

János Fodor
Janusz Kacprzyk (Eds.)

Aspects of Soft Computing, Intelligent Robotics and Control



Springer

János Fodor and Janusz Kacprzyk (Eds.)

Aspects of Soft Computing, Intelligent Robotics and Control

Studies in Computational Intelligence, Volume 241

Editor-in-Chief

Prof. Janusz Kacprzyk
Systems Research Institute
Polish Academy of Sciences
ul. Newelska 6
01-447 Warsaw
Poland
E-mail: kacprzyk@ibspan.waw.pl

Further volumes of this series can be found on our homepage: springer.com

- Vol. 220. Bettina Berendt, Dunja Mladenic, Marco de de Gemmis, Giovanni Semeraro, Myra Spiliopoulou, Gerd Stumme, Vojtech Svatek, and Filip Zelezny (Eds.)
Knowledge Discovery Enhanced with Semantic and Social Information, 2009
ISBN 978-3-642-01890-9
- Vol. 221. Tassilo Pellegrini, Sören Auer, Klaus Tochtermann, and Sebastian Schaffert (Eds.)
Networked Knowledge - Networked Media, 2009
ISBN 978-3-642-02183-1
- Vol. 222. Elisabeth Rakus-Andersson, Ronald R. Yager, Nikhil Ichalkarane, and Lakhmi C. Jain (Eds.)
Recent Advances in Decision Making, 2009
ISBN 978-3-642-02186-2
- Vol. 223. Zbigniew W. Ras and Agnieszka Dardzinska (Eds.)
Advances in Data Management, 2009
ISBN 978-3-642-02189-3
- Vol. 224. Amandeep S. Sidhu and Tharam S. Dillon (Eds.)
Biomedical Data and Applications, 2009
ISBN 978-3-642-02192-3
- Vol. 225. Danuta Zakrzewska, Ernestina Menasalvas, and Liliana Byczkowska-Lipinska (Eds.)
Methods and Supporting Technologies for Data Analysis, 2009
ISBN 978-3-642-02195-4
- Vol. 226. Ernesto Damiani, Jechang Jeong, Robert J. Howlett, and Lakhmi C. Jain (Eds.)
New Directions in Intelligent Interactive Multimedia Systems and Services - 2, 2009
ISBN 978-3-642-02936-3
- Vol. 227. Jeng-Shyang Pan, Hsiang-Che Huang, and Lakhmi C. Jain (Eds.)
Information Hiding and Applications, 2009
ISBN 978-3-642-02334-7
- Vol. 228. Lidia Ogiela and Marek R. Ogiela
Cognitive Techniques in Visual Data Interpretation, 2009
ISBN 978-3-642-02692-8
- Vol. 229. Giovanna Castellano, Lakhmi C. Jain, and Anna Maria Fanelli (Eds.)
Web Personalization in Intelligent Environments, 2009
ISBN 978-3-642-02793-2
- Vol. 230. Uday K. Chakraborty (Ed.)
Computational Intelligence in Flow Shop and Job Shop Scheduling, 2009
ISBN 978-3-642-02835-9
- Vol. 231. Mislav Grgic, Kresimir Delac, and Mohammed Ghanbari (Eds.)
Recent Advances in Multimedia Signal Processing and Communications, 2009
ISBN 978-3-642-02899-1
- Vol. 232. Feng-Hsing Wang, Jeng-Shyang Pan, and Lakhmi C. Jain
Innovations in Digital Watermarking Techniques, 2009
ISBN 978-3-642-03186-1
- Vol. 233. Takayuki Ito, Minjie Zhang, Valentin Robu, Shaheen Fatima, and Tokuro Matsuo (Eds.)
Advances in Agent-Based Complex Automated Negotiations, 2009
ISBN 978-3-642-03189-2
- Vol. 234. Aruna Chakraborty and Amit Konar
Emotional Intelligence, 2009
ISBN 978-3-540-68606-4
- Vol. 235. Reiner Onken and Axel Schulte
System-Ergonomic Design of Cognitive Automation, 2009
ISBN 978-3-642-03134-2
- Vol. 236. Natalio Krasnogor, Belén Melián-Batista, José A. Moreno-Pérez, J. Marcos Moreno-Vega, and David Pelta (Eds.)
Nature Inspired Cooperative Strategies for Optimization (NICSO 2008), 2009
ISBN 978-3-642-03210-3
- Vol. 237. George A. Papadopoulos and Costin Badica (Eds.)
Intelligent Distributed Computing III, 2009
ISBN 978-3-642-03213-4
- Vol. 238. Li Niu, Jie Lu, and Guangquan Zhang
Cognition-Driven Decision Support for Business Intelligence, 2009
ISBN 978-3-642-03207-3
- Vol. 239. Zong Woo Geem (Ed.)
Harmony Search Algorithms for Structural Design Optimization, 2009
ISBN 978-3-642-03449-7
- Vol. 240. Dimitri Plemenos and Georgios Miaoulis (Eds.)
Intelligent Computer Graphics 2009, 2009
ISBN 978-3-642-03451-0
- Vol. 241. János Fodor and Janusz Kacprzyk (Eds.)
Aspects of Soft Computing, Intelligent Robotics and Control, 2009
ISBN 978-3-642-03632-3

János Fodor and Janusz Kacprzyk (Eds.)

Aspects of Soft Computing, Intelligent Robotics and Control



Prof. János Fodor
Institute of Intelligent Engineering Systems
John von Neumann Faculty of Informatics
Budapest Tech
Bécsi út 96/b
H-1034 Budapest
Hungary
E-mail: fodor@bmf.hu

Prof. Janusz Kacprzyk
Systems Research Institute
Polish Academy of Sciences
Newelska 6, 01-447 Warsaw
Poland
E-mail: kacprzyk@ibspan.waw.pl

ISBN 978-3-642-03632-3

e-ISBN 978-3-642-03633-0

DOI 10.1007/978-3-642-03633-0

Studies in Computational Intelligence

ISSN 1860-949X

Library of Congress Control Number: Applied for

© 2009 Springer-Verlag Berlin Heidelberg

This work is subject to copyright. All rights are reserved, whether the whole or part of the material is concerned, specifically the rights of translation, reprinting, reuse of illustrations, recitation, broadcasting, reproduction on microfilm or in any other way, and storage in data banks. Duplication of this publication or parts thereof is permitted only under the provisions of the German Copyright Law of September 9, 1965, in its current version, and permission for use must always be obtained from Springer. Violations are liable to prosecution under the German Copyright Law.

The use of general descriptive names, registered names, trademarks, etc. in this publication does not imply, even in the absence of a specific statement, that such names are exempt from the relevant protective laws and regulations and therefore free for general use.

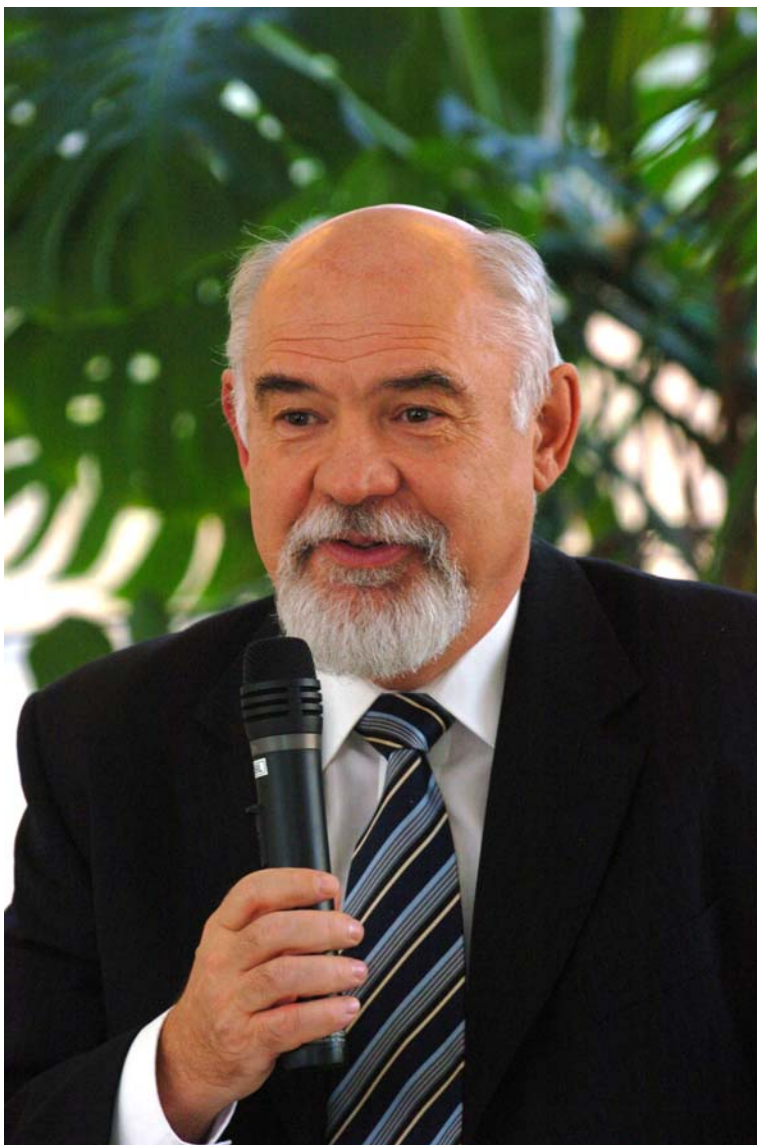
Typeset & Cover Design: Scientific Publishing Services Pvt. Ltd., Chennai, India.

Printed in acid-free paper

9 8 7 6 5 4 3 2 1

springer.com

This volume is dedicated to **Imre J. Rudas** on the occasion of his sixtieth birthday



Preface

Fifteen years ago Lotfi A. Zadeh proposed a new approach for machine intelligence, by distinguishing soft computing techniques based computational intelligence from hard computing techniques based artificial intelligence.

Soft computing is oriented towards the analysis and design of intelligent systems. It is based on fuzzy logic, artificial neural networks and probabilistic reasoning including genetic algorithms, with characteristics of approximation and tolerance for imprecision and uncertainty, in order to achieve an acceptable solution at a low cost and tractability.

The synergy derived from its components has made soft computing very effective and popular. The integration of constituent technologies provides complementary methods that allow developing flexible computing tools and solving complex problems.

A wide area of natural applications of soft computing techniques consists of the control of dynamic systems, including robots. Loosely speaking, control can be understood as driving a process to attain a desired goal. Intelligent control can be seen as an extension of this concept, to include autonomous human-like interactions of a machine with the environment.

Intelligent robots can be characterized by the ability to operate in an uncertain, changing environment with the help of appropriate sensing. They have the power to autonomously plan and execute motion sequences to achieve a goal specified by a human user without detailed instructions. In broader sense, intelligent robotics includes traditional robotics, computational intelligence, machine learning, data mining, evolutionary computation, neural nets and fuzzy logic, and other related research areas.

The present volume is a collection of 15 chapters written by leading experts of the fields, contributing to diverse aspects of soft computing and its applications. There is a distinguished person behind who mediates the subfields. He is professor Imre J. Rudas, who has been 60 this year. His wide spectrum of interests is reflected in the variety of these contributions.

Imre J. Rudas graduated from Bánki Donát Polytechnic, Budapest in 1971, received the Master Degree in Mathematics from the Eötvös Loránd University, Budapest, the Ph.D. in Robotics from the Hungarian Academy of Sciences in 1987, while the Doctor of Science degree from the Hungarian Academy of Sciences in 2004. He received his first Doctor Honoris Causa degree from the Technical

University of Košice, Slovakia and the second one from “Polytechnica” University of Timisoara, Romania.

He served as the Rector of Budapest Tech from August 1, 2003 for a period of four years, and was reelected for five years in 2007. He is active as a full university professor.

He is a Fellow of IEEE, Senior Administrative Committee member of IEEE Industrial Electronics Society, member of Board of Governors of IEEE SMC Society and Chair of IEEE Hungary Section.

He is the Vice-President of IFSA (International Fuzzy System Association), he was the President of Hungarian Fuzzy Association for ten years, Steering Committee Member of the Hungarian Robotics Association and the John von Neumann Computer Society.

He serves as an associate editor of some scientific journals, including IEEE Transactions on Industrial Electronics, member of editorial board of Journal of Advanced Computational Intelligence, member of various national and international scientific committees. He is the founder of the IEEE International Conference Series on Intelligent Engineering Systems (INES) and IEEE International Conference on Computational Cybernetics (ICCC), and some regional symposia. He has served as General Chairman and Program Chairman of numerous scientific international conferences.

His present areas of research activity are Computational Cybernetics, Robotics with special emphasis on Robot Control, Soft Computing, Computer-aided Process Planning, Fuzzy Control and Fuzzy Sets. He has published books, more than 400 papers in books, various scientific journals and international conference proceedings.

Imre J. Rudas' personal qualities of commitment, integrity, leadership and initiative leave lasting impression on his colleagues, students and friends. This volume is a token of their appreciation and friendship.

This volume has fifteen chapters, written by eminent scientists from different parts of the world, dealing with three major topics. The first part of the book is devoted to fundamental aspects of soft computing. This includes mathematical results on pseudo-analysis and aggregation functions, a description of neural networks and fuzzy systems, and recent results on new types of interactive evolutionary computation. The second part of the book addresses issues of intelligent robotics, including humanoid robots' gait in unstructured environments, multi-locomotion robot with passive dynamic autonomous control, harmonic motion generator for smooth robot arm motion, a fuzzy inference based mentality expression for eye robot, and fuzzy signatures in the field of intelligent mobile robots. The last part concerns with different problems, issues and methods of intelligent control. This includes controllability and stabilizability results concerning linear switching systems, an indirect adaptive control scheme using Hopfield-based dynamic neural network, fuzzy immune controller synthesis for ABR traffic control in high-speed networks, Takagi-Sugeno type fuzzy automaton model, control and dynamics of fractional order systems, an automatic learning based adaptive approach elaborated for the control of nonlinear dynamic systems.

The editors are grateful to the authors for their excellent work. Thanks are also due to Ms. Anikó Szakál for her editorial assistance and sincere effort in bringing out the volume nicely in time.

June 2009

J. Fodor
J. Kacprzyk
Budapest, Warsaw

Contents

Part I: Soft Computing

Pseudo-Analysis in Soft Computing	3
<i>Endre Pap</i>	

Aggregation Functions in Fuzzy Systems	25
<i>János Fodor</i>	

Neural Networks or Fuzzy Systems	51
<i>Bogdan M. Wilamowski</i>	

New IEC Research and Frameworks	65
<i>Hideyuki Takagi</i>	

Part II: Intelligent Robotics

How to Generate and Realize Bipedal Gait in Unstructured Environments?	79
<i>Miomir Vukobratović, Branislav Borovac</i>	

PDAC-Based Brachiating Control of the Multi-locomotion Robot	101
<i>Toshio Fukuda, Tadayoshi Aoyama, Yasuhisa Hasegawa, Kosuke Sekiyama, Shigetaka Kojima</i>	

A Simple Method for Generating Smooth Robot Arm Motion	123
<i>Antal K. Bejczy</i>	

Fuzzy Inference-Based Mentality Expression for Eye Robot in Affinity Pleasure-Arousal Space	129
<i>Yoichi Yamazaki, Hai An Vu, Phuc Quang Le, Hitoho Oikawa, Kazuya Fukuda, Yui Matsuura, Fangyan Dong, Kaoru Hirota</i>	

Fuzzy Communication and Motion Control by Fuzzy Signatures in Intelligent Mobile Robots.....	147
<i>Áron Ballagi, László T. Kóczy, Tamás D. Gedeon</i>	
Part III: Intelligent Control	
Linear Switching Systems: Attainability and Controllability	167
<i>József Bokor, Zoltán Szabó, László Nádai</i>	
Indirect Adaptive Control Using Hopfield-Based Dynamic Neural Network for SISO Nonlinear Systems	189
<i>Ping-Cheng Chen, Chi-Hsu Wang, Tsu-Tian Lee</i>	
Fuzzy Immune Controller Synthesis for ABR Traffic Control in High-Speed Networks	205
<i>Georgi M. Dimirovski, Yuanwei Jing, Tao Ren</i>	
Takagi-Sugeno Type Fuzzy Automaton Model	223
<i>Janos L. Grantner, George A. Fodor</i>	
Control and Dynamics of Fractional Order Systems.....	235
<i>J.A. Tenreiro Machado, Isabel S. Jesus, Ramiro S. Barbosa, Manuel F. Silva</i>	
Adaptive Control Using Fixed Point Transformations for Nonlinear Integer and Fractional Order Dynamic Systems ...	253
<i>József K. Tar, János F. Bitó</i>	
Author Index	269

Part I

Soft Computing

Pseudo-Analysis in Soft Computing

Endre Pap

Department of Mathematics and Informatics, 21 000 Novi Sad,
Trg Dositeja Obradovića 4, Serbia
pape@eunet.yu, pap@im.ns.ac.yu

Abstract. There are presented the basic operations on real intervals: pseudo-addition and pseudo multiplication which induce the semiring structure. Application of special pseudo-operations on the unit interval: t-norms and t-conorms, in the theory of fuzzy sets and fuzzy logics are given. Pseudo-convolution as a generalization of the classical convolution is given, with many important special cases. Further applications of pseudo-additive measures, pseudo-integrals and pseudo-convolutions are given in the theory of fuzzy numbers, information theory, system theory and control theory, and probabilistic metric spaces.

1 Introduction

Soft computing gives non-standard models for many important events, and therefore require new mathematical methods. Three main problems which usually occurs in mathematical models in soft computing: uncertainty, nonlinearity and optimization.

We shall present a mathematical background for treating all three mentioned problems. Instead of the usual plus-product structure of real numbers a semiring structure on extended reals with respect to some other operations (pseudo-operations) is considered. For example, max-min, max-plus, max-product or operations generated by some additive generator g are included, and specially triangular conorm- triangular norm. We present some parts of mathematical analysis in analogy with the classical mathematical analysis as for example measure theory, integration, integral operators, convolution, delta-sequences, Laplace transform, etc.

Many problems in fuzzy logic, fuzzy sets, neural nets, fuzzy-neural nets, multicriteria decision making, etc. can be treated by this mathematical tool. There are also many applications in different fields as optimization, nonlinear differential and difference equations, economy, game theory.

In section 2 there are presented the basic operations on real intervals: pseudo-addition and pseudo multiplication which induce the semiring structure.

Section 3 is devoted to the application of special pseudo-operations on the unit interval: t-norms and t-conorms, in the theory of fuzzy sets and fuzzy logics. Pseudo-convolution as a generalization of the classical convolution is given in section 4, with many important special cases. Further applications of pseudo-additive measures, pseudo-integrals and pseudo-convolutions are given in the theory of fuzzy numbers (section 5), information theory (section 6), system theory and control theory (section 7), and probabilistic metric spaces (section 8).

2 Pseudo-Operations

Let $[a,b]$ be a closed (in some cases semiclosed) subinterval of $[-\infty, \infty]$. We consider here a total order \leq on $[a,b]$ (although it can be taken in the general case a partial order). The operation \oplus (pseudo-addition) is a function $\oplus : [a,b] \times [a,b] \rightarrow [a,b]$ which is commutative, nondecreasing, associative and has a zero element, denoted by $\mathbf{0}$. Let $[a,b]_+ = \{x \mid x \in [a,b], x \geq \mathbf{0}\}$.

The operation \odot (pseudo-multiplication) is a function $\odot : [a,b] \times [a,b] \rightarrow [a,b]$ which is commutative, positively nondecreasing, i.e. $x \leq y$ implies $x \odot z \leq y \odot z$, $z \in [a,b]_+$, associative and for which there exist a unit element $\mathbf{1} \in [a,b]$, i.e., for each $x \in [a,b]$ we have $\mathbf{1} \odot x = x$.

We suppose, further, $\mathbf{0} \odot x = \mathbf{0}$ and that \odot is a distributive pseudo-multiplication with respect to \oplus , i.e.,

$$x \odot (y \oplus z) = (x \odot y) \oplus (x \odot z).$$

The structure $([a,b], \oplus, \odot)$ is called a *semiring*.

In this paper we will consider only special semirings ([4], [18], [8]) with the following continuous operations:

Case I (i) $x \oplus y = \min(x,y)$, $x \odot y = x + y$, on the interval $]-\infty, \infty]$. We have $\mathbf{0} = \infty$ and $\mathbf{1} = 0$.

(ii) $x \oplus y = \max(x,y)$, $x \odot y = x + y$, on the interval $[-\infty, \infty[$. We have $\mathbf{0} = -\infty$ and $\mathbf{1} = 0$.

Case II Semirings with pseudo-operations defined by monotone and continuous generator g ([25, 26, 27,]). In this case we will consider only strict pseudo-addition, i.e., such that the function \oplus is continuous and strictly increasing in $]a,b[\times]a,b[$. By Aczél's representation theorem ([1], [26]) for each strict pseudo-addition \oplus there exists a monotone function g (generator for \oplus),

$g : [a, b] \rightarrow [-\infty, \infty]$ (or with values in $[0, \infty]$) such $g(\mathbf{0}) = 0$ and $u \oplus v = g^{-1}(g(u) + g(v))$. Using a generator g of strict pseudo-addition \oplus , we can define pseudo-multiplication \odot : $u \odot v = g^{-1}(g(u)g(v))$. This is the only way to define pseudo-multiplication \odot , which is distributive with respect to \oplus generated by the function g .

Case III (i) Let $\oplus = \max$ and $\odot = \min$ on the interval $[-\infty, \infty]$.

(ii) Let $\oplus = \min$ and $\odot = \max$ on the interval $[-\infty, \infty]$.

We restrict now on the real interval $[0, 1]$.

Definition 1. A *triangular norm* T (*t-norm* briefly) is a function $T : [0, 1]^2 \rightarrow [0, 1]$ such that

- (T1) $T(x, y) = T(y, x)$ (commutativity)
- (T2) $T(x, T(y, z)) = T(T(x, y), z)$ (associativity)
- (T3) $T(x, y) \leq T(x, z)$ for $y \leq z$ (monotonicity)
- (T4) $T(x, 1) = x$ (boundary condition).

Example 1. The following are the basic t-norms

$$T_M(x, y) = \min(x, y),$$

$$T_P(x, y) = xy,$$

$$T_L(x, y) = \max(0, x + y - 1),$$

$$T_D(x, y) = \begin{cases} \min(x, y) & \text{if } \max(x, y) = 1 \\ 0 & \text{otherwise.} \end{cases}$$

Example 2. The family $(T_\lambda^Y)_{\lambda \in [0, \infty]}$ of *Yager t-norms* is given by

$$T_\lambda^Y(x, y) = \begin{cases} T_D(x, y) & \text{if } \lambda = 0, \\ T_M(x, y) & \text{if } \lambda = \infty, \\ \max\left(0, 1 - \left((1-x)^\lambda + (1-y)^\lambda\right)^{\frac{1}{\lambda}}\right) & \text{otherwise.} \end{cases}$$

The corresponding dual operation for t-norm is given by

Definition 2. A *triangular conorm* S (*t-conorm* briefly) is a function $S : [0, 1]^2 \rightarrow [0, 1]$ such that

- (S1) $S(x,y) = S(y,x)$ (commutativity)
- (S2) $S(x,S(y,z)) = S(S(x,y),z)$ (associativity)
- (S3) $S(x,y) \leq S(x,z)$ for $y \leq z$ (monotonicity)
- (S4) $S(x,0) = x$ (boundary condition).

We see that t-norms and t-conorms differs only by boundary conditions.

Example 3. The following are the basic t-conorms:

$$\begin{aligned} S_M(x,y) &= \max(x,y), \\ S_P(x,y) &= x + y - xy, \\ S_L(x,y) &= \min(1,x+y), \\ S_D(x,y) &= \begin{cases} \max(x,y) & \text{if } \min(x,y) = 0 \\ 1 & \text{otherwise.} \end{cases} \end{aligned}$$

Many other important t-norms and t-conorms can be found in [14].

Coming back to general pseudo-operations defined on $[0,1]$ such that the neutral element is inside of the interval, such operations were introduced under the name uninorms in [40], and as special (generated) compensatory operators by in [13].

Definition 3. An aggregation function $U : [0,1]^n \rightarrow [0,1]$ which is symmetric, associative and possesses a neutral element $e \in]0,1[$ is called a *uninorm*.

Uninorms are strongly connected with t-norms and t-conorms. For a given uninorm U with a neutral element e , we introduce the related t-norm $T_U : [0,e]^2 \rightarrow [0,e]$ and the t-conorm $S_U : [e,1]^2 \rightarrow [e,1]$, given by

$$T_U(x,y) = \frac{U(ex,ey)}{e}$$

and

$$S_U(x,y) = \frac{U(e+(1-e)x, e+(1-e)y) - e}{1-e}.$$

The following characterization was obtained in [10]

Proposition 1. Let $U : [0,1]^2 \rightarrow [0,1]$ be a uninorm with neutral element $e \in]0,1[$. Then there are three binary aggregation functions $T, S, H : [0,1]^2 \rightarrow [0,1]$ such that T is a t-norm, S a t-conorm and H is a symmetric mean aggregation function, and for any $(x,y) \in [0,1]^2$ we have

$$U(x, y) = \begin{cases} T(x, y) & \text{if } (x, y) \in [0, e]^2 \\ S(x, y) & \text{if } (x, y) \in [e, 1]^2 \\ H(x, y) & \text{otherwise.} \end{cases}$$

3 Fuzzy Logics and Fuzzy Sets

We shall present very briefly where in the fuzzy logics and fuzzy sets occur the preceding operations. We restrict ourselves on triangular norms and triangular conorms.

Given a (crisp) universe of discourse X , as it is well-known a *fuzzy subset* A of X ([41], see [14]) is characterized by its *membership function* $\mu_A : X \rightarrow [0, 1]$, where for $x \in X$ the number $\mu_A(x)$ is interpreted as the *degree of membership* of x in the fuzzy set A or, equivalently, as the *truth value* of the statement ‘ x is element of A ’. The membership function μ_A of a fuzzy subset A of X is a quite natural generalization of the *characteristic function* $\mathbf{1}_B : X \rightarrow \{0, 1\}$ of a crisp subset B of X , assigning the value 1 to all elements of X which belong to B , and the value 0 to all remaining elements of X . Therefore, the crisp subsets of X (in particular, the universe X and the empty set \emptyset) are special cases of fuzzy subsets of X . The intersection $A \cap B$ of two fuzzy subsets of X is characterized by the membership function $\mu_{A \cap B} : X \rightarrow [0, 1]$ defined by

$$\mu_{A \cap B}(x) = \min(\mu_A(x), \mu_B(x)). \quad (1)$$

The intersection \cap of fuzzy sets given in the preceding equality is a commutative, associative and monotone operation on the class of all fuzzy subsets of X , and the universe X acts as its neutral element. We remark that, for each $\alpha \in [0, 1]$, we have $[A \cap B]_\alpha = [A]_\alpha \cap [B]_\alpha$, where $[A]_\alpha = \{x \in \mathbb{R} \mid \mu_A(x) \geq \alpha\}$ is the α -cut of A , and the operation \cap on the right hand side is the usual intersection of crisp sets.

We present the investigations from [15]. The only possible negation $\mathbf{c} : [0, 1] \rightarrow [0, 1]$ which gives the complement of fuzzy sets satisfying

$\mu_{A^c}(x) = \mathbf{c}(\mu_A(x))$ and giving $A \cap A^c = \emptyset$ for all fuzzy subsets of X is the so-called Gödel negation $\mathbf{c}_G : [0,1] \rightarrow [0,1]$ defined by [12]

$$\mathbf{c}_G(x) = \begin{cases} 1 & \text{if } x = 0, \\ 0 & \text{otherwise.} \end{cases}$$

However, the Gödel negation is not involutive. If we wish the complement of fuzzy sets to be involutive and if $A \cap A^c = \emptyset$ should hold for all fuzzy subsets A of X , the only way out is to replace the minimum by a more general operation. The commutativity, associativity and monotonicity together with the requirement that X be its neutral element necessarily lead to a T -intersection \cap_T of fuzzy sets defined by

$$\mu_{A \cap_T B}(x) = T(\mu_A(x), \mu_B(x)),$$

where $T : [0,1]^2 \rightarrow [0,1]$ is some triangular norm.

We shall need the following result proven in [37].

Proposition 2. *A function $c : [0,1] \rightarrow [0,1]$ is a strong negation, i.e., an involutive decreasing function if and only if there is a decreasing bijection $t : [0,1] \rightarrow [0,1]$ such that for all $x \in [0,1]$*

$$\mathbf{c}(x) = t^{-1}(1 - t(x)). \quad (2)$$

Given a strong negation \mathbf{c} , there are infinitely many decreasing functions t generating it by (2), e.g., the standard negation $\mathbf{c}_s : [0,1] \rightarrow [0,1]$ given by $\mathbf{c}_s(x) = 1 - x$ is obviously generated by $t : [0,1] \rightarrow [0,1]$ given by $t(x) = 1 - x$, but also by any other decreasing bijection satisfying $t(x) + t(1 - x) = 1$ for all $x \in [0,1]$.

Given a strong negation \mathbf{c} we can now find a t-norm T such that $A \cap_T A^c = \emptyset$ for all fuzzy subsets A of X .

Theorem 1. *Let $c : [0,1] \rightarrow [0,1]$ be a strong negation, let $t : [0,1] \rightarrow [0,1]$ be a decreasing bijection generating \mathbf{c} by (2), and let $T : [0,1]^2 \rightarrow [0,1]$ be the t-norm which has t as additive generator. Then, for all fuzzy subsets A of X , we have $A \cap_T A^c = \emptyset$.*

If T is a t-norm such that $A \cap_T A^c = \emptyset$, then for each t-norm T^* with $T^* \leq T$ we also have $A \cap_{T^*} A^c = \emptyset$. As an example, starting with the

standard negation \mathbf{c}_s and its generator $t : [0,1] \rightarrow [0,1]$ given by $t(x) = 1 - x$, the construction in Theorem 1 leads to the Łukasiewicz t-norm T_L and, subsequently, each t-norm T with $T \leq T_L$ satisfies $A \cap_T A^{\mathbf{c}_s} = \emptyset$ for all fuzzy subsets A of X (however, in this case we get $A \cap_T A = A$ only if A is a crisp set). Examples of such t-norms are all Yager t-norms T_λ^Y with $\lambda \in [0,1]$.

Taking a t-norm T , the Zadeh strong negation \mathbf{c} given by $c(x) = 1 - x$ and, implicitly, with the t-conorm S dual to T given by

$$S(x, y) = \mathbf{c}T(\mathbf{c}(x), \mathbf{c}(y)),$$

we can introduce the basic connectives in a $[0,1]$ -valued logic as follows:

$$\text{conjunction: } x \wedge_T y = T(x, y),$$

$$\text{disjunction: } x \vee_T y = S(x, y).$$

If x and y are the truth values of two propositions A and B , respectively, then $x \wedge_T y$ is the truth value of ‘ A AND B ’, $x \vee_T y$ is the truth value of ‘ A OR B ’, and $c(x)$ is the truth value of ‘NOT A ’. Obviously, when restricting ourselves to Boolean (i.e., two-valued) logic with truth values 0 and 1 only, then we obtain the classical logical connectives. However, $([0,1], T, S, \mathbf{c}, 0, 1)$ never yields a Boolean algebra.

As in the classical logic, it is possible to construct implication, bi-implication and so on by means of negation, conjunction and disjunction. Taking into account that in Boolean logic ‘NOT A OR B ’ is equivalent to ‘IF A THEN B ’, one possibility of modelling the implication in a $[0,1]$ -valued logic (based on T , \mathbf{c} and S) is to define the function $I_T : [0,1]^2 \rightarrow [0,1]$ by

$$I_T(x, y) = S(\mathbf{c}(x), y) = \mathbf{c}(T(x, \mathbf{c}(y))).$$

It is clear that in this case the *law of contraposition*

$$I_T(x, y) = I_T(\mathbf{c}(y), \mathbf{c}(x))$$

is always valid.

For the two basic t-norms T_M , T_L we obtain the following implications:

$$I_{T_L}(x, y) = \begin{cases} y & x + y \geq 1, \\ 1 - x & \end{cases}$$

$$I_{T_M}(x, y) = \begin{cases} 1 & x \leq y, \\ 1 - x + y & \end{cases}$$

Another way of extending the classical binary implication operator (acting on $\{0,1\}$) to the unit interval $[0,1]$ uses the *residuation* (see [9, 14, 32])

$$R_T(x,y) = \sup \{z \in [0,1] \mid T(x,z) \leq y\}.$$

For the two previous basic t-norms T_M , T_L we obtain the following residuations:

$$\begin{aligned} R_{T_M}(x,y) &= \begin{cases} 1 & \text{if } x \leq y, \\ y & \text{otherwise;} \end{cases} \\ R_{T_L}(x,y) &= \begin{cases} 1 & \text{if } x \leq y, \\ 1-x+y & \text{otherwise;} \end{cases} \end{aligned}$$

In general, I_T and R_T are different (although both are extensions of the Boolean implication), but that $I_{T_L} = R_{T_L}$.

Let $X_1 \times X_2$ is the crisp Cartesian product of two crisp sets X_1 and X_2 . Then a *fuzzy relation* R on $X_1 \times X_2$ is a fuzzy set on $X_1 \times X_2$. The notion of *fuzzy relation equation*, first introduced by Sanchez [33] for T_M , is important in many applications, as for example in automatic control by fuzzy controllers. We state here only a result on the solution of a special type of fuzzy relation equation (see [9, 33]).

Theorem 2. *Let A, B be fuzzy subsets of the crisp sets X_1 and X_2 , respectively, and let T a t-norm. Then there exists a fuzzy relation R on $X_1 \times X_2$ which is the solution of the fuzzy relation equation*

$$B = A \circ_T R,$$

where

$$R \circ_T Q : \mu_{R \circ_T Q}(x,y) = \sup_{z \in X_2} T(\mu_R(x,z), \mu_Q(z,y)) \quad ((x,y) \in X_1 \times X_3)$$

for two fuzzy relations R and Q on $X_1 \times X_2$ and $X_2 \times X_3$, respectively, if and only if the fuzzy relation $R_T(A,B)$ on $X_1 \times X_2$ solves (remark), where $R_T(A,B)$ is given by

$$\mu_{R_T(A,B)}(x,y) = R_T(\mu_A(x), \mu_B(y)),$$

and

$$R_T(x,y) = \sup \{z \in [0,1] \mid T(x,z) \leq y\}.$$

Additionally, if (1.3) is solvable, the fuzzy relation $R_T(A,B)$ is the largest solution.

Fuzzy neural networks give more information with respect to the classical neural networks, which are more or less Black Boxes (see [24]). Since the t-norm T_M can be obtained as a limit of a family of continuous Archimedean t-norms (see [14]), taking enough big value for this parameter we obtain satisfactory approximation. In the Archimedean case (t-norm or t-conorm) we have an additive generator h . For example, if the activation function of the neuron u_j is given by a differentiable function h which is induced by a t-norm or t-conorm, then for activation a_{u_i} by neuron u_i we have

$$\frac{\delta \text{net}_{u_j}^{(p)}}{\delta a_{u_i}^{(p)}} = \frac{h'(a_{u_i}^{(p)})}{h'^{(-1)}(\sum_k h(a_{u_k}^{(p)}))},$$

where the sum goes through all neurons u_k which have connection with the neuron u_j (see [24]).

4 Pseudo-Integral and Pseudo-Convolution

Let \mathcal{A} be a σ -algebra of subsets of X . An \oplus -measure is a function $m : \mathcal{A} \rightarrow [a, b]$ which satisfy $m(A \cup B) = m(A) \oplus m(B)$ for all $A, B \in \mathcal{A}$ such that $A \cap B = \emptyset$, and $m(\emptyset) = \mathbf{0}$. If additionally it is also continuous from above then it is called σ - \oplus -measure, see [27].

Definition 4. The *pseudo-integral* of a simple function

$$s = \bigoplus_{i=1}^n a_i \odot \mathbf{1}_{A_i}$$

with respect to the σ - \oplus -measure m is given by

$$\int_X^\oplus s \odot dm = \bigoplus_{i=1}^n a_i \odot m(A_i).$$

The *pseudo-integral* of a bounded measurable function $f : X \rightarrow [a, b]$, such that, if \oplus is not idempotent, for each $\varepsilon > 0$ there exists a monotone ε -net in $f(X)$, is defined by (see [25, 27])

$$\int_X^\oplus f \odot dm = \lim_{n \rightarrow \infty} \int_X^\oplus s_n \odot dm,$$

where $\{s_n\}_{n \in \mathbb{N}}$ is the sequence of simple functions converging to f .

The pseudo-integral over A , when A is an arbitrary subset of X , is given by:

$$\int_A^{\oplus} f \odot dm = \int_X^{\oplus} \mathbf{1}_A \odot f \odot dm,$$

where $\mathbf{1}_A$ is pseudo-characteristic function of set A .

Let G be subset of \mathbb{R} and $*$ a commutative binary operation on \mathbb{R} such that $(G, *)$ is semigroup with unit element e and $G_+ = \{x \mid x \in G, x \geq e\}$. We have by [30].

Definition 5. The *generalized pseudo-convolution of the first type* of two functions $f : G_+ \rightarrow [a, b]$ and $h : G_+ \rightarrow [a, b]$ with respect to a $\sigma-\oplus$ -decomposable measure m is given in the following way

$$(f \star h)(x) = \int_{G_+^x}^{\oplus} f(u) \odot dm_h(v),$$

where $G_+^x = \{(u, v) \mid u * v = x, v, u \in G_+\}$, $m_h(A) = \sup_{x \in A} h(x)$ if (for $\oplus = \max$) is a sup-decomposable measure, $m_h(A) = \inf_{x \in A} h(x)$ if (for $\oplus = \min$) is a inf-decomposable measure, and if \oplus has an additive generator g , then $dm_h = h \odot d(g^{-1} \circ \lambda)$, where $\lambda = g \circ m$ is the Lebesgue measure (g -calculus [26]).

We consider also the *second type of generalized pseudo-convolution* of two functions $f : G \rightarrow [a, b]$ and $h : G \rightarrow [a, b]$ when $(G, *)$ is a group and the pseudo-integral is taken over whole set G :

$$(f \star h)(x) = \int_G^{\oplus} f(x * (-t)) \odot dm_h(t),$$

where $(-t)$ is unique inverse element for t , $x \in G$, $m_h(A) = \sup_{x \in A} h(x)$ if (for $\oplus = \max$) is a sup-decomposable measure, $m_h(A) = \inf_{x \in A} h(x)$ if (for $\oplus = \min$) is a inf-decomposable measure, and if \oplus has an additive generator g , then $dm_h = h \odot d(g^{-1} \circ \lambda)$, where $\lambda = g \circ m$ is the Lebesgue measure.

Remark 1. (i) When $*$ is the usual addition on \mathbb{R} and G is \mathbb{R} pseudo-convolutions of the first and the second type, for $x \in \mathbb{R}^+$, are

$$(f \star h)(x) = \int_{[0, x]}^{\oplus} f(x - t) \odot dm_h(t),$$

$$(f \star h)(x) = \int_{\mathbb{R}}^{\oplus} f(x-t) \odot dm_h(t),$$

respectively.

(ii) Convolution of two functions is defined by

$$(f \star h)(x) = \int_{[0,x]} f(x-t) dh(t) \quad (4)$$

for all $x \in]0, \infty[$, $(f \star h)(0) = 0$ and $(f \star h)(\infty) = 1$. Convolution defined in such manner is commutative, associative operation with identity. Using this approach we can introduce a different type of generalized pseudo-convolution of the first type, e.g., for g -case when $* = +$ and $G = \mathbb{R}$:

$$(f \star h)(x) = g^{-1} \left(\int_{[0,x]} g(f(x-t)) dg(h(t)) \right).$$

Convolution (4) can be transformed into the form

$$(f \star h)(x) = \int_{\{x\}} d\Pi(f(u), h(v))$$

where $\text{Sum}\{x\} = \{(u, v) \mid u + v < x; u, v \in \mathbb{R}^+\}$ and $\Pi(x, y) = x \cdot y$.

The main difference between this definition and Definition 5 is the existence of identity, which is not certain for generalized pseudo-convolution (see g -case).

Definition 6. Let pseudo-addition \oplus is an idempotent operation. *Pseudo-delta function* is given by

$$\delta^{\oplus, \odot}(x) = \begin{cases} \mathbf{1} & x = e, \\ \mathbf{0} & x \neq e, \end{cases}$$

where $\mathbf{0}$ is the zero element for the idempotent \oplus , $\mathbf{1}$ is the unit element for \odot and e is the zero element for $*$.

Example 4. Let $* = +$ and $G = \mathbb{R}$.

Case I)

(i) For the semiring $([-\infty, \infty[, \max, +)$ pseudo-integral, with respect to sup-measure $m, m(A) = \sup_{x \in A} h(x)$, is given by

$$\int_{\mathbb{R}}^{\oplus} f \odot dm = \sup_{\mathbb{R}} (f(x) + h(x)),$$

and the pseudo-convolution of the first type of the functions f and h will be

$$(f \star h)(x) = \sup_{0 \leq t \leq x} (f(x-t) + h(t)),$$

and the pseudo-convolution of the second type is

$$(f \star h)(x) = \sup_{t \in \mathbb{R}} (f(x-t) + h(t)),$$

Unit element for this pseudo-convolutions is the following pseudo-delta function

$$\delta^{\max,+}(x) = \begin{cases} \mathbf{1} (= 0) & \text{if } x = 0, \\ \mathbf{0} (= -\infty) & \text{if } x \neq 0. \end{cases}$$

(ii) For the semiring $(]-\infty, \infty], \min, +)$ pseudo-integral is given by

$$\int_{\mathbb{R}}^{\oplus} f \odot dm = \inf_{x \in \mathbb{R}} (f(x) + h(x)),$$

where the function h defines the \inf -measure m . The domain of functions will be $[0, \infty]$ (or some subset of $[0, \infty]$) and the domain of the semiring can be any subinterval of $]-\infty, \infty]$ which contains 0 and ∞ . The zero element for the \oplus is ∞ and the unit element for the \odot is 0. Pseudo-delta function is given by

$$\delta^{\min,+}(x) = \begin{cases} \mathbf{1} (= 0) & \text{if } x = 0, \\ \mathbf{0} (= \infty) & \text{if } x \neq 0. \end{cases}$$

Previous pseudo-delta function is the unit element for the operation of pseudo-convolution of the first type

$$(f \star h)(x) = \inf_{0 \leq t \leq x} (f(x-t) + h(t)),$$

and of the second type

$$(f \star h)(x) = \inf_{t \in \mathbb{R}} (f(x-t) + h(t)).$$

Case II)

Pseudo-convolution of the first type in the sense of the g -integral is given in the following way

$$(f \star h)(x) = g^{-1} \left(\int_0^x g(f(x-t)) \cdot g(h(t)) dt \right).$$

Pseudo-convolution of the second type in the same sense is

$$(f \star h)(x) = g^{-1} \left(\int_{-\infty}^{\infty} g(f(x-t)) \cdot g(h(t)) dt \right).$$

Case III)

For the semiring $([-\infty, \infty], \max, \min)$ pseudo-integral is given by

$$\int_{\mathbb{R}}^{\oplus} f \odot dm = \sup_{x \in \mathbb{R}} (\min(f(x), h(x))),$$

where the function h defines the sup-measure m . The domain of functions will be \mathbb{R} (or some subset of \mathbb{R}) and the domain of the semiring is $[-\infty, \infty]$ (or any subinterval). The zero element for the \oplus is $-\infty$ and the unit element for the \odot is ∞ . Pseudo-delta function is given by

$$\delta^{\max, \min}(x) = \begin{cases} \mathbf{1} \ (\infty) & \text{if } x = 0, \\ \mathbf{0} \ (-\infty) & \text{if } x \neq 0. \end{cases}$$

Pseudo-delta function is the unit element for the pseudo-convolution of the first type and the pseudo-convolution of the second type:

$$(f \star h)(x) = \sup_{0 \leq t \leq x} (\min(f(x-t), h(t))) \quad , \quad \text{the first type},$$

$$(f \star h)(x) = \sup_{t \in \mathbb{R}} (\min(f(x-t), h(t))) \quad . \quad \text{the second type}.$$

Example 5. Let $G = \mathbb{R} \setminus \{0\}$ and $* = ..$

Case I) For the semiring $([-\infty, \infty[, \max, +)$ pseudo-integral, with respect to sup-measure $m, m(A) = \sup_{x \in A} h(x)$, is given by

$$(f \star h)(x) = \sup_{1 \leq t \leq x} (f(\frac{x}{t}) + h(t)), \quad ; \text{ the first type};$$

$$(f \star h)(x) = \sup_{t \in \mathbb{R} \setminus \{0\}} (f(\frac{x}{t}) + h(t)), \quad . \text{ the second type}.$$

Case II) Pseudo-convolution in the sense of the g -integral is given in the following way

$$(f \star h)(x) = g^{-1} \left(\int_1^x g(f(\frac{x}{t})) \cdot g(h(t)) dt \right), \quad ; \quad \text{the first type};$$

$$(f \star h)(x) = g^{-1} \left(\int_{\mathbb{R} \setminus \{0\}} g(f(\frac{x}{t})) \cdot g(h(t)) dt \right), \quad \text{the second type}.$$

Case III) For the semiring $([-\infty, \infty], \max, \min)$ pseudo-integral is given by

$$(f \star h)(x) = \sup_{1 \leq t \leq x} (\min(f(\frac{x}{t}), h(t))), \quad ; \text{ the first type},$$

$$(f \star h)(x) = \sup_{t \in \mathbb{R} \setminus \{0\}} (\min(f(\frac{x}{t}), h(t))), \quad . \text{ the second type}$$

The unit element for the previous pseudo-convolutions is a bit different from the unit element for the case $* = +$ and $G = \mathbb{R}$. Since, in this case, we have $e = 1$, pseudo-delta function is given by

$$\delta^{\oplus, \odot}(x) = \begin{cases} \mathbf{1} & x = 1, \\ \mathbf{0} & x \neq 1, \end{cases}$$

where $\mathbf{0}$ is a zero element for pseudo-addition \oplus and $\mathbf{1}$ is a unit element for pseudo-multiplication \odot .

The basic properties of the generalized pseudo-convolution for idempotent pseudo-addition are given in the following theorem from [30].

Theorem 3. Let \mathcal{F} be a class of functions f such that $f : G_+ \rightarrow [a, b]$, where $(G, *)$ is an commutative semigroup with unit element e . Let \odot be continuous (up to some distinguished points) pseudo-multiplication of the first or the second type on interval $[a, b]$.

Then, the pseudo-convolution of the first type for the idempotent pseudo-addition (cases I and III)) is commutative, associative operation with the unit element $\delta^{\oplus, \odot}$.

Example 6. Let $G = \mathbb{R}$, $x * y = x + y + xy$, $f : \mathbb{R} \rightarrow [0, 1]$ and $h : \mathbb{R} \rightarrow [0, 1]$. Let T be an arbitrary t-norm. The pseudo-convolution of the first type for $\oplus = \max$, $\odot = T$ and $x \in G_+ = [0, \infty]$ is given by

$$\begin{aligned} (f \star h)(x) &= \sup \{T(f(u), h(v)) \mid u + v + uv = x, u, v \in [0, \infty]\} \\ &= \sup_{0 \leq t \leq x} Tf \frac{x-t}{1+t}, h(t) \\ &= \int_{[0, x]}^{\oplus} f \frac{x-t}{1+t} \odot dm_h(t). \end{aligned}$$

There were introduced and investigated also pseudo-Laplace transform [29, 31].

5 Fuzzy Numbers

A fuzzy subset of \mathbb{R} , whose membership function is normalized, upper semicontinuous and convex [5], is called a fuzzy number. The sum $A + B$ of two (triangular) fuzzy numbers A and B , based on the extension principle, is given by

$$\mu_{A+B}(x) = \sup_{t \in \mathbb{R}} \min(\mu_A(t), \mu_B(x-t)).$$

Observe that, for each $\alpha \in [0,1]$, we have $[A+B]_\alpha = [A]_\alpha + [B]_\alpha$, where $[A]_\alpha$ again denotes the α -cut of A (which is always an interval if A is a fuzzy number) and the addition on the right hand side is the addition of intervals.

Example 7. Triangular fuzzy numbers A is determined by triples (a, l, r) with $a \in \mathbb{R}$ and $l, r > 0$ by

$$\mu_A(x) = \max \left(\min \left(\frac{a-x+l}{l}, \frac{x-a+r}{r} \right), 0 \right),$$

where a denotes the modal value of A , and l and r are the left and right spreads of A , respectively. Given two triangular fuzzy numbers $A_1 = (a_1, l_1, r_1)$ and $A_2 = (a_2, l_2, r_2)$, we obtain

$$A_1 + A_2 = (a_1 + a_2, l_1 + l_2, r_1 + r_2),$$

which means that the left (right) spread of the sum $A_1 + A_2$ equals the sum of the respective left (right) spreads of A_1 and A_2 .

It was proposed in [6] to replace the minimum T_M by some t-norm T , leading to the sum $A \oplus_T B$ given by

$$\mu_{A \oplus_T B}(x) = \sup\{T(\mu_A(t), \mu_B(x-t)) \mid t \in \mathbb{R}\},$$

what is a pseudo-convolution with $\oplus = \max$ and $\odot = T$.

Example 8. The sum $A \oplus_T B$ of two triangular fuzzy numbers A and B is again a triangular fuzzy number if and only if $T \leq T_L$ or if T is a member of the family of Yager t-norms $(T_\lambda^Y)_{\lambda \in [0, \infty]}$ see [17].

Given two triangular fuzzy numbers $A_1 = (a_1, l_1, r_1)$ and $A_2 = (a_2, l_2, r_2)$, we obtain in the case $T \leq T_L$ (note again that this includes the case of Yager t-norms T_λ^Y with $\lambda \in [0, 1]$ because of $T_L = T_1^Y$)

$$A_1 \oplus_T A_2 = (a_1 + a_2, \max(l_1, l_2), \max(r_1, r_2)),$$

in the case of Yager t-norms T_λ^Y with $\lambda \in]1, \infty[$ we have

$$\begin{aligned} A_1 \oplus_{T_\lambda^Y} A_2 &= \\ &= a_1 + a_2, l_1^\mu + l_2^{q \frac{1}{q}}, r_1^q + r_2^{q \frac{1}{q}}, \end{aligned}$$

where $\mu = \frac{\lambda}{\lambda-1}$, and in the case $\lambda = \infty$ we are back to minimum because of $T_M = T_\infty^Y$. Therefore, an appropriate choice of the parameter $\lambda \in [1, \infty]$ of the Yager t-norm T_λ^Y allows the increase of the spreads when adding triangular fuzzy numbers to be controlled: $\lambda = 1$ corresponds to the minimal output spread (equal to the maximal input spread), and $\lambda = \infty$ leads to the maximal output spread.

Important issue in fuzzy number theory is whether fuzzy numbers are comparable. Set of fuzzy numbers can be ordered partially. The idea is to extend operations \min and \max in the sense of Zadeh's extension principle:

$$\text{MIN}(A, B)(z) = \sup_{\min(x, y)=z} \min(A(x), B(y)),$$

$$\text{MAX}(A, B)(z) = \sup_{\max(x, y)=z} \min(A(x), B(y)),$$

where it is taken for t-norm $T_M = \min$ and $*$ is \min or \max on reals. Since \min and \max are continuous operations $\text{MIN}(A, B)$ and $\text{MAX}(A, B)$ are fuzzy numbers and they are pseudo-convolutions of the second type for $\oplus = \max$ and $\odot = \min$. Properties of new operations MIN and MAX are commutativity, associativity, existence of idempotent element, absorption, distributivity.

6 Information Theory

We shall show how pseudo-convolution appears in the Information theory. The information theory based on the notion of a probability has been introduced in 1948 by Wiener and Shannon. Let (Ω, \mathcal{A}, p) be a probability space. For an event $A \in \mathcal{A}$ $J(A) = -\log p(A)$ is called information determined by realization of the event A . The mapping $J : \mathcal{A} \rightarrow [0, \infty]$ is called an information measure.

More general definition of information measure has been introduced in 1967 by Kampè de Fèriet and Forte.

Definition 7. Let (Ω, \mathcal{A}, p) be a probability space. Then the following mapping $J : \mathcal{A} \rightarrow [0, \infty]$ is called an *information measure* if it satisfy the following conditions:

(I1) $J(\Omega) = 0, J(\emptyset) = \infty$;

- (I2) $B \subset A$ implies $J(B) \geq J(A)$;
- (I3) if A and B are independent in the sense of Banach-Marczewski, then

$$J(A \cap B) = J(A) + J(B);$$
- (I4) $J(A \cup B) = F(J(A), J(B))$ whenever $A \cap B = \emptyset$ for some two-place function F ;
- (I5) $J(\bigcup_{i=1}^{\infty} A_i) = \lim_{n \rightarrow \infty} J(\bigcup_{i=1}^n A_i).$

The function F that appears in the previous definition is called a *composition law*. Usually, for F are required:

- continuity,
- symmetry ($F(x, y) = F(y, x)$),
- associativity ($F(F(x, y), z) = F(x, F(y, z))$),
- monotonicity (F is non-decreasing in both components),
- neutral element ($F(x, \infty) = x$).

In 1969 Schweizer and Sklar [34] proposed that information J should be treated as a random variable on $[0, \infty]$ instead as a non-negative real number. The idea is similar to that of Menger's generalization of metric spaces. So, we have distribution function $K(A):[0, \infty] \rightarrow [0, 1]$ that is a left-continuous non-decreasing mapping with $K(A)(0) = 0$.

Now, let $J(A)$ be a random information on $[0, \infty]$ for each $A \in \mathcal{A}$, $K(A, x)$ the probability that the information given by the realization of A is less than x . Axioms (I1)–(I5) can be rewritten in the style of Schweizer and Sklar [34]. The additivity axiom has been translated into the following form

(I4') for $A, B \in \mathcal{A}$ that $A \cap B = \emptyset$ it is $K(A \cup B) = \phi(K(A), K(B))$, where ϕ is a continuous, associative, commutative, non-decreasing two-place function on the system of distributions on $[0, \infty]$, with neutral element 0 and annihilator 1.

Let S be a continuous t-conorm. Then functions

$$\Pi_S(H, G, x) = S(H(u), G(v)), \quad \tau_S(H, G, x) = \sup_{u+v=x} S(H(u), G(v)),$$

where $u, v, x \in [0, \infty]$ and H, G are distributions on $[0, \infty]$, fulfill the required axiom. The second one is an generalized pseudo-convolution of the first type with respect to (\max, S) .

7 System Theory and Control Theory

Generalized pseudo-convolutions are important tools in the system theory as the classical convolution was (see [2, 21, 31]).

We stress here an important nonlinear PDE, so called Hamilton-Jacobi-Bellman equation

$$\frac{\partial u(x,t)}{\partial t} + H\left(\frac{\partial u}{\partial x}, x, t\right) = 0,$$

(see [21, 31]). Hamilton-Jacobi equation is specially important in the control theory. Unfortunately, usually the interesting models are represented by Hamilton-Jacobi equation in which the non-linear Hamiltonian H is not smooth, for example the absolute value, min or max operations. Hence we can not apply on such cases the classical mathematical analysis. There is so called "viscosity solution" method (see [19]) which gives upper and lower solutions but not a solution in the classical sense, i.e., that its substitution into the equation reduces the equation to the identity. Using the pseudo-analysis with generalized pseudo-convolution it is possible to obtain solutions which can be interpreted in the mentioned classical way. For more details see [21, 31].

8 Probabilistic Metric Spaces

We shall finish where somehow all started (t-norms and triangular functions). The basic notion of the theory of probabilistic metric spaces, the triangle function, is based on the pseudo-convolution of the first type.

Definition 8. A *distance distribution function* is a function F , $F : [0, \infty] \rightarrow [0, \infty]$, such that $F(0) = 0$ and $F(\infty) = 1$ and it is left continuous on $[0, \infty)$.

The family of all distance distribution functions is denoted by Δ^+ . Now we shall introduce an operation τ on Δ^+ .

Definition 9. A *triangle function* τ is a binary operation on Δ^+ that is commutative, associative and non-decreasing in each place, and has ε_0 as identity, where

$$\varepsilon_0(x) = \begin{cases} 0 & x = 0, \\ 1 & 0 < x \leq \infty. \end{cases}$$

The following definition introduce the basic space (see [11, 35]).

Definition 10. A probabilistic metric space is a triple $(M, \mathcal{F} \Leftrightarrow \tau)$ where M is a nonempty set, $\mathcal{F}: M^2 \rightarrow \Delta^+$ is given by $(p, q) \mapsto F_{pq}$, τ is a triangle function, such that the following conditions are satisfied for all $p, q, r \in M$

- (i) $F_{pp} = \varepsilon_0$; (ii) $F_{pq} \neq \varepsilon_0$ for $p \neq q$; (iii) $F_{pq} = F_{qp}$; (iv) $F_{pr} \geq \tau(F_{pq}, F_{qr})$.

Let $F, H \in \Delta^+$ and $u, v, x \in [0, \infty]$. Taking for triangle function $\tau = \tau_T$, where

$$\tau_T(F, H)(x) = \sup \{T(F(u), H(v)) \mid u + v = x\},$$

(generalized pseudo-convolution of the first type with respect to (\max, T) and $* = +$) for a left continuous t -norm T we obtain a special important probabilistic metric space, the Menger space. The fact that function τ_T is triangle function yields from Theorem 3.

It is important to obtain rich source for different triangle functions which would enable the construction of new probabilistic metric spaces. One of the useful construction goes in the following way.

Definition 11. \mathcal{L} is the class of all binary operators L on $[0, \infty[$ which satisfy the following conditions

- (i) L maps $[0, \infty[^2$ onto $[0, \infty[$;
- (ii) L is non-decreasing in both coordinate;
- (iii) L is continuous on $[0, \infty[^2$ (except possibly at the points $(0, \infty)$ and $(\infty, 0)$).

We introduce now, using the family \mathcal{L} the following binary operation on Δ^+ .

Definition 12. For a t-norm T and $L \in \mathcal{L}$, a function $\tau_{T,L}$ defined on $(\Delta^+)^2$ and with values in $[0, \infty[$ is given by

$$\tau_{T,L}(F, G)(x) = \sup \{T(F(u), G(v)) \mid L(u, v) = x\}.$$

In a special case $L(x, y) = x + y$, we obtain $\tau_{T,L} = \tau_T$.

The following theorem guarantees under mild conditions the triangularity of $\tau_{T,L}$ (see [35]).

Theorem 4. If T is left continuous t-norm and L from \mathcal{L} is commutative, associative, has 0 as identity and satisfy the condition

- if $u_1 < u_2$ and $v_1 < v_2$, then $L(u_1, v_1) < L(u_2, v_2)$,
- then $\tau_{T,L}$ is a triangle function.

Condition (5) is weaker than strictly increasingness of L in each place. So \min and \max satisfies it, although they are not strictly increasing in each place.

Example 9. $\tau_{T,\max}$ is a triangle function for any left continuous t-norm T .

It can be proved in a similar way for $\oplus = \min$ and $\odot = S$, where S is continuous t-conorm that functions

$$\tau_S(F, H)(x) = \inf \{S(F(u), H(v)) \mid u + v = x\},$$

$$\tau_{S,L}(F, H)(x) = \inf \{S(F(u), H(v)) \mid L(u, v) = x\}$$

are triangular functions (binary operation L has all properties from previous theorem and $F, H \in \Delta^+$).

Example 10. $\tau_{S,\min}$ is a triangle function for any continuous t-conorm S .

Many nonlinear equations under uncertainty, e.g., random equations, can be solved with fixed point methods in probabilistic metric spaces, see [11].

Conclusion

We have shown the usefulness of generalized real analysis, so called pseudo-analysis in soft computing, specially in the theory fuzzy sets and fuzzy logics, fuzzy neural nets, and related fields as information theory, system theory, control theory, probabilistic metric spaces. We have discussed some situations in fuzzy set theory where triangular norms different from T_M allow a more appropriate model of the investigated event. The concepts based on T_M can be viewed as "worst case scenarios" in the sense that, whenever a T_M -based model works, then also a general T -based model is appropriate.

References

- [1] Aczel, J.: Lectures on Functional Equations and their Applications. Academic Press, New York (1966)
- [2] Baccelli, F., Cohen, G., Olsder, G.J.: Quadrat: Synchronization and Linearity: an Algebra for Discrete Event Systems. John-Wiley and Sons, New York (1992)
- [3] Bellman, R.E., Dreyfus, S.E.: Applied Dynamic Programming. Princeton University Press, Princeton (1962)
- [4] Cuninghame-Green, R.A.: Minimax Algebra. Lecture Notes in Economics and Math. Systems, vol. 166. Springer, Heidelberg (1979)
- [5] Dubois, D., Kerre, E., Mesiar, R., Prade, H.: Fuzzy Interval Analysis. The Handbook of Fuzzy Sets Series, pp. 483–582. Kluwer Academic Publishers, Boston (2000)

- [6] Dubois, D., Prade, H.: Additions of Interactive Fuzzy Numbers. *IEEE Trans. Automat. Control.* 26, 926–936 (1981)
- [7] Dubois, D., Prade, H.: A Class of Fuzzy Measures Based on Triangular Norms. *Internat. J. Gen. System* 8, 43–61 (1982)
- [8] Golan, J.S.: The Theory of Semirings with Applications in Mathematics and Theoretical Computer Sciences. Pitman Monog. and Surveys in Pure and Appl. Maths, vol. 54. Longman, New York (1992)
- [9] Gottwald, S.: Characterizations of the Solvability of Fuzzy Equations. *Elektron. Informationsverarb. Kybernetik EIK* 22, 67–91 (1986)
- [10] Grabisch, G., Marichal, J.L., Mesiar, R., Pap, E.: Aggregation Functions. Cambridge University Press, Cambridge (2009)
- [11] Hadžić, O., Pap, E.: Fixed Point Theory in Probabilistic Metric Spaces. Mathematics and Its Applications, vol. 536. Kluwer Academic Publishers, Dordrecht (2001)
- [12] Hajek, P.: Metamathematics of Fuzzy Logic. Kluwer Academic Publishers, Dordrecht (1998)
- [13] Klement, E.P., Mesiar, R., Pap, E.: On the Relationship of Associative Compensatory Operators to Triangular Norms and Conorms. *Inter. J. Uncertainty, Fuzziness and Knowledge Based Systems* 4, 129–144 (1996)
- [14] Klement, E.P., Mesiar, R., Pap, E.: Triangular Norms. Kluwer Academic Publisher, Dordrecht (2000)
- [15] Klement, E.P., Mesiar, R., Pap, E.: Fuzzy Set Theory: "AND" is More Just the Minimum. In: Hryniwicz, O., Kacprzyk, J., Kuchta, D. (eds.) *Issues in Soft Computing Decisions and Operation Research*, Akademicka Oficyna Wydawnicza EXIT, Warsaw, pp. 39–52 (2005)
- [16] Klir, G.J., Folger, T.A.: Fuzzy Sets, Uncertainty, and Information. Prentice-Hall International, Inc., Englewood Cliffs (1992)
- [17] Kolesarova, A.: Triangular Norm-based Addition of Linear Fuzzy Numbers. *Tatra Mt. Math. Publ.* 6, 75–81 (1995)
- [18] Kuich, W.: Semirings, Automata, Languages. Springer, Berlin (1986)
- [19] Lions, P.L.: Generalized Solutions of Hamilton-Jacobi Equations. Pitman, London (1982)
- [20] Maslov, V.P.: On a New Superposition Principle in Optimization Theory. *Uspehi mat. nauk* 42, 39–48 (1987)
- [21] Maslov, V.P., Samborskij, S.N. (eds.): Idempotent Analysis. Advances in Soviet Mathematics, vol. 13. Amer. Math. Soc., Providence, Rhode Island (1992)
- [22] Mesiar, R.: Choquet-like integrals. *J. Math. Anal. Appl.* 194, 477–488 (1995)
- [23] Murofushi, T., Sugeno, M.: Fuzzy t-conorm Integrals with Respect to Fuzzy Measures: Generalization of Sugeno Integral and Choquet Integral. *Fuzzy Sets and Systems* 42, 57–71 (1991)
- [24] Nauck, D., Klawonn, F., Kruse, R.: Neuronale Netze und Fuzzy- Systeme. Vieweg, Braunschweig (1994)
- [25] Pap, E.: Integral Generated by Decomposable Measure. *Univ. u Novom Sadu Zb. Rad. Prirod.-Mat. Fak. Ser. Mat.* 20(1), 135–144 (1990)
- [26] Pap, E.: g -calculus. *Univ. u Novom Sadu Zb. Rad. Prirod. Mat. Fak. Ser. Mat.* 23(1), 145–150 (1993)
- [27] Pap, E.: Null-Additive Set Functions. Kluwer Academic Publishers, Dordrecht (1995)
- [28] Pap, E.: Pseudo-Analysis as a Mathematical Base for Soft Computing. *Soft Computing* 1, 61–68 (1997)
- [29] Pap, E.: Pseudo-Additive Measures and Their Applications. In: Pap, E. (ed.) *Handbook of Measure Theory*, pp. 1403–1465. Elsevier, Amsterdam (2002)

- [30] Pap, E., Štajner, I.: Generalized Pseudo-Convolution in the Theory of Probabilistic Metric Spaces, Information, Fuzzy Numbers, System Theory. *Fuzzy Sets and Systems* 102, 393–415 (1999)
- [31] Pap, E., Ralevic, N.: Pseudo-Laplace Transform. *Nonlinear Analysis* 33, 533–550 (1998)
- [32] Pedrycz, W.: Fuzzy Control and Fuzzy Systems. Technical report 82 14, Delft University of Technology, Department of Mathematics (1982)
- [33] Sanchez, E.: Solution of Fuzzy Equations with Extended Operations. *Fuzzy Sets and Systems* 12, 237–248 (1984)
- [34] Schweizer, B., Sklar, A.: Measures aleatoires de l'information. *C. R. Acad. Sci. Paris Ser. A* 269, 721–723 (1969)
- [35] Schweizer, B., Sklar, A.: Probabilistic Metric Spaces. North-Holland, Amsterdam (1983)
- [36] Sugeno, M., Murofushi, T.: Pseudo-additive measures and integrals. *J. Math. Anal. Appl.* 122, 197–222 (1987)
- [37] Trillas, E.: Sobre funciones de negacion en la teora de conjuntos difusos. *Stochastica* 3, 47–60 (1979)
- [38] Wang, Z., Klir, G.J.: Fuzzy Measure Theory. Plenum Press, New York (1992)
- [39] Weber, S.: \perp -Decomposable Measures and Integrals Archimedian t-conorm. *J. Math. Anal. Appl.* 101, 114–138 (1984)
- [40] Yager, R.R., Rybalov, A.: Uninorm Aggregation Operators. *Fuzzy Sets and Systems* 80, 111–121 (1996)
- [41] Zadeh, L.A.: Fuzzy Sets. *Inform. and Control* 8, 338–353 (1965)

Aggregation Functions in Fuzzy Systems

János Fodor

Budapest Tech
Bécsi út 96/B, H-1034 Budapest, Hungary
fodor@bmf.hu

Abstract. Aggregation of information represented by membership functions is a central matter in intelligent systems where fuzzy rule base and reasoning mechanism are applied. Typical examples of such systems consist of, but not limited to, fuzzy control, decision support and expert systems. In most cases, the aggregation operators are defined on a pure axiomatic basis and are interpreted either as logical connectives (such as t-norms and t-conorms) or as averaging operators allowing a compensation effect (such as the arithmetic mean). On the other hand, it can be observed by some empirical tests that the above-mentioned classes of operators differ from those ones that people use in practice. Therefore, it is important to find operators that are, in a sense, mixtures of the previous ones, and allow some degree of compensation. This chapter summarizes fundamental as well as non-conventional classes of aggregation functions for fuzzy information. This includes, but is not limited to, the class of uninorms and nullnorms, absorbing norms, distance- and entropy-based operators, quasi-conjunctions and nonstrict means.

1 Introduction

Soft computing is oriented towards the analysis and design of intelligent systems. It is based on fuzzy logic, artificial neural networks and evolutionary computation. Fuzzy logic is mainly concerned with imprecision and approximate reasoning, neural networks mainly with learning and curve fitting, while evolutionary computation with searching and optimization. Constituents of soft computing are complementary rather than competitive.

In a narrow sense, fuzzy logic is a logical system that aims at a formalization of approximate reasoning. As such, it is rooted in multi-valued logic, but its agenda is quite different from that of traditional multi-valued logical system. Many of its concepts are not a part of traditional multi-valued logic (e.g. linguistic variable, fuzzy if-then rule, fuzzy quantifier). In a broad sense, fuzzy logic is almost synonymous with fuzzy set theory – a theory of classes with unsharp boundaries.

Most concepts dealt with or described in our world are fuzzy. Fuzziness refers to nonstatistical imprecision, approximation and vagueness in information and data. In classical logic, known also as crisp or Boolean logic, an element either *is* or *is not* a member of a set (membership degree either equals 1 or 0). In a fuzzy set, membership values (typically numbers from the closed unit interval) reflect the membership grades of the elements in the set.

The problem of aggregating information represented by membership functions (i.e., by fuzzy sets) in a meaningful way has been of central interest since the late 1970s. In most cases, the aggregation operators are defined on a pure axiomatic basis and are interpreted either as logical connectives (such as t-norms and t-conorms) or as averaging operators allowing a compensation effect (such as the arithmetic mean).

It can also be recognized by some empirical tests that the above-mentioned classes of aggregations differ from those ones that people use in practice (see [31]). Therefore, it is important to find aggregation functions that are, in a sense, mixtures of the previous ones, and allow some degree of compensation.

One can also discern that people are inclined to use standard classes of aggregation operators also as a matter of routine. For example, when one works with binary conjunctions and there is no need to extend them for three or more arguments, as it happens e.g. in the inference pattern called generalized modus ponens, associativity of the conjunction is an unnecessarily restrictive condition. The same is valid for the commutativity property if the two arguments have different semantical backgrounds and it has no sense to interchange one with the other.

The present paper intends to give an overview of fundamental as well as non-conventional classes of aggregation functions for fuzzy information. First we briefly consider essential properties of aggregation functions individually. Then we formulate consistent aggregation as it is usual in the literature. Consistency indicates a functional equation for the aggregation functions involved. We summarize some fundamental results on solutions of particular forms of these equations under some additional properties of the aggregations functions. We show also some non-conventional aggregation functions such as distance-based or entropy-based aggregations.

2 Fundamental Properties of Aggregation Functions

Since membership values are just real numbers from the closed unit interval, we restrict ourselves to the study of functions $F_{(n)}$ from $[0,1]^n$ to $[0,1]$, where n is a positive integer. Any n -ary aggregation function must be such a mapping, owning additional properties as well. Since the number n of input values can be arbitrary, an aggregation operator is a mapping

$$\mathbf{F} : \bigcup_{n \in \mathbb{N}} [0, 1]^n \rightarrow [0, 1].$$

In other words, it is a family of n -ary aggregation functions for all positive integer n . The aggregation of a single value must be equal to that value, so we must have $\mathbf{F}(x) = x$ for all $x \in [0, 1]$.

2.1 Basic Mathematical Properties

Now we consider some fundamental properties that an aggregation function may possess. In general, when we consider an aggregation function we simply write F and omit the subscript (n) , unless otherwise stated. When $n = 2$, aggregation functions are alternatively called binary *operations* or *operators*, emphasizing the strong algebraic background behind them.

Boundary conditions. Let $F : [0, 1]^n \rightarrow [0, 1]$ be a function. When all the inputs equal either 0 or 1, the aggregated value must be the same boundary value. That is, F must satisfy the *boundary conditions*

$$F(0, \dots, 0) = 0 \text{ and } F(1, \dots, 1) = 1. \quad (1)$$

Monotonicity. A function $F : [0, 1]^n \rightarrow [0, 1]$ is called *increasing* (non-decreasing) if

$$x_1 \leq y_1, \dots, x_n \leq y_n \text{ imply } F(x_1, \dots, x_n) \leq F(y_1, \dots, y_n). \quad (2)$$

An increasing function F is called *strictly increasing* if, in addition to (2), $(x_1, \dots, x_n) \neq (y_1, \dots, y_n)$ implies $F(x_1, \dots, x_n) < F(y_1, \dots, y_n)$.

Idempotency. Consider a function $F : [0, 1]^n \rightarrow [0, 1]$. An element $x \in [0, 1]$ is called an *idempotent element* of F if $F(x, \dots, x) = x$. We call F an *idempotent function* if each $x \in [0, 1]$ is an idempotent element of F . Notice that an increasing and idempotent function is *compensatory*: it satisfies the inequality

$$\min(x_1, \dots, x_n) \leq F(x_1, \dots, x_n) \leq \max(x_1, \dots, x_n).$$

Symmetry. A function $F : [0,1]^n \rightarrow [0,1]$ is called *symmetric* if the function value does not depend on the ordering of inputs. More formally, if $\pi = (\pi(1), \dots, \pi(n))$ is a permutation of $(1, \dots, n)$, then F must satisfy

$$F(x_1, \dots, x_n) = F(x_{\pi(1)}, \dots, x_{\pi(n)}).$$

When $n = 2$, symmetry is also called *commutativity*.

Continuity. In applications continuity of functions is a required property. It guarantees that a small change in the input does not cause dramatic change in the output. More formally, a function $F : [0,1]^n \rightarrow [0,1]$ is called *continuous* if for all $x_1, \dots, x_n \in [0,1]$ and for all $\{x_{1j}\}_{j \in \mathbb{N}}, \dots, \{x_{nj}\}_{j \in \mathbb{N}} \in [0,1]^\mathbb{N}$ we have

$$\left(\lim_{j \rightarrow \infty} x_{ij} = x_i, \text{ for } i = 1, \dots, n \right) \Rightarrow \lim_{j \rightarrow \infty} F(x_{1j}, \dots, x_{nj}) = F(x_1, \dots, x_n).$$

Because $[0,1]^n$ – the domain of F – is a compact set, continuity of F is equivalent to its *uniform continuity*.

If someone wants to define the broadest possible class of functions to be considered as aggregations, there are two inevitable properties that such functions must satisfy. This is formulated in the next definition.

Definition 1. A function $F : [0,1]^n \rightarrow [0,1]$ is called an *aggregation function* if it satisfies the boundary conditions (1) and it is increasing (2).

2.2 Consistency

The problem of *consistent aggregation* was posed by Klein [20] and, for ease of exposition, is formulated as follows, and is illustrated in Figure 1.

There are n inputs that contribute to the outputs of m producers. The j^{th} producer's output depends upon the inputs x_{j1}, \dots, x_{jn} to that producer through possibly producer-specific (microeconomic) production functions F_j ($j = 1, \dots, m$). The question is, do there exist aggregation functions for the outputs (G) and for each kind of inputs (G_k ; $k = 1, \dots, n$) so that the aggregated output depend only upon the n aggregated inputs through a macroeconomic function F .

$$\begin{array}{llll}
 x_{11} \dots x_{1k} \dots x_{1n} & F_1 \longrightarrow y_1 \\
 \vdots & \vdots & \vdots & \vdots \\
 x_{j1} \dots x_{jk} \dots x_{jn} & F_j \longrightarrow y_j \\
 \vdots & \vdots & \vdots & \vdots \\
 x_{m1} \dots x_{mk} \dots x_{mn} & F_m \longrightarrow y_m
 \end{array}$$

$$\begin{array}{ccccc}
 G_1 & G_k & G_n & & G \\
 \downarrow & \downarrow & \downarrow & & \downarrow \\
 z_1 \dots z_k \dots z_n & F \longrightarrow u
 \end{array}$$

Fig. 1. Scheme of consistent aggregation

We get the functional equation of $m \times n$ rectangular *generalized bisymmetry* that defines consistency of the aggregation procedure:

$$G(F_1(x_{11}, \dots, x_{1n}), \dots, F_m(x_{m1}, \dots, x_{mn})) = F(G_1(x_{11}, \dots, x_{m1}), \dots, G_n(x_{1n}, \dots, x_{mn})). \quad (3)$$

Note that several district problems may lead to (particular forms of) this equation; see e.g. [11, 15]. We consider two of them now: associativity and bisymmetry.

Associativity. A function $F : [0,1] \times [0,1] \rightarrow [0,1]$ is called *associative* if

$$F(x, F(y, z)) = F(F(x, y), z), \quad x, y, z \in [0,1]. \quad (4)$$

From aggregation point of view, associativity is an excellent "tool" for extending a binary function to an n -ary one.

Bisymmetry. A function $F : [0,1] \times [0,1] \rightarrow [0,1]$ is called *bisymmetric* if it satisfies

$$F(F(x, y), F(u, v)) = F(F(x, u), F(y, v)), \quad (5)$$

for all $x, y, u, v \in [0,1]$. The property was introduced by Aczél in [1]. It is easy to see that if a function $F : [0,1] \times [0,1] \rightarrow [0,1]$ is symmetric and associative then F is bisymmetric. The converse statement is not true in general. If, however, F is symmetric and has a neutral element, then bisymmetry of F implies that F is associative [27].

3 Traditional Operations

The original fuzzy set theory was formulated in terms of Zadeh's standard operations of intersection, union and complement. The axiomatic skeleton used for characterizing fuzzy intersection and fuzzy union are known as *triangular norms* (*t-norms*) and *triangular conorms* (*t-conorms*), respectively. For more details we refer to the books [16] and [22].

3.1 Triangular Norms and Conorms

Definition 2. A *triangular norm* (shortly: a *t-norm*) is a function $T : [0,1]^2 \rightarrow [0,1]$ which is associative, increasing and commutative, and satisfies the boundary condition $T(1, x) = x$ for all $x \in [0,1]$.

Definition 3. A *triangular conorm* (shortly: a *t-conorm*) is an associative, commutative, increasing $S : [0,1]^2 \rightarrow [0,1]$ function, with boundary condition $S(0, x) = x$ for all $x \in [0,1]$.

Notice that continuity of a t-norm and a t-conorm is not taken for granted.

The following are the four basic t-norms, namely, the minimum T_M , the product T_P , the Łukasiewicz t-norm T_L , and the drastic product T_D , which are given by, respectively:

$$\begin{aligned} T_M(x, y) &= \min(x, y), \\ T_P(x, y) &= x \cdot y, \\ T_L(x, y) &= \max(x + y - 1, 0), \\ T_D(x, y) &= \begin{cases} 0 & \text{if } (x, y) \in [0,1]^2, \\ \min(x, y) & \text{otherwise.} \end{cases} \end{aligned}$$

These four basic t-norms have some remarkable properties. The drastic product T_D and the minimum T_M are the smallest and the largest t-norm, respectively. The minimum T_M is the only t-norm where each $x \in [0,1]$ is an idempotent element. The product T_P and the Łukasiewicz t-norm T_L are prototypical examples of two important subclasses of t-norms (of strict and nilpotent t-norms, respectively).

Definition 4. A non-increasing function $N : [0,1] \rightarrow [0,1]$ satisfying $N(0) = 1$, $N(1) = 0$ is called a *negation*. A negation N is called *strict* if N is strictly decreasing and continuous. A strict negation N is said to be a *strong negation* if N is also involutive: $N(N(x)) = x$ for all $x \in [0,1]$.

The standard negation is simply $N_s(x) = 1 - x$, $x \in [0,1]$. Clearly, this negation is strong. It plays a key role in the representation of strong negations.

We call a continuous, strictly increasing function $\varphi : [0,1] \rightarrow [0,1]$ with $\varphi(0) = 0$, $\varphi(1) = 1$ an *automorphism* of the unit interval.

Note that $N : [0,1] \rightarrow [0,1]$ is a strong negation if and only if there is an automorphism φ of the unit interval such that for all $x \in [0,1]$ we have

$$N(x) = \varphi^{-1}(N_s(\varphi(x))).$$

In what follows we assume that T is a t-norm, S is a t-conorm and N is a strong negation.

Clearly, for every t-norm T and strong negation N , the operation S defined by

$$S(x, y) = N(T(N(x), N(y))), \quad x, y \in [0,1]$$

is a t-conorm. In addition, $T(x, y) = N(S(N(x), N(y)))$ ($x, y \in [0,1]$). In this case S and T are called N -duals. In case of the standard negation (i.e., when $N(x) = 1 - x$ for $x \in [0,1]$) we simply speak about duals. Obviously, equality (6) expresses the De Morgan's law in the fuzzy case.

Generally, for any t-norm T and t-conorm S we have

$$T_D(x, y) \leq T(x, y) \leq T_M(x, y)$$

and

$$S_M(x, y) \leq S(x, y) \leq S_D(x, y),$$

where S_M is the dual of T_M , and S_D is the dual of T_D .

These inequalities are important from practical point of view as they establish the boundaries of the possible range of mappings T and S .

Between the four basic t-norms we have these strict inequalities:

$$T_{\mathbf{D}} < T_{\mathbf{P}} < T_{\mathbf{L}} < T_{\mathbf{M}}.$$

Further various aspects of t-norms and related operations can be found in the fundamental book [20].

4 Recent Associative and Commutative Operations

4.1 Uninorms and Nullnorms

4.1.1 Uninorms

Uninorms were introduced by Yager and Rybalov [29] as a generalization of t-norms and t-conorms. For uninorms, the neutral element is not forced to be either 0 or 1, but can be any value in the unit interval.

Definition 5. [29] A uninorm U is a commutative, associative and increasing binary operator with a neutral element $e \in [0,1]$, i.e., for all $x \in [0,1]$ we have $U(x,e) = x$.

T-norms do not allow low values to be compensated by high values, while t-conorms do not allow high values to be compensated by low values. Uninorms may allow values separated by their neutral element to be aggregated in a compensating way. The structure of uninorms was studied by Fodor *et al.* [17]. For a uninorm U with neutral element $e \in]0,1[$, the binary operator T_U defined by

$$T_U(x,y) = \frac{U(ex,ey)}{e}$$

is a t-norm; for a uninorm U with neutral element $e \in [0,1[$, the binary operator S_U defined by

$$S_U(x,y) = \frac{U(e + (1-e)x, e + (1-e)y) - e}{1 - e}$$

is a t-conorm. The structure of a uninorm with neutral element $e \in]0,1[$ on the squares $[0,e]^2$ and $[e,1]^2$ is therefore closely related to t-norms and t-conorms. For $e \in]0,1[$, we denote by ϕ_e and ψ_e the linear transformations defined by

$\phi_e(x) = \frac{x}{e}$ and $\psi_e(x) = \frac{x-e}{1-e}$. To any uninorm U with neutral element $e \in]0, 1[$, there corresponds a t-norm T and a t-conorm S such that:

- (i) for any $(x, y) \in [0, e]^2$: $U(x, y) = \phi_e^{-1}(T(\phi_e(x), \phi_e(y)))$;
- (ii) for any $(x, y) \in [e, 1]^2$: $U(x, y) = \psi_e^{-1}(S(\psi_e(x), \psi_e(y)))$.

On the remaining part of the unit square, i.e. on $E = ([0, e[\times]e, 1]) \cup (]e, 1] \times [0, e[)$, it satisfies

$$\min(x, y) \leq U(x, y) \leq \max(x, y),$$

and could therefore partially show a compensating behaviour, i.e. take values strictly between minimum and maximum. Note that any uninorm U is either *conjunctive*, i.e. $U(0, 1) = U(1, 0) = 0$, or *disjunctive*, i.e. $U(0, 1) = U(1, 0) = 1$.

4.1.2 Representation of Uninorms

In analogy to the representation of continuous Archimedean t-norms and t-conorms in terms of additive generators, Fodor *et al.* [17] have investigated the existence of uninorms with a similar representation in terms of a single-variable function. This search leads back to Dombi's class of *aggregative operators* [10]. This work is also closely related to that of Klement *et al.* on associative compensatory operators [21].

Consider $e \in]0, 1[$ and a strictly increasing continuous $[0, 1] \rightarrow \overline{\mathbb{R}}$ mapping h with $h(0) = -\infty$, $h(e) = 0$ and $h(1) = +\infty$. The binary operator U defined by

$$U(x, y) = h^{-1}(h(x) + h(y))$$

for any $(x, y) \in [0, 1]^2 \setminus \{(0, 1), (1, 0)\}$, and either $U(0, 1) = U(1, 0) = 0$ or $U(0, 1) = U(1, 0) = 1$, is a uninorm with neutral element e . The class of uninorms that can be constructed in this way has been characterized [17].

Consider a uninorm U with neutral element $e \in]0, 1[$, then there exists a strictly increasing continuous $[0, 1] \rightarrow \overline{\mathbb{R}}$ mapping h with $h(0) = -\infty$, $h(e) = 0$ and $h(1) = +\infty$ such that

$$U(x, y) = h^{-1}(h(x) + h(y))$$

for any $(x, y) \in [0, 1]^2 \setminus \{(0, 1), (1, 0)\}$ if and only if

- (i) U is strictly increasing and continuous on $]0, 1[^2$;
- (ii) there exists an involutive negator N with fixpoint e such that

$$U(x, y) = N(U(N(x), N(y))))$$

for any $(x, y) \in [0, 1]^2 \setminus \{(0, 1), (1, 0)\}$.

The uninorms characterized above are called *representable* uninorms. The mapping h is called an *additive generator* of U . The involutive negator corresponding to a representable uninorm U with additive generator h , as mentioned in condition (ii) above, is denoted N_U and is given by

$$N_U(x) = h^{-1}(-h(x)). \quad (7)$$

Clearly, any representable uninorm comes in a conjunctive and a disjunctive version, i.e. there always exist two representable uninorms that only differ in the points $(0, 1)$ and $(1, 0)$. Representable uninorms are almost continuous, i.e. continuous except in $(0, 1)$ and $(1, 0)$, and Archimedean, in the sense that $(\forall x \in]0, e[)(U(x, x) < x)$ and $(\forall x \in]e, 1[)(U(x, x) > x)$. Clearly, representable uninorms are not idempotent. A very important fact is that the underlying t-norm and t-conorm of a representable uninorm must be strict and cannot be nilpotent. Moreover, given a strict t-norm T with decreasing additive generator f and a strict t-conorm S with increasing additive generator g , we can always construct a representable uninorm U with desired neutral element $e \in]0, 1[$ that has T and S as underlying t-norm and t-conorm. It suffices to consider as additive generator the mapping h defined by

$$h(x) = \begin{cases} -f\left(\frac{x}{e}\right) & , \text{if } x \leq e \\ g\left(\frac{x-e}{1-e}\right) & , \text{if } x \geq e \end{cases}. \quad (8)$$

On the other hand, the following property indicates that representable uninorms are in some sense also generalizations of nilpotent t-norms and nilpotent t-conorms: $(\forall x \in [0, 1])(U(x, N_U(x)) = N_U(e))$. This claim is further supported by studying the residual operators of representable uninorms in [9].

As an example of the representable case, consider the additive generator h defined by $h(x) = \log \frac{x}{1-x}$, then the corresponding conjunctive representable uninorm U is given by $U(x, y) = 0$ if $(x, y) \in \{(1, 0), (0, 1)\}$, and

$$U(x, y) = \frac{xy}{(1-x)(1-y) + xy}$$

otherwise, and has as neutral element $\frac{1}{2}$. Note that N_U is the standard negator: $N_U(x) = 1 - x$.

The class of representable uninorms contains famous operators, such as the functions for combining certainty factors in the expert systems MYCIN (see [28, 8]) and PROSPECTOR [8]. The MYCIN expert system was one of the first systems capable of reasoning under uncertainty [5]. To that end, certainty factors were introduced as numbers in the interval $[-1, 1]$. Essential in the processing of these certainty factors is the modified combining function C proposed by van Melle [5]. The $[-1, 1]^2 \rightarrow [-1, 1]$ mapping C is defined by

$$C(x, y) = \begin{cases} x + y(1-x) & , \text{ if } \min(x, y) \geq 0 \\ x + y(1+x) & , \text{ if } \max(x, y) \leq 0 \\ \frac{x+y}{1-\min(|x|, |y|)} & , \text{ otherwise .} \end{cases}$$

The definition of C is not clear in the points $(-1, 1)$ and $(1, -1)$, though it is understood that $C(-1, 1) = C(1, -1) = -1$. Rescaling the function C to a binary operator on $[0, 1]$, we obtain a representable uninorm with neutral element $\frac{1}{2}$ and as underlying t-norm and t-conorm the product and the probabilistic sum. Implicitly, these results are contained in the book of Hájek *et al.* [19], in the context of ordered Abelian groups.

4.1.3 Nullnorms

Triangular norms and conorms possess absorbing elements: we have $T(x, 0) = 0$ and $S(x, 1) = 1$ for all $x \in [0, 1]$. We can introduce aggregation functions with absorbing elements lying anywhere in the unit interval as follows.

Definition 6. [6] A nullnorm V is a commutative, associative and increasing binary operator with an absorbing element $a \in [0, 1]$, i.e. $(\forall x \in [0, 1])(V(x, a) = a)$, and that satisfies

$$(\forall x \in [0, a])(V(x, 0) = x) \quad (9)$$

$$(\forall x \in [a, 1])(V(x, 1) = x) \quad (10)$$

The absorbing element a corresponding to a nullnorm V is clearly unique. By definition, the case $a = 0$ leads back to t-norms, while the case $a = 1$ leads back to t-conorms. In the following proposition, we show that the structure of a nullnorm is similar to that of a uninorm. In particular, it can be shown that it is built up from a t-norm, a t-conorm and the absorbing element [6].

Theorem 1. Consider $a \in [0, 1]$. A binary operator V is a nullnorm with absorbing element a if and only if

- (i) if $a = 0$: V is a t-norm;
- (ii) if $0 < a < 1$: there exists a t-norm T_V and a t-conorm S_V such that $V(x, y)$ is given by

$$\begin{cases} \phi_a^{-1}(S_V(\phi_a(x), \phi_a(y))), & \text{if } (x, y) \in [0, a]^2 \\ \psi_a^{-1}(T_V(\psi_a(x), \psi_a(y))), & \text{if } (x, y) \in [a, 1]^2 \\ a, & \text{elsewhere} \end{cases} \quad (11)$$

- (iii) if $a = 1$: V is a t-conorm.

Recall that for any t-norm T and t-conorm S it holds that $T(x, y) \leq \min(x, y) \leq \max(x, y) \leq S(x, y)$, for all $(x, y) \in [0, 1]^2$. Hence, for a nullnorm V with absorbing element a it holds that $(\forall (x, y) \in [0, a]^2)(V(x, y) \geq \max(x, y))$ and $(\forall (x, y) \in [a, 1]^2)(V(x, y) \leq \min(x, y))$. Clearly, for any nullnorm V with absorbing element a it holds for all $x \in [0, 1]$ that

$$V(x, 0) = \min(x, a) \text{ and } V(x, 1) = \max(x, a). \quad (12)$$

Notice that, without the additional conditions (9) and (10), it cannot be shown that a commutative, associative and increasing binary operator V with absorbing element a behaves as a t-conorm and t-norm on the squares $[0, a]^2$ and $[a, 1]^2$.

Nullnorms are a generalization of the well-known *median* studied by Fung and Fu [18], which corresponds to the case $T = \min$ and $S = \max$. For a more general treatment of this operator, we refer to [13]. We recall here the characterization of that median as given by Czogala and Drewniak [7]. Firstly, they observe that an idempotent, associative and increasing binary operator O has as absorbing element $a \in [0,1]$ if and only if $O(0,1) = O(1,0) = a$. Then the following theorem can be proven.

Theorem 2. [7] Consider $a \in [0,1]$. A continuous, idempotent, associative and increasing binary operator O satisfies $O(0,1) = O(1,0) = a$ if and only if it is given by

$$O(x,y) = \begin{cases} \max(x,y), & \text{if } (x,y) \in [0,a]^2 \\ \min(x,y), & \text{if } (x,y) \in [a,1]^2 \\ a, & \text{elsewhere} \end{cases}$$

Nullnorms are also a special case of the class of T - S aggregation functions introduced and studied by Fodor and Calvo [fodcal98].

Definition 7. Consider a continuous t-norm T and a continuous t-conorm S . A binary operator F is called *T - S aggregation function* if it is increasing and commutative, and satisfies the boundary conditions

$$\begin{aligned} (\forall x \in [0,1]) (F(x,0) = T(F(1,0),x)) \\ (\forall x \in [0,1]) (F(x,1) = S(F(1,0),x)). \end{aligned}$$

When T is the algebraic product and S is the probabilistic sum, we recover the class of aggregation functions studied by Mayor and Trillas [25]. Rephrasing a result of Fodor and Calvo, we can state that the class of associative T - S aggregation functions coincides with the class of nullnorms with underlying t-norm T and t-conorm S .

5 Generalized Conjunctions and Disjunctions

5.1 The Role of Commutativity and Associativity

One possible way of simplification of axiom skeletons of t-norms and t-conorms may be not requiring that these operations have the commutative and the associative properties. Non-commutative and non-associative operations are widely used in mathematics, so, why do we restrict our investigations by keeping these axioms? What are the requirements of the most typical applications?

From theoretical point of view the commutative law is not required, while the associative law is necessary to extend the operation to more than two variables. In applications, like fuzzy logic control, fuzzy expert systems and fuzzy systems modeling fuzzy rule base and fuzzy inference mechanism are used, where the information aggregation is performed by operations. The inference procedures do not always require commutative and associative laws of the operations used in these procedures. These properties are not necessary for conjunction operations used in the simplest fuzzy controllers with two inputs and one output. For rules with greater number of inputs and outputs these properties are also not required if the sequence of variables in the rules are fixed.

Moreover, non-commutativity of a conjunction may in fact be desirable for rules because it can reflect different influences of the input variables on the output of the system. For example, in fuzzy control, the positions of the input variables the "error" and the "change in error" in rules are usually fixed and these variables have different influences on the output of the system. In the application areas of fuzzy models when the sequence of operands is not fixed, the property of non-commutativity may not be desirable. Later some examples will be given for parametric non-commutative and non-associative operations.

The axiom systems of t-norms and t-conorms are very similar to each other except the neutral element, i.e. the type is characterized by the neutral element. If the neutral element is equal to 1 then the operation is a conjunction type, while if the neutral element is zero the disjunction operation is obtained. By using these properties, the concepts of conjunction and disjunction operations were introduced in [4].

Definition 8. Let T be a mapping $T : [0, 1] \times [0, 1] \rightarrow [0, 1]$. T is a *conjunction operation* if $T(x, 1) = x$ for all $x \in [0, 1]$.

Definition 9. Let S be a mapping $S : [0, 1] \times [0, 1] \rightarrow [0, 1]$. S is a *disjunction operation* if $S(x, 0) = x$ for all $x \in [0, 1]$.

Conjunction and disjunction operations may also be obtained one from another by means of an involutive negation $N : S(x, y) = N(T(N(x), N(y)))$, and $T(x, y) = N(S(N(x), N(y)))$.

It can be seen easily that conjunction and disjunction operations satisfy the following boundary conditions: $T(1, 1) = 1$, $T(0, x) = T(x, 0) = 0$, $S(0, 0) = 0$, $S(1, x) = S(x, 1) = 1$. By fixing these conditions, new types of generalized operations are introduced.

Definition 10. Let T be a mapping $T : [0, 1] \times [0, 1] \rightarrow [0, 1]$. T is a *quasi-conjunction operation* if $T(0, 0) = T(0, 1) = T(1, 0) = 0$, and $T(1, 1) = 1$.

Definition 11. Let S be a mapping $S : [0, 1] \times [0, 1] \rightarrow [0, 1]$. S is a *quasi-disjunction operation* if $S(0, 1) = S(1, 0) = S(1, 1) = 1$, and $S(0, 0) = 0$.

It is easy to see that conjunction and disjunction operations are quasi-conjunctions and quasi-disjunctions, respectively, but the converse is not true.

Omitting $T(1, 1) = 1$ and $S(0, 0) = 0$ from the definitions further generalization can be obtained.

Definition 12. Let T be a mapping $T : [0, 1] \times [0, 1] \rightarrow [0, 1]$. T is a *pseudo-conjunction operation* if $T(0, 0) = T(0, 1) = T(1, 0) = 0$.

Definition 13. Let S be a mapping $S : [0, 1] \times [0, 1] \rightarrow [0, 1]$. S is a *pseudo-disjunction operation* if $S(0, 1) = S(1, 0) = S(1, 1) = 1$.

Theorem 3. Assume that T and S are non-decreasing pseudo-conjunctions and pseudo-disjunctions, respectively. Then there exist the absorbing elements 0 and 1 such as $T(x, 0) = T(0, x) = 0$ and $S(x, 1) = S(1, x) = 1$.

5.2 A Parametric Family of Quasi-Conjunctions

Let us cite the following result, which is the base of the forthcoming parametric construction, from [4].

Theorem 4. Suppose T_1, T_2 are quasi-conjunctions, S_1 and S_2 are pseudo disjunctions and $h, g_1, g_2 : [0, 1] \rightarrow [0, 1]$ are non-decreasing functions such that $g_1(1) = g_2(1) = 1$. Then the following functions

$$T(x, y) = T_2(T_1(x, y), S_1(g_1(x), g_2(y))) \quad (13)$$

$$T(x, y) = T_2(T_1(x, y), g_1 S_1(x, y)) \quad (14)$$

$$T(x, y) = T_2(T_1(x, y), S_2(h(x), S_1(x, y))) \quad (15)$$

are quasi-conjunctions.

By the use of this Theorem the simplest parametric *quasi*-conjunction operations can be obtained as follows:

$$T(x, y) = x^p y^q, \quad (16)$$

$$T(x, y) = \min(x^p, y^q), \quad (17)$$

$$T(x, y) = (xy)^p (x + y - xy)^q \quad (18)$$

where $p, q \geq 0$.

5.3 Distance-Based Operations

Let e be an arbitrary element of the closed unit interval $[0, 1]$ and denote by $d(x, y)$ the distance of two elements x and y of $[0, 1]$. The idea of definitions of distance-based operators is generated from the reformulation of the definition of the min and max operators as follows

$$\begin{aligned} \min(x, y) &= \begin{cases} x, & \text{if } d(x, 0) \leq d(y, 0) \\ y, & \text{if } d(x, 0) > d(y, 0) \end{cases}, \\ \max(x, y) &= \begin{cases} x, & \text{if } d(x, 0) \geq d(y, 0) \\ y, & \text{if } d(x, 0) < d(y, 0) \end{cases} \end{aligned}$$

Based on this observation the following definitions can be introduced, see [4].

Definition 14. The *maximum distance minimum operator* with respect to $e \in [0, 1]$ is defined as

$$\max_e^{\min}(x, y) = \begin{cases} x, & \text{if } d(x, e) > d(y, e) \\ y, & \text{if } d(x, e) < d(y, e) \\ \min(x, y), & \text{if } d(x, e) = d(y, e) \end{cases} \quad (19)$$

Definition 15. The *maximum distance maximum operator* with respect to $e \in [0, 1]$ is defined as

$$\max_e^{\max}(x, y) = \begin{cases} x, & \text{if } d(x, e) > d(y, e) \\ y, & \text{if } d(x, e) < d(y, e) \\ \max(x, y), & \text{if } d(x, e) = d(y, e) \end{cases} \quad (20)$$

Definition 16. The *minimum distance minimum operator* with respect to $e \in [0, 1]$ is defined as

$$\min_e^{\min}(x, y) = \begin{cases} x, & \text{if } d(x, e) < d(y, e) \\ y, & \text{if } d(x, e) > d(y, e) \\ \min(x, y), & \text{if } d(x, e) = d(y, e) \end{cases} \quad (21)$$

Definition 17. The *minimum distance maximum operator* with respect to $e \in [0, 1]$ is defined as

$$\min_e^{\max}(x, y) = \begin{cases} x, & \text{if } d(x, e) < d(y, e) \\ y, & \text{if } d(x, e) > d(y, e) \\ \max(x, y), & \text{if } d(x, e) = d(y, e) \end{cases} \quad (22)$$

It can be proved by simple computation that if the distance of x and y is defined as $d(x, y) = |x - y|$ then the distance-based operators can be expressed by means of the min and max operators as follows.

$$\max_e^{\min} = \begin{cases} \max(x, y), & \text{if } y > 2e - x \\ \min(x, y), & \text{if } y < 2e - x, \\ \min(x, y), & \text{if } y = 2e - x \end{cases} \quad (23)$$

$$\min_e^{\min} = \begin{cases} \min(x, y), & \text{if } y > 2e - x \\ \max(x, y), & \text{if } y < 2e - x \\ \min(x, y), & \text{if } y = 2e - x \end{cases} \quad (24)$$

$$\max_e^{\max} = \begin{cases} \max(x, y), & \text{if } y > 2e - x \\ \min(x, y), & \text{if } y < 2e - x, \\ \max(x, y), & \text{if } y = 2e - x \end{cases} \quad (25)$$

$$\min_e^{\max} = \begin{cases} \min(x, y), & \text{if } y > 2e - x \\ \max(x, y), & \text{if } y < 2e - x \\ \max(x, y), & \text{if } y = 2e - x \end{cases} \quad (26)$$

5.4 Entropy-Based Conjunction and Disjunction Operators

The question of how fuzzy is a fuzzy set has been one of the issues associated with the development of the fuzzy set theory. In accordance with a current terminological trend in the literature, measure of uncertainty is being referred as *measure of fuzziness*, or *fuzzy entropy* [23].

Throughout this part the following notations will be used; X is the universal set, $\mathcal{F}(X)$ is the class of all fuzzy subsets of X , \mathbb{R}^+ is the set of non negative real numbers, \bar{A} is the fuzzy complement of $A \in \mathcal{F}(X)$ and $|A|$ is the cardinality of A .

Definition 18. Let X be a universal set and A is a fuzzy subset of X with membership function μ_A

The *fuzzy entropy* is a mapping $\mathcal{F}(X) \rightarrow \mathbb{R}^+$ which satisfies the following axioms:

AE 1 $e(A) = 0$ if A is a crisp set.

AE 2 If $A \prec B$ then $e(A) \leq e(B)$. Here $A \prec B$ means that A is sharper than B .

AE 3 $e(A)$ assumes its maximum value if and only if A is maximally fuzzy.

AE 4 $e(A) = e(\bar{A})$, $\forall A \in X$.

Let e_p be equilibrium of the fuzzy complement N and specify **AE 2** and **AE 3** as follows:

AES 2 A is sharper than B in the following sense:

$\mu_A(x) \leq \mu_B(x)$ for $\mu_B(x) \leq e_p$ and $\mu_A(x) \geq \mu_B(x)$ for $\mu_B(x) \geq e_p$, for all $x \in X$.

AES 3 A is defined maximally fuzzy when $\mu_A(x) = e_p \quad \forall x \in X$.

Let A be a fuzzy subset of X and define the following function $f_A : X \rightarrow [0,1]$ by

$$f_A : x \mapsto \begin{cases} \mu_A(x) & \text{if } \mu_A(x) \leq e_p \\ N(\mu_A(x)) & \text{if } \mu_A(x) > e_p \end{cases} \quad (27)$$

Denote Φ_A the fuzzy set generated by f_A as its membership function.

Theorem 5. The $g(|\Phi_A|)$ is an entropy, where $g : \mathbb{R} \rightarrow \mathbb{R}$ is a monotonically increasing real function and $g(0) = 0$.

Definition 19. Let A be a fuzzy subset of X . f_A is said to be an *elementary fuzzy entropy function* if the cardinality of the fuzzy set Φ_A is an entropy of A .

It is obvious that f_A is an elementary entropy function.

Now we introduce some operations based on entropy. For more details we refer to [4].

Definition 20. Let A and B be two fuzzy subsets of the universe of discourse X and denote φ_A and φ_B their elementary entropy functions, respectively. The *minimum entropy conjunction operation* is defined as $I_\varphi^* = I_\varphi^*(A, B)$, where

$$\mu_{U_\varphi^*} : x \mapsto \begin{cases} \mu_A(x) & \text{if } \varphi_A(x) < \varphi_B(x) \\ \mu_B(x) & \text{if } \varphi_B(x) < \varphi_A(x) \\ \min(\mu_A(x), \mu_B(x)) & \text{if } \varphi_A(x) = \varphi_B(x) \end{cases} \quad (28)$$

Definition 21. Let A and B be two fuzzy subsets of the universe of discourse X and denote φ_A and φ_B their elementary entropy functions, respectively. The *maximum entropy disjunction operation* is defined as $U_\varphi^* = U_\varphi^*(A, B)$, where

$$\mu_{U_\varphi^*} : x \mapsto \begin{cases} \mu_A(x) & \text{if } \varphi_A(x) > \varphi_B(x) \\ \mu_B(x) & \text{if } \varphi_B(x) > \varphi_A(x) \\ \max(\mu_A(x), \mu_B(x)) & \text{if } \varphi_A(x) = \varphi_B(x) \end{cases} \quad (29)$$

Several important properties of these operations as well as their construction can be found in [4].

6 Nonstrict Means

The aggregation functions recalled in section 3.1 are logical operations. Their range excludes function values between min and max. In the present section we summarize some results on important subclasses of means, satisfying the *bisymmetry* equation. It can also be considered as a generalization of simultaneous commutativity and associativity. This functional equation has been investigated by several authors. For a list of references see Aczél (1966). The equation is given as follows:

$$M[M(x, y), M(u, v)] = M[M(x, u), M(y, v)], \quad (30)$$

where M is a function from $[a, b]^2$ to $[a, b]$ ($a < b$ are real numbers). This is a particular case of the consistent aggregation equation. Without loss of generality, we restrict ourselves to the case $a = 0, b = 1$ in this paper.

This equation is used for characterizing *quasi-arithmetic means*

$$M(x, y) = f^{-1}\left(\frac{f(x) + f(y)}{2}\right), \quad (31)$$

and in general, *quasilinear functions*

$$M(x, y) = f^{-1} (Af(x) + Bf(y) + C), \quad (32)$$

where f is a continuous and strictly monotonic function, f^{-1} is its inverse, and A, B, C are real constants such that $A \neq 0, B \neq 0$.

Note that (32) contains the following particular cases:

- a) $A = B = 1/2, C = 0$: quasi-arithmetic means;
- b) $A + B = 1, A, B \geq 0, C = 0$: quasilinear means;
- c) $A = B = 1, C = 0$: strict t-norms.

The following properties of a function $M : [0,1]^2 \rightarrow [0,1]$ play important role in the sequel. Such an M is called

- *reducible on both sides* if $M(t, z_1) \neq M(t, z_2), M(z_1, t) \neq M(z_2, t)$ hold for $z_1 \neq z_2$;
- *nondecreasing* if $x \leq t$ and $y \leq z$ imply $M(x, y) \leq M(t, z)$;
- *Archimedean* if M satisfies $\max\{M(x, 0), M(0, x)\} < x < \min\{M(x, 1), M(1, x)\}$ for all $x \in]0, 1[$ and it is continuous;
- *internal* if $x < M(x, y) < y$ holds for $x < y, x, y \in]0, 1[$.

It has been proved in Aczél (1966) that the quasi-arithmetic mean is the general continuous, on both sides reducible, real solution of the bisymmetry equation, under the additional conditions of idempotency and symmetry. It was also noted that reducibility on both sides can be replaced by internality to have the same representation.

The aim of the present section is to recall the general continuous, idempotent, symmetric and nondecreasing real solutions of the bisymmetry equation originally published in [15].

6.1 Archimedean Bisymmetric Functions

Before determining the general nonstrict solutions, we need an equivalent form of the representation theorem, and another characterization of the quasi-arithmetic means when internality is replaced by the Archimedean property.

Let us denote by \mathcal{M}_α the class of all continuous, idempotent, symmetric, nondecreasing real functions $M : [0,1]^2 \rightarrow [0,1]$ which satisfy the bisymmetry equation and have the boundary condition $M(0,1) = \alpha$ ($\alpha \in [0,1]$ is fixed). Let

$\mathcal{M} = \bigcup_{\alpha \in [0,1]} \mathcal{M}_\alpha$. Then any member of \mathcal{M} is called a *nonstrict bisymmetric mean*.

Theorem 6. A function $M \in \mathcal{M}$ is Archimedean if and only if there exists a continuous and strictly monotonic real function f defined on the unit interval such that representation (31) holds.

The general solution (31) can be expressed also in the following form that will be useful in the sequel.

Theorem 7. The general continuous, Archimedean, idempotent, symmetric real solution M of the bisymmetry equation is given by the following form

$$(a) \quad M(x, y) = \varphi^{-1}(\sqrt{\varphi(x)\varphi(y)}) \text{ if } M(0,1) = 0;$$

$$(b) \quad M(x, y) = 1 - \varphi^{-1}(\sqrt{\varphi(1-x)\varphi(1-y)}) \text{ if } M(0,1) = 1;$$

$$(c) \quad M(x, y) = \varphi^{-1}\left(\frac{\varphi(x)+\varphi(y)}{2}\right) \text{ if } 0 < M(0,1) < 1,$$

where φ is an automorphism of the unit interval.

This theorem says that there are three basic classes of operations satisfying the mentioned properties: the first one contains means isomorphic to the *geometric mean*; the second consists of means isomorphic to the *dual of the geometric mean*; finally, the third class contains means isomorphic to the *arithmetic mean*.

6.2 Characterization of the Class \mathcal{M}_0

Suppose that $M \in \mathcal{M}_0$ (that is, $M(0,1) = 0$).

Let φ_i be an automorphism of the unit interval. For typographic reason, we introduce the following short notation when x and y are in $[a_i, b_i] \subseteq [0,1]$:

$$L_i(x, y) := \varphi_i^{-1}\left(\sqrt{\varphi_i\left(\frac{x-a_i}{b_i-a_i}\right)\varphi_i\left(\frac{y-a_i}{b_i-a_i}\right)}\right).$$

We summarize the characterization of the class \mathcal{M}_0 in the following theorem.

Theorem 8. A function M belongs to \mathcal{M}_0 if and only if either

(a) there exists an automorphism φ of the unit interval such that

$$M(x, y) = \varphi^{-1}(\sqrt{\varphi(x)\varphi(y)}),$$

or

$$(b) \quad M(x, y) = \min(x, y),$$

or

(c) there exist an index set K , a family of disjoint subintervals $\{[a_i, b_i]\}$ of $[0,1]$ and for each $i \in K$ an automorphism φ_i of the unit interval such that $M(x, y) = a_i + (b_i - a_i)L_i(\min(x, b_i), \min(y, b_i))$ if $\min(x, y) \in (a_i, b_i)$, and otherwise $M(x, y) = \min(x, y)$.

6.3 Characterization of the Class \mathcal{M}_1

Turning to the case $M \in \mathcal{M}_1$, we can use the above result for \mathcal{M}_0 . Indeed, one can easily prove that $M \in \mathcal{M}_1$ if and only if $M^* \in \mathcal{M}_0$ with

$$M^*(x, y) = 1 - M(1-x, 1-y).$$

Therefore, characterization of the class \mathcal{M}_1 is immediately obtained by Theorem 8. This is summarized in the following theorem.

Theorem 9. A function M belongs to \mathcal{M}_1 if and only if either

(a) there exists an automorphism φ of the unit interval such that

$$M(x, y) = 1 - \varphi^{-1}(\sqrt{\varphi(1-x)\varphi(1-y)}),$$

or

$$(b) M(x, y) = \max(x, y),$$

or

(c) there exist an index set K , a family of disjoint subintervals $\{[a_i, b_i]\}$ of $[0,1]$ and for each $i \in K$ an automorphism φ_i of the unit interval such that $M(x, y) = a_i + (b_i - a_i)M_i(\max(x, a_i), \max(y, a_i))$

if $\max(x, y) \in (a_i, b_i)$, and otherwise we have

$$M(x, y) = \max(x, y),$$

where $M_i(u, v) = 1 - L_i(1-u, 1-v)$ for $u, v \in [a_i, b_i]$.

6.4 Characterization of the Class \mathcal{M}_α for $0 < \alpha < 1$

In this section we characterize the class \mathcal{M}_α with $0 < \alpha < 1$.

Define a set $X \subseteq [0,1]$ by

$$X = \{x \in [0,1] \mid M(x, 1) = x \text{ or } M(x, 0) = x\}.$$

Obviously, $0, 1 \in X$ since $M(0, 0) = 0$ and $M(1, 1) = 1$. Moreover, X is closed, by continuity of M . Therefore, $Y = [0, 1] \setminus X$ is open and bounded. Thus, there exists an index set K and a family of non-overlapping open intervals $\{]a_i, b_i[\}_{i \in K}$ such that

$$Y = \bigcup_{i \in K}]a_i, b_i[.$$

Since $0 < M(0, 1) = \alpha < 1$, there are two possibilities: either $\alpha \in X$ (that is, we have $M(\alpha, 1) = \alpha$ or $M(\alpha, 0) = \alpha$), or there exists an index $j \in K$ such that $\alpha \in]a_j, b_j[$.

First we state the main theorem when $\alpha \in X$.

Theorem 10. *If $\alpha \in X$ then there exist $M_0 \in \mathcal{M}_0$ and $M_1 \in \mathcal{M}_1$ such that*

$$M(x, y) = \begin{cases} \alpha M_1\left(\frac{x}{\alpha}, \frac{y}{\alpha}\right) & \text{if } x, y \leq \alpha \\ \alpha + (1 - \alpha) M_0\left(\frac{x - \alpha}{1 - \alpha}, \frac{y - \alpha}{1 - \alpha}\right) & \text{if } x, y \geq \alpha \\ \alpha & \text{otherwise} \end{cases}$$

Let us turn now to the remaining case when there exists an $]a_j, b_j[$ such that $\alpha \in]a_j, b_j[$. Denote this interval simply by $]a, b[$ for short. Notice that we have $M(0, \alpha) < \alpha < M(1, \alpha)$ now.

The main result related to the present subcase can be stated as follows.

Theorem 11. *Suppose α is such that $0 < \alpha < 1$, and $M(0, \alpha) < \alpha < M(1, \alpha)$. Then $M \in \mathcal{M}_\alpha$ if and only if there exist $M_0 \in \mathcal{M}_0$, $M_1 \in \mathcal{M}_1$ and numbers $0 \leq a < b \leq 1$, such that*

$$M(x, y) = a M_0\left(\frac{x}{a}, \frac{y}{a}\right) \text{ if } x, y \in [0, a];$$

$$M(x, y) = a + (b - a) \varphi^{-1}\left(\frac{\varphi\left(\frac{x-a}{b-a}\right) + \varphi\left(\frac{y-a}{b-a}\right)}{2}\right) \text{ if } x, y \in [a, b];$$

$$M(x, y) = b + (1 - b) M_1\left(\frac{x-b}{1-b}, \frac{y-b}{1-b}\right) \text{ if } x, y \in [b, 1];$$

$$M(x, y) = \alpha \text{ if } \min(x, y) \leq a, \max(x, y) \geq b;$$

$$M(x, y) = a + (b - a) \varphi^{-1}\left(\frac{1}{2} \cdot \varphi\left(\frac{y-a}{b-a}\right)\right) \text{ if } x \in [0, a], y \in [a, b];$$

$$M(x, y) = a + (b - a) \varphi^{-1}\left(\frac{1}{2} + \frac{1}{2} \cdot \varphi\left(\frac{y-a}{b-a}\right)\right) \text{ if } x \in [b, 1], y \in [a, b].$$

Conclusion

In this paper we summarized some results on (partly our contributions to) the theory of aggregation functions used in fuzzy set theory. Further details and another classes of aggregation operators can be found in [4]. The picture cannot be complete, due to space limitations. For instance, we could not touch upon the interesting class of *copulas* playing important role both in probability theory and fuzzy sets. The interested reader can read the book [26].

Acknowledgments. The author gratefully acknowledges the support obtained within the frames of Bilateral Romanian-Hungarian S&T Co-operation Project conducted by the Research and Technology Fund in Hungary, a support in part by OTKA K063405, and by COST Actions IC0602 and IC0702.

References

- [1] Aczél, J.: On Mean Values. *Bulletin of the American Math. Society* 54, 392–400 (1948)
- [2] Aczél, J., Maksa, G.: Solution of the Rectangular $m \times n$ Generalized Bisymmetry Equation and of the Problem of Consistent Aggregation. *Journal of Mathematical Analysis and Applications* 203, 104–126 (1996)
- [3] Aczél, J., Maksa, G., Taylor, M.: Equations of Generalized Bisymmetry and of Consistent Aggregation: Weakly Surjective Solutions which be Discontinuous at Laces. *Journal of Mathematical Analysis and Applications* 214, 22–35 (1997)
- [4] Batyrshin, I., Kaynak, O., Rudas, I.: Fuzzy Modeling Based on Generalized Conjunction Operations. *IEEE Transactions on Fuzzy Systems* 10, 678–683 (2002)
- [5] Buchanan, B., Shortliffe, E.: Rule-based Expert Systems. In: The MYCIN Experiments of the Stanford Heuristic Programming Project. Addison-Wesley, Reading (1984)
- [6] Calvo, T., De Baets, B., Fodor, J.: The Functional Equations of Frank and Alsina for Uninorms and Nullnorms. *Fuzzy Sets and Systems* 120, 385–394 (2001)
- [7] Czogała, E., Drewniak, J.: Associative Monotonic Operations in Fuzzy Set Theory. *Fuzzy Sets and Systems* 12, 249–269 (1984)
- [8] De Baets, B., Fodor, J.: Van Melle’s Combining Function in MYCIN is a Representable Uninorm: An Alternative Proof. *Fuzzy Sets and Systems* 104, 133–136 (1999)
- [9] De Baets, B., Fodor, J.: Residual Operators of Uninorms. *Soft Computing* 3, 89–100 (1999)
- [10] Dombi, J.: Basic Concepts for the Theory of Evaluation: the Aggregative Operator. *European J. Oper. Res.* 10, 282–293 (1982)
- [11] Dubois, D., Fodor, J.C., Prade, H., Roubens, M.: Aggregation of Decomposable Measures with Application to Utility Theory. *Theory and Decision* 41, 59–95 (1996)
- [12] Fodor, J.C.: A New Look at Fuzzy Connectives. *Fuzzy Sets and Systems* 57, 141–148 (1993)
- [13] Fodor, J.: An extension of Fung-Fu’s Theorem. *Internat. J. Uncertain. Fuzziness Knowledge-based Systems* 4, 235–243 (1996)

- [14] Fodor, J., Calvo, T.: Aggregation Functions Defined by t-norms and t-conorms. In: Bouchon-Meunier, B. (ed.) *Aggregation and Fusion of Imperfect Information*, pp. 36–48. Physica-Verlag (1998)
- [15] Fodor, J.C., Marichal, J.-L.: On Nonstrict Means. *Aequationes Mathematicae* 54, 308–327 (1997)
- [16] Fodor, J.C., Roubens, M.: *Fuzzy Preference Modelling and Multicriteria Decision Support*. Kluwer, Dordrecht (1994)
- [17] Fodor, J., Yager, R., Rybalov, A.: Structure of Uninorms. *Internat. J. Uncertain. Fuzziness Knowledge-Based Systems* 5, 411–427 (1997)
- [18] Fung, L., Fu, K.: An Axiomatic Approach to Rational Decision-Making in a Fuzzy Environment. In: Tanaka, K., Zadeh, L., Fu, K., Shimura, M. (eds.) *Fuzzy Sets and their Applications to Cognitive and Decision Processes*, pp. 227–256. Academic Press, New York (1975)
- [19] Hajek, P., Havranek, T., Jirousek, R.: *Uncertain Information Processing in Expert Systems*. CRC Press, Boca Raton (1992)
- [20] Klein, L.R.: Remarks on the Theory of Aggregation. *Econometrica* 14, 303–312 (1946)
- [21] Klement, E.P., Mesiar, R., Pap, E.: On the Relationship of Associative Compensatory Operators to Triangular Norms and Conorms. *Internat. J. Uncertain. Fuzziness Knowledge-based Systems* 4, 129–144 (1996)
- [22] Klement, E.P., Mesiar, R., Pap, E.: *Trends in Logic*, vol. 8. Kluwer Academic Publishers, Dordrecht (2000)
- [23] Klir, J.G., Folger, T.A.: *Fuzzy Sets, Uncertainty, and Information*. Prentice-Hall International Editions, USA (1988)
- [24] Maksa, G.: *Associativity and Bisymmetry Equations*. Thesis for the title “Doctor of the Hungarian Academy of Sciences” (2004) (in Hungarian)
- [25] Mayor, G., Trillas, E.: On the Representation of some Aggregation Functions. In: Proc. Internat. Symposium on Multiple-Valued Logic, pp. 110–114 (1986)
- [26] Nelsen, R.B.: *An Introduction to Copulas*, 2nd edn. Springer, Heidelberg (2006)
- [27] Sander, W.: Some Aspects of Functional Equations. In: Klement, E.P., Mesiar, R. (eds.) *Logical, Algebraic, Analytic and Probabilistic Aspects of Triangular Norms*, pp. 43–187. Elsevier, Amsterdam (2005)
- [28] Tsadiras, A., Margaritis, K.: The MYCIN Certainty Factor Handling Function as Uninorm Operator and its Use as a Threshold Function in Artificial Neurons. *Fuzzy Sets and Systems* 93, 263–274 (1998)
- [29] Yager, R., Rybalov, A.: Uninorm Aggregation Operators. *Fuzzy Sets and Systems* 80, 111–120 (1996)
- [30] Zadeh, L.A.: Fuzzy Sets. *Information and Control* 8, 338–353 (1965)
- [31] Zimmermann, H.-J., Zysno, P.: Latent Connectives in Human Decision Making. *Fuzzy Sets and Systems* 4, 37–51 (1980)

Neural Networks or Fuzzy Systems

Bogdan M. Wilamowski

Electrical and Computer Engineering, Auburn University
420 Broun Hall, Auburn, Alabama, USA

Abstract. The paper describes basic concepts of neural networks and fuzzy systems. It shows that most commonly used neural network architecture of MLP – Multi Layer Perceptron is also one of the least efficient ones. Also most commonly used EBP – Error Back Propagation algorithm is not only very slow, but also it is not able to find solutions for optimal neural network architectures. EBP can solve problems only when large number of neurons is used, but this way neural network loses its generalization property. Performances of both fuzzy systems and neural networks are compared leading to the conclusion that neural networks can produce much more accurate nonlinear mapping and they are simple to implement. At the end of the presentation several concepts of neuro-fuzzy systems are compared.

Keywords: Learning, neural networks, fuzzy systems, perceptron, neuro-fuzzy.

1 Introduction

Both neural networks and fuzzy systems perform nonlinear mapping and both systems internally operate within a limited signal range between zero and one. In general, all parameters of fuzzy systems are designed, while parameters of neural networks are being obtained by a training process. It is relatively easy for humans to follow the computation process of fuzzy systems, while it is almost impossible to do as in the case of neural networks. Neural networks can handle basically an unlimited number of inputs and outputs while fuzzy systems have one output and number of inputs is practically limited to 2 or 3. The resulted nonlinear function produced by neural networks is smooth while functions produced by fuzzy systems are relatively rough (see Fig. 1).

It is relative easy to design fuzzy systems based on a designer's intuition. In case of neural networks a designer may face many challenges. The first challenge

is that it is difficult to decide how many neurons to use and how they have to be connected. Second problem, which often leads to frustration, is how to train neural networks. As a result far from optimum neural network architectures are selected and learning algorithms which are not able to produce a good solution are used. These issues will be discussed in section 2 of this presentation. However, if difficulties with neural networks are solved then neural networks generate not only a better and smoother control surface, but also its microcontroller implementations requires shorter code and faster operation [1]. Of course it is possible to merge these two technologies by developing neuro-fuzzy systems.

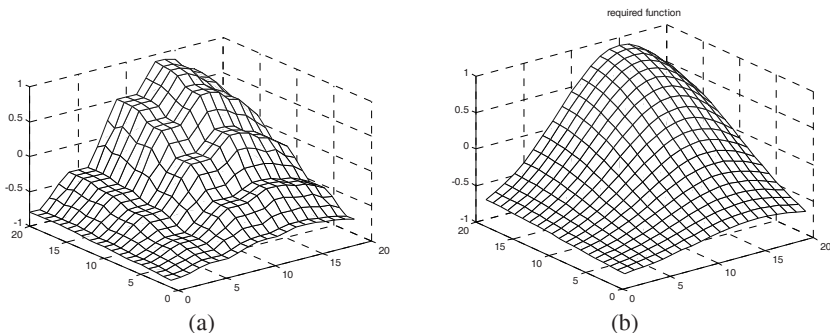


Fig. 1. Comparison of control surfaces obtained with (a) fuzzy controller with 6 and 5 membership function for both inputs (b) neural controller with 3 neurons

2 Neural Networks

Artificial neural networks consist of many neurons with a sigmoid activation function as shown in Fig. 2. These neurons are connected in such a way that the feed forward signal flow is assured. Connecting weights may have both positive and negative values and the resulted neuron excitation *net* is calculated as a sum of products of incoming signals multiplied by weights:

$$net = \sum_{i=I}^n w_i x_i \quad (1)$$

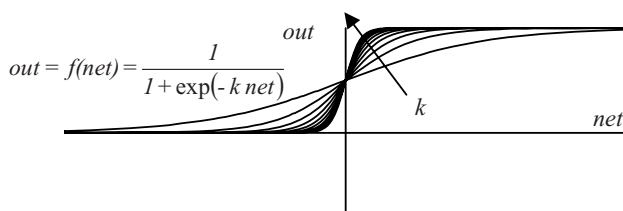


Fig. 2. Unipolar activation function of a neuron

2.1 Neural Network Architectures

The most commonly used architecture is MLP – Multi Layer Perceptron as shown in Fig. 3. The only advantage of MLP is that it is relatively easy to write software for this architecture. Unfortunately when using MLP topology more neurons are needed to solve problems. A better option is to use MLP with connections across layers. This architecture is not only more powerful but it can be trained faster, assuming that we have written a proper software. The most powerful architecture is the cascade architecture, also known as FCN – Fully Connected Network shown in Fig. 4.

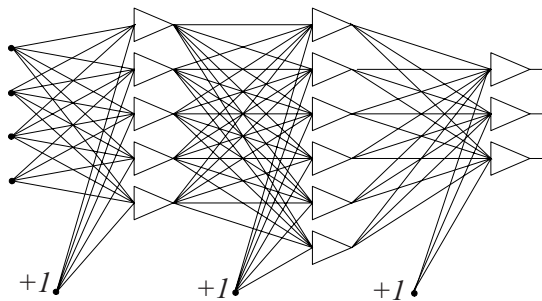


Fig. 3. MLP - Multi Layer Perceptron architecture for neural networks

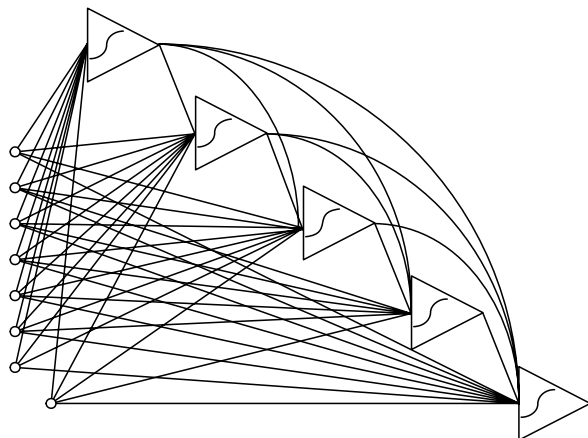


Fig. 4. FCN – Fully Connected Network or cascade network architecture

2.2 Neural Network Training

The most common training algorithm is EBP – Error Back Propagation [2]. It is relatively simple and it does not require a lot of computer resources. This algorithm however seldom leads to a good solution and is extremely slow. The EBP show some advantages for MLP networks [3], [4]. Much better results can be obtained with the LM – Levenberg-Marquardt Algorithm [5]. Even better results can be obtained with NBN – Neuron by Neuron algorithm [6]. Note that in the LM algorithm an N by N matrix must be inverted in every iteration. This is the reason why for large size neural networks the LM algorithm is not practical. Also most of implementations of LM algorithms (like popular MATLAB NN Toolbox) are developed only for MLP. The Neuron by Neuron (NBN) algorithm was developed in order to eliminate most disadvantages of the LM algorithm. Detailed descriptions of the algorithm can be found in [6], [7].

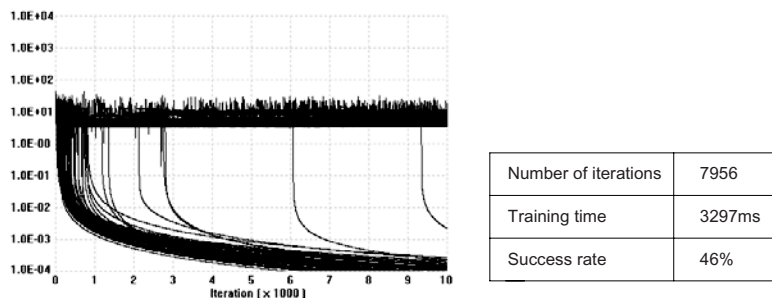


Fig. 5. Result of parity-4 training using EBP algorithm with 4-3-3-1 architecture

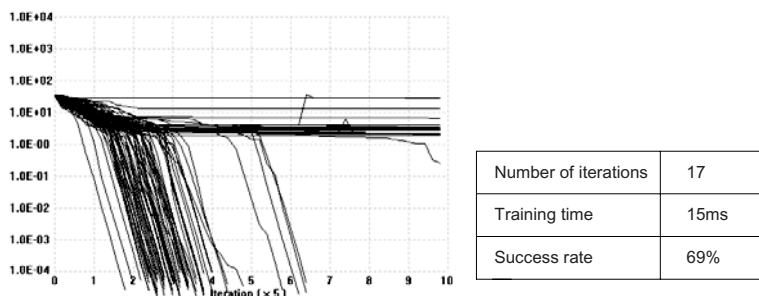


Fig. 6. Result of parity-4 training using LM algorithm with 4-3-3-1 architecture

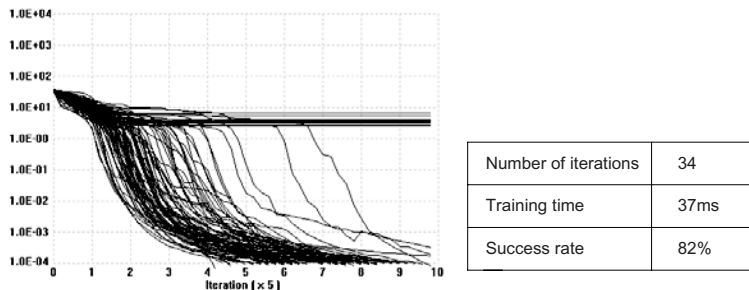


Fig. 7. Result of parity-4 training using NBN algorithm with 4-3-3-1 architecture

Figures 5 through 7 shows results of training of MLP architecture for the Parity- 4 problem. One may notice that EBP training requires 200 times more iterations and 100 times longer time to train. Also the success rate is smaller than in the case of other algorithms. LM algorithm is slightly faster but it has a smaller success rate in comparison to NBN algorithm. For the FCN architecture, with 3 neurons connected in cascade, the parity problem can be solved with significantly smaller number of neurons (3 instead of 7). Unfortunately EBP algorithm cannot solve this problem with less than 10,000 iterations. The standard LM algorithm is not suitable for FCN architecture; but NBN algorithm can solve this problem in a short time with the success rate of 98%. Training results for Parity-4 problem are summarized in Table 1.

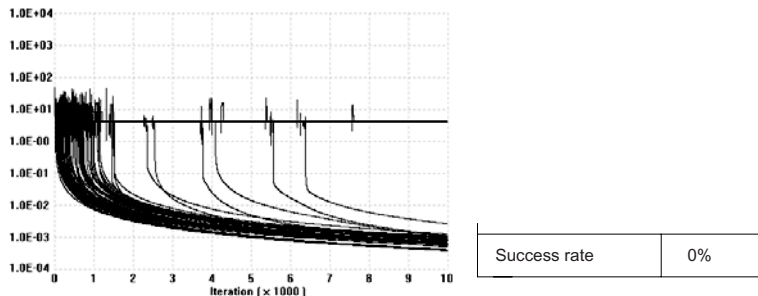


Fig. 8. Result of parity-4 training using EBP algorithm with 4-1-1-1 architecture

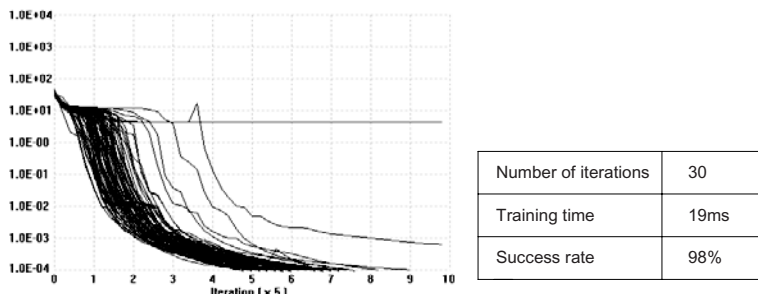


Fig. 9. Result of parity-4 training using NBN algorithm with 4-1-1-1 architecture

Table 1. Comparison of solutions of PARITY-4 problem with various Algorithms for two different architectures

	Iterations	Time [ms]	Success rate
MLP with 4331 architecture without connections across layers (desired error=0.0001)			
EBP ($\eta=3$)	7956.4	3296.6	46%
LM (Gauss-Jordan)	16.5	14.9	69%
NBN (Gauss-Jordan)	33.6	37.07	82%
FCN with 4111 architecture with connections across layers (desired error=0.0001)			
EBP ($\eta=3$)	N/A	N/A	0%
LM (Gauss-Jordan)	<i>Is not able to handle FCN with connections across layers</i>		
NBN (Gauss-Jordan)	30.2	19.1	98%

For MLP topologies it seems that the EBP algorithm is most robust and has the largest success rate for random weight initialization. At the same time the EBP algorithm requires over 200 times larger number of iterations to converge.

If the number of neurons in FCN is increased to 4 then also EBP algorithm can solve the problem with success rate of 98%. The NBN algorithm can solve this problem in 150 times shorter time with 100% success rate. Results are shown in Table 2. One may also notice that with increasing of network complexity neural networks are losing their ability for generalization (if neural network is used for nonlinear mapping).

Table 2. Comparison of solutions of PARITY-4 problem with various Algorithms on 4-1-1-1-1 topology

Type size (pts.)	Averages from 100 runs		
	Success rate	iterations	Computing time
EBP	98%	3977.15	1382.78ms
LM	N/A	N/A	N/A
NBN	100%	12.36	8.15ms

For experiments shown in Table 3 the LM algorithm was modified so not only MLP networks but all arbitrarily connected neural networks could be trained. Also in both LM and NBN algorithms the matrix inversion, the Gauss-Jordan method, was replaced by the LU decomposition. As a consequence the training time was significantly reduced.

One may notice that if too large neural networks are used the system can find solutions which produce very small error for the training patterns, but for patterns which were not used for training errors actually could be much larger than in the case of much simpler network.

Table 3. Comparison of solutions of various increased complexity problems using various algorithms and FCN architectures

	Iterations	Time [ms]	Success rate
Parity 4 problem with 4111 architecture (desired error=0.001)			
EBP ($\eta=1$)	17505	3384.6	93%
LM (modified)	14.6	0.16	98%
NBN (modified)	20.6	1.01	99%
Parity 8 problem with 411111 architecture (desired error=0.001)			
EBP ($\eta=1$)	failed	failed	0%
LM (modified)	32.1	152.2	8%
NBN (modified)	40.6	192.7	28%
Parity 12 problem with 41111111 architecture (desired error=0.001)			
EBP ($\eta=1$)	failed	failed	0%
LM (modified)	77.3	9656.	3%
NBN (modified)	66.7	14,068.	14%

What many people are not also aware of is that not all popular algorithms can train every neural network. Surprisingly, the most popular EBP (Error Back Propagation) algorithm cannot handle more complex problems while other more advanced algorithms can. Also, in most cases neural networks trained with popular algorithms such as EBP produce far from optimum solutions [3], [4].

3 Fuzzy Systems

The fuzzy set system theory was developed by Zadeh [8]. Fuzzy logic is similar to Boolean algebra, but it operates on analog values between zero and one. Also, instead of AND and OR operators the MIN and MAX operators are used as is shown in Fig. 10.

<i>Boolean</i>			<i>Fuzzy</i>		
$A \cap B$		$A \cup B$	$A \cap B$		$A \cup B$
0	0	0	0.2	0.3	0.2
0	1	0	0.2	0.8	0.2
1	0	0	0.7	0.3	0.3
1	1	1	0.7	0.8	0.7

Fig. 10. Comparison Boolean algebra with fuzzy logic

In order to solve problem of nonlinear mapping two similar approaches are usually taken: Mamdani [9] and TSK [10], [11]. Block diagrams for these two controllers are shown in Figures 11 and 12.

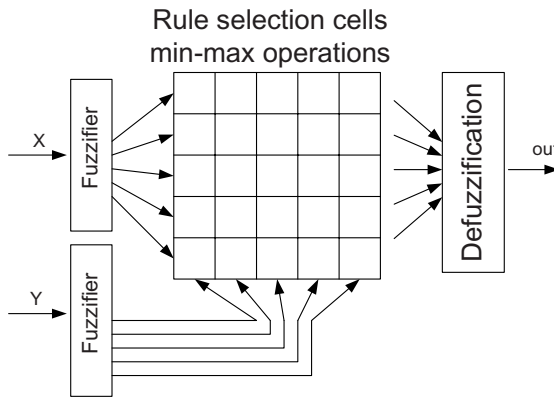


Fig. 11. Block diagram of a Mamdani type fuzzy controller

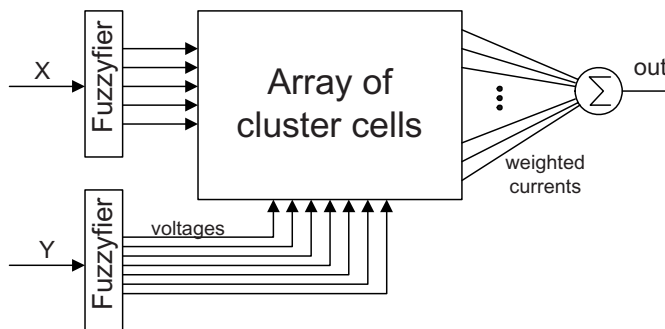


Fig. 12. TSK (Takagi-Sugeno-Kang) fuzzy architecture.

4 Neuro-fuzzy Systems

Most commonly used neuro-fuzzy architecture is shown in Fig. 13. It has neural network topology, but its operation does not reassemble biological neuron operations. This concept of neuro-fuzzy architecture requires signal multiplication and division and as result it is not easy to implement this concept in hardware.

It is, however, possible to implement fuzzy systems using typical neurons with sigmoid activation functions. One such implementation may follow the the concept of conterpropagation neural networks [4]. Actually TSK fuzzy systems have a

very similar topology. Unfortunately, the conterpropagation networks operate correctly only on normalized inputs. Normalization of inputs lead to removal of important information so it cannot be used. However, by increasing the dimensionality of input dimensionality it is possible to project input data on sphere (or hypersphere) without losing important information. The neuro-fuzzy system based on the conterpropagation network with input pattern transformation is shown in Fig. 14. In the network of Fig. each neuron is responsible for one fuzzy rule.

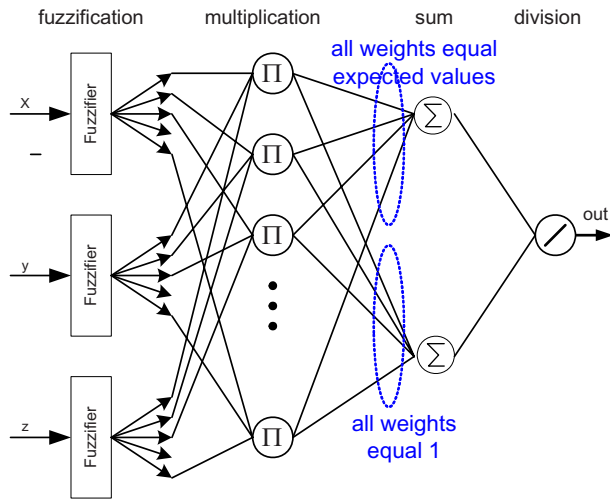


Fig. 13. Classical Neuro-Fuzzy Architecture

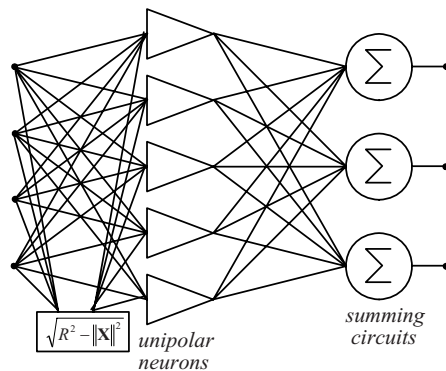


Fig. 14. Fuzzy controller based on conterpropagation network

All neurons in Fig. 14 have a unipolar activation function and if the system is properly designed, then for any input vector in certain areas only the neuron of this area produces +1 while all remaining neurons have zero values. In the case of when the input vector is close to a boundary between two or more regions, then all participating neurons are producing fractional values and the system output is

generated as a weighted sum. For proper operation it is important that the sum of all outputs of the second layer must be equal to +1. In order to assure the above condition, an additional normalization block can be introduced, in a similar way as it is done in TSK fuzzy systems as shown in Fig. 12.

Another concept of replacing fuzzy systems with neural networks is shown in Fig. 14 [12]. This network can be considered as a fuzzy system with sigmoid membership functions [12].

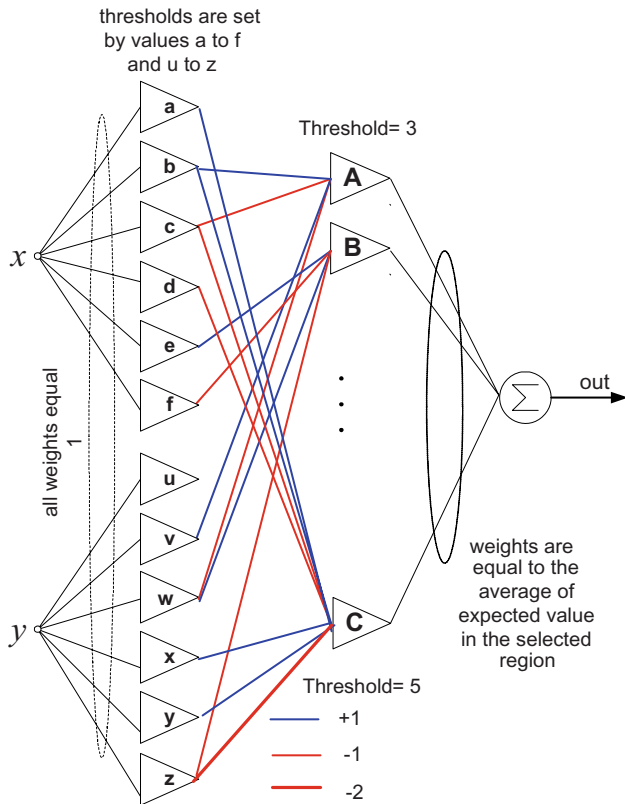


Fig. 14. Simple neural networks performing the function of TSK fuzzy system

It is shown above that a simple neural network of Fig. 14 can replace a fuzzy system. All parameters of this network are directly derived from requirements specified for a fuzzy system and there is no need for a training process.

One may observe that if the training process is allowed then the network architecture of Fig. 14 can be significantly simplified. Let us compare in the following subsections the commonly used neural network architectures.

5 Comparison of Neural Networks and Fuzzy Systems

Fuzzy systems utilize the expert information in the form of a set of rules. There are several reasons for using fuzzy systems in control engineering practice. First, the dynamics of the system under interest is generally complicated, but sometimes its behavior can be defined more easily in linguistic terms. Second, fuzzy systems are suitable architectures for modification and tuning process, which provides some kind of adaptiveness through the on-line adjustment of parameters. The major advantage of fuzzy logic based systems is their ability to utilize expert knowledge and perception based information.

Artificial neural networks are well known by their property of performing complex nonlinear mappings. Earlier works on the mapping properties of these architectures have shown that neural networks are universal approximators [13, 14].

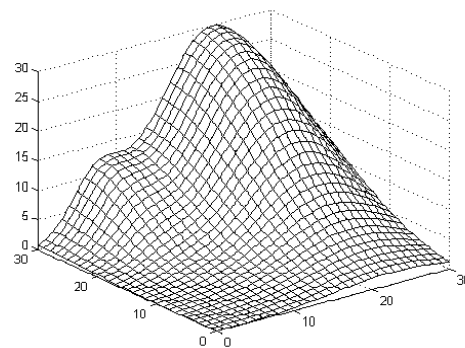


Fig. 15. Required control function and a comparison of the results obtained with microcontroller implementation using fuzzy and neural systems

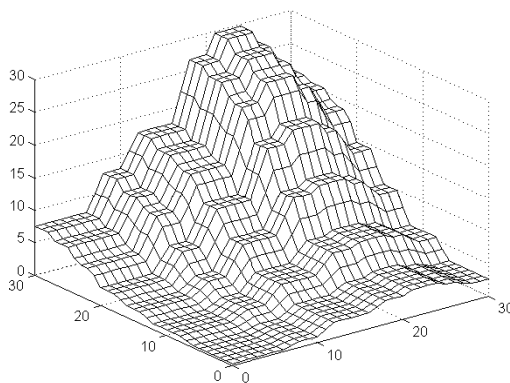


Fig. 16. Control surfaces obtained with Motorola microcontroller HC11 using fuzzy approach with trapezoidal membership functions (7 functions per input) and TSK defuzzification [1]

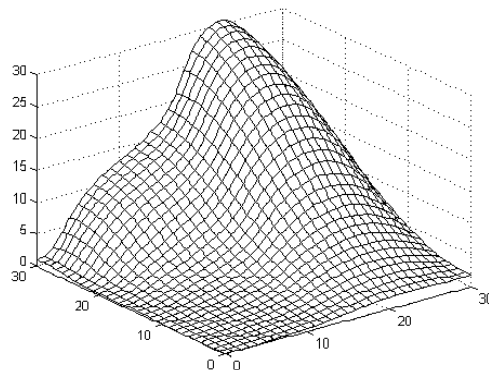


Fig. 17. Control surfaces obtained with Motorola microcontroller HC11 using fuzzy approach with six neurons 2-1-1-1-1 architecture and Elliot activation function [1]

Figures 15 to 17 show a comparison of fuzzy and neural networks based system implemented in Motorola HC11 microcontroller. Motorola's 68HC711E9 is a low cost, 8-bit microprocessor; the on-board features of which are 512 bytes of RAM and EEPROM and 12K bytes of UV erasable EPROM. The processor was used with an 8 MHz crystal, allowing an internal clock frequency of 2 MHz.

Currently, fuzzy controllers are the most popular choice for hardware implementation of complex control surfaces because they are easy to design. Neural controllers are more complex and harder to train, but provide an outstanding control surface with much less error than that of a fuzzy controller.

A drawback of neural controllers is that the design process is more complicated than that of fuzzy controllers. However, this difficulty can be easily overcome with proper design tools. One severe disadvantage of a fuzzy system is its limited ability of handling problems with multiple inputs. In the case of neural networks such a limitation does not exist. Furthermore, control surfaces obtained from neural controllers also do not exhibit the roughness of fuzzy controllers that can lead to unstable or rough control.

Table 4. Comparison of solutions of various increased complexity problems using various algorithms and FCN architectures

	Fuzzy System (Zadeh)	Fuzzy System (TSK)	Neural Network 2-1-1-1	Neural Network 2-1-1-1-1-1
Length of code	2324	1502	680	1119
Time (ms)	1.95	28.5	1.72	3.3
MSE Error	0.945	0.309	0.000578	0.000093

Both neural networks and fuzzy systems are capable of approximating any nonlinear function, but their implementation in silicon is not easy. Both neural and fuzzy systems have their advantages and limitations.

One may notice that TSK fuzzy controller can be easily replaced by neural network with very simple architecture. In this case the intuitive fuzzy rules can be used as patterns to train neural networks. This approach is not only very simple but it also produces a smooth control surface. In most cases these neural networks which are replacing fuzzy systems require hardware.

Conclusion

The paper describes basic concepts of neural networks and fuzzy systems. It is shown that most commonly used neural network architecture of MLP – Multi Layer Perceptron is also one of the least efficient ones. Also most commonly used EBP – Error Back Propagation algorithm is not only very slow, but also it is not able to find solutions for optimal neural network architectures. EBP can solve problems only when large number of neurons is used, but this way neural network loses its generalization property. Performances of both fuzzy systems and neural networks are compared leading to the conclusion that neural networks can produce much more accurate nonlinear mapping that are simple to implement. At the end of the presentation several concepts of neuro-fuzzy systems are compared.

References

- [1] Wilamowski, B.M., Bin fet, J.: Microprocessor Implementation of Fuzzy Systems and Neural Networks. In: International Joint Conference on Neural Networks (IJCNN 2001), Washington DC, July 15-19, 2001, pp. 234–239 (2001)
- [2] Rumelhart, D.E., Hinton, G.E., Williams, R.J.: Learning Representations by Back-Propagating Errors. *Nature* 323, 533–536 (1986)
- [3] Wilamowski, B.M.: Advanced Learning Algorithms. In: INES 2009 – 13th International Conference on Intelligent Engineering Systems, Barbados, April 16-18, 2009, pp. 9–17 (2009)
- [4] Wilamowski, B.M.: Special Neural Network Architectures for Easy Electronic Implementations. In: POWERENG 2009 - International Conference on Power Engineering, Energy and Electrical Drivers, Lisbon, Portugal, March 18-20 (2009)
- [5] Hagan, M.T., Menhaj, M.: Training Feedforward Networks with the Marquardt Algorithm. *IEEE Transactions on Neural Networks* 5(6), 989–993 (1994)
- [6] Wilamowski, B.M., Cotton, N.J., Kaynak, O., Dundar, G.: Computing Gradient Vector and Jacobian Matrix in Arbitrarily Connected Neural Networks. *IEEE Trans. on Industrial Electronics* 55(10), 3784–3790 (2008)
- [7] Wilamowski, B.M., Cotton, N., Hewlett, J., Kaynak, O.: Neural Network Trainer with Second Order Learning Algorithms. In: 11th INES 2007 -International Conference on Intelligent Engineering Systems, Budapest, Hungary, June 29 2007-July 1 (2007)
- [8] Zadeh, L.A.: Fuzzy Sets. *Information and Control* 8, 338–353 (1965)

- [9] Mamdani, E.H.: Application of Fuzzy Algorithms for Control of Simple Dynamic Plant. *IEEE Proceedings* 121(12), 1585–1588 (1974)
- [10] Sugeno, M., Kang, G.T.: Structure Identification of Fuzzy Model. *Fuzzy Sets and Systems* 28(1), 15–33 (1988)
- [11] Takagi, T., Sugeno, M.: Fuzzy Identification of Systems and Its Application to Modeling and Control. *IEEE Transactions on System, Man, Cybernetics* 15(1), 116–132 (1985)
- [12] Wilamowski, B.M.: Methods of Computational Intelligence for Nonlinear Control Systems. In: *ICCAE 2005 International Conference on Control, Automation and System*, Gyeonggi-Do, Korea, June 2-5, 2005, pp. P1–P8 (2005)
- [13] Kolbusz, J., Paszczyński, S., Wilamowski, B.M.: Network Traffic Model for Industrial Environment. *IEEE Transaction on Industrial Informatics* 2(4), 213–220 (2006)
- [14] Wilamowski, B.M., Kaynak, O.: Oil Well Diagnosis by sensing Terminal Characteristics of the Induction Motor. *IEEE Transactions on Industrial Electronics* 47(5), 1100–1107 (2000)

New IEC Research and Frameworks

Hideyuki Takagi

Kyushu University, 4-9-1, Shiobaru, Minami-ku, Fukuoka, 815-8540 Japan
takagi@design.kyushu-u.ac.jp

Abstract. We introduce recent research on new types of interactive evolutionary computation (IEC) applications and that on reducing IEC user fatigue. IEC is an optimization technique to embed IEC user's subjective evaluations based on his/her domain knowledge, experiences, and preferences into several designs and has been applied to wide varieties of applications in artistic, engineering, and others for these 20 years. The approach of almost them can be said as a system optimization based on IEC user's subjective evaluations. We review recent new research topics including an IEC as a tool for analyzing human mind, an IEC with physiological responses, and an IEC with evolutionary multi-objective optimization. We also introduce recent approaches for reducing IEC user fatigue by modeling user's evaluation characteristics and expanding an IEC framework.

1 Introduction

Interactive Evolutionary Computation (IEC) is an optimization framework consisting of a target optimization system, evolutionary computation (EC), and an IEC user, and it can be said that IEC is an EC whose fitness function is replaced with a human user. IEC is suitable for optimization tasks that are hard or almost impossible to be evaluated numerically or whose fitness functions are difficult to be designed. These tasks are, for example, fitting a hearing-aid to let its user satisfy his/her sound preference or designing cute motions of robot's behaviors. Although it is hard to evaluate these tasks quantitatively, we can apply IEC to them if we can evaluate them subjectively based on our domain knowledge, experiences, and preferences. We may say that IEC is a method for embedding our capability of global decision making, or *KANSEI* in general, into the process of optimization or design.

IEC started from R. Dowkins's biomorph (1986). Its applications were biased to computer graphics in the former half of 1990's, but it was widely applied to several areas; they include artistic applications such as graphics, music, industrial design, or facial design, engineering applications such as acoustic and image signal processing, data mining, robotics, or control, and other applications such as geology, education or games [20].

One of recent remarkable features is the increase of its practical applications. The applications that aim practical real world applications include MEMS design with concrete fabrications [8], conceptual designing of software using Unifies Modeling Language [18], developing medicines [3, 10, 17], joint research of hearing-aid fitting with hearing aid companies, Rion Co., Ltd. and Matsushita Communication Industrial Co., Ltd (in those days) [24], joint research of concept design of aircrafts with British Aerospace, engine control of Yamaha Motor Co., Ltd.

Other research direction is to aim practical IEC by reducing IEC user fatigue; it include reducing mental stresses of decision making for evaluation, fatigue of input operations, and boringness due to iterated evaluations. These approaches are categorized into (a) improving input/output interface, (b) accelerating EC convergence, (c) user intervening into EC search, and (d) making a model of user evaluation characteristics based on machine learning and simulating IEC with the model as a pseudo-IEC user.

The (a) is to improve the interfaces of inputting fitness values from an IEC user and displaying individuals to the user [20]. This kind of research includes evaluation of trade-off of more fitness levels that are precise but increase IEC user fatigue and fewer fitness levels that have their reverse characteristics, displaying individuals sorted by fitness to help IEC user's comparisons, multiple windows for displaying many individuals on a limited space of a PC display, a secondary window for displaying an enlarged image to check the detail of an individual, explicit display of an elite individual to help sequential comparisons with other individuals of sounds or movies, and others.

The (b) is to fasten EC convergence. It is an efficient approach for reducing the number of evaluations, but it must work well under the restricted conditions of fewer population size and fewer generation numbers. This kind of research includes acceleration of EC convergence on a simplified searching landscape roughly approximated by a simple unimodal function [21], developing optimization methods and EC operators that work well under the above mentioned restricted conditions of IEC, combination of IEC with normal EC using a fitness function, and others.

The (c) aims to reduce user's mental stress caused by boring iterations of IEC evaluations by letting an IEC user not only join to IEC evaluations but also intervene in EC search actively. It is also useful to accelerate IEC convergence. This kind of research includes reducing dimensions of a searching space by fixing the value of a certain optimization parameter when an IEC user thinks that its corresponding phenotype looks good if the relationship of its phenotype and genotype is one-to-one, adding a new searching point, i.e. an individual, based on visual guessing on the 2-D searching space that is mapped from an original n -D searching space [4], and others.

Refer the reference [20] for these descriptions without citations. We will describe about the (d) in section 3.1.

IEC has the below features:

- (1) an optimization with fewer population size and fewer generation numbers,
- (2) nevertheless, it is not so difficult to obtain satisfactory solutions,

- (3) relative evaluations in general, and
- (4) discrete n -evaluation levels.

The feature (1) is a restriction due to an IEC user fatigue for iterative evaluations. As mentioned, when we develop EC acceleration methods, it is essential that the methods must work well under this restriction. This feature becomes a bottleneck for keeping enough number of training data for making a model of user evaluation characteristics that will be mentioned in the later of this paper.

The reason of the feature (2) is that any solutions are the same for an IEC user if he/she cannot distinguish them. It is easy to understand if we think that IEC searches global optimization *area*, while normal EC searches the global optimization point. For example, in our experience of IEC-based hearing-aid fitting using a commercial hearing-aids and real hearing-aid users, it frequently became difficult for the users to evaluate which sounds are good after five generations even if they can perceive the difference of the sounds themselves.

The reason of the feature (3) is that it is general for an IEC user to compare individuals relatively and then evaluate them. Since a normal EC generates offspring individuals using EC operations and fitness values of only its parent generation, it is not a problem to generate offspring using relative fitness. If absolute fitness values are used with fewer n -evaluation level of the feature (4), fitness values of almost individuals in early generations become poor and those in later generations become better, which reduces selection pressure and hinders IEC convergence.

The feature (4) causes quantization noise in fitness and may influence on IEC convergence. Unlike a fitness function, it is not easy for an IEC user to evaluate slight differences among individuals. This is a reason why rough evaluation levels, such as five-level or seven-level evaluations, are used for IEC. The ultimate level is one bit of *selected/unselected* used for simulated breeding that originates from a selection of artificial breeding. As the n -level evaluation rounds slight differences among real individuals and ignores them, subjective fitness values of an IEC user must include quantization noise. Even though it is said that genetic algorithms (GA) is robust for fitness noise or fluctuations in general, IEC convergence must be influenced badly by fitness noises: noises originating in reduced evaluation quantization levels, fluctuations of an IEC user's evaluations, and input inaccuracy. We may say that simulated breeding is the IEC with the most quantization noise in a sense. By contraries, psychological fatigue reduces in inverse proportion to the evaluation levels, and the simulated breeding requests fewer number of input operations, i.e. just clicking individuals without evaluating how good/bad they are. When we consider methods for reducing human fatigue discussed in section 3, we must think about the balance of IEC convergence speed and the easiness of operations and evaluations.

IEC simulators are useful for IEC research. Although IEC research should be evaluated with IEC users at the final stage, human users are not always the best for the IEC research. When we need to repeat experimental evaluations under the completely the same conditions, what we need is not human users who cannot provide us reliable objective data but an IEC simulator.

The IEC simulator looks similar to normal EC because the evaluation characteristics of an IEC user are replaced with a function. Their different point is whether the previously mentioned features (3) and (4) are included. The IEC simulator is designed by embedding a converter that converts values from a fitness function to relative and discrete fitness values into an EC framework. The evaluation characteristics of a pseudo-IEC user are expressed as those of a fitness function with the converter.

The converter equally divides the interval between the maximum and minimum fitness values into n and converts continuous fitness values to the relative and discrete ones of $1-n$ points [25]. Since there may be multiple best individuals with the same best fitness value of n points, elite individual(s) are selected randomly among the best individuals when elite strategy is used.

Refer the reference [20] for general IEC tutorial and a survey of wide variety of IEC applications and research on reducing IEC user fatigue. In this paper, we introduce new type of IEC research that is not found in 1990's.

2 New Type of IEC Applications

2.1 *As a Tool for Analyzing Human Mind*

Since IEC optimizes a target system based on a user's subjective evaluation scale in mind, we may be able to analyze his/her psychological measure or mental characteristics by analyzing the optimized target system. We may say that it corresponds to reverse engineering of software.

From the IEC-based fitting of hearing-aids or cochlea implants, it is expected that new facts in audio-psychology or audio-physiology may be able to be found by analyzing the optimized characteristics of hearing-aids or cochlea implants. It was made clear that the best characteristics of hearing-aids fitted using voice and those using music were different [14, 24.] It means that human beings hear voice and music with different manners, and we should keep it in our mind as a new fact for hearing compensation. Cochlear implant fitting has conducted based on the common sense that the more electric channels and the wider dynamic range of each channel, the better. However, the cochlear implant fitted by IEC had fewer channels than conventional ones and dynamic ranges of some channels were quite narrower. Nevertheless, it was reported that a correctness ratio of cochlear implant user improved from about 45% with a cochlear implant fitted based on conventional method to 92% with that fitted by IEC [11]. This fact implies that there is unknown mechanism of audio-psychology/physiology, and therefore there are possibility that new knowledge in this area may be found.

IEC was applied to measure the mental dynamic range of *happy–sad* [22]. Three schizophrenics and five mental healthy students were asked to make *happy* impression and *sad* impression using the IEC-based computer graphics (CG) lighting design system [1]. More than 30 subjects evaluated these 8 CG of each impression using the Nakaya's variation [13] of the Sheffé's method for paired comparisons [19], and a psychological scale was constructed. An order scale of *happy–sad* was also calculated from the obtained two scales for *happy* and *sad* impressions. This experimental result showed that it was significantly harder for these three schizophrenics to design *happy* impression than mental healthy subjects, while there was no significant difference for designing *sad* impression. Although the number of experimental subjects is too few to conclude, the experimental result implies that the dynamic range of schizophrenics for *happy–sad* is narrower than that of mental healthy people, which matches the thoughts of some therapists based on their experiences. If it is confirmed through further research, there is a possibility that this IEC-based method can provide useful information for psychiatric diagnostics.

2.2 Extended IEC Based on Physiologic Responses

Extended IEC based on IEC user's physiologic responses is an extension of conventional IEC that is based on psychological evaluations.

The first trial use of physiologic responses was that IEC inputted IEC user's physiologic responses and optimized physical parameters of sounds, images, or movies to bring his/her physiological condition to a certain target condition, such as relaxed or stressed one. Movies and music move us. Although their stories or scenes may be the biggest factors for influencing our emotion, physical features such as colors, motions, switching scenes, sound volume affect our physiological responses, too. If we can control these physical features, we may be able to control the physiological responses of listeners or viewers.

IEC inputs the differences of physiological responses, such as blood pressure, heart rates, or breathe rates, between the targeted relaxed or excited condition and current measured ones as fitness. We form the framework of the extended IEC's loop that the EC optimizes the physical features of the stimuli to an IEC user based on his/her physiological inputs iteratively [23].

The second trial was to use eye tracking for inputting IEC user's subjective evaluations instead of a mouse or keyboard [15]. This approach is based on the assumption that an IEC user watches individuals of his/her interest longer than others. Although there are remained problems such as verifying the assumption, detecting individuals of the interest from eye trajectory that always moves, comparing the superiority of this method to other input methods, and others, eye tracking-based IEC has potential for the cases that we do not want to use intentional inputs or cannot use it, and when trajectory itself has useful information rather than detecting the individuals in which a user is interested.

2.3 IEC with Evolutionary Multi-objective Optimization

The number of items that we want to optimize is not always one. Multi-objective optimization methods are used for this case. The number of research on evolutionary multi-objective optimization (EMO) has increased rapidly in this decade.

When it is hard or impossible to quantify some of these optimization objectives, IEC is combined with the EMO. For example, the conventional EMO is available to find the best apartments whose room sizes, tenant fees, and distances to the nearest stations are wide, less expensive, and near, respectively, but it cannot be used when new searching conditions of beauty of room inside/outside and great views from a room besides the above quantitative optimization objectives. In this case, we need to combine subjective visual evaluation with the EMO.

IEC and EMO were applied to design MEMS (or micromachine). UC Berkeley and other teams have tried to replace conventional CAD-based MEMS design with EMO-based design to automate the conventional manual designing. The EMO approach tries to find out designs of a MEMS acceleration sensor whose spring stiffness is strong enough, resonance frequency is close enough to the specification frequency, and area size is small enough, for example. However, fabricated MEMS does not always show the same characteristics as a MEMS simulator shows. It happens when MEMS simulation does not use the finite element method that shows high precision but request high computational cost. Besides it, there is an essential reason that we cannot design fitness functions for all evaluation items, and therefore, manual designing method has not been able to be automated completely.

To solve this problem, IEC that optimizes MEMS design based on MEMS designer's experiences and domain knowledge was combined with EMO [8]. As experienced MEMS designers can evaluate total quality of MEMS designs by just glancing at them, we can accelerate designing MEMS by embedding their evaluation into EC search.

Architectural design is its other application. Architects design room floor layouts under several restrictions and objects, for example, requirements of architectural laws such as window sizes, the pass condition from an entrance to a veranda through only public spaces such as house passages, a living room, and a kitchen, a room shape condition that requests rectangular or similar one but allows slight irregular room shapes, conditions that each room size is close to the target specific size, and others. Besides them, there are qualitative objects in architectural designs such as architects' experiences and their sense of beauty, and preference of clients, and therefore IEC and EMO are necessary for supporting its designs [2, 6].

There are several combination ways of IEC and EMO: a method that IEC runs first and narrows searching areas from the global view point and then EMO search starts; a contrary combination that EMO searches Pareto solutions first, and then IEC fine-tunes the solutions; a method that EMO runs several generations behind an IEC user's evaluation at every IEC generation. There are comparative reports, but the best combination of IEC and EMO and its performance may depend on application tasks.

We introduced IEC+EMO research within an ordinary IEC framework that an IEC user evaluates the output of the target system and EC inputs user's evaluations and optimizes the target system. This type of research is few. Note that there are many EMO papers with confusing names of interactive EMO or similar ones, and they do not mean IEC+EMO but mean that a human being selects Pareto solutions based on his/her visual inspection. For example, we cannot distinguish which type of research the reference [16] is from its paper title, but it is the latter type of EMO research. They may be categorized in IEC of wide definition IEC [20].

3 Research to Reduce IEC User Fatigue

3.1 *Learning User Models and Its Applications*

(a) Learning User Models

Since inputs and outputs to an IEC user are outputs of the target system (exactly speaking, values of optimization variables from EC) and subjective evaluations to EC, respectively, computer can observe both of them. If the computer can learn the relationship between these inputs and outputs, we can make a model of an IEC user's evaluation characteristics. Once we obtain the model, we can estimate user's evaluation previously. We may be able to accelerate IEC convergence by using the model as a pseudo-IEC user, simulating IEC process with a big population size and many generations, showing the best m individuals that the pseudo-IEC user finds out to a real human IEC user. Furthermore, when we obtain the user's evaluation model, there is a possibility that we can know the optimization parameters or hidden factors to which an IEC user attaches much importance by analyzing the model. Once we know the user's evaluation factors, we may use them to accelerate an IEC convergence.

There are three major approaches to make a model of IEC user's evaluation characteristics, i.e. a prediction model of user's evaluation values: (1) distance-based models, (2) neural networks (NN) learning, and (3) fuzzy systems.

Predicting user's evaluations based on the distance-based model is similar to the case-based reasoning in knowledge engineering. Distances on a searching space from the individual with unknown fitness to individuals whose fitness values were known in past generations are calculated, the known fitness values are weighed with inverse of the distances and the average of the weighted known fitness values is used as the estimated fitness.

The advantage of this method is that costly learning is not necessary and estimated user's fitness can be calculated from a few individuals in past generations. This feature is quite preferable for IEC that searches with small population size. Its

disadvantage is that its estimated fitness is not precisely obtained from Euclidian distances on a searching space when importance levels that an IEC user attaches to each of optimization parameters are different. In this case, we need to estimate the importance levels and calculate weighted Euclidian distances. If fitness values are not in proportion to distances in a searching space, nonlinear estimation methods, such as NN, are necessary for this distance-based model.

NN-based estimation is to learn the relationship between input and output data using a supervised learning, which methodology is easy to understand. This method works even when the contributions of optimization parameters to the total fitness are not equal or the relation between the parameters and the fitness is nonlinear. However, it is not easy to collect enough number of NN training data because the features of IEC are small population size and small number of searching generations. When enough number of training data is obtained after many generations, IEC may reach to the end of its search and the trained model may not be able to be used. There are several improvements for practical use of this NN approach, such as finding new NN that does not require many training data.

A fuzzy system that was off-line designed previously was used as a user model of evaluation characteristics [9]. The advantage of the off-line design is to use the model for predicting user's evaluation to accelerate IEC search from the first generation regardless the approaches of fuzzy systems or NN learning. The cases when the model is off-line designed are that same user applies IEC to the same optimization task or that the evaluation characteristics of multiple IEC users are similar. The case of the latter depends on application tasks; the variance of evaluations based on domain knowledge of multiple domain experts is small, while those based on user's preferences are big. Since evaluations for MEMS designs are based on experienced MEMS designers' domain knowledge and experts' evaluations are similar in general, the reference [9] could adopt this off-line method.

To obtain enough number of training data, just collecting fitness values in past generations is not good to learn user's evaluation characteristics because IEC fitness values are relative in each generation and therefore the best fitness in past generation may be worse than the worst fitness of the current generation. However, it is almost impossible to collect enough number of data for learning the user's evaluation characteristics without using fitness values in past generations.

The solution for this dilemma is to transform relative fitness values to absolute ones that can be compared over generations. One of the transformation is to evaluate the same individual in continuous two generations, assume the difference of the two fitness values to be the evaluation difference of two generations, and correcting all individuals of either of the two generation with the difference [25]. This simple transformation may accumulate transformation errors according to generations, but the simulation results showed that IEC with the prediction model was better than IEC without the model and that IEC with a prediction model trained with absolute fitness transformed by this simple method was better than that with relative fitness.

(b) Usage of Other Users' Evaluation Models

As described in the previous section, once an evaluation characteristics model of an IEC user is obtained, we can simulate IEC search with a pseudo-IEC user behind real user's evaluation. The IEC simulation can use big population size and many generations as much as computation time allows and provide the best m individuals, which helps to accelerate IEC convergence. This is a good approach to reduce IEC user fatigue. However, this method cannot be used in early generations until the model is learnt. If many generations are necessary for training the model, this method may not be used well till the end of the IEC search.

One solution for this problem is to prepare models of several users' evaluation characteristics previously, choose the most similar model to the real IEC user in each generation, and use the chosen model instead of the model of the real IEC user until the real IEC user's model is learnt [5]. In each generation, all models of other IEC users evaluate all individuals as the same as the real IEC user does, and evaluation vectors of the real IEC user and each of other models are compared, and the other user's model whose evaluation vector is the closest to that of the real IEC user is chosen as the alternative of the IEC user's model.

We can expect the better performance of the IEC simulation from the first generation if the chosen other user model and the real IEC user's one are similar; if they are not similar, the IEC simulation works worse. It is convenient if we can check the similarity before we really apply this method.

We made the boarder of effective and ineffective clear through simulation. We made two mixture Gaussian models of evaluation characteristics of users A and B. The similarity between two models is changed gradually by changing the parameters of the B model, and the effect of IEC simulation is measured. At the same time, the fitness differences of two models are normalized by the n of evaluation levels to absorb the difference of the evaluation levels. From these experiences, we can estimate whether the method of using other IEC user's models works well by checking the differences of users' fitness values previously. This is, we show some individuals to several IEC users previously, normalize their fitness values, calculate the difference of normalized ones, and decide whether we use this method by checking the fitness difference is smaller than the boarder of effectiveness and ineffectiveness.

3.2 New IEC Frameworks

(a) Tournament IEC

In typical conventional IEC, all individuals are shown to an IEC user and relatively evaluated in n -evaluation levels. This relative evaluation by comparing all individuals is heavy load for an IEC user, and especially evaluating sound or movie individuals that we cannot compare spatially increases user's mental load as if a

tramp concentration game. Its solution is a tournament IEC that does not request an IEC user to compare all individuals but pairs of individuals [7].

Tournament IEC makes pairs of all individuals randomly in each generation. The half of winner individuals at the first game go up to the second game, and this evaluation is iterated until one champion individual is obtained. Fitness is given to each individual according to the number of winning. The simplest way is to give the same fitness to all looser individuals at the same game. More precise fitting method takes into account the evaluation difference between an individual pair instead of 1 bit of win and loss. Thanks to taking into account the fitness difference, even if the second best individual is beaten by the champion individual at the first game, the second best does not become the worst looser [7]. This method corrects the fitness differences after a tournament game is over from the last game to the first game or its inverse order.

As the tournament IEC has less information than normal IEC that compares all individuals, its convergence may become slower than normal IEC. However, tournament IEC user's fatigue is improved largely thanks to paired comparison.

As the term of *tournament selection* is used in EC community, it is necessary to distinguish two *tournaments* when you survey IEC papers.

(b) Interactive PSO

Any individual-based optimization methods that do not request the information of a search space such as differential information can be used in an IEC framework. Since different optimization methods have different characteristics, we should investigate the best optimization method whose searching performance with fewer individuals and fewer generations is excellent for new IEC.

Particle swarm optimization (PSO) is one of such optimization methods. The comparative experiments of PSO and GA showed that PSO that uses space information for its velocity vector converges faster than GA for less complex benchmark functions such as DeJong's F_1 and F_2 but the PSO becomes worse than GA according to increasing complexity of benchmark functions [12]. As the landscape of IEC searching space is that of evaluation characteristics in IEC user's mind, it is hard to believe that the landscape is complex enough and fitness changes dramatically when values of optimization parameters change slightly. In many IEC applications, satisfied solutions can be obtained with smaller population size within fewer generations, and it is the proof that the IEC landscape is quite simple. Thus, we can expect that PSO is better than GA for IEC.

However, experimental comparison showed that interactive PSO is poorer than interactive GA for any simple benchmark functions unlike the comparison of PSO and GA. We analyzed the reason and found that fitness quantization noise that cannot be avoid due to the feature (4) mentioned in section sec:1 gave bad influence to the calculations of the global best and the local bests and the imprecise velocity vectors made the convergence of interactive PSO worse [12]. Less tolerance of PSO to fitness noise is a disadvantageous feature to use for IEC. In other words, if we can reduce the influence of the quantization noise, we can expect that interactive POS

converges faster than interactive GA. We proposed some methods for improvements and showed that it was true [12].

Conclusion

We overviewed the features of IEC research mainly in 2000's following remarks for developing IEC techniques in this paper. Most IEC research is within the typical IEC framework; EC optimizes the target system based on IEC user's subjective evaluation. Besides them, new types of IEC research can be found in this decade, and we introduced such research: measuring a psychological scale of an IEC user by analyzing the system optimized based on his/her psychological scale, IEC based on physiological responses, and IEC+EMO. Other features of IEC research are several trials to reduce IEC user fatigue and the start of new type/framework of IEC research.

Author is thinking that IEC is one of tools that realize *Humanized Computational Intelligence* and there must be several approaches to realize it besides the IEC. We would like to continue to research toward this big framework.

References

- [1] Aoki, K., Takagi, H.: 3-D CG Lighting with an Interactive GA. In: 1st Int. Conf. on Conventional and Knowledge-based Intelligent Electronic Systems (KES 1997), Adelaide, Australia, May 1997, pp. 296–301 (1997)
- [2] Brinstrup, A.M., Takagi, H., Tiwari, A., Ramsden, J.J.: Evaluation of Sequential, Multi-Objective, and Parallel Interactive Genetic Algorithms for Multi-Objective Optimization Problems 6, 319–354 (2006)
- [3] Ecemis, M.I., Wikle, J., Bingham, C., Bonabeau, E.: A Drug Candidate Design Environment Using Evolutionary Computation 12(5), 591–603 (2008)
- [4] Hayashida, N., Takagi, H.: Acceleration of EC convergence with Landscape Visualization and Human Intervention 1(4F), 245–256 (2002)
- [5] Henmi, S., Iwashita, S., Takagi, H.: Interactive Evolutionary Computation with Evaluation Characteristics of Multi-IEC Users. In: IEEE Int. Conf. on Systems, Man, and Cybernetics (SMC 2006), Taipei, Taiwan, October 2006, pp. 3475–3480 (2006)
- [6] Inoue, M., Takagi, H.: Layout Algorithm for an EC-based Room Layout Planning Support System. In: Int. Conf. on Soft Computing in Industrial Applications (SMCia 2008), Muroran, Hokkaido, Japan, June 2008, pp. 165–170 (2008)
- [7] Johanson, B.: Automated Fitness Raters for the GP-Music System Technical report, Masters Degree Final Project at University of Birmingham, UK (September 1997)
- [8] Kamalian, R., Takagi, H., Agogino, A.M.: Optimized Design of MEMS by Evolutionary Multi-Objective Optimization with Interactive Evolutionary Computation. In: Genetic and Evolutionary Computation (GECCO 2004), Seattle, WA, USA, June 2004, pp. 1030–1041 (2004)
- [9] Kamalian, R.R., Yeh, R., Zhang, Y., Agogino, A.M., Takagi, H.: Reducing Human Fatigue in Interactive Evolutionary Computation through Fuzzy Systems and Machine Learning Systems. In: Int. Conf. on Fuzzy Systems (FUZZ-IEEE 2006), Vancouver, Canada, July 2006, pp. 3295–3301 (2006)

- [10] Lameijer, E.-W., Kok, J.N., Bäck, T., Ijzerman, A.P.: The Molecule Evaluator. An Interactive Evolutionary Algorithm for the Design of Drug-like Molecules. *J. of Chemical Information and Modeling* 46(2), 545–552 (2006)
- [11] Legrand, P., Bourgeois-Republique, C., Péan, V., Harboun-Cohen, E., Levy-Vehel, J., Frachet, B., Lutton, E., Collet, P.: Interactive Evolution for Cochlear Implants Fitting 8(4), 319–354 (2007)
- [12] Nakano, N., Takagi, H.: Influence of Fitness Quantization Noise on the Performance of Interactive PSO. In: Nakano, N., Takagi, H. (eds.) *IEEE Congress on Evolutionary Computation (CEC 2009)*, Trondheim, Norway (May 2009)
- [13] Nakaya, S.: A Modification of Scheffe's Method for Paired Comparisons. In: Proc. of the 11th Meeting of Sensory Test, pp. 1–12 (1970) (in Japanese)
- [14] Ohsaki, M.: A Study on the Compensation for Hearing Impairment Based on Evolutionary Computation. In: Doctoral Dissertation, Kyushu Institute of Design (December 1999) (in Japanese)
- [15] Pallez, D., Collard, P., Baccino, T., Dumercy, L.: Eye-Tracking Evolutionary Algorithm to Minimize User Fatigue in IEC Applied to Interactive One-Max Problem. In: *Genetic and Evolutionary Computation (GECCO 2007)*, London, UK, pp. 2883–2886 (2007)
- [16] Sathe, M.: VDM Verlag, Saarbrücken, Germany (2008)
- [17] Sedwell, A.N., Parmee, I.C.: Techniques for the Design of Molecules and Combinatorial Chemical Libraries. In: *IEEE Congress on Evolutionary Computation (CEC 2007)*, pp. 2435–2442 (2007)
- [18] Simons, C.L., Parmee, I.C.: A Cross-Disciplinary Technology Transfer for Search-based Evolutionary Computing: From Engineering Design to Software Engineering Design 39(5), 631–648 (2007)
- [19] Scheffé, H.: An Analysis of Variance for Paired Comparisons 47, 381–400 (1952)
- [20] Takagi, H.: Interactive Evolutionary Computation: Fusion of the Capabilities of EC Optimization and Human Evaluation 89(9), 1275–1296 (2001)
- [21] Takagi, H., Ingu, T., Ohnishi, K.: Accelerating a GA Convergence by Fitting a Single-Peak Function 15(2), 219–229 (2003) (in Japanese)
- [22] Takagi, H., Takahashi, T., Aoki, K.: Applicability of Interactive Evolutionary Computation to Mental Health Measurement. In: *IEEE Int. Conf. on Systems, Man, and Cybernetics (SMC 2004)*, The Hague, The Netherlands, October 2004, pp. 5714–5718 (2004)
- [23] Takagi, H., Wang, S., Nakano, S.: Proposal for a Framework for Optimizing Artificial Environments Based on Physiological Feedback 24(1), 77–80 (2005)
- [24] Takagi, H., Ohsaki, M.: Interactive Evolutionary Computation-based Hearing-Aid Fitting 11(3), 414–427 (2007)
- [25] Wang, S., Takagi, H.: Improving the Performance of Predicting Users'. Subjective Evaluation Characteristics to Reduce their Fatigue in IEC 24(1), 81–85 (2005)

Part II

Intelligent Robotics

How to Generate and Realize Bipedal Gait in Unstructured Environments?

Miomir Vukobratović¹ and Branislav Borovac²

¹ Institute Mihajlo Pupin, Volgina 15, 11000 Belgrade, Serbia
vuk@robot.imp.bg.ac.yu

² Faculty of Technical Sciences, University of Novi Sad, 21000 Novi Sad, Serbia
Trg Dositeja Obradovića 6, Serbia
borovac@uns.ns.ac.yu

Abstract. When walking in an unstructured environment, human is realizing various trajectories, often arising due to an instantaneous situation that could not be predicted in advance. This imposes the requirement for on-line trajectory planning and constant changing of gait parameters (turning, stopping, acceleration and deceleration, switching from the walk on a flat to the walk on an inclined surface or staircases, etc.). In view of the prospect that humanoid robots of the future will share with humans living and working space it will be normally expected from them to possess similar walking capabilities. This work aims to demonstrate the possibility of on-line generation of complex motion as a combination of simple motions at particular joints, called primitives. Each primitive has its parameters and constraints that are determined on the basis of similar man's motions. The set of all primitives represents the base from which primitives are selected and combined for the purpose of performing the corresponding complex movement. The proof that a correct selection of primitives is made and that the movement is the appropriate one is obtained on the basis of the maintainance of dynamic balance, which is realized by monitoring the ZMP position, as well as based on the pattern of the very movement.

Keywords: humanoid, pattern generation, dynamic balance, ZMP, primitives.

1 Introduction

In the recent years we have witnessed an explosive development of Humanoid Robotics. However, in the realization of their movements, many humanoid robots perform motions that are synthesized in advance [1-4]. If robots are to share the

living and working space with humans, which assumes their motion in unstructured environments, it is not possible to program them in advance since they will have to react to the situations in real time during the motion realization, which will not be possible to plan in advance. This work demonstrates a way of how to approach solving of this problem.

The main task of humanoid in bipedal gait is to avoid overturning, so that maintenance of dynamic balance represents the primary control task. In [5], different control algorithms were analyzed with the aim of eliminating the effect of small disturbances. The task is split into two parts: maintenance of dynamic balance (the ZMP position is constantly measured during the gait and compared with the reference one, so that the task of this part of control law is to minimize the deviation) and preserving the anthropomorphic shape of motion. It should be pointed out that the priority of realization of the two parts of the same control task changes during the motion. When dynamic balance is endangered, its preservation (fall prevention) has an absolute priority, and when there is no danger of falling down, attention can be paid to the other tasks. The notion of dynamic balance has been considered in detail in [6, 7], especially from the aspect of biological principles that are used to preserve it, as well as in the case of a nonstandard foot-ground contact. In [8], a comparison was made of the fuzzy logic control and PID control. The mentioned strategies were mainly adequate for compensating small disturbances, whereas the compensation of large disturbances requires a different approach. The problem of classifying disturbances as small and large ones has been considered in detail in [9].

In the case of occurrence of large disturbances (e.g. when the robot is pushed by a large force or when it kicks its foot against an obstacle) the dynamic balance is instantaneously jeopardized; hence the system has to fully abandon the realization of the reference motion and undertake an urgent action to preserve dynamic balance, i.e. to prevent the fall. For example, an urgent action may be a step sideways if the disturbance was a strong lateral force. Only after reestablishing dynamic balance, the system can return to the reference motion and resume its further realization by imposing the reference control.

A main problem in compensating large disturbances in described way is the extremely short time available to form a compensating movement, since the shortage of time does not allow realization of complex computing and time demanding algorithms. Hence, in this work (it draws heavily upon [10]) we propose an approach that enables on-line generation of compensating movements for bipedal robots, based on using simple primitives, whose basic shape is known, whereby some of its parameters can be relatively easily modified on the basis of the disturbance characteristics. In [11-15], the authors used the entire movement as a primitive (overall gait, transition from standing to walking, etc.). An essential difference between such approach and the one proposed in this work is that the motion is formed on-line by a combination of primitives, and not of the movements recorded in advance. Complex movements are decomposed into simple ones, called primitives (e.g. leg stretching, leg bending, hip turning, etc.). It should be pointed out that in the course of a "normal" motion a human is realizing reflexly a whole

series of basic motions (primitives), modifying them in real time, by which the trajectory changes on-line and adapts to the instantaneous situation. Thus, for example, if a need arises to modify the motion (e.g. if there appears an obstacle that is to be swerved around or the need to climb the staircases) man does not waste time on the calculation of a new and complex motion to be realized and of new kinematic and dynamic parameters of motion, but he selects the most appropriate primitive from the already learned ones, by adjusting only some of the basic parameters such as the height of the leg lifting, angle of leg bending, or the stride length. By introducing the base of primitives that are realized by taking as a model human's movements, the aim of this work was to demonstrate that the appropriate selection and combination of primitives can yield the realization of a complex motion that was not planned in advance, and, at the same time, allows preservation of dynamic balance.

In this work we focus on the basic explanations of the notion and forms of primitives, and the approach is illustrated on the example of gait realization in the absence of disturbances. Further development of this approach, especially for the case of occurrence of large disturbances, will be reported in our forthcoming articles.

The article describes first the motion synthesis by semi-inverse method and then describes the primitives to be realized and the way they are used in the gait realization. Then we present the model of humanoid robot used for the simulation. Finally, we review the simulation results obtained on the basis of the presented approach for generating complex movements using primitives and compare them with the motion synthesized by semi-inverse method, serving as a reference. We also demonstrate the possibility of on-line modification of motion to allow the humanoid to swerve around an obstacle, as well the synthesis of the motion of staircase climbing.

2 Gait Synthesis

In this section we recall first the semi-inverse method and then describe several primitives and the way of their use.

2.1 *Gait Synthesis Using Semi-inverse Method*

The model of the system's dynamics relates the independent motion coordinates \mathbf{q}' and joint drives $\boldsymbol{\tau}$. In the single-support phase, all joint coordinates are independent and hence $\mathbf{q}'=\mathbf{q}''$, where the superscript n denotes the overall number of DOFs of the system, while in the double-support phase the number of independent coordinates is reduced due to the contact of the front leg with the ground. Depending

on the character of contact (heel-strike, flat-foot, etc.), the degree of this reduction will be different. In the current discussion, we concentrate on the single-support phase without compromising the generality of conclusions. Since $\mathbf{q}' = \mathbf{q}''$, the dynamic model is:

$$\boldsymbol{\tau} = \mathbf{H}(\mathbf{q})\ddot{\mathbf{q}} + \mathbf{h}(\mathbf{q}, \dot{\mathbf{q}}) + \mathbf{G}(\mathbf{q})$$

where \mathbf{H} is the system inertia matrix, \mathbf{h} is a vector comprising all 'velocity' influences (Coriolis, centrifugal, etc.), while \mathbf{G} is a vector of moments due to gravitational forces. The model is used for the synthesis of reference motion and the feed-forward control.

In the synthesis of reference motion, the overall number of DOFs whose motion is to be defined (\mathbf{n}) may be divided in the following way: $\mathbf{n} = \mathbf{n}_l + \mathbf{n}_a + \mathbf{n}_n + \mathbf{n}_w$, where \mathbf{n}_l corresponds to the joints of the legs, \mathbf{n}_a to the joints of the arms, \mathbf{n}_n to the joints of the neck, whereas \mathbf{n}_w corresponds to the joints of the waist. During the walk, certain 'subsystems' of the locomotion mechanism should realize an exactly defined function (e.g. the legs are to realize desired pace type, the arms have to perform a certain movement, etc.). In order to ensure this, the motion of that part of the system should be prescribed in advance. In this work, the basic legs' motion pattern was obtained by recording the performance of a human subject. The remaining part of the system should be solved in such a way to preserve the system's dynamic balance (during the whole motion duration it should be ensured that $\mathbf{M}_X = 0$ and $\mathbf{M}_Y = 0$) and under the condition that the posture of the locomotion system at the beginning and at the end of one step is identical (i.e. it is necessary to realize the repeatability conditions). In this way, the gait is ensured by repeating one synthesized step. The term "semi-inverse" denotes that part of the system's motion is prescribed in advance and for the rest it is determined so to satisfy the given conditions. Let us explain this in more detail.

Let us suppose that the humanoid walks in a certain manner. This may be achieved by prescribing (imposing) motion to the joints of the legs. With humans, these are learned patterns that can be recorded and applied to humanoids. Thus, let the motion of \mathbf{n}_l joints of the legs be prescribed (the motion copied from a human subject) and let their changes with time be given by $\mathbf{q}'(t)$. In [18], the trajectories of all 27 angular coordinates of the legs involved in one half-step were presented. The motion of the rest DOFs ($\mathbf{n}_a + \mathbf{n}_n + \mathbf{n}_w$) can be defined in the following way:

- If any arm activity (manipulation or some other activity) is to be performed¹ along with walking, then the arm joints motions are considered prescribed. Let there be \mathbf{n}_a such joints and let their changes be defined as $\mathbf{q}''(t)$.

¹ The arms may also be immobile with respect to the trunk during the walk.

- The neck has to orient the head in a prescribed direction involving n_n DOFs, and let their changes in the considered time period be $\dot{q}''(t)$. Thus, the motion at the total of $(n_l + n_a + n_n)$ joints is prescribed. The motion in the waist (n_w DOFs) is still undefined.
- Let there be $n_w = 3$ waist DOFs: \dot{q}'' ; two of them are utilized to maintain the dynamic balance ($n_{wZMP} = 2$): the trunk rotations left-right and forward-backward (motion in the frontal and sagittal planes).

To achieve balance, these motions should be calculated. First, it is necessary to define the ZMP position in the support area in the given time instant. Then the motion at two waist joints (which move the trunk in the frontal and sagittal planes) should be determined so that for the given ZMP dynamic balance conditions ($M_x = 0$ and $M_y = 0$) are fulfilled. Besides, in order the motion could be continued, it is necessary the mechanism postures at the beginning and at the end of a step are identical, i.e. that the repeatability conditions are fulfilled.

The remaining waist motion ($n_{w\text{rotation about } Z \text{ axis}} = 1$), can be either prescribed (if the given task requires it) or can be calculated so as to reduce the friction torque between the foot and the ground. Note that in the situation when the arms are not engaged in any functional activity, they usually move so as to assist the waist in reducing the friction torque [18]. In this way it is possible to determine motions at all joints of the locomotion system ($n_l + n_a + n_n + n_{wZMP} + n_{w\text{rotation about } Z \text{ axis}}$) so as to ensure dynamic balance and repeatability conditions, whereby the reference motion of the complete system is defined.

2.2 Basics of Motion Primitives

The term motion primitive (or shorter, primitive) stands for a basic and simple reflex or learned movement that a human or robot is capable to realize. A primitive itself should be simple in order it could be easily combined with the other primitives. Each primitive is parametrized and has the following parameters:

- intensity of the movement in the span of 0-1, which determines the extent to which, for example, a leg is to be bent or stretched,
- time instant at which the primitive execution should be started, and
- duration of the primitive, i.e. the time in which the primitive is to be executed.

Each of the primitives is realized by activating one or more DOFs. Fig. 1a shows stick diagrams representing bending of the leg that is in swing phase. In this case the joints at the hip, the knee, and the ankle are activated, so that a consequence of the simultaneous activation of all these joints is the leg lifting the way presented in Fig. 1a). Fig. 1b) shows the primitive by which the already bent leg in

swing phase is stretching, whereby use is made of the joints at the hip, knee, and ankle, as well as the link of the toes of the leg being in swing phase. This primitive is realized so to produce an appropriate stretching of the leg which will become supporting leg in the beginning of the double-support phase. It should be noticed that the given value of the angle at the hip at the end of leg stretching is different from zero (this value can change), and hence the leg after stretching remains stuck out forward.

Thus, as explained above, the primitive for bending the leg in swing phase involves activation of the joints at the hip, knee and ankle of the swing leg. Fig. 2 shows the primitives at each of these joints for the leg bending shown in Fig. 1a). Let us point out that the magnitude of the angle at the knee is twice larger than the magnitudes of the angles at the hip and the ankle. It is of the opposite sign, too. It should be noticed that in this case the angle of the toes link remained constant all the time and equal zero; hence its diagram has not been shown. Also, it is worth noting that the primitives can be reshaped very easily in the sense of varying the range of the changing angle (by multiplying with a factor smaller than 1 the span of the angle change will be narrower compared to q_{max} , where q_{max} represents the maximal value of the angle allowed by the structure of the given joint, so that there is no sense to multiply the q_{max} by a factor that is greater than 1), as well as by changing the duration of its realization (faster or slower movement execution).

Apart from the primitives imposed onto the swing leg, the primitives acting on the supporting leg: stretching of the supporting leg (Fig. 3a), as well as the primitive for the mechanism's inclination forward (Fig. 3b), were also realized.

In the realization of the primitive for stretching of the supporting leg (Fig. 3a) use is made of the ankle, knee, and hip joints. By the realization of primitives for stretching the supporting leg these joints move so to ensure that at the end of the movement, when the stretching intensity was preset to 1, the leg is fully stretched, which corresponds to the angles at the joints of 0 rad. Of course, it is possible to change the intensity of leg stretching, by which is changed the span of the motion the joints, and, by the same token, the characteristics of the movement.

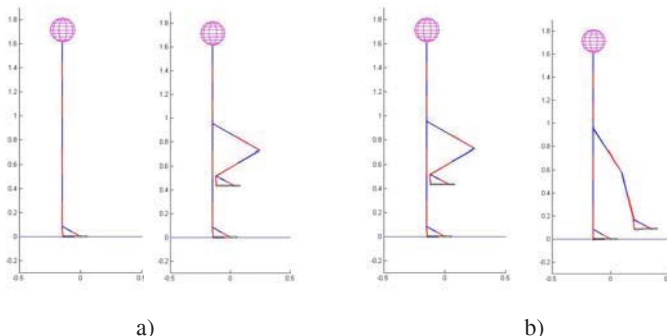


Fig. 1. Stick diagrams of the humanoid robot model in the realization of primitives by the swing leg: a) leg bending, b) leg stretching

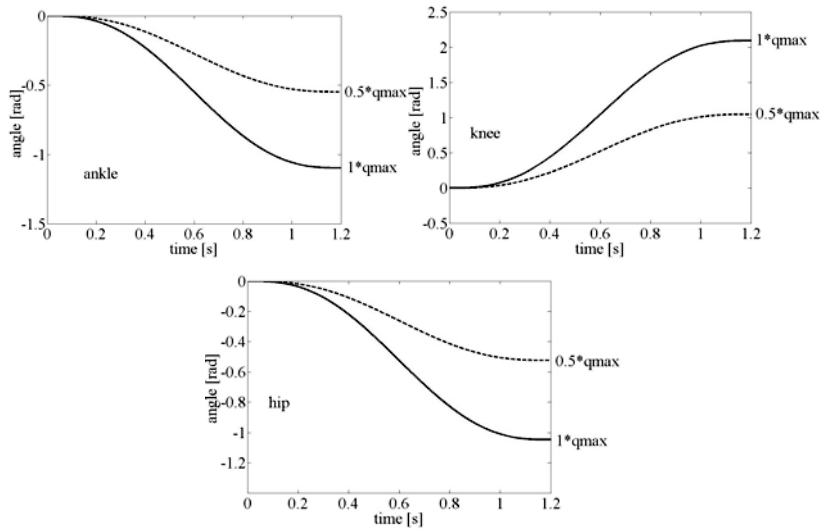


Fig. 2. Change of the angles at the ankle, knee, and hip in the leg bending during swing phase

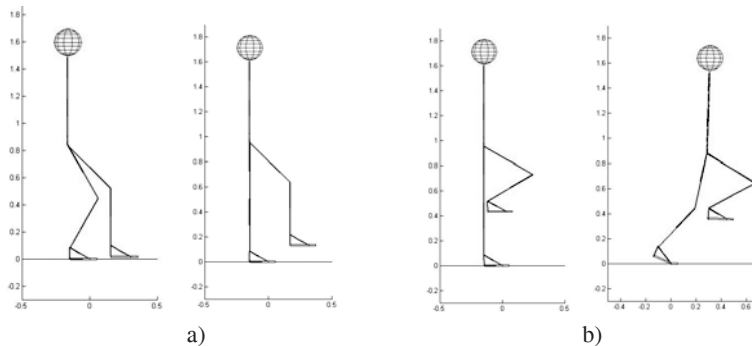


Fig. 3. Stick diagrams of the model of humanoid robot in the realization of primitives by the supporting leg: a) stretching, b) inclining the overall system, by which the system as a whole moves forward.

In the realization of the primitive for inclining, the supporting leg is activated again, and the same joints are used as in the realization of the primitive for stretching the supporting leg (Fig. 3b), but now the toes link is also activated since the rear part of the foot (heel) separates from the ground and the system remains supported only on the link of the toes. With this primitive, the angles at the joints of the knee and hip are of the opposite sign to the angles at the links of the toes and ankle, to ensure keeping the trunk in the upright position with respect to the external coordinate frame.

The realization of the next primitive (Figs. 4 a and b) yields the leg lifting. This primitive is similar to that of leg bending. The only difference is in that that the values of internal coordinates at the knee are imposed the way in which the shinbone remains parallel to itself during the gait realization, that is the value of internal coordinates at the knee is the same as at the hip, but with an opposite sign. The internal coordinates at the ankle of the swing leg remain unchanged in the course of imposing this primitive. The leg lowering movement is realized by a primitive that is completely inverse to the primitive of leg lifting. Figs. 4 a and b depicts the stick diagram of the humanoid realizing leg lifting, while leg lowering is not shown.

The last primitive to be dealt with is stepping sideways, which is applied when it is necessary to swerve around an obstacle but keeping the general direction of motion. The sideway stepping represents a synchronized and simultaneous movement of the both hip joints (the joint axes in Fig. 5 are \vec{e}_8 and \vec{e}_{16}), so that the legs move apart. At the same time the ankle axes (in Fig. 5 these are the axes \vec{e}_{11} and \vec{e}_{19}) turn appropriately to maintain the feet parallel to the ground. Fig. 4 shows the stick diagram of stepping sideways: Fig. 4c) depicts the mechanism in the initial position, Fig. 4d) stepping sideways at an intensity of 0.5, while Fig. 4e) illustrates stepping sideways at an intensity of 1. After the realization of stepping sideways the mechanism remains in the posture with the legs stretched apart, so that in order to return to "normal" posture it is necessary in the subsequent phase to "eliminate" the stepping sideways, i.e. to bring the angles of the axes \vec{e}_8 , \vec{e}_{16} , \vec{e}_{11} and \vec{e}_{19} back to their reference values.

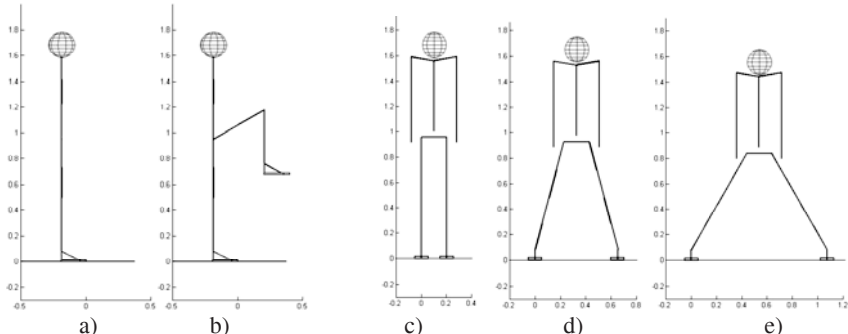


Fig. 4. Stick diagrams of the humanoid robot in the realization of two additional primitives. The first one (a and b) is leg lifting up, whereas the leg lowering is a completely inverse operation, and hence it is not shown. The other primitive (Figs. c, d and e) is the stepping sideways. Stepping sideways at an intensity of 0.5 is shown in d), and at intensity of 1 in e), while c) shows the initial posture. It should be noted that for realizing this primitive, before continuing the gait, it is necessary to bring back the humanoid from the straddle position to the initial posture.

3 Experimental Results

3.1 Mechanism Structure

The algorithm for mathematical modeling of the biped mechanism has already been well described in [16]. The mechanism used in this work [10] possesses four kinematic chains and 50 DOFs (see Fig. 5). The first and second kinematic chains form the left and right leg of the humanoid; the third represents the trunk and right arm, while the fourth one stands for the left arm.

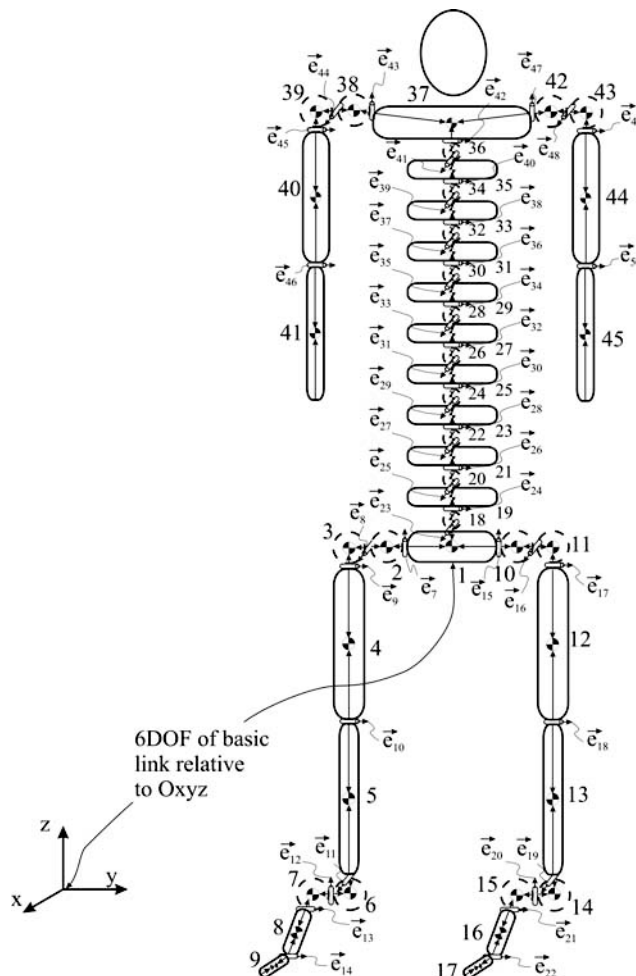


Fig. 5. Kinematic sketch of the free-flying mechanism with 50 DOFs

The trunk is not realized as a single link but as a 10-link one. Each of the joints connecting the trunk links has 2 DOFs and each of them allows relative rotation about the axes that are oriented in the directions of the x and y axes.

The software used for modeling and simulation of the humanoid robot motion has the possibility of realizing and disrupting contact between the mechanism and surrounding objects. Thus, for the purpose of gait simulation, an object is introduced that represents the ground on which the robot moves. In our case this was a flat surface. During the walk the robot is always in contact with the ground, at least via one foot. When the robot is in the single-support phase, the contact exists between the supporting leg and the ground, and in the double-support phase both feet are in contact with the ground. At the moments of transition from the single-support to the double-support phase and vice versa, the realization and breaking off the contact take place, respectively.

Evidently, the humanoid model considered here is very complex, especially from the aspect of the multilink trunk. We decided to use such a complex model because we expect it to be very convenient and indispensable in the subsequent phases of research, although the additional complexity of the trunk has no essential influence on the results presented in this paper.

3.2 Gait Synthesis – Walking on the Flat Surface

To assess its quality the motion realized by applying primitives was compared with that synthesized by the semi-inverse method [1-4], serving as reference. In this method, the motion of the legs² and the ZMP position are given in advance and the trunk motion is synthesized so as to ensure realization of the prescribed ZMP position. Since the ZMP is located in the predicted position inside of the support area, the robot is dynamically balanced during the whole half-step. Fig. 7 shows the stick diagrams of the reference motion during a half-step in frontal and side view, while Fig. 6 shows the reference trajectory of the ZMP.

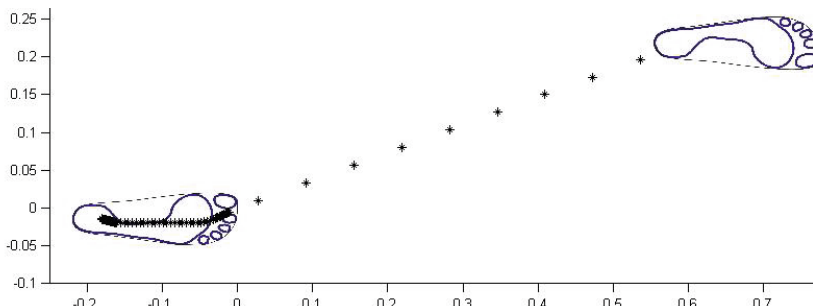


Fig. 6. ZMP trajectory for the reference half-step

² The motion of the legs was obtained based on human walk.

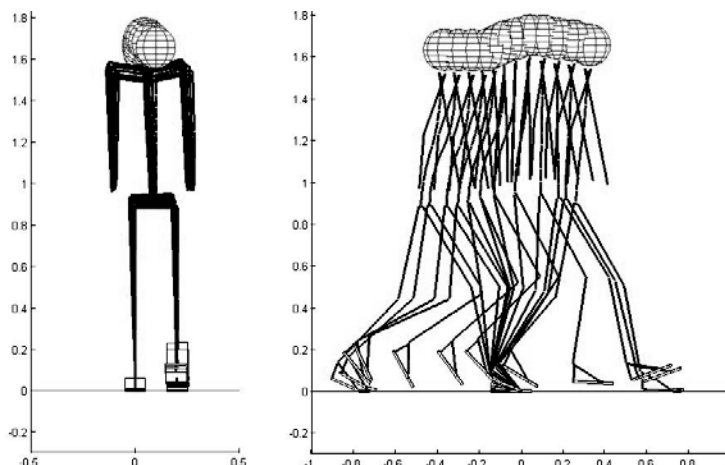


Fig. 7. Stick diagrams of dynamically balanced reference half-step synthesized by semi-inverse method

The example on which we will illustrate the realization of primitives is the humanoid gait that aims at being anthropomorphic. In order to realize it, the reference motion at the joints by which the robot moves forward (the joints corresponding to the rotation about the y axis, i.e. the joints 9, 10, and 14 for the right leg, and the joints 17, 18 and 21 for the left leg) is replaced with the corresponding primitives. The motion of the legs joints whose axes are parallel to the x and z axes and all motions of the trunk and arms were taken over from the reference motion. The state identical to the initial state in the reference motion was taken as the starting state. All movements presented lasted 2.4 s, which was realized in the simulation at the sampling interval of $\Delta t=0.00066$ s, corresponding to a total of 3600 iterations.

The newly obtained motion of the legs consists of the following combination of primitives. As first, bending of the swing leg was imposed at an intensity of 0.5 (dashed line on the diagrams in Fig. 2). The starting moment of the swing leg bending was the beginning of the movement (first iteration), and duration of the primitive was 1800 iterations. At the same time, the primitive for stretching (straightening) of supporting leg was imposed at the intensity of 1, which lasted 1200 iterations. This movement was followed by the primitives of the swing leg stretching and inclination of the supporting leg. Stretching of swing leg involved the following parameters: intensity 1, the primitive was started at the iteration no. 1800, and lasted the next 1800 iterations, i.e. till the end of the movement. The intensity of inclination of the supporting leg was 1, the primitive was imposed starting from the 1200th iteration and lasted also till the end of the movement, i.e. the next 2400 iterations. In this way we obtained a motion combined of different primitives, with duration of 3600 iterations, like the reference one. The motion obtained is represented by stick diagrams shown in Fig. 8.

Fig. 9 shows the magnitudes of the angles at the ankle, hip and knee of the supporting leg for the reference movement and for the movement obtained by using primitives for one half-step. It should be noticed that the motion in all presented diagrams for the supporting leg was a result of the combination of two primitives taking place in the sequence, i.e. stretching and inclining.

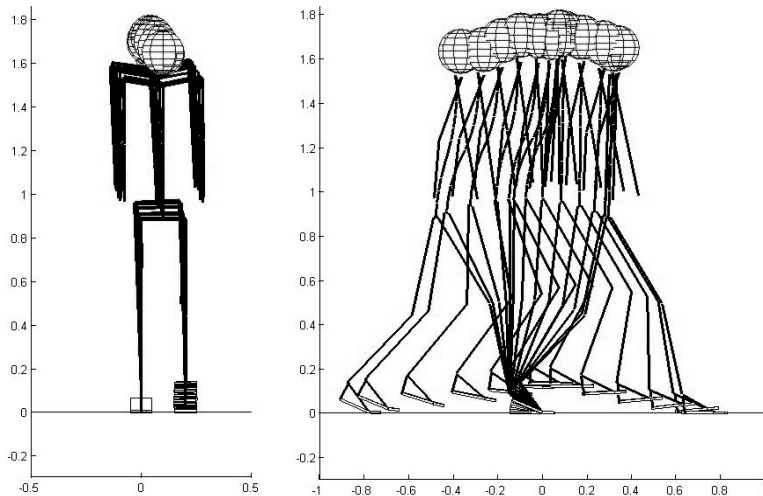


Fig. 8. Stick diagrams of the half-step when the motion was realized with the aid of primitives.

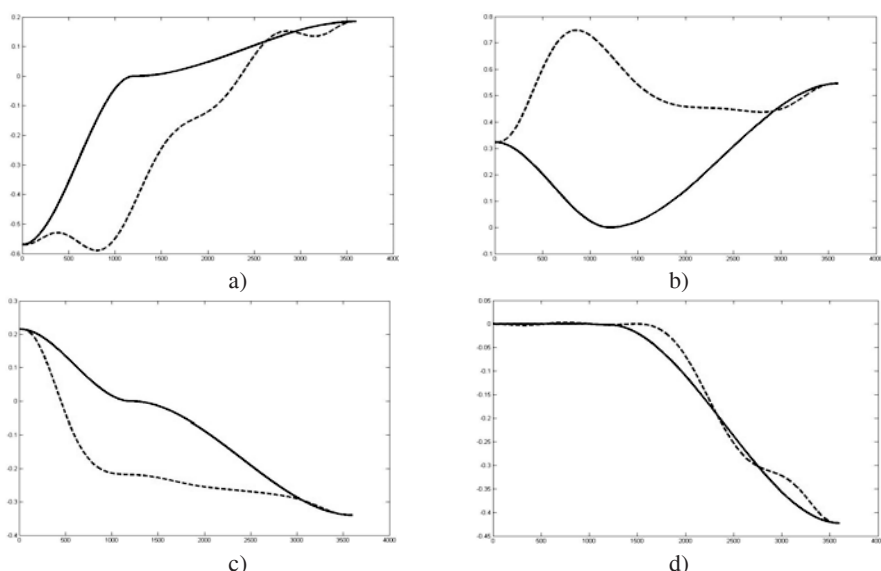


Fig. 9. Changes of the angles at the joints of the supporting leg for the reference half-step (dashed line) and the half-step obtained on the basis of primitives (full line): a) hip, b) knee, c) ankle, d) toes

The applying of the new, changed, motion, formed on the basis of primitives at the prespecified joints while keeping the reference motion at the other joints, yielded a significant distortion of the ZMP trajectory, as shown in Fig. 10. As can be seen, the robot would inevitably fall down. Hence it was necessary to correct the motion imposed at the joints, in order to preserve dynamic balance. The correction was made in the following way. Since the general pattern of motion was satisfactory it should be changed to a smallest possible extent, because it was only necessary to change the ZMP position. Hence, it was decided to change the acceleration at the ankle of the supporting leg in each sampling period to a sufficient extent so that the ZMP would be brought sufficiently close to its reference position (an acceptable deviation from the reference position was prescribed, and, when the ZMP entered that zone, the task was considered fulfilled). Double integration of the corrected accelerations yielded the corrected trajectories at the ankle.

Fig. 11 shows the stick diagrams of a half-step of the humanoid robot when the motion of the legs was realized by using primitives and applying correction at the ankle of the supporting leg, while Fig. 12 illustrates the ZMP trajectory in the case of the corrected motion.

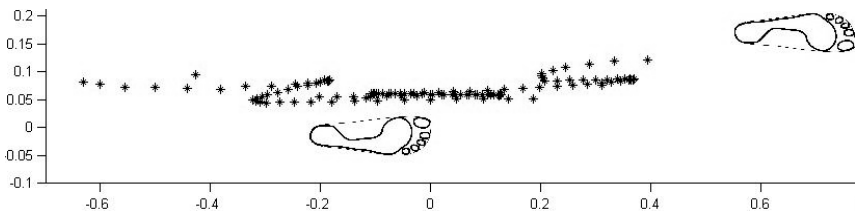


Fig. 10. ZMP trajectory for the half-step obtained by imposing primitives onto the legs

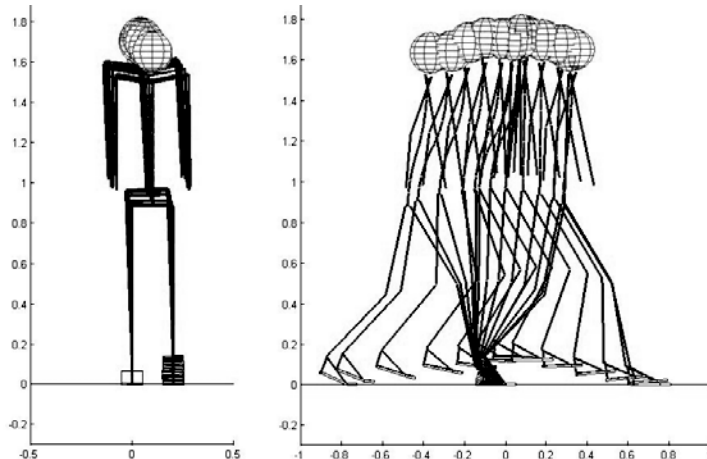


Fig. 11. Stick diagrams of the half-step when the primitives are imposed onto the legs, with the correction at the ankle

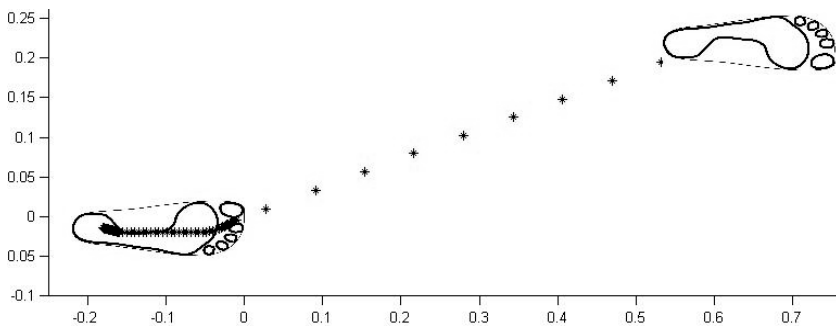


Fig. 12. ZMP trajectory with the correction at the ankle

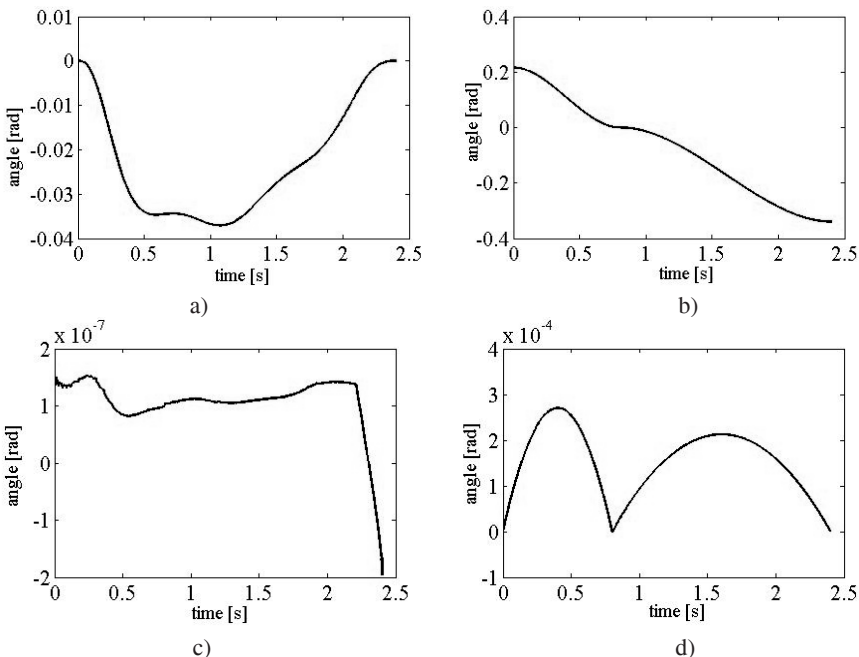


Fig. 13. Magnitudes of the angles with and without correction at the ankle at which correction was performed and the difference arising due the correction: a) angle about the x axis at the ankle (lines representing trajectories with and without correction coincide with each other), b) angle about the y axis at the ankle (lines representing trajectories with and without correction also coincide), c) the difference of the angles about the x axis of the ankle due to the correction, d) the difference of the angles about the y axis of the ankle due to the correction applied

Magnitudes of the angles about the x and y axes with and without correction at the ankle of the supporting leg are presented in Figs. 13 c) and d). It should be noted that both curves in Figs. 13 a) and b) coincide with each other, so that they are practically seen as one curve. As can be seen from Figs. 13 c) and d), the deviations at the ankle before and after the correction are minimal, and did not introduce significant change, as far as the movement pattern is concerned. Maximal

difference between the angles at the ankle before and after the correction does not exceed the value of 3×10^{-4} rad. By comparing Figs. 11 and 13 we can also see that the motion did not change significantly and that the desired pattern of the half-step has been preserved. However, a comparison of Figs. 10 and 12 reveals that the application of the correction yielded an essential improvement in the ZMP trajectory, and it is very similar to the reference trajectory of the ZMP shown in Fig. 6. This correction at the ankle, which, as already mentioned, did not influence the movement pattern, yielded a successful realization of a dynamically balanced gait using primitives.

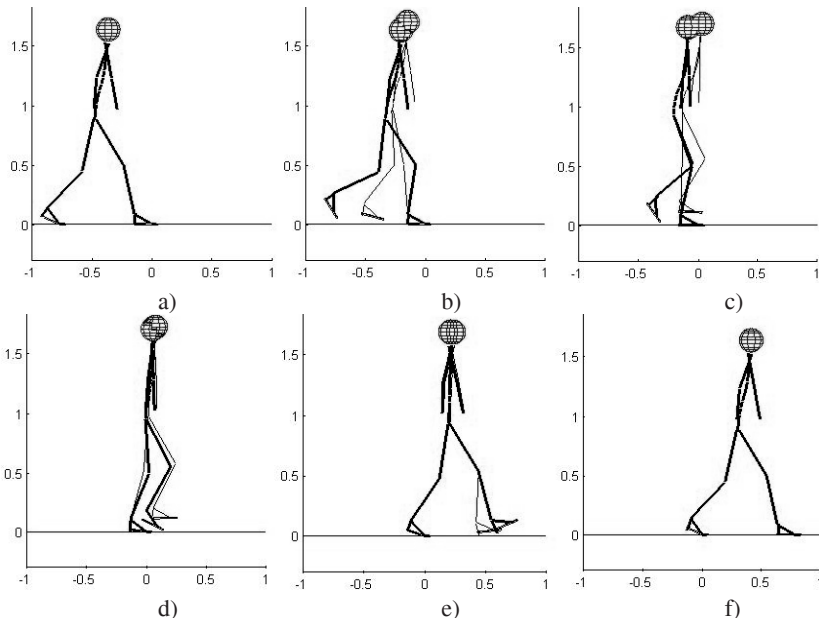


Fig. 14. Comparison of the motion of humanoid robot for the case when the motion was synthesized by semi-inverse method (thick line) and using primitives (thin line)

A question arises as to whether the correction of primitives in the way demonstrated in this work would be applicable if the robot had to perform on-line modification of its motion. We believe that this would be possible, for at least two reasons. As first, in the on-line modification of the motion it is not necessary to change completely the primitives imposed onto the legs, but only modify some of the parameters such as, for example, extending the stride, lifting the leg a little bit higher to surmount the obstacle that appeared in the way, or rotating additionally the leg at the hip to swerve around an obstacle. The other reason is the fact that the correction can be applied in the form of position control of the ZMP (correction of small disturbances), by which dynamic balance would be preserved (as was demonstrated in our previous work [5]), synthesized by the semi-inverse method (thick line) and with the aid of primitives (thin line).

Let us discuss briefly the comparison of the characteristics of the gaits synthesized by the semi-inverse method (Fig. 14, thick line) and by applying primitives (Fig. 14, thin line). The figure shows the superimposed stick diagrams for the two synthesized motions. It is clear that the postures at the beginning and at the end of motion coincide, which was a consequence of the appropriately prescribed limiting conditions, but between the limiting points the system did not move in a completely identical way in the two cases. This we do not consider as a shortcoming but as a potential advantage, because there is no any objective reason for the system to move in the same way. However, it should be pointed out that the system during the entire motion was dynamically balanced, and that there was no threat of falling down at any time instant. We expect that the results would be also similar in the case of an on-line modification of the motion.

3.3 Gait Synthesis – Walking on the Flat Surface with Obstacle Avoidance

An especially important task that should be realized by a "brand-new robot" entering the world of humans is the capability of moving in an unstructured environment. In that case it is not possible to program the motion in advance but it is necessary to change trajectory during the motion; in fact, it is necessary to enable its generation in real time. It should be noted that in this case a certain motion already exists, and its modification will yield a modified (arbitrary) trajectory. In this example we assumed that the already existing motion is an established rectilinear motion on the flat surface. There are a lot of ways in which such motion can be modified by slowing down, speeding up, swerving around an obstacle, obstacle overstepping, switching from the walking on the flat surface to climbing up the stairs, etc. Of course, all of them can not be dealt appropriately with in one article, so that we will present here only an illustrative example, and the other cases can be generated in a similar way. We chose the walk on the flat ground with obstacle avoidance as an example of the on-line modification of humanoid motion. We decided to realize obstacle avoidance by stepping sidewise (in this case the step is made by the right leg to the right side) with no rotation about vertical axis of the hip of the supporting leg, so that the system during the modification performs a translatory motion without changing direction of the motion. In other words, the humanoid that followed a rectilinear trajectory switches to a new path which is parallel to the previous one.

The rectilinear walk on flat surface, synthesized in the previous section (half-step duration of 2.4 s, i.e. 3600 iterations) served as the already existing motion. To the half-step of this motion the primitives were added for stepping sideways, causing the legs to move apart in the frontal plane, while in the subsequent half-step the motion of the joints at the hips and at the ankle return back to the reference trajectory. The primitive for stepping sideways is presented Figs. 4 c-e and described Sec. 2.2.

A total of three half-steps were synthesized. In the first half-step nothing was added to the reference motion, i.e. the robot was realizing "pure" reference motion. The second half-step, starting from the 1440th iteration, was modified by adding to the both hip joints the primitive of stepping sideways by the right leg at an intensity of 0.2, which lasted to the end of the half-step. Of course, the corresponding motion at the joints of both ankles was also modified.

In the third half-step, starting from the 360th iteration, a motion was imposed that was inverse to the primitive of stepping sideways (the legs are brought closer to the normal position), i.e. to return the system back to the normal position at an intensity 1 (the leg returns back to the state before applying stepping sideways primitive), so that both legs will move afterwards in parallel planes.

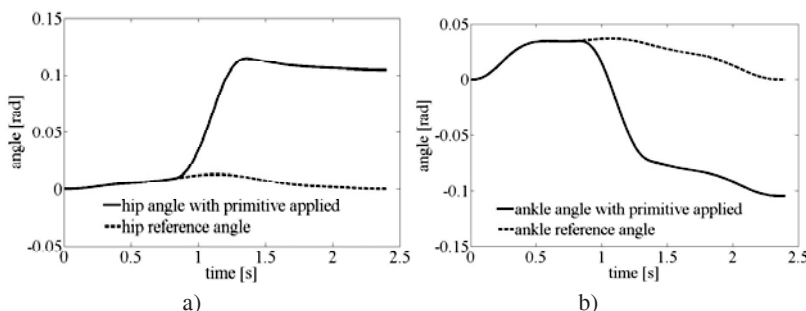


Fig. 15. Reference motion and motion modified by adding primitives: a) at the hip joint, and b) at the ankle

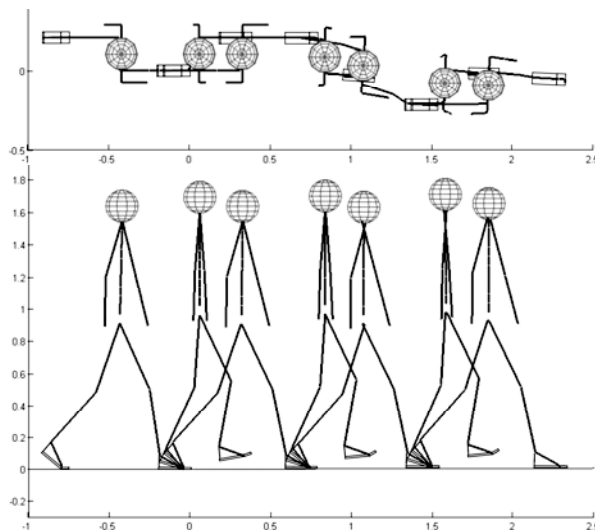


Fig. 16. Top view (upper) and side view (lower) at the stick diagrams representing the realization of humanoid's motion by stepping out to the right-hand side

After that follows the realization of the reference motion, but now along a trajectory that is not collinear to the reference one but is parallel to it at a distance that is equal to the size of the half-step. Fig. 15 shows the reference trajectories and the primitive-modified trajectories of the angles at the hip and ankle joints, while stick diagrams of humanoid's walk with obstacle avoidance are shown in Fig. 16.

3.4 Gait Synthesis – Climbing Up Stairs

The issue of switching from the realization of one type of motion to another, completely different motion, is a very interesting task. A good example of this is switching from the walk on a flat ground to climbing up stairs.

In order to make the climbing up stairs possible the base of primitives was expanded by adding two new primitives for the leg in swing phase. The first primitive is the leg lifting to the desired height, the maximum being determined by the maximum of the motion range at the hip joint, which depends on its construction. The other primitive is the leg landing, and it is completely inverse to the primitive of leg lifting.

In order to make clearer the process of the synthesis of motion up stairs, the motion was split into three phases. First, the robot from a regular walk is brought to the initial upright posture which is adopted to be the initial position for imposing the primitive for climbing up stairs. Then, it is to realize climbing the first step and afterwards the second step. Further climbing can be realized by repeating the movements performed to climb up the second step.

It should be pointed out that there is no reference motion for such type of walk, and the overall motion is to be realized by superimposing primitives. Climbing the first step is realized by combining the following primitives. First, to the robot in the upright position the leg-bending primitive is imposed, by which the leg takes off from the ground and passes to the swing phase. This primitive lasts 1650 itera-

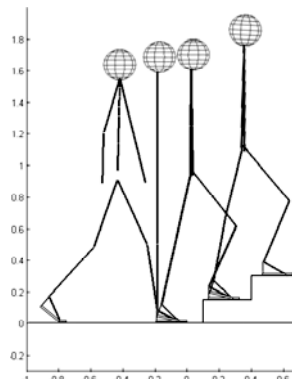


Fig. 17. Stick diagram (only four postures are shown) of humanoid robot climbing up stairs

tions at an intensity of 0.44. At the same time is imposed the primitive for lifting up the same leg. This primitive is imposed beginning from the 275th iteration and lasts to the 1925th iteration at an intensity of 0.2. In the span from the 1100th to the 2750th iteration the two primitives – for stretching the supporting leg and bringing down the swing leg – are imposed simultaneously at the intensities of 0.35 and 0.1, respectively. An additional primitive for inclining forward is imposed to the supporting leg from the 1350th to the 3000th iteration at intensity of 0.25.

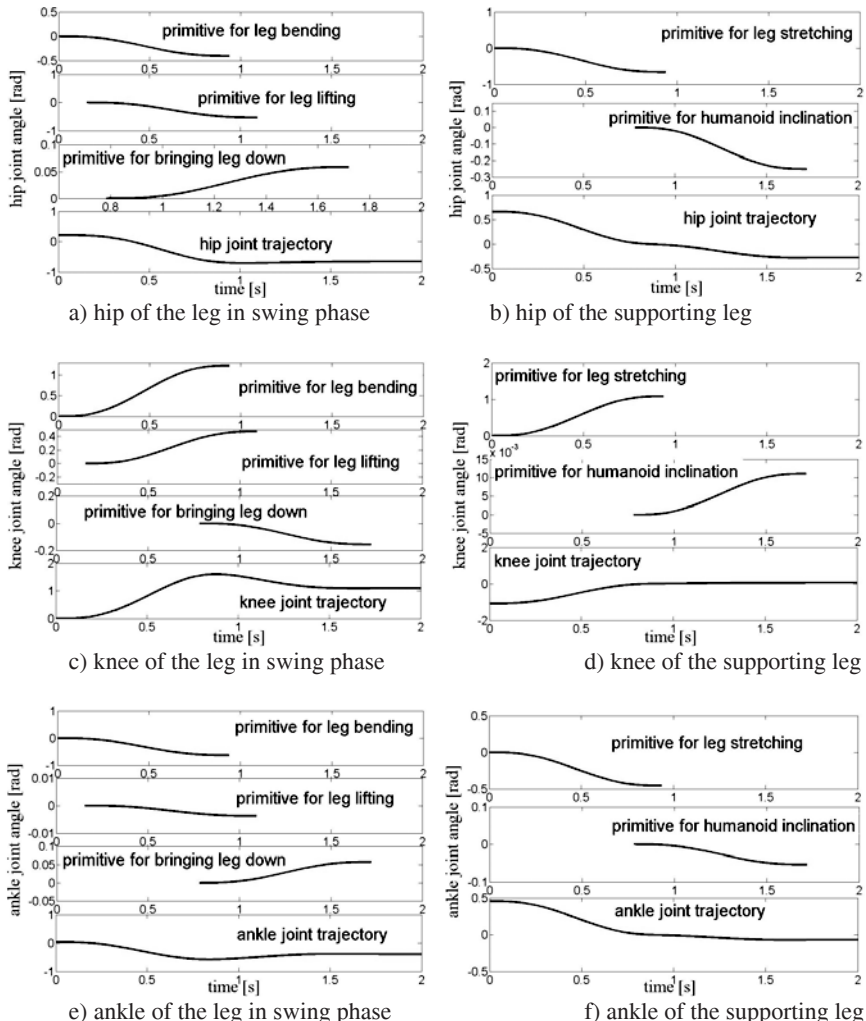


Fig. 18. Diagrams of forming the motion at the leg joints at the hip, knee and ankle (downwards) of the swing (left) and supporting (right) leg by superimposing primitives

The third phase is the climbing up the second step, the initial posture being different from the one prior to climbing the first step. In this phase is realized the leg bending lasting from the first to the 1650th iteration at an intensity of 0.44. The primitive for stretching the supporting leg is applied simultaneously (lasting also from the first to 1650th iteration at an intensity of 1). After that follows the lifting up of the swing leg, and this primitive lasts from the 275th to the 1925th iteration at an intensity of 0.23. Then comes the realization of the inclination³ (in Fig. 18 denoted as the primitive for humanoid inclination) of the supporting leg from the 1350th to the 3000th iteration at the intensity of 0.28, and finally, the landing of the swing leg lasting the same time at an intensity of 0.1. Afterwards, the procedure is repeated from the beginning.

Fig. 17 shows the stick diagrams of the humanoid climbing up stairs, while Fig. 18 illustrates all the primitives applied for the realization of climbing the second step and the overall motion at the joints of the hip, knee, and ankle for both legs of the humanoid.

Conclusion

Humanoid robots of the future will have to move in an unstructured environment, so that it will not be possible to plan and generate the entire robot's motion in advance. The direction and motion parameters will have to be determined and modified during the motion realization. Hence the need to develop a new approach that will enable modification of the current motion, or the synthesis of a completely new one, in real time, will be an inevitability.

In this work we presented one of the ways in which this problem may be approached. In contrast to the approaches in which the motion of the overall system is generated as a whole, we propose to compose the entire motion of the humanoid of a series of motions at particular joints. If a need appears that the humanoid has to adapt to the situation it found itself in the given moment, it is possible to simply modify the motion at the particular joints (e.g. to swerve around an obstacle), by adding appropriate primitive. It should be noticed that the combination of several simple primitives can lead to a significantly more complex movement.

The objective of this work was to clearly explain the basics of the notion, form and application of primitives, restricted to the realization of only the humanoid gait in the absence of disturbances.

The first example presented illustrates the synthesis of motion on a flat ground using appropriate primitives, the reference motion being synthesized by the

³ Inclination is realized by activating the joint by which the link of toes is connected to the rest of the foot, thus inclining the overall humanoid forward. To preserve the verticality of the trunk this inclination has to be compensated for, so that the curves of the "primitive for humanoid inclination" are applied at all joints of the supporting leg, which can be seen in the right-hand diagrams of Fig. 18.

semi-inverse method. Constant care was paid to preserving dynamic balance of the humanoid during the whole motion, which was also realized successfully.

Further, we showed that humanoid robot, using this approach of adding simply the appropriate primitives to the existing motion, can in real time modify its trajectory and swerve around an obstacle.

We also showed an example of the synthesis of motion of climbing up stairs, from which it is clear that once synthesized motion can be very easily modified and adapted to climbing stairs of different dimensions.

In the future research, this approach will be expanded by adding new primitives, which will allow the realization of much more complex motions.

References

- [1] Vukobratović, M.: How to Control the Artificial Anthropomorphic Systems. IEEE Trans. on System, Man and Cybernetics SMC-3, 497–507 (1973)
- [2] Vukobratović, M.: Legged Locomotion Systems and Anthropomorphic Mechanisms. Mihajlo Pupin Institute, Belgrade (1975); also published, Nikkan Shimbun Ltd. Tokyo (in Japanese), MIR, Moscow (1976) (in Russian), Beijing (1983) (in Chinese)
- [3] Vukobratović, M., Borovac, B., Surla, D., Stokić, D.: Biped Locomotion – Dynamics, Stability, Control and Application. Springer, Berlin (1990)
- [4] Vukobratović, M., Borovac, B.: Zero-Moment Point- Thirty Five Years of its Life. Int. Jour. of Humanoid Robotics 1(1), 157–173 (2004)
- [5] Vukobratović, M., Borovac, B., Raković, M., Potkonjak, V., Milinović, M.: On Some Aspects of Humanoid Robots Gait Synthesis and Control at Small Disturbances. Int. Jour. of Humanoid Robotics 5(1), 119–156 (2008)
- [6] Vukobratović, M., Herr, H., Borovac, B., Raković, M., Popovic, M., Hofmann, A., Jovanović, M., Potkonjak, V.: Biological Principles of Control Selection for a Humanoid Robot's Dynamic Balance Preservation. Int. Jour. of Humanoid Robotics 5(4), 639–678 (2008)
- [7] Vukobratović, M., Borovac, B., Potkonjak, V., Jovanović, M.: Dynamic Balance of Humanoid Systems in Regular and Irregular Gaits: an Expanded Interpretation. To appear in Intl. Journal of Humanoid Robotics 6(1) (2009)
- [8] Vukobratović, M., Borovac, B., Raković, M.: Comparison of PID and Fuzzy Logic Controllers in Humanoid Robot Control of Small Disturbances. In: Eurobot Conference 2008, pp. 69–79. MATFYZPRESS, Heidelberg (2008)
- [9] Vukobratović, M., Borovac, B., Potkonjak, V.: Towards a Unified Understanding of Basic Notions and Terms in Humanoid Robotics. Robotica 25, 87–101 (2007)
- [10] Vukobratović, M., Borovac, B., Raković, M., Nikolić, M.: Generating Complex Movements of Humanoid Robots by Using Primitives. In: Eurobot Conference 2009, La Ferte Bernard, France (May 2009) (to appear)
- [11] Hauser, K., Bretl, T., Latombe, J.-C.: Using Motion Primitives in Probabilistic Sample-Based Planning for Humanoid Robots. In: Algorithmic Foundation of Robotics VII, vol. 47, pp. 507–522. Springer, Heidelberg (2008)
- [12] Zhang, L., Bi, S., Liu, D.: Dynamic Leg Motion Generation of Humanoid Robot Based on Human Motion Capture. In: Xiong, C.-H., Liu, H., Huang, Y., Xiong, Y.L. (eds.) ICIRA 2008. LNCS (LNAI), vol. 5314, pp. 83–92. Springer, Heidelberg (2008)

- [13] Denk, J., Schmidt, G.: Synthesis of Walking Primitive Databases for Biped Robots in 3D-Environments. In: Proceedings of the IEEE International Conference on Robotics and Automation (ICRA), Taipei, Taiwan, vol. 1, pp. 1343–1349 (2003)
- [14] Nakaoka, S., Nakazawa, A., Yokoi, K., Ikeuchi, K.: Leg Motion Primitives for a Humanoid Robot to Imitate Human Dances. *Journal of Three Dimensional Images* 18(1), 73–78 (2004)
- [15] Ha, S., Han, Y., Hahn, H.: Adaptive Gait Pattern Generation of Biped Robot based on Human's Gait Pattern Analysis. *International Journal of Mechanical Systems Science and Engineering* 1(2), 80–85 (2007)
- [16] Potkonjak, V., Vukobratović, M., Babković, K., Borovac, B.: General Model of Dynamics of Human and Humanoid Motion: Feasibility, Potentials and Verification. *Int. Jour. of Humanoid Robotics* 3(2), 21–48 (2006)

PDAC-Based Brachiating Control of the Multi-locomotion Robot

Toshio Fukuda¹, Tadayoshi Aoyama¹, Yasuhisa Hasegawa², Kosuke Sekiyama¹, and Shigetaka Kojima³

¹ Department of Micro-Nano Systems Engineering, Nagoya University
Furo-cho, Chikusa-ku, Nagoya, 464-8603, Japan
fukuda@mein.nagoya-u.ac.jp, aoyama@robo.mein.nagoya-u.ac.jp,
sekiyama@mein.nagoya-u.ac.jp

² Department Intelligent Interaction Technologies, University of Tsukuba
1-1-1 Tenodai, Tsukuba, 305-8573, Japan
hase@esys.tsukuba.ac.jp

³ Department of Mechanical Science and Engineering, Nagoya University
Furo-cho, Chikusa-ku, Nagoya, 464-8603, Japan
kojima@robo.mein.nagoya-u.ac.jp

Abstract. This paper introduces the multi-locomotion robot which has multiple types of locomotion at first. The robot has been developed to achieve a bipedal walk, a quadrupedal walk, and a brachiation, mimicking locomotion ways of a gorilla. It therefore has higher mobility by selecting a proper locomotion type according to its environment and purpose. When we consider a transition motion connecting one locomotion form to another, two designed controllers corresponding to each locomotion type are not enough. A new control algorithm that covering control properties of two locomotion controllers should be developed, because the intermediate motion cannot be realized by fusing control outputs from two controllers. Previously, based on this notion, we have proposed a novel method named Passive Dynamic Autonomous Control (PDAC) that realized not only a bipedal walk but also a quadruped walk. In this paper, the PDAC is also applied to a brachiation motion on the irregular ladder; then the proposed controller is validated by the experiment.

Keywords: multi-locomotion robot; brachiation; PDAC; motion control.

1 Introduction

In recent years there have been many successful researches that focus on dynamic and skillful motions performed by animals [15-17, 19, 24]. Especially, brachiation

is an interesting form of locomotion performed by long-armed apes by using their arms to swing from branch to branch. This motion is a dynamic and dexterous action routinely performed by some kinds of apes [23]. Many kinds of brachiation robots have been developed. A pioneering research analyzed dynamics of brachiation and proposed using a six-link brachiation robot [7]. Fukuda *et al.* [8, 20, 21] developed a 2-link brachiation robot, “Brachiator II”, and proposed a heuristic method to find feasible motions. A self-scaling reinforcement learning algorithm was also proposed to achieve robustness against some disturbances [9]. As an analytical approach, Nakanishi *et al.* proposed the “Target Dynamics Method”, in which the target dynamics are used as inputs to the controller; they investigated the “ladder”, “swing up”, “rope” and “leap” problems [18]. Considering the control of higher degrees of freedom, Fukuda *et al.* then developed “Brachiator III” [22]. The dimension and location of the joints are based on those of a long-armed ape’s. As a hierarchical behavior-based approach, Hasegawa *et al.* proposed an adaptation method that measures effects of each local behavior on the target motion and determines activation levels of each local behavior controller [10]. Then, Kajima *et al.* proposed an enhanced control method which can adjust the timing of local behaviors of a robot in order to achieve two types of brachiation: over-hand and side-hand motions [14]. However, they were mainly focused on a single type of locomotion, such as brachiation.

On the other hand, many animals, such as primates, use a primary form of locomotion but switch to other types depending on their surroundings, situation and purpose. For instance, a gorilla has high mobility in a forest by adopting bipedal walking in a narrow space, quadrupedal walking on rough terrain and brachiation in the forest canopy. Inspired by these high mobility of an animal, we have developed a anthropoid-like “Multi-locomotion robot” that can perform several types of locomotion and choose the proper one on an as-needed basis (Fig. 1) [1, 3, 11, 13, 26]. A development of a bio-inspired robot which has multiple locomotion types for high mobility is one of challenging issues, because a problem is remaining in addition to research issues on humanoid robot study. That is a control architecture that synthesizes some controllers for each locomotion. When we consider a transient motion connecting one locomotion to another, two designed controllers corresponding to each locomotion type are not enough. A new control algorithm that covering control properties of two locomotion controllers should be developed because the intermediate motion cannot be realized by fusing control outputs from two controllers. Based on this notion, we have proposed a novel method named Passive Dynamic Autonomous Control (PDAC) [4] that realize not only a bipedal walk [5, 6] but also a quadrupedal walk [2]. In this paper, the PDAC is also applied to a brachiation motion on the irregular ladder; then the proposed controller is validated by the experiment.

This paper continues as follows. In Section 2 we introduce the Gorilla Robot III that has been developed as a prototype of the multi-locomotion robot. In Section 3 we explain about PDAC concisely. Section 4 describes the design of the irregular ladder brachiation and Section 5 shows the experimental results. Finally, we summarize this paper in Section 6.

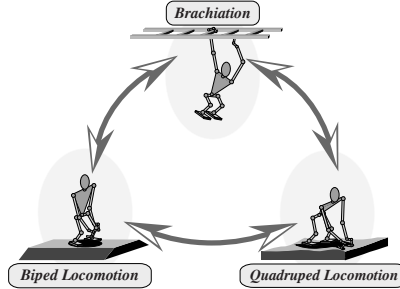


Fig. 1. Concept of the multi-locomotion robot

2 Multi-locomotion Robot

The dimensions of the multi-locomotion robot we developed is determined by those of a gorilla, and therefore the robot is called “Gorilla Robot III”. Figure 2 shows the overview of Gorilla Robot III and its link structure. This robot is about 1.0 [m] tall, weighs about 24.0 [kg], and consists of 25 links and 24 AC motors including two grippers. The real-time operating system VxWorks (Wind River Systems Inc) runs on a Pentium III PC for processing sensory data and generating its behaviors. Two kinds of sensors are attached to each hand. The rate gyroscope, CRS03-04 manufactured by Silicon Sensing Systems Japan Ltd., measures the angular velocity around the contact bar to calculate the pendulum angle during the motion. The force sensor, IFS-67M25A made by NITTA CORPORATION, measures reaction forces from contact bars in order to judge whether the robot successfully grasps the bar or not.

This robot has been designed to perform biped locomotion, quadruped locomotion and brachiation. We designed the controller for all locomotion using the same algorithm “PDAC”. The approach of PDAC is to describe the robot dynamics as a 1-DOF autonomous system around a contact point, using an interlocking so that the robot could keep the robot inherent dynamics. The PDAC is explained in the next section. 3-dimensional natural dynamic walking is achieved as shown in Fig. 3 [6]. We also designed a controller for a quadrupedal walk [2] using the same PDAC. The snapshots of the quadrupedal walk are shown in Fig. 4.

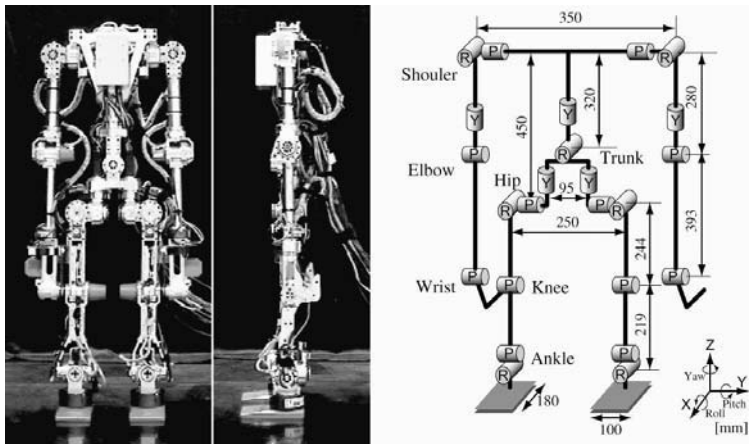


Fig. 2. Gorilla Robot III

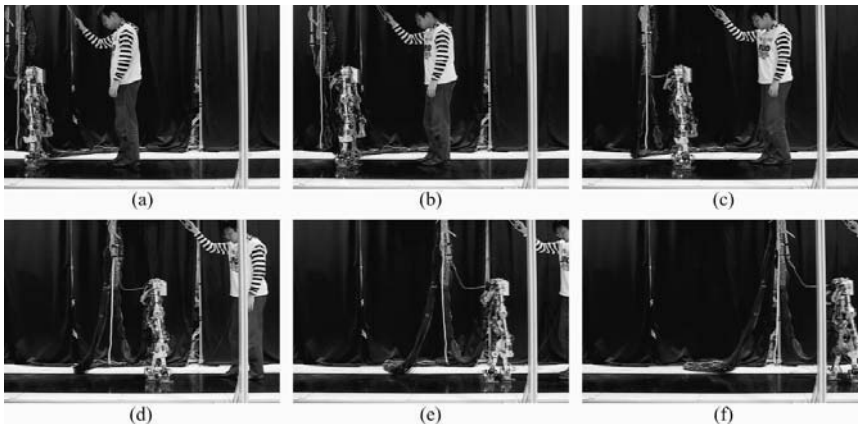


Fig. 3. Snapshots of the bipedal walking using PDAC. Each figure shows the snapshots at (a) 1st, (b) 7th, (c) 12th, (d) 16th, (e) 19th, (f) 22th step.

3 Passive Dynamic Autonomous Control (PDAC)

In this section, Passive Dynamic Autonomous Control (PDAC), which was proposed before [4], is explained briefly. PDAC employs the two following premises: point-contact (underactuation) and *Virtual Constraint* [25]. Virtual Constraint is the

holonomic constraint applying virtually to the robot dynamics. These premises make it possible to describe whole robot dynamics as 1-dimensional autonomous system, that is, the phase around contact-point. This phase makes it possible to analyze the locomotion motion in the irregular ladder environment, which is explained about later.

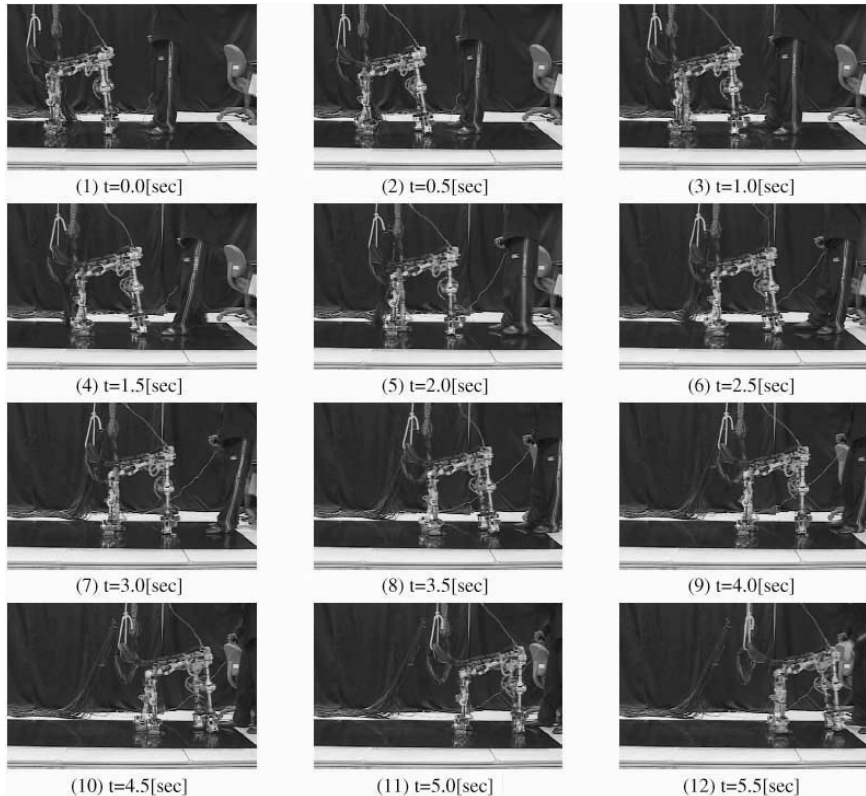


Fig. 4. Snapshots of the quadrupedal walking using PDAC

Assuming that PDAC is applied to the serial n-link rigid robot (θ_i and τ_i are the angle and the torque of i^{th} joint respectively. m_i and J_i are the mass and the moment of inertia of i^{th} link respectively), these two premises are expressed as follows:

$$\tau_1 = 0, \quad (1)$$

$$\begin{aligned} \Theta &= [\theta_1, \theta_2, \dots, \theta_n]^T = [f_1(\theta), f_2(\theta), \dots, f_n(\theta)]^T \\ &=: \mathbf{f}(\theta), \end{aligned} \quad (2)$$

where θ is the inclination of the first link in the absolute coordinate system. Since the first joint is unactuated, the way to define the coordinate system of the first joint and the robot dynamics itself are irrelevant. Thus, the coordinate system of the first joint is defined as the absolute one, that is, $\theta_1 = f_1(\theta) = \theta$.

The dynamic equations of this model are given by

$$\frac{d}{dt} (\mathbf{M}(\Theta) \dot{\Theta}) - \frac{1}{2} \frac{\partial}{\partial \Theta} (\dot{\Theta}^T \mathbf{M}(\Theta) \dot{\Theta}) - G(\Theta) = \boldsymbol{\tau}, \quad (3)$$

where $\mathbf{M}(\Theta) = [\mathbf{m}_1(\Theta)^T, \mathbf{m}_2(\Theta)^T, \dots, \mathbf{m}_n(\Theta)^T]^T$, $\Theta = [\theta_1, \theta_2, \dots, \theta_n]^T$, $G(\Theta) = [G_1(\Theta), G_2(\Theta), \dots, G_n(\Theta)]^T$, $\boldsymbol{\tau} = [\tau_1, \tau_2, \dots, \tau_n]^T$, $\frac{\partial}{\partial \Theta} = \left[\frac{\partial}{\partial \theta_1}, \frac{\partial}{\partial \theta_2}, \dots, \frac{\partial}{\partial \theta_n} \right]^T$. Since in this model the dynamic equation around the contact point has no term of the Coriolis force, it is given as

$$\frac{d}{dt} (\mathbf{m}_1(\Theta)^T \dot{\Theta}) - G_1(\Theta) = \tau_1. \quad (4)$$

By differentiating Eq. (2) with respect to time, the following equation is acquired,

$$\dot{\Theta} = \frac{\partial \mathbf{f}(\theta)}{\partial \theta} \dot{\theta} = \left[\frac{\partial f_1(\theta)}{\partial \theta}, \frac{\partial f_2(\theta)}{\partial \theta}, \dots, \frac{\partial f_n(\theta)}{\partial \theta} \right]^T \dot{\theta}. \quad (5)$$

Substituting Eq. (1), (2) and (5) into Eq. (4) yields the following dynamic equation,

$$\frac{d}{dt} (M(\theta) \dot{\theta}) = G(\theta), \quad (6)$$

where

$$M(\theta) := \mathbf{m}_1 \mathbf{f}(\theta)^T \frac{\partial \mathbf{f}(\theta)}{\partial \theta}, \quad (7)$$

$$G(\theta) := G_1 \mathbf{f}(\theta). \quad (8)$$

By multiplying both sides of Eq. (6) by $M(\theta)\dot{\theta}$ and integrating with respect to time, the dynamics around the contact point is obtained as follows:

$$\int M(\theta)\dot{\theta} \frac{d}{dt}(M(\theta)\dot{\theta}) dt = \int M(\theta)G(\theta)\dot{\theta} dt \quad (9)$$

$$\Leftrightarrow \dot{\theta} = \frac{1}{M(\theta)} \sqrt{\int 2G(\theta)M(\theta) d\theta}. \quad (10)$$

Assuming that the integration in right side of Eq. (10) is calculated as $\int G(\theta)M(\theta) d\theta = D(\theta) + C$, Eq. (10) is described as the following 1-DOF autonomous system,

$$\dot{\theta} = \frac{1}{M(\theta)} \sqrt{2D(\theta) + C} \quad (11)$$

$$:= F(\theta). \quad (12)$$

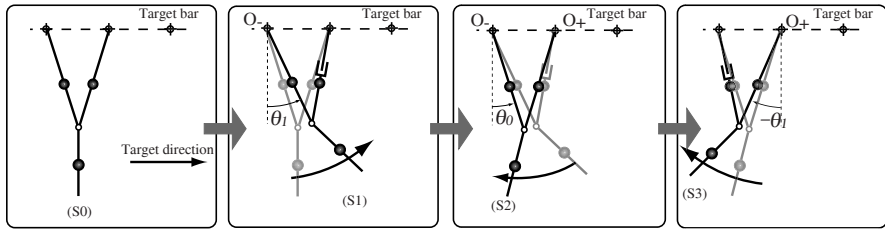
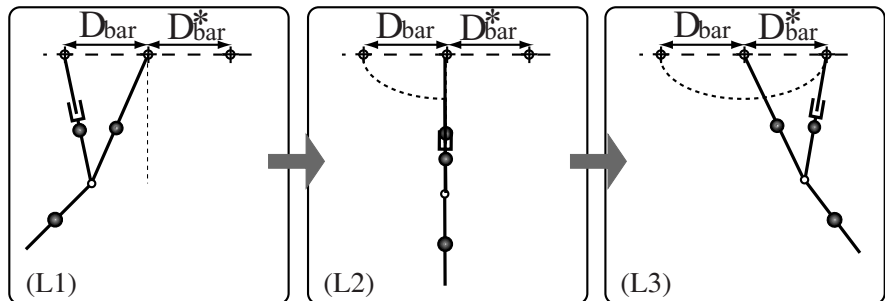
We term Eq. (11) and (12) converged dynamics. The remarkable point is that if there is no error such as the model error or disturbance, the actual dynamics of $\dot{\theta}$ is identical with the converged dynamics definitely, since it is obtained from the robot inherent dynamics.

4 Continuous Brachiation on the Irregular Ladder

4.1 Motion Design of the Brachiation

In this paper, in order to simplify the controller design, the whole robot is modeled as the 3-link: swing-arm, support-arm and torso. In the actual motion, the elbow of swing-arm is bended during locomotion; however, this paper assumes that its effect on dynamics can be neglected since the bending angle is relatively small. Support-arm is controlled to be kept stretched. Both legs are actuated to be fixed and not moved so that torso and legs can be seemed a link. Note that the torque around a bar cannot be applied. Thus, the main issue regarding brachiation is how to control and actuate the swing-arm and the torso in order to achieve the continuous and stable brachiation.

The brachiation controller is composed of two actions: swing action (Fig. 5) and locomotion action (Fig. 6). In the swing action phase, the robot injects the energy by swinging back the torso prior to the locomotion action. In the locomotion phase, the robot moves toward the target direction after releasing the rear bar and grasps the front bar at the end of the action.

**Fig. 5.** Swing action**Fig. 6.** Locomotion action

As for the uniform ladder problem, it is possible to design the locomotion action symmetrically along the gravitational direction, that is, the first-half motion (from (L1) to (L2)) and the last-half motion (from (L2) to (L3)) are symmetrical. Under the condition of symmetric motion along the gravity force, the effects of the first-half motion and the last-half motion on the dynamics are antithetical, hence the mechanical energy in (L1) and (L3) are identical. We proposed previously the control method of the uniform ladder brachiation based on this symmetric property [12].

However, in the irregular ladder environment, symmetric motion cannot be designed as shown in Fig. 7. Thus, it is impossible to apply the same strategy as the uniform ladder brachiation. In order to achieve the irregular ladder brachiation, it is necessary to estimate the energy difference between (L1) and (L3) caused by symmetry breaking. In order to evaluate the energy difference, we apply PDAC to the locomotion action. Swing motion is adjusted so as to satisfy the desired energy calculated from energy difference. The motion scheme is explained in detail below.

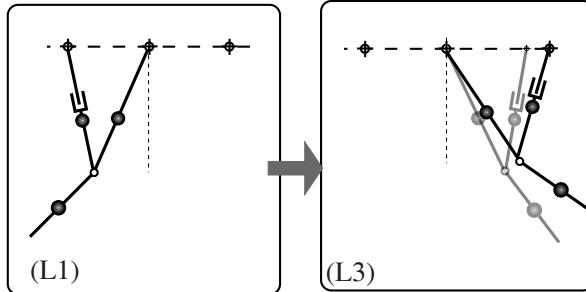


Fig. 7. Symmetry breaking

4.2 Locomotion Action

As mentioned previously, this paper employs 3-link model as shown in Fig. 8. Link 1 is stretched arm, link 2 is a swinging arm, and link 3 is a torso and legs. P is the position of a shoulder, O is the hand position of the support-arm, Q is the hand position of the swing-arm, and G is the position of the center of gravity. m_i , l_i , and θ_i are the mass, the length, and angle of the link i ($i = 1, 2, 3$). D_{bar} is the distance between bars. θ_p is the pendulum angle. Note that the angle around the contact point cannot be actuated.

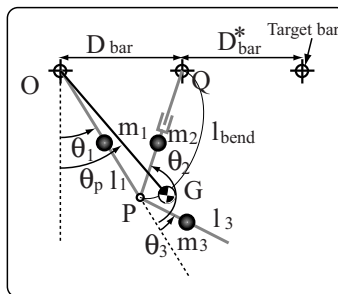


Fig. 8. 3-link model. θ_1 , θ_2 and θ_3 are the angles of support-arm, swing-arm and torso respectively. D_{bar} is the present bar-distance and D_{bar}^* is the target bar-distance.

The first dynamic equation around the contact point, O, is derived as follows (Note that the angle around the contact point cannot be actuated i.e. $\tau_1 = 0$):

$$\frac{d}{dt} \left(M_1 \dot{\theta}_1 + M_2 \dot{\theta}_2 + M_3 \dot{\theta}_3 \right) - (h_1 + h_2 + h_3) = 0, \quad (13)$$

where

$$M_1 = J_1 + J_2 + J_3 + m_1 a_1^2 + m_2 l_1^2 - 2m_2 l_1 a_2 \cos \theta_2 + m_3 l_1^2 + m_3 a_3^2 + 2m_3 l_1 a_3 \cos \theta_3, \quad (14)$$

$$M_2 = J_2 + m_2 a_2^2 - l_1 a_2 \cos \theta_2, \quad (15)$$

$$M_3 = J_3 + m_3 a_3^2 + l_1 a_3 \cos \theta_3, \quad (16)$$

$$h_1 = -(m_1 a_1 + m_2 l_1 + M_3 l_1) g \sin \theta_1, \quad (17)$$

$$h_2 = -m_2 g a_2 \sin(\theta_2 - \theta_1), \quad (18)$$

$$h_3 = -m_3 g a_3 \sin(\theta_1 + \theta_3). \quad (19)$$

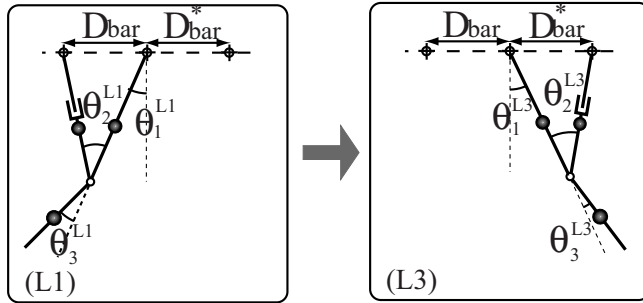


Fig. 9. The beginning and the ending of locomotion action. Superscripts denotes the state (L1) or (L3).

In accordance with the process of PDAC, the holonomic constraints between joints are designed. In order for the locomotion action and the swing action to switch smoothly, the constraint is necessary to satisfy the following conditions:

$$\begin{aligned} \theta_1 &= \theta_1^{L1} \rightarrow \dot{\theta}_2 = 0, \dot{\theta}_3 = 0, \\ \theta_2 &= \theta_2^{L1}, \theta_3 = \theta_3^{L1}. \end{aligned} \quad (20)$$

$$\begin{aligned} \theta_1 &= \theta_1^{L3} \rightarrow \dot{\theta}_1 = 0, \dot{\theta}_2 = 0, \dot{\theta}_3 = 0, \\ \theta_2 &= \theta_2^{L3}, \theta_3 = \theta_3^{L3}. \end{aligned} \quad (21)$$

In this paper, we determine the constraint so as to satisfy (20) and (21) as follows:

$$\theta_2 = A \left(\theta_1^2 - \theta_1^{L1} \right) + B = f(\theta_1), \quad (22)$$

$$\theta_3 = A' \left(\theta_1^2 - \theta_1^{L1} \right) + B' = g(\theta_1), \quad (23)$$

$$\begin{aligned} A &= -\frac{2(\theta_2^{L1} - \theta_2^{L3})}{(\theta_1^{L1} - \theta_1^{L3})^2}, \\ A' &= -\frac{2(\theta_3^{L1} - \theta_3^{L3})}{(\theta_1^{L1} - \theta_1^{L3})^2}, \end{aligned} \quad (24)$$

$$B = \frac{\left((\theta_1^{L3})^2 + (\theta_2^{L1})^2 - 2\theta_1^{L1}\theta_1^{L3}\theta_2^{L1} + \theta_1^{L1}\theta_2^{L1} \right)}{(\theta_1^{L1} - \theta_1^{L3})^2}, \quad (25)$$

$$B = \frac{\left((\theta_1^{L3})^2 + (\theta_3^{L1})^2 - 2\theta_1^{L1}\theta_1^{L3}\theta_3^{L1} + \theta_1^{L1}\theta_3^{L1} \right)}{(\theta_1^{L1} - \theta_1^{L3})^2}, \quad (26)$$

$$\dot{\theta}_2 = \frac{df}{d\theta_1} \frac{d\theta_1}{dt} = f'(\theta_1) \dot{\theta}_1, \quad (27)$$

$$\dot{\theta}_3 = \frac{dg}{d\theta_1} \frac{d\theta_1}{dt} = g'(\theta_1) \dot{\theta}_1. \quad (28)$$

Substituting Eq. (22)-(28) into Eq. (13) yields the following equation,

$$\frac{d}{dt} \left(M(\theta_1) \dot{\theta}_1 \right) = h(\theta_1), \quad (29)$$

(30)

where

$$M(\theta_1) = \hat{M}_1 + \hat{M}_2 f'(\theta_1) + \hat{M}_3 g'(\theta_1), \quad (31)$$

$$h(\theta_1) = \hat{h}_1 + \hat{h}_2 f'(\theta_1) + \hat{h}_3 g'(\theta_1), \quad (32)$$

$$\hat{M}_i = M_i \mid_{(\theta_2, \theta_3) = (f(\theta_1), g(\theta_1))}, \quad (33)$$

$$\hat{h}_i = h_i \mid_{(\theta_2, \theta_3) = (f(\theta_1), g(\theta_1))}, \quad (34)$$

$$(i = 1, 2, 3).$$

Finally, the phase around contact point is obtained as below,

$$\dot{\theta}_1 = \frac{1}{M(\theta_1)} \sqrt{\int 2M(\theta_1)h(\theta_1)d\theta_1} \quad (35)$$

$$\doteq \frac{1}{M(\theta_1)} \sqrt{D(\theta_1) + C} \quad (36)$$

$$(C = -D(\theta_1^{L3})) \\ \doteq F(\theta_1). \quad (37)$$

The $\dot{\theta}_1^{L1}$ can be calculated by substituting θ_1^{L1} into Eq. (12). By use of $\dot{\theta}_1^{L1}$, it is possible to estimate the energy difference between (L1) and (L3) as below,

$$\Delta E_{loco} = \frac{1}{2}(m_1 a_1^2 + J_1)(\dot{\theta}_1^{L1})^2. \quad (38)$$

Fig. 10 depicts the relationship among the present bar-distance D_{bar} , the target bar-distance D_{bar}^* , and the energy difference ΔE_{loco} .

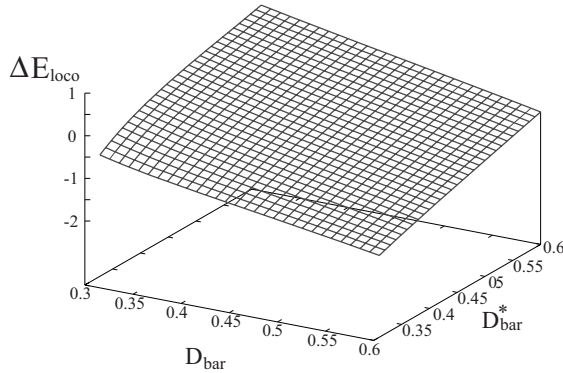


Fig. 10. Relationship among D_{bar} , D_{bar}^* and ΔE_{loco}

4.3 Swing Action

In this subsection, the controller of the swing action is described. At the initial state denoted by $S0$, the arms are symmetric with length l_0 , which is equal to the length of the stretched arm, and the torso is hanging down vertically. The robot swings up the torso (counterclockwise) while bending its elbow. The rear contact point

denoted by O can be considered as the pivot point of the pendulum during the swing-up motion. $S1$ denotes the state when the pendulum angular velocity is zero. After that, the robot swings back the torso (clockwise) with elbow-extending action synchronized with the pendulum motion. The arms are symmetric with length l_0 at the state denoted by $S2$, during this swing-back action. At this moment, the pivot point of the pendulum switches from the rear contact point O to the front contact point Q . Then, the pendulum angular velocity is zero at $S3$. Immediately after $S3$, the robot releases the rear bar and starts the locomotion action. The overview of the swing action is shown in Fig. 5. Note that the robot just repeats the swing-back action from the state $S1$ to $S3$ after the locomotion action.

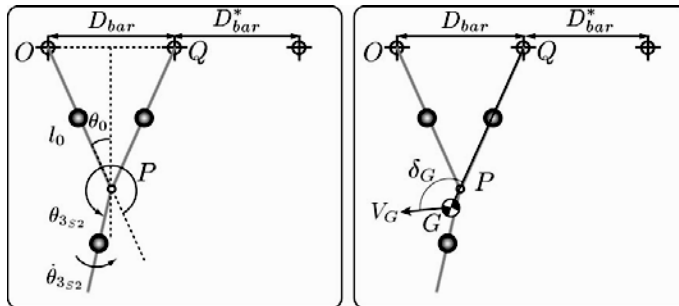


Fig. 11. Parameter setting at $S2$

The elbow-bending during the swing action is geometrically designed to realize a double pendulum motion as well as keep grasping the bar so that the model can be looked upon as a double pendulum consisted of link 1 and link 3. The desired trajectories l_b^d is given as a cubic spline function $F_{spl}(t)$ shown in Fig. 12.

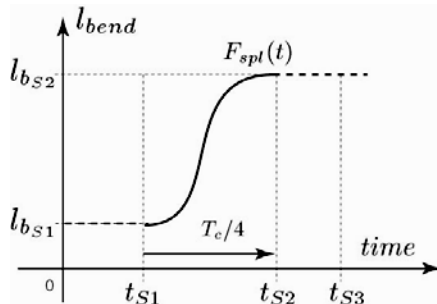


Fig. 12. Disered trajectory of l_{bend}

The boundary conditions at t_{s1} and t_{s2} are specified as follow:
 $l_b^d(t_{s1}) = l_{2s1}$, $l_b^d(t_{s2}) = l_o$, $\dot{l}_b^d(t_{s1}) = \dot{l}(t_{2s}) = 0$. θ_2^d is given as function of θ_1 and l_b^d . θ_3^d is expressed by using a cosine wave function($t_{s1} \leq t_{s2}$) and a cubic spline $F'_{spl}(t)(t_{s2} \leq t)$ as shown in Fig. 13. These parameters are described as follows:

$$x_p = l_0 \sin \theta_1, \quad y_p = -l_0 \cos \theta_1, \quad (39)$$

$$x_q = d_{bar}, \quad y_q = 0, \quad (40)$$

$$l_b^d = F_{spl}(l_{2s1}, l_{2s2}, T_2, t), \quad (41)$$

$$\begin{aligned} \theta_2^d &= \cos^{-1}\left(\frac{x_q - x_p}{l_2}\right) - \theta_1 + \frac{\pi}{2} \\ &= \cos^{-1}\left(\frac{d_{bar} - l_0 \sin \theta_1}{l_2}\right) - \theta_1 + \frac{\pi}{2}, \end{aligned} \quad (42)$$

$$\theta_3^d = A_s \cdot \cos\left(\frac{2\pi}{T_s}(t - t_{s1})\right), \quad (43)$$

$$A_s := \theta_{3s1} - \theta_{3s2}, \quad (44)$$

$$\dot{\theta}_{3s2} = -A_s \cdot \frac{\pi}{T_s}, \quad (45)$$

where D_{bar} is the distance between bars, l_o is the length of a straight arm, A_s is the amplitude and T_s is the period of the oscillation.

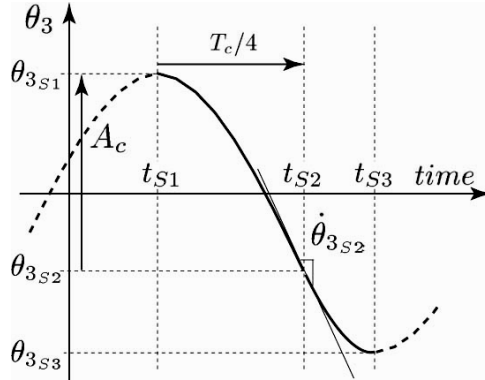


Fig. 13. Desired trajectory of θ_3

The input parameters A_s and T_s are determined by the energy-based control method. The angular velocity, $\dot{\theta}_{3S2}$, is controlled so that the robot obtains the enough energy to reach the target bar in the successive locomotion phase. The posture at S2 affects its motions since the center of rotation of the pendulum switches from the rear contact point O to the front contact point Q .

In this paper, θ_{3S2} is given to satisfy the following condition,

$$QG \cdot V_G = 0, \quad (46)$$

where QG is the position vector of the center of gravity, V_g is the velocity vector of the center of gravity. Fig. 11 shows these vectors. This equation means the velocity vector V_G is orthogonal on the position vector QG so that the loss of the angular momentum at the moment $S2$ is zero.

The target energy at S2 is estimated by the following equation,

$$E_{S2}^d = E^* + \Delta E_{loco}, \quad (47)$$

where E^* is the potential energy at L3.

The kinetic energy(K_{S2}) and potential energy(P_{S2}) at S2 are given as follows:

$$E_{S2} = P_{S2} + K_{S2}, \quad (48)$$

$$P_{S2} = P_1 + P_2 + P_3, \quad (49)$$

$$P_1 = m_1 g \frac{l_0}{2} \cos \theta_0, \quad (50)$$

$$P_2 = P_1, \quad (51)$$

$$P_3 = m_3 g \left(l_0 \cos \theta_0 + \frac{l_3}{2} \cos(\theta_0 + \theta_{3_{S2}}) \right), \quad (52)$$

$$K_{S2} = \frac{1}{2} m_3 \left(\frac{l_3}{2} \dot{\theta}_{3_{S2}} \right)^2, \quad (53)$$

where

$$\theta_0 = \sin^{-1} \left(\frac{D_{bar}}{2l_0} \right). \quad (54)$$

The required energy at S2 is obtained from Eq. (47) and (48),

$$K_{S2}^d = E_{S2}^d - P_{S2}^d \quad (55)$$

$$= E^* + \Delta E_{loco} - P_{S2}^d. \quad (56)$$

By substituting Eq. (56) into Eq. (53), the desired angular velocity is acquired as follows:

$$\dot{\theta}_3^d = -\frac{2}{l_3} \sqrt{\frac{2}{m_3} (E^* + \Delta E_{loco} - P_{S2}^d)}. \quad (57)$$

From above equations, the desired period, T_s , is decided as the following equation,

$$T_s = l_3 (\theta_{3_{S1}} - \theta_{3_{S2}}) \pi \sqrt{\frac{m_3}{2(E^* + \Delta E_{loco} - P_{S2}^d)}}. \quad (58)$$

5 Experiment

In this section, we validate the proposed method for the irregular ladder problem by the experiment using the Gorilla Robot III. At first, the experimental setup is described, and then we show the experimental results.

5.1 Experimental Setup

The experiment is conducted by using the Gorilla Robot III introduced in the Section 2. The control system of the Gorilla Robot III is shown in Fig. 14. Each joint is driven by AC servo motor through the harmonic drive gear, partially through the timing belt. Maximum output power of the motor is 30 [W]. The power supply and the computer are installed outside of the robot for weight saving.

The distance between bars d_{bar} remains constant at 0.4 [m] and all bars are set at the same height at 2.7 [m]. The mass of arms m_1 or m_2 is 7.0 [kg], that of the torso m_3 is 15.0 [kg], the length of the stretched arm l_0 is 0.64 [m], and that of the torso l_3 is 0.85 [m].

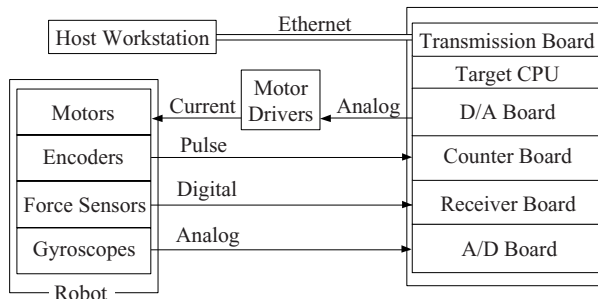


Fig. 14. Control System of MLR

Table 1. T_S of irregular labber brachiation

	$\Delta = -0.1[m]$	$\Delta = 0.1[m]$
$T_S[s]$ where $D_{bar} = 0.4$	2.196	-
$T_S[s]$ where $D_{bar} = 0.3$	-	1.536

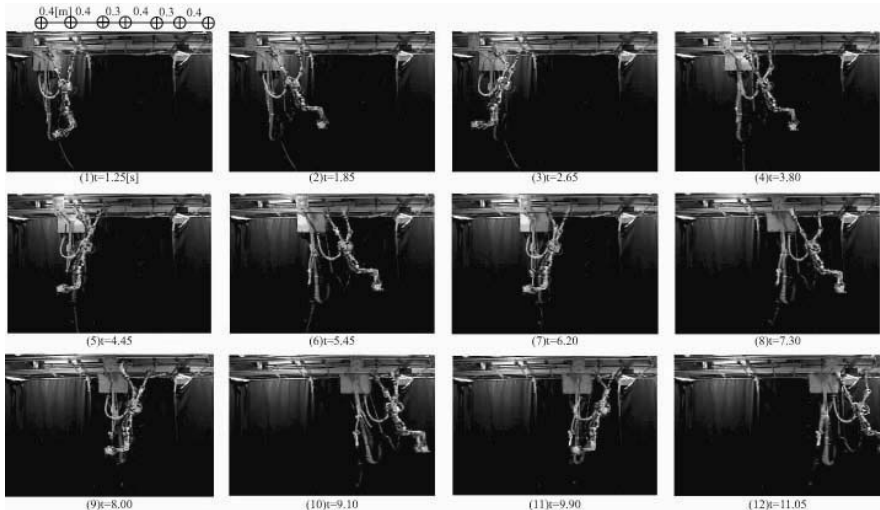
Table 2. Pendulum angle θ_p at S3 and L3

	1 st	2 nd	3 rd	4 th	5 th	6 th	7 th
D_{bar}^*	0.40	0.30	0.40	0.30	0.40	0.30	0.40
θ_p^{S3} [deg]	-31.5	-30.0	-28.0	-30.0	-27.0	-30.5	-26.0
θ_p^{L3} [deg]	28.0	27.0	30.0	28.0	29.5	28.0	-28.0

5.2 Experimental Results

In order to confirm the validity of the proposed method, we performed the experiment of the irregular ladder brachiation. In this paper, as the experimental environment, the bar-distance is set up to be 4.0 [m] and 3.0 [m] alternately. Note that the robot is given the information of the bar distance and that how to acquire that information (for example, with a camera) is future work.

As a result, the stable continuous brachiation on the irregular ladder was achieved. Table 1 shows the value of T_s employed in the experiment and Table 2 shows the pendulum angle, θ_p at S3 and L3 of the i th action. As shown in this table, θ_p^{L3} increases compared to θ_p^{S3} under the condition of $D_{bar}^* = 0.4$, on the

**Fig. 15.** Snapshots of the irregular ladder brachiation

other hand, θ_p^{L3} decreases compared to θ_p^{S3} under the condition of $D_{bar}^* = 0.3$. Fig. 15 shows the snapshots of the experiment and Fig. 16 depicts the experimental results of the pendulum angle, θ_p , and the torso angle, θ_3 .

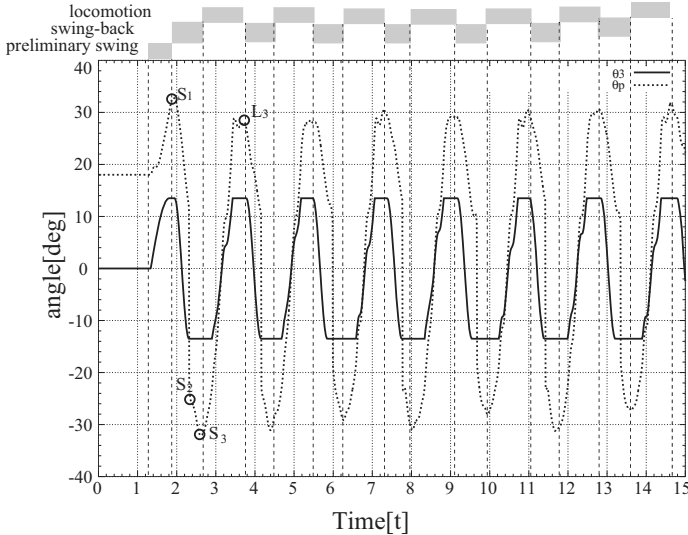


Fig. 16. Experimental results

The proposed method can apply the various irregular ladder, however the hardware capability limits the robot performance. For example, we found that it was impossible to realize the brachiation from 3.0 [m] to 5.0 [m] bar-distance. It is conceivable that improvement of the hardware or proposal of more efficient method can enhance the performance.

Summary

In this paper, the concept of bio-inspired robotics named multi-locomotion robot was introduced at first. Multi-locomotion robot has the high ability to ambulate by achieving several kinds of locomotion in stand-alone. In addition, the Gorilla Robot III was introduced as a prototype of the multi-locomotion robot. Second, we explained the Passive Dynamic Autonomous Control (PDAC) which has proposed previously. The PDAC realized not only bipedal walking but also quadrupedal walking in our previous works. Third, we also applied the PDAC to a brachiation and designed the brachiating controller on the irregular ladder. The controller estimates the energy difference caused by symmetry breaking. Finally, we validated the proposed controller by realizing the continuous irregular ladder brachiation with the Gorilla Robot III.

References

- [1] Aoyama, T., Sekiyama, K., Hasegawa, Y., Fukuda, T.: Analysis of Relationship between Limb Length and Joint Load in Quadruped Walking on the Slope. In: Proceedings of the IEEE/RSJ International Conference on Intelligent Robots and Systems, pp. 3908–3913 (2008)
- [2] Asano, Y., Doi, M., Hasegawa, Y., Matsuno, T., Fukuda, T.: Quadruped Walking by Jointinterlocking Control Based on the Assumption of Point-contact. Transactions of the Japan Society of Mechanical Engineers, Series C 73(727), 230–236 (2007) (in Japanese)
- [3] Doi, M., Hasegawa, Y., Fukuda, T.: Passive Trajectory Control of the Lateral Motion in Bipedal Walking. In: Proceedings of the IEEE International Conference on Robotics and Automation, pp. 3049–3054 (2004)
- [4] Doi, M., Hasegawa, Y., Fukuda, T.: Passive Dynamic Control of Bipedal Walking. In: Proceedings of the IEEE-RAS/RSJ International Conference on Humanoid Robots, pp. 811–829 (2004)
- [5] Doi, M., Hasegawa, Y., Fukuda, T.: 3D Dynamic Walking Based on the Inverted Pendulum Model with two Degree of Underactuation. In: Proceedings of the IEEE/RSJ International Conference on Intelligent Robots and Systems, pp. 2788–2793 (2005)
- [6] Fukuda, T., Doi, M., Hasegawa, Y., Kajima, H.: Multi-Locomotion Control of Biped Locomotion and Brachiation Robot. In: Fast Motions in Biomechanics and Robotics, pp. 121–145. Springer, Berlin (2006)
- [7] Fukuda, T., Hosokai, H., Kondo, Y.: Brachiation Type of Mobile Robot. In: Proceedings of the IEEE International Conference on Advanced Robotics, pp. 915–920 (1991)
- [8] Fukuda, T., Saito, F., Arai, F.: A Study on the Brachiation Type of Mobile Robot (Heuristic Creation of Driving input and Control Using CMAC). In: Proceedings of the IEEE/RSJ International Conference on Intelligent Robots and Systems, pp. 478–483 (1991)
- [9] Hasegawa, Y., Fukuda, T., Shimojima, K.: Self-Scaling Reinforcement Learning for Fuzzy Logic Controller –Applications to Motion Control of Two-Link Brachiation Robot. IEEE Transactions on Industrial Electronics 46, 1123–1131 (1999)
- [10] Hasegawa, Y., Ito, Y., Fukuda, T.: Behavior Coordination and its Modification on Brachiation-Type Mobile Robot. In: Proceedings of the IEEE International Conference on Robotics and Automation, pp. 3984–3989 (2000)
- [11] Kajima, H., Doi, M., Hasegawa, Y., Fukuda, T.: A Study on a Brachiation Controller for a Multi-Locomotion Robot –Realization of Smooth, Continuous Brachiation. Advanced Robotics 18(10), 1025–1038 (2004)
- [12] Kajima, H., Hasegawa, Y., Doi, M., Fukuda, T.: Energy-based Swing-Back Control for Continuous Brachiation of a Multilocomotion Robot. International Journal of Intelligent Systems 21, 1025–1043 (2006)
- [13] Kajima, H., Hasegawa, Y., Fukuda, T.: Study on Brachiation Controller -Adjustment Method of Strength and Timing Parameters-. In: Proceedings of the IEEE/RSJ International Conference on Intelligent Robots and Systems, pp. 2497–2502 (2002)
- [14] Kajima, H., Hasegawa, Y., Fukuda, T.: Learning Algorithm for a Brachiating Robot. Applied Bionics and Biomechanics 1(1), 57–66 (2003)
- [15] Kajita, S., Yamaura, T., Kobayashi, A.: Dynamic Walking Control of a Biped Robot Along a Potential Energy Conserving Orbit. IEEE Transaction on Robotics and Automation 8(4), 431–438 (1992)

- [16] Li, Q., Takanishi, A., Kato, I.: Learning Control of Compensative Trunk Motion for Biped Walking Robot Based on ZMP. In: Proceedings of the IEEE/RSJ International Conference on Intelligent Robots and Systems, pp. 597–603 (1992)
- [17] McGeer, T.: Passive Dynamic Walking. *The International Journal of Robotics Research* 9(2), 62–82 (1990)
- [18] Nakanishi, J., Fukuda, T., Koditschek, D.E.: A Brachiating Robot Controller. *IEEE Transactions on Robotics and Automation* 16(2), 109–123 (2000)
- [19] Raibert, M.H.: Legged Robots that Balance. MIT Press, Cambridge (1986)
- [20] Saito, F., Fukuda, T., Arai, F.: Swing and Locomotion Control for Two-Link Brachiating Robot. In: Proceedings of the IEEE International Conference on Robotics and Automation, pp. 719–724 (1993)
- [21] Saito, F., Fukuda, T., Arai, F.: Swing and Locomotion Control for a Two-Link Brachiating Robot. *IEEE Control System Magazine* 14(1), 5–12 (1994)
- [22] Saito, F., Fukuda, T.: A First Result of The Brachiator III -A New Brachiating Robot Modeled on a Siamang. In: Artificial Life V, pp. 354–361. MIT Press, Cambridge (1997)
- [23] Simons, E.L.: Primate Evolution: An Introduction to Man's Place in Nature. Macmillan, New York (1972)
- [24] Spong, M.: The Swing up Control Problem for the Acrobot. *IEEE Control System Magazine* 15(1), 49–55 (1995)
- [25] Westervelt, E.R., Buche, G., Grizzle, J.W.: Experimental Validation of a Framework for the Design of Controllers that Induce Stable Walking in Planar Bipeds. *The International Journal of Robotics Research* 24(6), 559–582 (2004)
- [26] Yoneda, H., Sekiyama, K., Hasegawa, Y., Fukuda, T.: Vertical Ladder Climbing Motion with Posture Control for Multi-Locomotion Robot. In: Proceedings of the IEEE/RSJ International Conference on Intelligent Robots and Systems, pp. 3579–3584 (2008)

A Simple Method for Generating Smooth Robot Arm Motion

Antal K. Bejczy

Senior Research Scientist
JPL/CALTECH (retiree), Pasadena, California, USA
antbej@earthlink.net

Abstract. A computer algorithm is described for generating smooth robot arm motion in task space trajectories. The algorithm is based on observations and analysis of task space trajectory profiles produced by human operators manually, using a six degree-of-freedom position hand controller. The algorithm is formulated in the *velocity-position phase space* and employs a *harmonic (sinusoid)* base function in the phase space. Hence the name: Harmonic Motion Generator (HMG). Performance capabilities of HMG are illustrated, including its combination with force-moment sensor based active compliance control and with task space (Cartesian space) position servo control.

1 Introduction

Robot arm motion can be generated in two ways: *manually* by an operator using a suitable manual control input device, and *algorithmically* by a computer program. A novel algorithmic motion generator technique which circumvents the usual time-based robot arm motion generators, normally acting in the robot arm's joint space, is briefly described in this paper. The described novel technique offers a motion generator capability which closely resembles the kinematical profiles of trajectories generated by operators manually in position control mode acting in the Cartesian task space. Indeed, the novel algorithmic technique is based on observations and analysis of manually generated robot arm trajectories in position command mode in the task space.

First a brief analysis of manually generated trajectories is presented in position control mode. Then an algorithmic scheme is formulated matching the profile of manually generated trajectories in position control mode in the task space. Performance results are then presented illustrating capabilities of the algorithmic control scheme.

2 Manually Generated Trajectories

Manually generated trajectories in position control mode express much more than just position commands or position profiles versus time, they implicitly also express both velocity and acceleration and deceleration profiles. Using a six-degree of freedom Force Reflecting Hand Controller (FRHC) of the Jet Propulsion Laboratory (JPL) Advanced Teleoperator Laboratory, many series of position versus time motion profiles were generated and recorded for moving the robot hand from point A to point B in a distance of about 50 cm in position control mode. A close inspection and analysis of manually generated robot arm trajectories in position mode of control revealed important features as seen in the *phase space*.

(1) The trajectories have three kinematical segments: acceleration after start of motion, constant velocity, and deceleration to stop. The significant element is the constant velocity segment.

(2) In the quoted motion range, the acceleration/deceleration segments cover about 5 cm distance in about 0.5 sec. time.

(3) The operator's hand motion is not controlled by a clock (or time): there are some time variations for a fixed distance. The operators rather observe the distance to be traveled and start the deceleration accordingly.

(4) The start and stop of motion are gradual but definite.

(5) The transition from acceleration to constant velocity and from constant velocity to deceleration is *very smooth, without jerks*.

(6) The maximum comfortable velocity for operator's hand motion is about 20 to 25 cm/sec.

(7) The velocity-position *phase diagrams* of manually generated trajectories in position control mode resemble an “*augmented*” harmonic (*sine*) function. The notion “*augmented*” refers to the second (constant velocity) segment of the trajectory. The notion “*harmonic function*” refers to the first quadrant of a sine function for the acceleration segment and to the second quadrant of a sine function for the deceleration segment of the trajectory.

3 Algorithmically Generated Trajectories

Based on observations and analysis of manually generated trajectories in position control mode outlined above – and specifically defined under point (7) there – an “*augmented*” Harmonic Motion Generator (HMG) algorithm with *sinusoidal velocity-position phase space function profile* was formulated and implemented at JPL. For a straight line motion, for instance, the HMG only needs three parameter values to be specified by the operator or, in case of an automated system, by a higher level program: i) The total distance to be traveled. ii) The maximum constant velocity to be attained. iii) The distance to be used for acceleration and deceleration.

When a straight line trajectory is, for instance, specified by X, Y, Z coordinate values, then the total distance to be traveled is first computed. Since the motion generated by the “augmented” HMG algorithm is characterized by the peak velocity and the distance used for acceleration and deceleration, the velocity as a function of distance to be traveled will consist of three segments:

- *Acceleration*: velocity increases as a first-quarter sine function of distance from zero to the given maximum (constant) velocity value.
- *Coasting*: velocity is kept constant at the given maximum value till the start of deceleration.
- *Deceleration*: velocity is reduced as a second-quarter sine function of the distance left till the end point of motion.

The use of the first- and second-quarter sine function profiles for the acceleration and deceleration segments, respectively, will guarantee *smooth (corner- or jitter-free)* transition to and from the peak velocity.

In every servo loop the velocity is computed first. The position is computed as an integral of the velocity. The position is then decomposed into X, Y, Z components according to the direction cosines of the straight line function. (Note that the direction cosines are constant along a straight line.) Fig. 1 illustrates the augmented HMG position-velocity (*phase space*) function, and Fig. 2 illustrates the corresponding position and velocity versus time (*state space*) functions.

The augmented HMG algorithm can fully and easily replace the position command generating function of the FRHC since the output of this algorithm equals the output of the JPL FRHC which is the incremental position change in the task (X,Y,Z) space coordinates at a fixed (1 KHz) rate. For telerobotic applications, the algorithm can be coded either in the control station site computer or in the remote site computer where the robot arm works. In the first case, the communication from the control station to the remote site is a constant data stream of incremental position commands similar to the data stream transmitted from the FRHC. In the second case, the communication from the control station to the remote site only contains the basic input parameter values to the augmented HMG, and eventually a “go” signal.

It is noted that any geometric function (like circle, ellipse, or any segment of them) can be specified to the augmented HMG as a path to be followed by a given robot arm. The velocity versus position phase space function will then first be computed along that geometric path. The X, Y, Z decomposition of position commands, however, will not have a constant set of direction cosines as it was for a straight line path. The direction cosines will now be functions of the path points which can be and shall be determined.

The augmented HMG algorithm is substantially different from the typical trajectory generator algorithms employed in robotics. The existing trajectory generating algorithms in robotics typically use *polynomials in the position versus time state space*. The augmented HMG algorithm is formulated in the *velocity versus position phase space, and employs a harmonic (sine) base function*. Moreover, the HMG algorithm provides task space trajectories; it does not require trajectory decomposition into the robot arm’s joint space which is the usual procedure in most

of the existing robotic trajectory generators. The HMG outputs (like the FRHC outputs) are executed as task space commands having passed through the Inverse Kinematical (IK) transformation of the given robot arm.

Another important feature of the HMG algorithm is that it allows inputs as relative distances to be traveled through and does not require specification of travel time. Only the maximum (coasting) velocity and the length of the acceleration/deceleration segments along the path need be specified. These features provide an easy operator interaction with the HMG algorithm. Furthermore, the HMG algorithm also can be directly combined with Cartesian servo scheme and with force-moment sensor based active compliance control as illustrated in the subsequent chapter.

4 Performance Results

A number of performance experiments have been performed with the augmented HMG. The experiments also implied the use of Cartesian servo scheme and the combination with active (force-moment sensor based) compliance control.

Cartesian (or task space) servo scheme is a novel feedback technique to minimize position errors in the task space directly. This implies an acting closed position loop in the Cartesian task space. The Cartesian space position errors are computed from actual joint space position values through the Forward Kinematical (FK) transformations and from the actual FRHC or HMG task space commands. (See Fig. 3)

For force-moment sensor based active compliance control two schemes are of major interest: *integrating-* and *spring-type compliance*. The integrating-type is useful, for instance, for maintaining a required cutting force when something must be cut with a tool in the robot hand. While the spring-type is useful, for instance, to put a peg into a narrow tolerance hole to prevent jamming. – More on Cartesian servo and the two types of active compliance control schemes can be found in [1] and [2].

Fig. 4 illustrates a forward (X-direction) straight line motion commanded by the HMG and performed *without* Cartesian servo. First note that the trajectory profile is practically identical with a trajectory commanded by the FRHC. Then note the Z-direction (up-down) errors. Ideally, these errors should have been zero since no motion was commanded in the Z-direction. Fig. 5 illustrates the results when the same HMG commanded forward (X-direction) motion was performed *with* Cartesian servo. The mean Z-direction errors became practically zero, the maximum value of the error time function is less than 1 mm. This dramatically illustrates the performance effect of the Cartesian servo scheme.

Fig. 6 illustrates the combination of HMG, Cartesian servo and active compliance control of the integrating type. Here, the HMG Y-direction lateral motion was combined with the requirement to maintain a constant forward (X-direction) force against a table while moving in the lateral Y direction. The Cartesian servo

was disabled along the X direction, but retained along the Y and Z directions. To make the performance test more interesting, the task board in the Y direction was misaligned by about 5 degrees relative to the nominal Y direction defined in the robot arm's base reference frame. That is, to maintain a constant force in the X direction while moving in the Y direction required an automatic position correction in the X direction *based upon force sensing*. As seen in Fig. 6, HMG performed excellently when combined with Cartesian servo and integrating-type active compliance control. – The task example quoted in Fig. 6 is equivalent to the cutting of a 40 cm long material on a vertical board with 5 N cutting force automatically, and such that misalignment between the vertical board and knife along the cutting direction is automatically corrected based on the sensing of the required cutting force.

In Fig. 7 a general straight line example is shown. Here, a *three-dimensional* general straight line (having X, Y, Z components in the task space) was commanded by the HMG. Note, that the tracking error time histories in Fig. 7 are *absolute errors*, equal to the square root of the sum of the squares of the X, Y, and Z errors. Therefore, the content of these time histories is not comparable to the ones shown in Figs. 4, 5, and 6 which are unprocessed real +/- tracking error time histories. It is, however, clear from Fig. 7 that the Cartesian task space servo considerably improves the tracking performance of the HMG generated 3D trajectory.

The reason for the improved tracking performance is that the Cartesian servo tends to compensate for sticktion, friction, and for other un-modeled dynamic effects in trajectory tracking, and to keep the control execution performance consistent with the geometric parameter values of the robot arm. It is true, however, that the calibration accuracy of the robot arms internal reference frame relative to the external word reference frame only can be improved by actual *external measurements*. This is well illustrated in Fig. 6 where contact force measurements correct for a 5-degree misalignment and for any other robot arm geometric parameter errors in the lateral Y direction.

Conclusion

In summary, the significance of the augmented HMG algorithm is twofold: (1) Its implementation and coding are relatively simple, and can easily run in real-time even at 1 KHz rate if needed, as indeed was shown in the JPL implementation. (2) It can easily and in a natural way be combined with sensed events and with Cartesian servo since the “driving force” in the HMG algorithm is not the running time but the task (or Cartesian) space events. As illustrated in Figs. 5, 6, and 7, the HMG algorithm's combination with Cartesian servo and active compliance control provides very encouraging performance. The above two significant points may also indicate that the augmented HMG algorithm could become an excellent partner to intelligent real-time or near-real-time planning programs for robot arms' motion.

Acknowledgments. This work was carried out at the Jet Propulsion Laboratory, California Institute of Technology, under contract with the National Aeronautics and Space Administration.

References

- [1] Bejczy, A.K., Szakaly, Z., Kim, W.S.: A Laboratory Breadboard System for Dual-Arm Teleoperation. In: Proc. of Third Annual Workshop on Space Operations, Robotics and Automation, JSC, Houston, TX, July 25-26, (1989); NASA Conf. Publ. No. 3059, pp. 649-660
- [2] Szakaly, Z., Bejczy, A.K.: Performance Capabilities of a JPL Dual-Arm Advanced Teleoperation System. In: Proc. of Space Operations, Automation and Robotics (SOAR) Workshop, Albuquerque, NM, June 26-27 (1990)

Fuzzy Inference-Based Mentality Expression for Eye Robot in Affinity Pleasure-Arousal Space

Yoichi Yamazaki¹, Hai An Vu², Phuc Quang Le², Hitoho Oikawa², Kazuya Fukuda², Yui Matsuura², Fangyan Dong², and Kaoru Hirota²

¹ Dept. of Electrical, Electronic & Information Engineering,
Kanto Gakuin University, Japan

yamazaki@kanto-gakuin.ac.jp

² Dept. of Computational Intelligence & Systems Science,
Tokyo Institute of Technology, Japan
hirota@hrt.dis.titech.ac.jp

Abstract. An eye robot focused on eye expression and a mascot robot system are proposed as a casual communication robot systems with human friendly expression. A mentality expression system based on the affinity pleasure-arousal space by eye robot is proposed. The three-dimensional affinity pleasure-arousal space is proposed to express mentality states with fuzzy inference. The eye robot that performs eye motions is developed based on the human mechanisms. A mascot robot system is proposed as an internet-based robot application for casual communication in home environment. This mascot robot system is a network composed of four fixed type eye robots, one mobile self-propelled type eye robot, an information recommendation module, and the speech recognition module. The mascot robot system's functionality is demonstrated in a living room, where casual communication is conducted based on speech recognition and mentality expression of eye robots. The validity of the proposed mentality expression system is confirmed by communication experiments with 2 scenarios. The proposed systems provide casual communication between a human interlocutor and a robot.

1 Introduction

In home environments, emotional interaction between robots and humans is more important than job performance. Facial expressions are important components of face-to-face communication. Therefore communication robots often take the form of a head-robot to express mentality, e.g., Kismet [1], SAYA [2], WE [3], and CRF [4]. The modality of facial expression of these robots is based on six basic facial expressions, which are based on the analysis of facial muscles.

The eye is another communication medium that can express mentality in face-to-face communication. Eye motion is an important component to express mentality, because eyes attract the attention of the interlocutor in human communication.

In order to achieve multiple robot type application at home environments, mentality expression system with eye robot is proposed. The eye robot has 5 degrees of freedom that needs a smaller number of actuators than that of other facial expression systems. Therefore, this system is appropriate for a multiple arranged type robot in terms of cost. This mentality expression by the eye robot makes up the mascot robot system that achieves casual communication with human in home environment.

An eye robot focused on eye expression and a mascot robot system are proposed as casual communication robot systems with human friendly expression. An overview of mentality expression by robots is given 2. A mentality expression system based on the affinity pleasure-arousal space by eye robot is described in 3. A mascot robot system as an internet-based information retrieval and recommendation application of the eye robot is presented in 4. This mascot robot system provides casual communication in home environment. The evaluations of the mentality expression with the eye robot are described in 5.

2 Mentality Expression by Robots

A sophisticated and diversified system is necessary for household robots that have to perform tasks indicated by a program. Moreover, they are requested to perform completely different tasks from conventional industrial robots, i.e., household robots need to communicate with human beings in as friendly a fashion as possible.

Some communication robots are proposed in [1]-[4]. They mostly take the form of a head-robot to express mentality information. Facial expressions are important components of communication. Kismet [1] can produce several facial expressions and can thus generate human aid efficiently because of the ease of communication with the human interlocutor. SAYA [2], the face robot implemented with artificial muscles, can express a number of facial expressions of real female adults. The WE [3] series have expressive robotic faces and robotic hands. The CRF robot [4] deforms facial expressions to communicate more effectively. The modality of facial expression of these robots is based on six basic facial expressions that are based on the analysis of facial muscles. Although these head robot systems look similar in terms of facial expressiveness, their research orientations are different from one another. Kismet emulates the social behavior of a 5-year old child that needs a caregiver to keep its emotional parameters at reasonable levels. SAYA has undergone several updates to the level where its size and appearance are comparable to that of an adult female human. The WE series robots are developed along with bipedal locomotion mechanisms, and the long-term objective of the research is to develop a humanoid robot that has limbs, a body, and a human-like head.

An eye robot focused on eye expression and a mascot robot system are proposed as casual communication robot system with human friendly expression. It is important for friendly communication to express mentality. Eye motion is classified

as nonverbal expression which has a tendency to express mentality. Eye expression is important in face-to-face communication as denoted in [5, 6].

3 Mentality Expression by an Eye Robot System

A mentality expression system based on the affinity pleasure-arousal space by eye robot is proposed for the interaction of humans and robots in a home environment. The three-dimensional affinity pleasure-arousal space is proposed to express the continuous evolution of mentality states during conversation. Fuzzy inference is used to express the mentality eye motions that are arranged in the affinity pleasure-arousal space. The eye robot that performs eye motions is developed based on the mechanisms of the human eye. An overview of the proposed system is given in 3.1. The architecture of the eye robot is presented in 3.2. The fuzzy mentality expression system based on affinity pleasure-arousal space is described in 3.3.

3.1 *Overview of the Mentality Expression by the Eye Robot System*

The architectural overview of the proposed system is shown in Fig. 3.1 where the input is language category information that is generated by the speech recognition system and the output is mentality expression motion with the robotic eyes.

The mechanical part of the eye robot that can perform eye motions is developed based on mechanisms of the human eye through familiarity considerations. The eye robot has an eyelid part and an ocular part. The modality of expression with the eyelid and ocular parts is based on a two-dimensional pleasure-arousal plane. In the pleasure-arousal plane, all mentality states (for example anger or excitement) are pre-assigned [6, 7]. The pleasure-arousal plane is the two-dimensional plane that has a pleasure-displeasure axis and an arousal-sleep axis. The pleasure-displeasure axis relates to the favor of the interlocutor. The arousal-sleep axis relates to liveliness in communication. In order to take into account the transition from one mentality state to another, a three-dimensional affinity pleasure-arousal space is proposed as an extension of the pleasure-arousal plane. The motivation for a given mentality expression is determined by fuzzy inference in the affinity pleasure-arousal space.

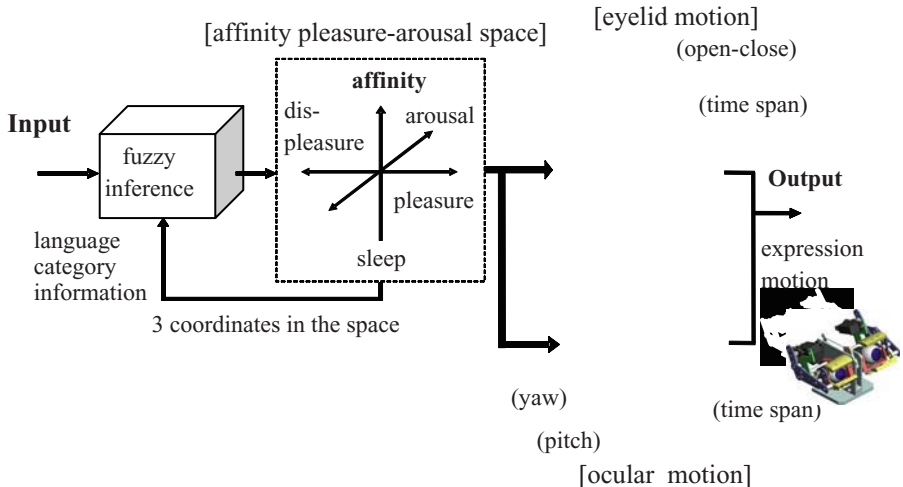


Fig. 3.1. Architectural overview of eye robot system

3.2 The Architecture of the Eye Robot

The eye robot that can express eye motions is developed based on the mechanisms of the human eye. Eye motions consist of eyelid motion and ocular motion.

The structure of the eyelids part and the ocular part is shown in Fig. 3.2. The eye robot has 2 degrees of freedom (DOF) for the eyelids part and 3 DOF for the ocular part based on human eye mechanism. The eye robot covers a wider range with each motion of the eye than is possible with human eyeballs. Therefore the eye robot can sufficiently simulate a human being's eye motions.

The appearance of a robot is important in robot-to-human communication. Many robots designed for entertainment are built up to the size of children because the size of children is considered as being more friendly. The size of the eye robot is 130 mm in width, 80 mm in height, and 75 mm in depth. This size is inspired by the size of a five-year-old child. The picture of the eye robot is shown in Fig. 3.3. The eye robot has five micro servomotors for actuators that are supported by an H8 microcontroller.

The eye motion of eye robot is defined as the combination of eyelid motion and ocular motion. Eyelid motion and ocular motion are independent in the pleasure-arousal plane. All motions of the eyelids and eyeballs have the tendency to change according to each axis of the pleasure-arousal plane. The motions are assigned to the 25 different partitions of the pleasure-arousal plane based on psychological knowledge and results from the questionnaire survey [6].

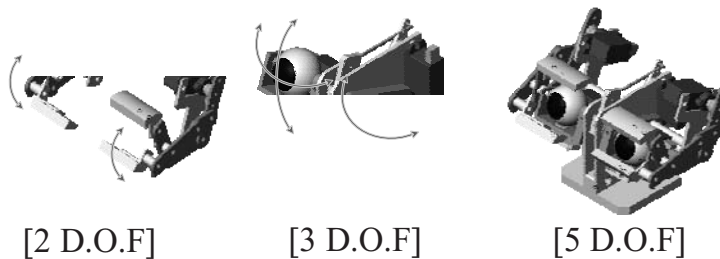


Fig. 3.2 The structure of the robot

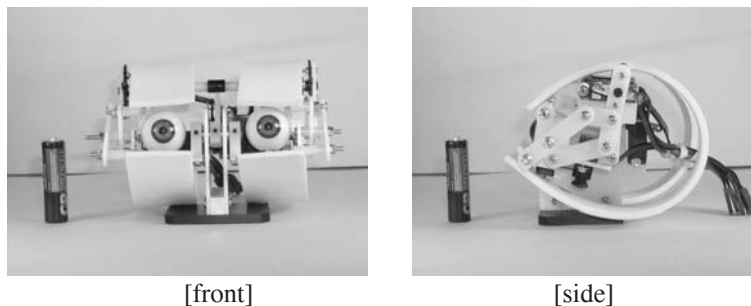


Fig. 3.3 The appearance of eye robot

All motions of the eyelids and eyeballs have the tendency to change according to each axis of the pleasure-arousal plane. The motions are assigned to the 25 different partitions of the pleasure-arousal plane based on psychological knowledge and results from the questionnaire survey [6].

When the level of arousal is high, the intervals and degrees of eyelid motions increase. When the state is closer to the sleep region, the eyelids tend to remain closed and the movement intervals are shorter. The higher the level of pleasure, the more the eyelids will tend to stay open. Accordingly, when displeasure is being expressed, the eyelids will tend to remain closed.

For ocular motion, when the mentality state is one of high arousal, the eyeballs are directed at the center of the face and the motion intervals are short. When the mentality state is closer to sleepiness, the eyeballs tend to be looking downward and the motion intervals are longer. The eyeballs tend to look straight ahead (that is looking at the face of the interlocutor) when the state is closer to pleasure. When the mentality state tends more to displeasure, the eyeballs tend to look away.

The suitable mentality expression motions for the eye robot are decided based on these macro level tendencies of the eyelid and ocular motions.

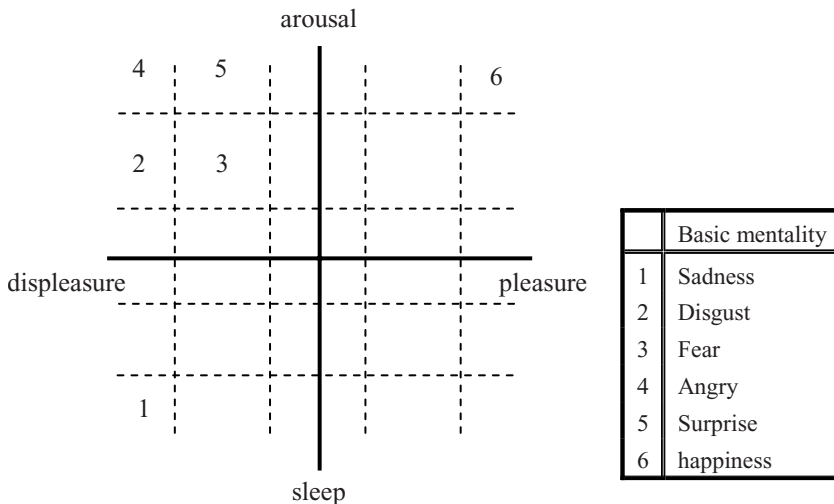


Fig. 3.4. Examples of the assignments of the typical mentalities on pleasure-arousal plane

The motions are arranged in the pleasure-arousal plane that is partitioned into 25 regions. These motions are subsequently validated by testing on 5 subjects. Moreover, the motions are further adjusted interactively by the test subjects, since eyelid motion is inseparably connected with facial muscle motion, which constitutes another form of non-verbal emotion expression. The examples of the assignments of typical mentality are shown in Fig. 3.4. These 6 motions are designed to express ‘surprise’, ‘disgust’, ‘anger’, ‘happiness’, ‘sadness’, and ‘fear’. The motions are based on 6 basic facial expressions. The assignment of the motions to the pleasure-arousal plane is based on the results in [6].

3.3 *Fuzzy Mentality Expression System Based on Affinity Pleasure-Arousal Space*

3.3.1 Affinity Pleasure-Arousal Space

The three-dimensional affinity pleasure-arousal space is proposed to describe the mentality state during communication. Specific eye motions are assigned to different regions of the pleasure-arousal plane. Using the pleasure-arousal plane, it is possible to express fixed mentality states and mentality states which change slowly, but it is difficult to deal with mentality states which are changing in real time according to the progress of the conversation and repetitive interaction.

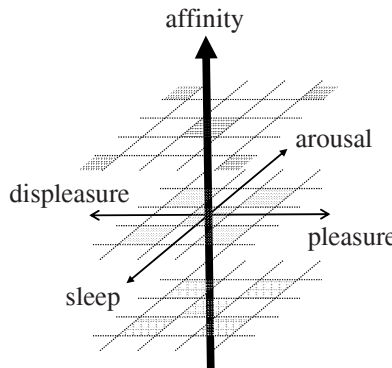


Fig. 3.5. The affinity pleasure-arousal space

To take into account rapid variations in the mentality state due to real time communication, an extra dimension, the affinity axis, is added. This results in a three-dimensional structure the affinity pleasure-arousal space, which is shown in Fig. 3.5. As the affinity state gets higher, the expression range becomes wider. At extremely low affinity states, some expressions in the pleasure-arousal plane get reversed. Essentially the affinity axis allows for a more varied range of interlocution with human beings.

3.3.2 Fuzzy Mentality Expression System

To express with eye motions the mentality states that are arranged in the affinity pleasure-arousal space, fuzzy inference is used. Four features are used as inputs for the fuzzy inference engine. One feature is language category information and three features are provided by three-dimensional coordinates in the affinity pleasure-arousal space.

Language category information is supposed to be generated by a speech recognition system. The category information is divided into 6 types. ‘1. positive to robot’ denotes positive words from the interlocutor to the robot, for example ‘I like you’, ‘you did a fine job’, and so on. ‘2. negative to robot’ denotes negative words from the interlocutor to the robot, for example ‘I hate you’, ‘you are useless’, and so on. ‘3. positive interlocutor’ denotes words where the interlocutor is making positive statements about himself, for example ‘I’m fine’, ‘I heard good news’, and so on. ‘4. negative interlocutor’ denotes words where the interlocutor is making negative statements about himself, for example ‘I’m down’, ‘I heard bad news’ and so on. These four categories serve as basis for mentality shifts. ‘5. difficult word’ denotes the words that the speech recognition system could not distinguish. ‘6. greeting’ is a specific category useful during communication, for example for signaling the beginning of a conversion, and many communication robots understand these words.

The inputs are represented by coordinates in the affinity pleasure-arousal space S and language category c . S is expressed as

$$S \in \mathbf{S}$$

$$S(x_{pl}, x_{ar}, x_{af}),$$

$$\begin{aligned} -200 &\leq x_{pl} \leq 200, \\ -200 &\leq x_{ar} \leq 200, \\ -100 &\leq x_{af} \leq 100 . \end{aligned} \quad (3.3.2.1)$$

Language category c is expressed as

$$c = \{1, 2, 3, 4, 5, 6\} . \quad (3.3.2.2)$$

The output is an update of the value of S , ΔS . ΔS is expressed as

$$\begin{aligned} \Delta S(x_{pl}, x_{ar}, x_{af}) &= (\Delta x_{pl}, \Delta x_{ar}, \Delta x_{af}), \\ -50 &\leq \Delta x_{pl} \leq 50, \\ -50 &\leq \Delta x_{ar} \leq 50, \\ -50 &\leq \Delta x_{af} \leq 50 . \end{aligned} \quad (3.3.2.3)$$

The Pleasure-displeasure axis and arousal-sleep axis use five-level scale, and affinity axis uses three-point scale. The 90 of the fuzzy rules are assigned in the space. These rules are defined based on the natural reactions of human.

To obtain fuzzy quantization, membership functions are defined for each input feature. To obtain the outputs, the center of gravity method is used as a defuzzification method. As shown in Fig. 3.1, the coordinates in the affinity pleasure-arousal space are generated by fuzzy inference. For each coordinate in the affinity pleasure arousal space, one unique region from the 25 partitions of the pleasure arousal plane is assigned. The eye robot expresses the mentality motions based on the specified region.

4 Casual Information Recommendation by Mascot Robot System

The robots that work in a home environment need to communicate with human beings in a friendly fashion. The robot system for casual communication needs to understand human speech and return the required information with friendly reactions.

A mascot robot system is proposed as an internet-based information retrieval and recommendation robot system for casual communication in home environment. The mascot robot system consists of 5 robots, i.e., 4 fixed robots (placed on a TV, a darts game machine, an information terminal, and a mini-bar) and 1 mobile robot. Each of them includes an eye robot, a speech recognition module, and a laptop PC that controls the robot and the speech recognition module. These robots connect together with a server through the internet by RT Middleware, thus constituting the robot system. The mascot robot system's functionality is demonstrated in an ordinary living room, where casual communication between 5 robots and 4 human beings (1 host, 2 guests, and 1 walk-in) is conducted based on speech recognition and mentality expression of eye robots.

An overview of the mascot robot system is mentioned in 4.1. A Speech Recognition Module (SRM) and the information recommendation and mentioned in 4.2. The oral experiments for casual communication using the mascot robot system are shown in [8, 9].

4.1 Mascot Robot System for Casual Communication

In home environment, robots need to communicate with users in casual fashion. The casual communication interface in home environments needs to recognize human speech and give back required and personalized recommended information on displays and emotional reactions of robots. A mascot robot system (MRS) is proposed as an internet-based information retrieval and recommendation robots system for casual communication in home environment. The mascot robot system is developed as a the national project with the purpose of developing the Common Basis of Next-Generation Robots led by the New Energy and Industrial Technology Development Organization (NEDO).

This mascot robot system is a network composed of four fixed type eye robots, one mobile self-propelled type eye robot, an information recommendation module, the speech recognition module (SRM), and a server that is responsible for overall management. Robot Technique Middleware (RT Middleware) developed by AIST Japan is used to connect between the system's components. With RT Middleware, each robot can be viewed as a network component and the whole system can be managed from high level. The outline of the system is shown in Fig. 4.1. The configuration is shown in Fig. 4.2. Every robot is composed of a controlled PC, a microphone, a Speech Recognition Module (SRM) and an eye robot. In the mascot robot system, one directional microphone is used for the mobile robot while four non-directional microphones are used the fixed robots. The SRM processes speech inputs and then indicates the recognition result on the PC display or writes down

the information in a log file through the RT Middleware network system. Depending on the recognition results, the eye robots, in Fig. 4.3, express their corresponding emotions through designated actions [6, 7].

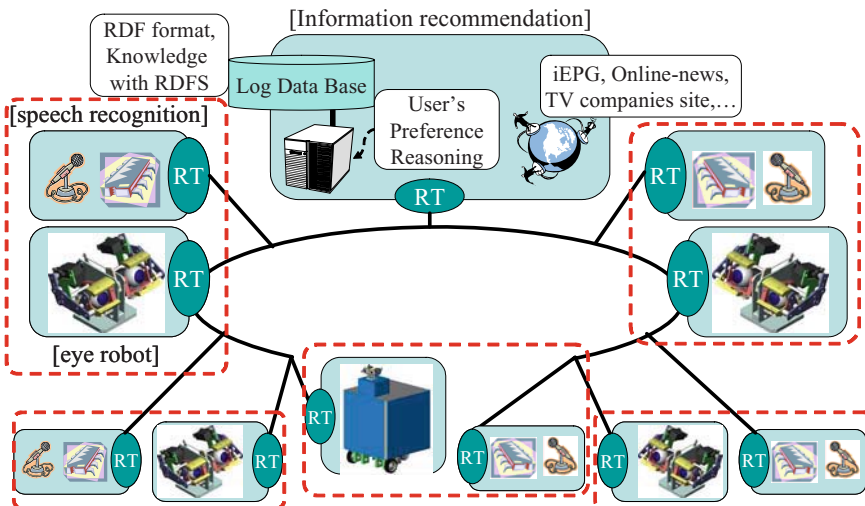


Fig. 4.1. The outline of the mascot robot system

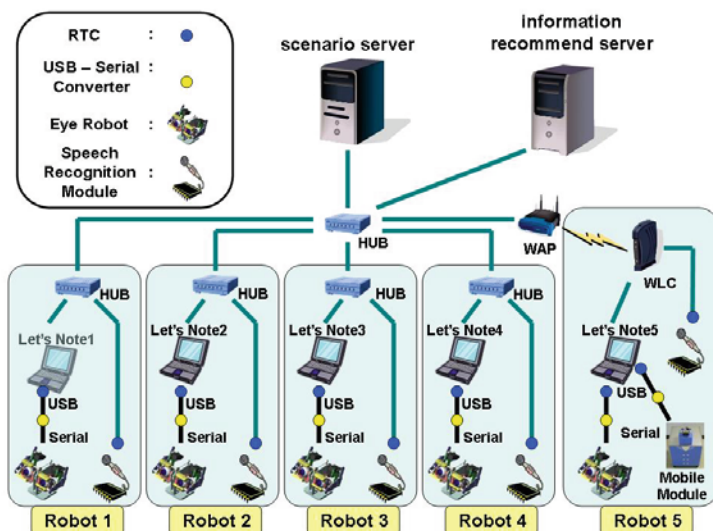


Fig. 4.2. The construction of the mascot robot system

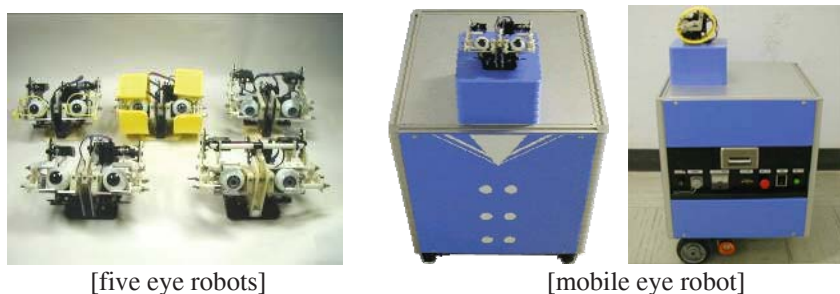


Fig. 4.3. The appearance of eye robots

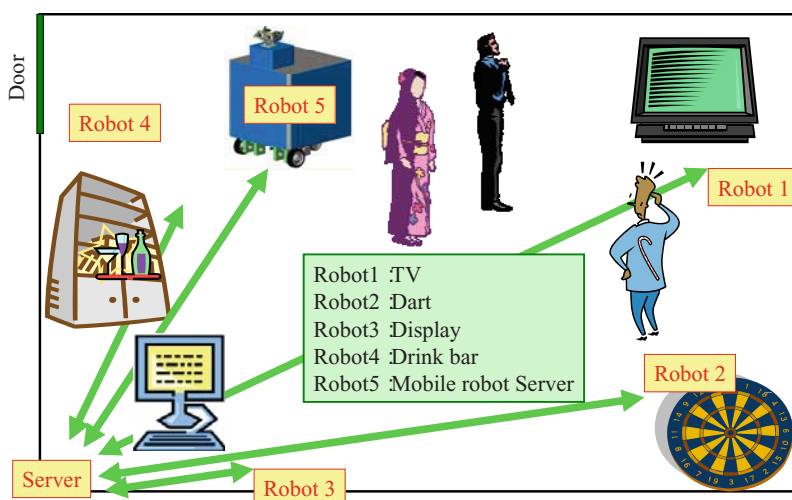


Fig. 4.4. The arrangement of the robots in the room

The SRM developed by NEC, Inc. is a compact hardware device with small size, low cost, low power consumption. This device is developed as one of three main parts in NEDO project.

This system has been tested in an interior space simulating a home environment. The fixed type robots are put on furniture and appliances such as the TV, a PC or a closet. The mobile self-propelled type eye robot, in Fig. 4.3, moves along with users. The arrangement of the system in a room is shown in Fig. 4.4 with the mobile self-propelled type eye robot. A host and two guests are considered as users

of the mascot robot system. In the environment, the mascot robot system is ascertained the validity based on a typical situation scenario where the mascot robot system performs representative function of the system. The specific of the scenario is as follows. When the user mentions something to the robots that requires an affinity response (for example, "this is interesting", "it's cold, isn't it?" etc...), the system searches for and subsequently provides information based on the user's speech. Communication between the user and the system is established by the user's speech to the robots and the robot's response as an emotional expression, as well as displaying information on a screen. For example, the mascot robot system can propose cocktail recipes or provide companionship during a game of darts and reacting accordingly to the performance of the players. The mascot robot system could also take cues from baseball games on TV and offer the user information about the players participating in the game [10].

4.2 Information Recommendation Based on Speech Recognition Module

A System interface needs to understand information from human by humanlike way for casual communication in home environment. In the system, speech recognition is used.

The information recommendation module collects information about users from their preference including their speech and the Web, proposes interesting information for users, and presents the assist information to uses [11].

The speech recognition module is developed for general robot systems by NEC Corporation in the Development Project for a Common Basis of Next-Generation Robots led by the NEDO organization. Its functions are single word speech recognition, noise canceller, sound source directional detection, speaker independent recognition and dictionary switching, i.e. it can select a specific dictionary fitting with current conversation topic. The speech recognition principle in the SRM is a word-matching search based on pre-defined dictionary. In addition, the noise canceller function of this module is improved by using directional and non-directional microphones. The situation of the information recommendation by the system is shown in Fig. 4.5.

The functionality of the mascot robot system is demonstrated in an interior space simulating a home environment. Experimentally, it is confirmed that the mascot robot system provides informative support to the human with casual communication in the home environment [8, 11].



Fig. 4.5. The information recommendation at the mascot robot system

5 Experiments for Impression Evaluation of the Expression by Eye Robot System

To verify the validity of the eye robot system, Mentality expression experiments with 2 scenarios are performed, and the results are evaluated by questionnaire. The experimental procedure is described in 5.1. The result is described in 5.2.

5.1 Experiment Procedures of an Experiment for Impression Evaluation

To verify the validity of the eye robot system, experiments are performed with human interlocutors. The purposes of the experiment are to check the transition from one mentality state to another and to evaluate the expressivity of the motions corresponding to each mentality expression. Mentality state transitions and mentality expression motions are closely linked to each other. The interlocutor cannot figure out the conversation's context by knowing only one of them, but instead needs both of them simultaneously to be able to perform an adequate evaluation.

The eye robot is positioned 1 m in front of the test subject and at the same level as that of his eyes. The eye robot is controlled by PC into which the operator inputs the language category information.

The procedure for the evaluation experiment is as follows:

- 1) The operator informs the interlocutor about the inputs and outputs.
- 2) The operator iteratively inputs the same language category information based on a scenario that is determined in advance. The type of language category information is shown to the interlocutor.
- 3) The interlocutor evaluates the motions of the robots eye balls and eye lids.
- 4) Steps 2) and 3) are repeated until the end of the scenario.

Two types of scenario are prepared for this evaluation experiment. These scenarios have 5 types of language category information as input. The start point of the affinity pleasure-arousal space is supposed to be the origin point. The first input is '6. Greeting' because conversations among humans are often started by the triggering effect of greeting words, e.g. "Hello!", "Do you have a moment please?". All Inputs of language category information for each scenario are shown in Table 5.1. The mentality state trajectory in the affinity pleasure-arousal space for scenario 1 and scenario 2 are shown in Fig. 5.1, respectively. The representative motions performed by the eye robot for scenario 1 and scenario 2 are shown in Fig. 5.2, respectively.

Table 5.1. Language category information inputs for each scenario

order	Input category	
	scenario1	scenario2
1	CAT6	CAT6
2	CAT3	CAT5
3	CAT2	CAT4
4	CAT5	CAT2
5	CAT1	CAT1

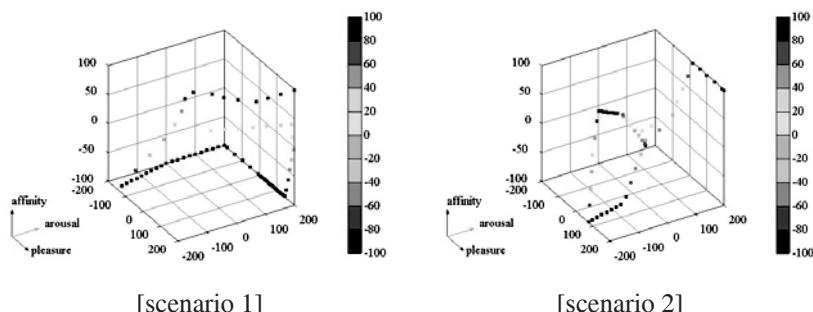


Fig. 5.1. The mentality state trajectory in the affinity pleasure-arousal space for each scenario

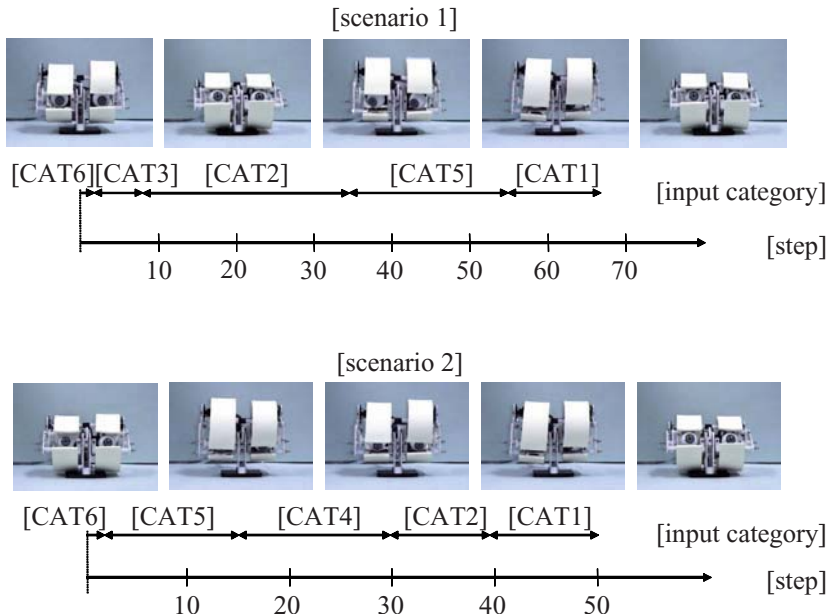


Fig. 5.2. The representative motions for each scenario

5.2 Evaluation Results of Impression Evaluation

The subjects consisted of twelve engineering students (nine men and three women). The results of the questionnaire for scenario 1 and scenario 2 are shown in Fig. 5.3, respectively. These figures show the mean evaluation values by all subjects for each category. These categories are arranged according to the timeline of each scenario. These figures show that the evaluation value increases as the timeline progresses. The mean of all categories in scenario 1 and scenario 2 are shown in Table 5.2. In this table, the average of evaluation value for scenario 1 is higher than that of scenario 2.

The overall evaluation value is 3.6 in Table 5.2, which confirms the validity of the eye robot system. The eye robot system expresses mentality states in a way that can be understood by human beings during conversation. This value might be negatively biased due to the fact that actual semantic content was not taken into account in the communication. This value would increase if the system had a speech recognition module.

The evaluation value increases as the timeline progresses. This may be due to the interlocutor gradually getting used to the eye robot's mentality expressions. The subject should be able to assimilate the mentality expression motions and motivations of the eye robot during the time span of the experiment. If that should be

the case, the eye robot system will perform better during real life communications in a home environment, since these would have typically longer time spans than those of the performed experiments.

The average score of scenario 1 is higher than that of scenario 2. The reason could be that the transition range of coordinates in the affinity pleasure-arousal space for scenario 2 is smaller than that for scenario 1. In scenario 2, the coordinates of the affinity pleasure-arousal space are moving in the negative direction along the affinity axis. In the area where the coordinate values of affinity are relatively small (about 0 to -50), the transition in the pleasure-arousal plane is restrained. The motions do not change their direction or frequency drastically. This should influence the evaluation of the interlocutor.

The same problem might in fact be present in human-to-human interlocution in a similar manner.

Table 5.2. Averages of evaluation value for all of language categories inputs in each scenario

	scenario1	scenario2	total
Average	3.68	3.45	3.57
Standard deviation	1.17	1.20	1.19

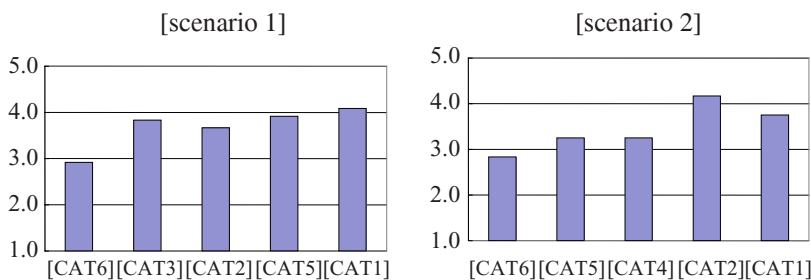


Fig. 5.3. Evaluation values for each language category input in each scenario

Conclusion

An eye robot focused on eye expression and a mascot robot system are proposed as casual communication robot systems with human friendly expression.

The mentality expression system based on the affinity pleasure-arousal space by eye robot is proposed for the interaction of humans and robots in a home environment. The three-dimensional affinity pleasure-arousal space is proposed to

express the continuous evolution of mentality states during conversation. The Pleasure-displeasure axis relates to favor displayed by the interlocutor. The arousal-sleep axis relates to liveliness in communication. Affinity relates to the relationship with the interlocutor that changes with time as the communication progresses.

Fuzzy inference is used to express the mentality eye motions that are arranged in the affinity pleasure-arousal space. The input for the fuzzy inference engine consists of four parameters, language category information, and three-dimensional coordinates in the affinity pleasure-arousal space. Language category information is supposed to be generated by a speech recognition system.

The eye robot that performs eye motions is developed based on the mechanisms of the human eye. Eye motions consist of eyelid motion and ocular motion. The eye robot has 2 DOF for the eyelid part and 3 DOF for the ocular part. The size of the eye robot is 130 mm in width, 80 mm in height, and 75 mm in depth, which is inspired by the size of the eyes of a five-year-old child. The eye robot has five micro servomotors that are controlled by an H8 microcontroller.

The eye motion of the eye robot is represented by a combination of eyelid motion and ocular motion. Eyelid motion is defined by two parameters: position and frequency. Ocular motion is defined by three parameters: ocular position in the pitch and yaw directions, and frequency. Mentality expression experiments with 2 scenarios are performed, and the results are evaluated by questionnaire. The experimental results show that the average evaluation value is 3.6 out of 5.0 as estimated by 12 interlocutors. From these results the validity of the proposed system is confirmed.

A mascot robot system is proposed as an internet-based information retrieval and recommendation system for casual communication in home environment.

This mascot robot system is a network composed of four fixed type eye robots, one mobile self-propelled type eye robot, an information recommendation module, the speech recognition module and a server that is responsible for overall management.

The eye robot expresses emotional reactions with the information presentation for casual communication in home environment. These reactions are determined by fuzzy inference in the proposed affinity pleasure-arousal space.

The information recommendation module collects information about users from their preferences which includes their speech. The web then proposes interesting information for users.

The speech recognition module is developed for general robot systems by NEC Corporation. Its functions are single word speech recognition, noise cancellation, sound source directional detection, speaker independent recognition and dictionary switching.

The eye robot, the information recommendation, and the speech recognition are developed as modules, and integrated with RT Middleware, a middleware for developing robot system developed by AIST.

The functionality of the mascot robot system is demonstrated in an interior space simulating a home environment. Experimentally, it is confirmed that the

mascot robot system provides informative support to the human with casual communication in the home environment.

The proposed system is suitable for a communication architecture between a human interlocutor and a robot. The system can form a suitable basic interface for an information terminal in a home environment. This is true in a society that is both aging fast and growing accustomed to easy to understand interfaces provided by advanced information processing techniques.

Acknowledgments. This research works were financially supported by 21st Century Center of Excellence (COE) Program “Creation of Agent-Based Social Systems Sciences” (ABSSS)as a project; “Mathematical System of Decision Making”, and NEDO as a project; “Development Project for a Common Basis of Next-Generation Robots/ Development of Speech Recognition Device and Module (FY2005-FY2007)”.

References

- [1] Breazeal, C.: Robot in Society: Friend or Appliance. In: Agents 1999 Workshop on Emotion-based Agent Architectures, pp. 18–26 (1999)
- [2] Senda, M., Kobayashi, H., Shiba, T., Yamazaki, Y.: Impression Evaluation of the realistic Face Robot. In: Proc. Human Interface Symposium, pp. 507–510 (2003)
- [3] Miwa, H., Takanishi, A., Takanobu, H.: Experimental Study on Robot Personality for Humanoid Head Robot. In: Proc. IEEE/RSJ Int. Conf. Robots and Systems, pp. 1183–1188 (2001)
- [4] Fukuda, T., et al.: Human-Robot Mutual Communication System. In: Proc. IEEE Int. Workshop on Robot and Human Communication, pp. 14–19 (2001)
- [5] Yarbus, A.L.: Eye Movements and Vision. Plenum, New York (1967)
- [6] Yamazaki, Y., Hatakeyama, Y., Dong, F., Nomoto, K., Hirota, K.: Fuzzy Inference-based Mentality Expression for Eye Robot in Affinity Pleasure-Arousal Space. J. of Advanced Computational Intelligence and Intelligent Informatics. 12(3), 304–313 (2008)
- [7] Yamazaki, Y., Dong, F., Uehara, Y., Hatakeyama, Y., Nobuhara, H., Takama, Y., Hirota, K.: Mentality Expression in Affinity Pleasure-Arousal Space using Ocular and Eyelid Motion of Eye Robot. In: Proc. Joint 3rd International Conference on Soft Computing and Intelligent Systems and 7th International Symposium on Advanced Intelligent Systems, pp. 422–425 (2006)
- [8] Yamazaki, Y., Dong, F., Masuda, Y., Uehara, Y., Kormushev, P., Vu, H.A., Le, P.Q., Hirota, K.: Intent Expression Using Eye Robot for Mascot Robot System. In: Proc. 8th International Symposium on Advanced Intelligent Systems, pp. 576–580 (2007)
- [9] Yamazaki, Y., Vu, H.A., Le, Q.P., Fukuda, K., Matsuura, Y., Hannachi, M.S., Dong, F., Takama, Y., Hirota, K.: Mascot Robot System by integrating Eye Robot and Speech Recognition using RT Middleware and its Casual Information Recommendation. In: Proc. 3rd International Symposium on Computational Intelligence and Industrial Applications, pp. 375–384 (2008)
- [10] Vu, H.A., Yamazaki, Y., Fukuda, K., Matsuura, Y., Le, P.Q., Oikawa, H., Ohnishi, K., Takama, Y., Dong, F., Hirota, K.: The Interrupt of Mascot Robot System Embedded in RT Middleware Based on Fuzzy Logic. Advanced Controls of Active and Robotic Systems 7(1), 11–28 (2009)
- [11] Namba, H., Iwase, Y., Takama, Y.: System Design Based on RT-middleware for Human-Robot Communication under TV Watching Environment. In: Proc. 8th International Symposium on Advanced Intelligent Systems, pp. 587–590 (2007)

Fuzzy Communication and Motion Control by Fuzzy Signatures in Intelligent Mobile Robots

Áron Ballagi¹, László T. Kóczy^{2,3}, and Tamás D. Gedeon⁴

¹Department of Automation, Széchenyi István University
Egyetem tér 1, H-9026, Győr, Hungary

ballagi@sze.hu

²Institute of Mechanical, Electrical Engineering and Information Technology, Széchenyi
István University

Egyetem tér 1, H-9026 Győr, Hungary

³Department of Telecommunications and Media Informatics, Budapest University of
Technology and Economics

Magyar tudósok krt. 2, H-1117 Budapest, Hungary

koczy@tmit.bme.hu

⁴Department of Computer Science, Australian National University
Acton, ACT (Canberra), Australia

tom.gedeon@anu.edu.au

Abstract. This paper presents two examples for the deployment of fuzzy signatures in the field of intelligent mobile robots. The first shows a complex lateral drift control method base on fuzzy signatures. This method considers the motion system of the robot as a whole, unlike as simple parts of a complex system. The state space is written down by fuzzy signatures which add up flexibility, adaptability and learning ability to the system. In the second experiment a new communication approach is investigated for intelligent cooperation of autonomous mobile robots. Effective, fast and compact communication is one of the most important cornerstones of a high-end cooperating system. In this paper we propose a fuzzy communication system where the codebooks are built up by fuzzy signatures. We use cooperating autonomous mobile robots to solve some logistic problems.

Keywords: fuzzy signatures, fuzzy communication, intention guessing, mobile robotics, motion control.

1 Introduction

Fuzzy signatures structure data into vectors of fuzzy values, each of which can be a further vector, are introduced to handle complex structured data [3, 5, 7, 8]. This will widen the application of fuzzy theory to many areas where objects are complex and sometimes interdependent features are to be classified and similarities / dissimilarities evaluated. Often, human experts can and must make decisions based on comparisons of cases with different numbers of data components, with even some components missing. Fuzzy signatures were created with this objective in mind. This tree structure is a generalization of fuzzy sets and vector valued fuzzy sets in a way modeling the human approach to complex problems. However, when dealing with a very large data set, it is possible that they hide hierarchical structure that appears in the sub-variable structures.

This paper deals with fuzzy signatures as complex state description method in field of control of mobile robots and robot cooperation. The first example stands near to control theory and gives a new aspect of motion control supervisory systems.

Intelligent cooperation is a new research field in autonomous robotics. If one would plan or build a cooperating robot system which has intelligent behaviors, one could not program the all scenarios which may appear in the life of the robots, and would realize that effective, fast and compact communication is one of the most important cornerstones of a high-end cooperating system. We assume settings where communication itself is very expensive, so generally speaking it is advisable to build up as large as possible contextual knowledge bases and codebooks in the distant on-board robot controller computers [10, 11]. Clearly, this is in order to shorten their communication process. This is appropriate if it significantly reduces the amount of information that must be transmitted from one to another, rather than to concentrate all contextual knowledge in one of them, and then to export its respective parts whenever they are needed in the other(s). It appears to be very important in the cooperation and communication of intelligent robots or physical agents that the information exchange among them is as effective and compressed as possible [4]. In this paper we propose a fuzzy communication system where the codebooks are built up by fuzzy signatures. After an overview of this type of fuzzy communication we will deal with some real scenarios of autonomous mobile robot cooperation. The base idea of this example has come from the partly unpublished research projects at LIFE [6]. The paper presents a cooperation system where a group of autonomous intelligent mobile robots is supposed to solve transportation problems according to the exact instruction given to the Robot Foreman (R_0). The other robots have no direct communication links with R_0 and all others, but can solve the task by intention guessing from the actual movements and positions of other robots, even though they might not be unambiguous.

2 Fuzzy Signatures

The original definition of fuzzy sets was $A : X \rightarrow [0,1]$, and was soon extended to *L-fuzzy sets* by Goguen [1]

$$A_s : X \rightarrow [a_i]_{i=1}^k, a_i = \begin{cases} [0,1] \\ [a_{ij}]_{j=1}^{k_i} \end{cases}, a_{ij} = \begin{cases} [0,1] \\ [a_{iji}]_{i=1}^{k_j} \end{cases}, \quad (1)$$

$A_L : X \rightarrow L$, L being an arbitrary algebraic lattice. A practical special case, *Vector Valued Fuzzy Sets* was introduced by Kóczy [3], where $A_{v,k} : X \rightarrow [0,1]^k$, and the range of membership values was the lattice of k -dimensional vectors with components in the unit interval. A further generalization of this concept is the introduction of fuzzy signature and signature sets, where each vector component is possibly another nested vector (right).

Fuzzy signature can be considered as special multidimensional fuzzy data. Some of the dimensions are interrelated in the sense that they form sub-group of variables, which jointly determine some feature on higher level. Let us consider an example. Fig. 1 shows a fuzzy signature structure.

The fuzzy signature structure shown in Fig. 1 can be represented in vector form as follow:

$$x = \begin{bmatrix} \begin{bmatrix} x_{11} \\ x_{12} \end{bmatrix} \\ \begin{bmatrix} x_{21} \\ \begin{bmatrix} x_{221} \\ x_{222} \\ x_{223} \end{bmatrix} \\ x_{23} \\ \begin{bmatrix} x_{31} \\ x_{32} \end{bmatrix} \end{bmatrix}^T \quad (2)$$

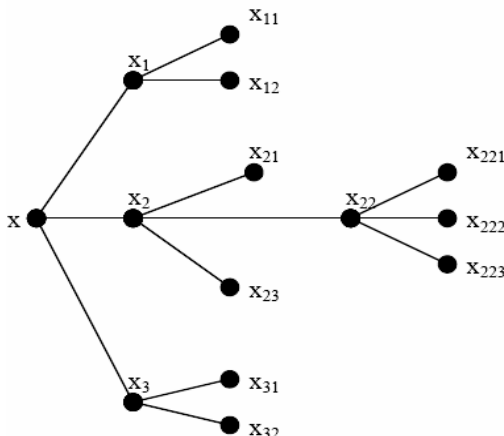


Fig. 1. A Fuzzy Signature Structure

Here $[x_{11} \ x_{12}]$ from a sub-group that corresponds to a higher level compound variable of x_1 . $[x_{221} \ x_{222} \ x_{223}]$ will then combine together to form x_{22} and $[x_{21} \ [x_{221} \ x_{222} \ x_{223}] \ x_{23}]$ is equivalent on higher level with $[x_{21} \ x_{22} \ x_{23}] = x_2$. Finally, the fuzzy signature structure will become $x = [x_{221} \ x_{222} \ x_{223}]$ in the example.

The relationship between higher and lower level is governed by the set of fuzzy aggregations. The results of the parent signature at each level are computed from their branches with appropriate aggregation of their child signature. Let a_1 be the aggregating associating x_{11} and x_{12} used to derive x_1 , thus $x_1 = x_{11}a_1x_{12}$. By referring to Fig. 1, the aggregations for the whole signature structure would be a_1, a_2, a_{22} and a_3 . The aggregations a_1, a_2, a_{22} and a_3 are not necessarily identical or different. The simplest case for a_{22} might be the min operation, the most well known t-norm. Let all aggregation be min except a_{22} be the averaging aggregation. We will show the operation based on the following fuzzy signature values for the structure in the example.

Each of these signatures contains information relevant to the particular data point x_0 , by going higher in the signature structure, less information will be kept. In some operations it is necessary to reduce and aggregate information obtained from another source (some detail variables missing or simply being locally omitted). Such a case occurs when interpolation within a fuzzy signature rule base is done, where the fuzzy signatures flanking an observation are not exactly of the same structure. In this case the maximal common sub-tree must be determined and all signatures must be reduced to that level in order to be able to interpolate between the corresponding branches or roots in some cases [8].

$$x = \begin{bmatrix} 0.3 \\ 0.4 \\ 0.2 \\ 0.6 \\ 0.8 \\ 0.1 \\ 0.9 \\ 0.1 \\ 0.7 \end{bmatrix}^T \quad (3)$$

After the aggregation operation is performed to the lowest branch of the structure, it will be described on higher level as:

$$x = \begin{bmatrix} 0.3 \\ 0.2 \\ 0.5 \\ 0.9 \\ 0.1 \end{bmatrix}^T \quad (4)$$

Finally, the fuzzy signature structure will be:

$$x = \begin{bmatrix} 0.3 \\ 0.2 \\ 0.1 \end{bmatrix}^T \quad (5)$$

3 Mobil Robot Motion Control System

The differentially steered drive system used in many robots is essentially the same arrangement as that used in a wheelchair. Thus, steering the robot is just a matter of varying the speeds of the drive wheels. At least two independent driving chains are used in most of differentially steered drive system. Each driver wheel has the own controller in a traditional motion system, which give a hard tuned, rigid arrangement. In this paper we propose a complex lateral drift control method base on fuzzy signatures. This method inspects the motion system as a whole, unlike as simple parts of a complex system. The state space is written down by fuzzy signatures which add up flexibility, adaptability and learning ability to system.

3.1 Lateral Drift Control Method

We propose a motion control method which treats the robot locomotion as whole, without inspection of drive and other system separately. The base of this method is the lateral drift measure. Every sampling time the sensors collect information about the difference between the theoretical trajectory and the real trajectory or position as Fig. 2 shows. For the sake of simplicity let us assume that the followed lane is parallel with the x-axis and linear. The $e(T_1)$ is the measured error (lateral drift) on the T_1 sampling time.

Essentially, this implementation attempts to control a secondary effect, the overall locomotion behavior of the robot, rather than a primary effect (individual motor speed).

Theoretically the measured error and changing of the error (speed and direction) give enough information to control and correct the lane-following of the robot. We built fuzzy signature base control algorithms to cope this relatively complex control problem.

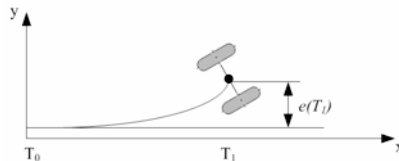


Fig. 2. Track of the robot on a Cartesian coordinate plane

3.2 Fuzzy Signature-Based Motion Control

In the lateral drift motion control method the controlled robot is a complex system which can be handled by fuzzy signatures based supervisory regulator [9]. The reference sub-tree (R_e) is the base of the controller, which depicts the state of the robot trajectory drift. Equation (6) and Fig. 4 show the scheme of fuzzy signature for R_e , where e is the measure of lateral error and de/dt is the velocity of error changing. A new branch appears on higher level: the Δe , the error changing between two sampling, signs the success of preview manipulation of controller. The Δe is very important for self-diagnosis and latter adaptation.

$$R_e = \begin{bmatrix} D \\ \Delta e \end{bmatrix} = \begin{bmatrix} \left[\begin{array}{c} e \\ \frac{de}{dt} \end{array} \right] \\ \Delta e \end{bmatrix} \quad (6)$$

The used linguistic value in signatures are:

$$e = \begin{cases} \text{Negative Big, Negative Small, Zero,} \\ \quad \text{Positive Small, Positive Big} \end{cases}$$

$$\frac{de}{dt} = \begin{cases} \text{Fast DownGrade, DownGrade, Zero,} \\ \quad \text{UpGrade, Fast UpGrade} \end{cases}$$

$$\Delta e = \begin{cases} \text{Negative Big, Negative Small, Zero,} \\ \quad \text{Positive Small, Positive Big} \end{cases}$$

The above described fuzzy signature can build a basic reference for motion control. If we want use a more sophisticated system then the fuzzy signature is had to complement some new branches or sub-trees. This is a real advantage over classical control structure, where the whole system is had to change in this case.

Let us add a behavior sub-tree (B) to our system. Here the behavior means the control strategy of trajectory following. For example, if the following behavior is soft then the controller softly correct the lateral drift from theoretical trajectory (Fig. 3).

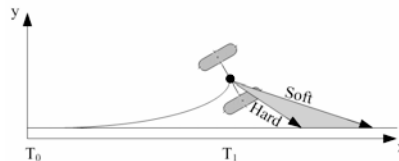


Fig. 3. Track correction behaviors

The motion control fuzzy signature complemented with controller behavior is the following:

$$C = \begin{bmatrix} R_e \\ B \end{bmatrix} = \begin{bmatrix} \left[\begin{bmatrix} e \\ \frac{de}{dt} \\ \Delta e \\ B \end{bmatrix} \right] \end{bmatrix} \quad (7)$$

where the behavior is $B = \{\text{Soft, Moderate, Hard}\}$.

The relationship between higher and lower level is governed by the set of fuzzy aggregations. The results of the parent signature at each level are computed from their branches with appropriate aggregation of their child signature. The fuzzy signature behavior is highly influenced by the chosen aggregations. In our case we use simple fuzzy aggregations, on lowest or leaf level *max*, on the second and third level *average* and on the highest level the *production* aggregation methods are used.

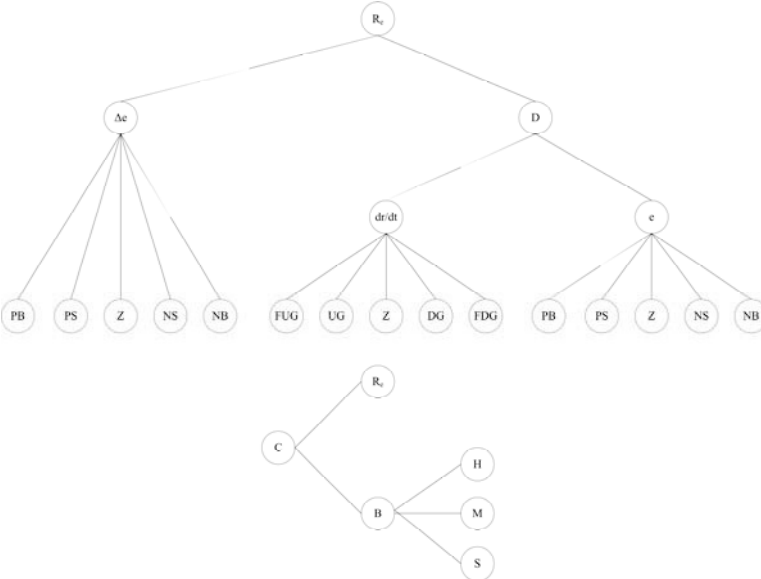


Fig. 4. R_e and the final C fuzzy signatures

This fuzzy signature writes down the state of the robot locomotion in every sampling time and makes a reference signal for control decision. The controller can work with a very simple fuzzy rule base because the fuzzy signature prepares the data for it.

Let us take an example with linguistic values and numerical signatures:

$$C_1 = \left[\begin{bmatrix} \text{Negative Big} \\ \text{UpGrade} \\ \text{Positive Small} \\ \text{Moderate} \end{bmatrix} \right] \rightarrow \left[\begin{bmatrix} 0.1 \\ 0.6 \\ 0.7 \\ 0.5 \end{bmatrix} \right] \quad (8)$$

After the low level aggregation the higher level will be described as:

$$C_1 = \left[\begin{bmatrix} 0.3 \\ 0.7 \\ 0.5 \end{bmatrix} \right] \quad (9)$$

Finally, the fuzzy signature structure will be:

$$C_1 = \begin{bmatrix} 0.5 \\ 0.5 \end{bmatrix} \rightarrow [0.25] \quad (10)$$

Therefore the C_1 control parameter is *Negative Small*, and the manipulation is taken according to this state and behavior fuzzy signature, the robot tend to go back to track with moderate characteristic.

4 Fuzzy Communication of Cooperating Robots

One of the most important parameters of effective cooperation is efficient communication. Because communication itself very expensive, it is much more advisable to build up as large as possible contextual knowledge bases and codebooks in robot controllers in order to shorten their communication process. That is, if it essentially reduces the amount of information that must be transmitted from one to another, than to concentrate all contextual knowledge in one of them and then to export its respective parts whenever they are needed in other robot(s). It appears to be very important in the cooperation and communication of intelligent robots or physical agents that the information exchange among them is as effective and compressed as possible [4].

4.1 The System in Hand

Let us examine a subset of our overall robot cooperation problem work in practice. There is a warehouse where some square boxes wait for ordering. Various configurations can be made from them, based on their color and tags. We have a group of autonomous intelligent robots which try to build the actual order of boxes according to the exact instructions given to the R_0 (foreman) robot. The other robots have no direct communication links with R_0 , but they are able to observe the behavior of R_0 and all others, and they all posses the same codebook containing the base rules of storage box ordering. Every box has an identity color and tag on one side of it. The individual boxes can be shifted or rotated, but always two robots are needed for actually moving a box, as they are heavy. If two robots are pushing the box in parallel the box will be shifted according the joint forces of the robots. If the two robots are pushing in opposite directions positioned at the diagonally opposite ends, the box will turn around the center of gravity. If two robots are pushing in parallel, and one is pushing in the opposite direction, the box will not move or rotate, just like when only a single robot pushes. Under these conditions the task can be solved, if all robots are provided with suitable

algorithms that enable intention guessing from the actual movements and positions, even though they might be unambiguous.

Fig. 5 presents some example of how eleven boxes can be arranged. The robots would move or push the boxes, so one box has max two neighbors on their opposite sides. The tag of the box, which is always on the Relative-North side of the box (as we will see below), must be visible (so do not adjoin any other object), so the box can touch others only the East or/and West sides.

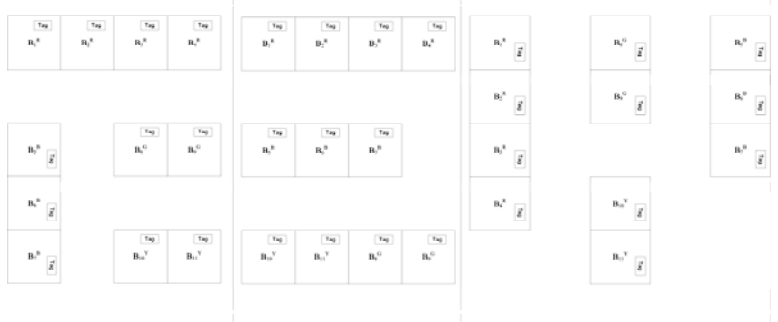


Fig. 5. Examples for box arrangement

In the description two direction sign systems are used, the absolute direction with letters N, E, S, W as in the usual sense for North, East, South and West. The second direction sign system is a box relative system where the sides of a box are N_B , E_B , S_B and W_B respectively (Fig. 6). The position of the objects (boxes and robots in this case) always can be described by the absolute course, latitude and longitude of the object. One object relative position to a box is described by the box relative system, i.e. which side of the box is touched by that object.

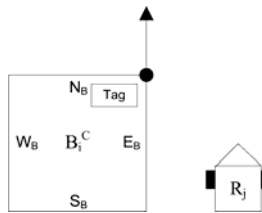


Fig. 6. Symbols of boxes and robots

The box has a B_i^C sign which means that is the i^{th} Box with C color (e.g.: R for red). Fig. 3 depicts the features of a box and robot. The R_j is the sign of the j^{th} robot. The R_0 is a distinct one, namely it is the robot foreman, the only robot that exactly knows the task on hand.

There are just a few essentially different robot positions allowed. Because two robots are needed for pushing or turning a box, at each side of the boxes, two spaces are available for the robots manipulating them: the “counterclockwise position” and the “clockwise position” (see Fig. 7). The position is described by

$P_r^b = [S, T]$ where r is the number of the robot, b is the number of the box, S is the side of the box where the robot touch it (N_B , E_B , S_B and W_B respectively) and the T is the turning position that means “counterclockwise position” or “clockwise position” (CC or CW).

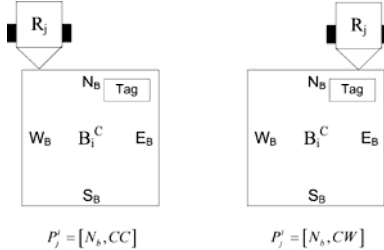


Fig. 7. Robot positions at the N_B side of the box

The cooperating combination of robots is denoted by $C_{i,j,(k)}^b$ where i, j and k is the number of the robots (k appears only in stopping combinations), and b is the number of the box. There are three essentially different combinations (Fig. 8), $C_{1,2}^i = P$ is the “pushing or shifting combination”, when two robots (R_1 and R_2) are side by side at the same side of the table; $C_{1,2}^i = RC$ stands for “counterclockwise rotation combination”; and $C_{1,2}^i = RW$ denotes “clockwise rotation combination”.

In the first case R_1 and R_2 are in the relative North (N_B) position, in the other two, North (N_B) and South (S_B). Of course, all the other three directions are similarly allowed. Any other combination of two robots is illegal, except see the next paragraph (“stopping combination”). The three essentially different combinations can be seen in Fig. 8.

Eventually, in Fig. 9, the combinations are shown where two robots intend to do a move operation (shift or rotate), and another robot that has recognized the goal box configuration positions itself to prevent a certain move. $C_{1,2,3}^i = ST$ is essentially a three robot combination, where either R_1 and R_2 are attempting a shift and R_3 positions itself to prevent it, or R_2 and R_3 / R_1 and R_3 are starting a rotation and R_1 and R_2 prevent it, knowing that the intended move is wrong from the point of view of the goal configuration.

However, in $C_{1,2,3}^i = ST$ it is sufficient that R_1 takes up its $P_1^i = [N_B, CC]$ position if R_3 is aware that both the shift and the rotate counterclockwise combinations would be wrong from the point of view of the goal, thus R_3 immediately stops the maneuver by assuming the $P_3^i = [S_B, CW]$ position, thus preventing both shift and clockwise rotation.

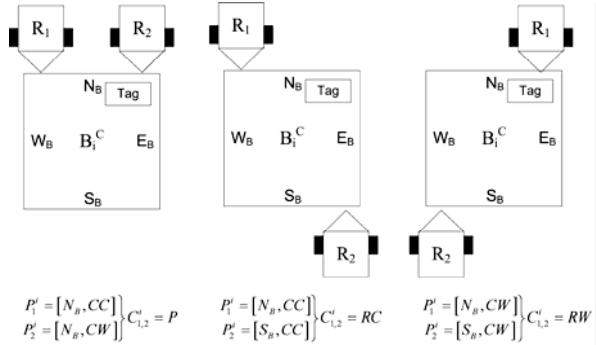


Fig. 8. Allowed combinations of two robots for moving the table

This is an exception where a two robot combination other than the ones listed in Fig. 8 is legal as a temporary combination, clearly signalizing “stop this attempt as it is in contrary to the goal”. A symmetrical pair of the three robot combination but for stopping shift to the South or a counterclockwise rotation can be seen in the second part of Fig. 9.

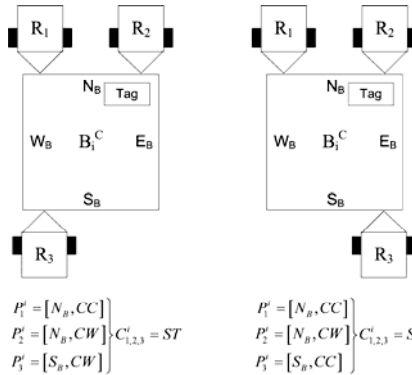


Fig. 9. Three and two robot stopping configurations

4.1.1 Fuzzy Signature Classes

On basis of the features of the boxes the robot can build a fuzzy signature for each box. This signature built up on a template or class, and every box has its own instance of the Box fuzzy Signature Class (BSC). This signature records the position, the arrangement, the dynamic and the robots working on the actually box. Let us see the construction of this fuzzy signature class. As can be seen in Eq. (11), the main signature has three sub-signatures.

$$B_i^c = \begin{bmatrix} P \\ AR \\ DY \end{bmatrix} \quad (11)$$

The first is the position (P) sub-signature which describes the actual fuzzy position of the box (e.g.: Nearly North). It has four leaves namely the points of the compass, North, East, South and West. The box is “in direction” if its reference side lays near to any main compass direction (Fig. 10).

It is important that the real position of a box has two other parameters: the latitude and the longitude of its reference point, but it does not have any importance to decision making only in navigation, so we abandon these parameters here.

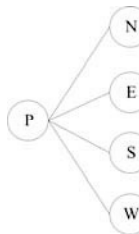


Fig. 10. Box position fuzzy signature

The second branch of box fuzzy signature is the arrangement that describes the box’s connections to other boxes. As it was described above, a box can connect to none, one or two other boxes. Therefore the signature has two main branches for the no connection case, and for the connected case, which has two other branches for connect to one, connect to two boxes. The leaves describe the side of connection. As we see this signature we can observe that there are some surprising permitted connect positions in it (e.g.: North or tag side). These are very useful for decision making about wrong positions and wrong dynamic of the box. Fig. 11 presents the arrangement signature (AR) where AL is the “alone” (no connection) branch, NB are the neighbor boxes: one or two and the direction of the join.

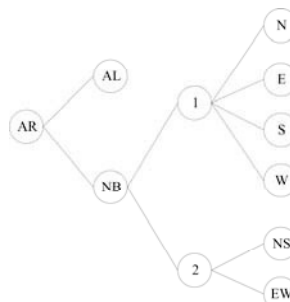


Fig. 11. Box arrangement fuzzy signature

The next branch is the dynamic feature (*DY*) of the box, which is valid if robots work on the box and records what the robots are doing: push or rotate, and in which direction. This signature includes all the valid combinations of robots, and all valid movements of boxes. This is shown in Fig. 12, with the number of robots at a box (*1R*, *2R*, *3R* respectively), the effect of this combination of robots (*SH* as shift and *R* as rotate) and the direction.

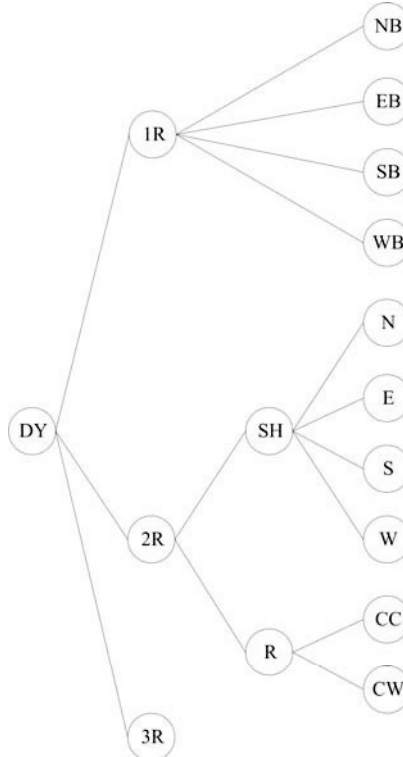


Fig. 12. Dynamic fuzzy signature

These three output fuzzy signatures are able to describe the actual states of the box and give a basis for the fuzzy decision process in the robot control. Every robot builds its actual knowledge-base from the fuzzy signature classes and then boxes are assigned individual signatures in each individual robot controller.

The second necessary fuzzy signature class is the Robot state fuzzy Signature Class (RSC), which describes the state of each robot. This represents the dynamic and working behavior of the robot. In this paper we do not consider the robot signatures in detail because they do not have an important role in the primary decision making.

4.1.2 Fuzzy Decision

The above described fuzzy signatures enable robots to recognize a situation in the warehouse, and then the robots use their codebooks to take action accordingly. Let us see the codebook, namely a hidden fuzzy decision tree, in the robot controller. For simplicity we have cut the decision tree to sub-trees, then arranged them in a logical sequence. The robot takes decisions from some simple cases to more complex ones. The Fig. 13 shows the entry point of the decision process. This figure depicts the steps of decision making based on fuzzy signatures, where the diamond shaped objects denote the elementary decisions (decision milestones) and hide the fuzzy signatures that are used. The used and hidden signatures are presented by a grey arrow with the signature name.

It is important to mention here this is only a local task and the final decision making needs the global signatures and other robot signatures, but these are beyond the scope of this paper. The first step in the local decision is to search for the nearest box, after which the box signature is built up or updated. In the next level, the position of the box is investigated which is described by the P signature. If the membership value of any good direction (N, E, S or W) is high enough, then the decision process steps to the next level and takes the arrangement (AR) and dynamic (DY) signatures of the box, if not then there is a simple decision: the box must rotate. Which direction? This is dependent on the global state of system, which is described by global signatures.

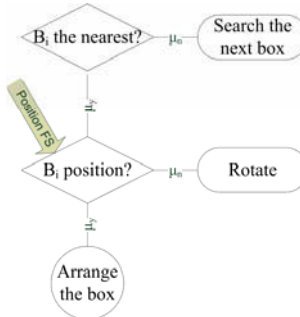


Fig. 13. Entry point of decision task

The arrangement and dynamic signatures are used in a partially parallel way. Fig. 14 shows the whole decision task from this point. The robot analyzes the arrangement and dynamic of the box. If three robots work on it then there is a Stop combination and our robot (R_i) does not have any task on this box, it must search the next box. If two robots work on it and the guessed result points to higher order then R_i leaves it and searches the next near box. If the box has one or two neighbors in a good combination then the membership degree of “on the place” is raised and any dynamic (shift or rotate) is forbidden so if there any robot combination the R_i should go to the Stop position. Of course, if the neighbors of the box are not in a good place then more analysis is necessary to take the appropriate

decision. If one robot waits for help there, then R_i decides which is a good position for pushing or turning the box and goes to this position. The most complex decision problem appears when any robot is not at the box; in this case R_i needs to take a decision about the box alone. This higher level problem is not covered in this paper.

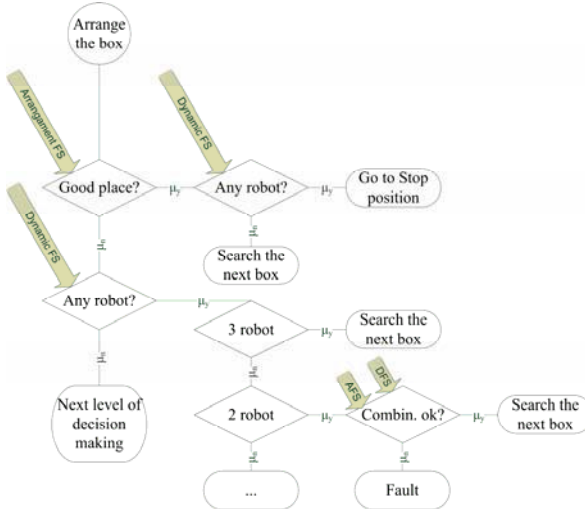


Fig. 14. The decision task

Based on the above considerations it is possible to build some elements of the context and codebook for cooperating robots. It takes the form of a decision tree, where the inputs are the fuzzy signatures of the observations, the first level outputs are intention guesses and the second level outputs the concrete actions of the corresponding robot.

5 Future Works

Research towards extending this fuzzy communication method to more complex robot cooperation is going on currently. We will build further algorithms for fuzzy communication which will be tested and developed in a simulation environment.

We have some micro-sized autonomous mobile robots as Fig. 15 shows. These robots can move, avoid collision and perform the simple shifting tasks of the nature we describe in this paper in a well-defined environment. At the next stage these robots will be used as a real cooperating system. In other works we are investigating scenarios in which the foreman is directly controlled by a human (in a game-like environment, this is effectively a human controlled agent), in particular extending the use of eye gaze to allow the assistant robots to better predict human intentions [2].

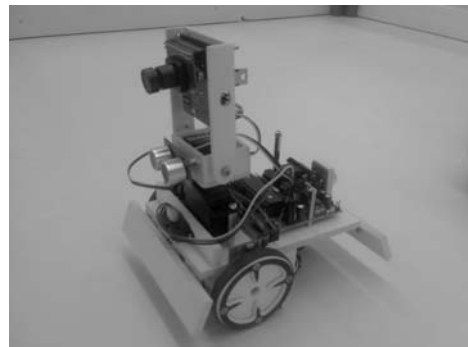


Fig. 15. The B-bot Micro

6 Conclusions

In this paper we presented the usage of fuzzy signature based algorithms on field of mobile robotics. These methods were used in totally other level of robot control. The motion control stays the lower layer of control hierarchy than the cooperation system which is a high level strategy control algorithm. We could see the applicability of fuzzy signatures on these two layers of mobile robot control.

We experimented with a new fuzzy signature based motion control system for a differentially driven mobile robot, which gives more flexibility and modularity on the control level with less computational complexity.

Fuzzy communication contains vague or imprecise components and it might lack abundant information. If two robots are communicating by a fuzzy channel, it is necessary that both ends possess an identical part within the codebook. The codebook might partly consist of common knowledge but it usually requires a context dependent part that is learned by communicating. Possibly it is continuously adapting to the input information. If such a codebook is not available or it contains too imprecise information, the information to be transmitted might be too much distorted and might lead to misunderstanding, misinterpretation and serious damage. If however the quality of the available codebook is satisfactory, the communication will be efficient i.e. the original contents of the message can be reconstructed. At the same time it is cost effective, as fuzzy communication is compressed as compared to traditional communication. This advantage can be deployed in many areas of engineering, especially where the use of the communication channels is expensive in some sense, or where there is no proper communication channel available at all.

Here we illustrate clearly that the communication among intelligent robots by intention guessing and fuzzy evaluation of the situation might lead to effective co-operation and the achievement of tasks that cannot be done without collaboration and communication.

Acknowledgments. The research was supported by HUNOROB (HU0045) EEA grant, a Széchenyi University Main Research Direction Grant 2009, and National Scientific Research Fund Grants OTKA T048832 and K75711.

References

- [1] Goguen, J.A.: L-Fuzzy Sets. *J. Math. Anal. Appl.* 18, 145–174 (1967)
- [2] Gedeon, T.D., Zhu, D., Mendis, B.S.U.: Eye Gaze Assistance for a Game-like Interactive Task. *International Journal of Computer Games Technology* 2008, Article ID 623752, 10 pages (2008)
- [3] Kóczy, L.T.: Vectorial I-Fuzzy Sets. In: Gupta, M.M., Sanchez, E. (eds.) *Approximate Reasoning in Decision Analysis*, pp. 151–156. North-Holland, Amsterdam (1982)
- [4] Kóczy, L.T., Gedeon, T.D.: Context Dependent Reconstructive Communication. In: 3rd International Symposium on Computational Intelligence and Intelligent Informatics, ISCIII 2007, Agadir, Morocco, March 28-30, 2007, pp. 13–19 (2007)
- [5] Kóczy, L.T., Vámos, T., Gy, B.: Fuzzy Signatures. In: Proceedings of EUROTUSE-SIC 1999, pp. 210–217 (1999)
- [6] Terano, T., et al.: Research Project at LIFE. In: Laboratory for International Fuzzy Engineering Research, Yokohama (1993/1994) (oral presentation)
- [7] Vámos, T., Kóczy, L.T., Gy, B.: Fuzzy Signatures in Data Mining. In: Proceedings of IFSA World Congress and 20th NAFIPS International Conference, pp. 2842–2846 (2001)
- [8] Wong, K.W., Chong, A., Gedeon, T.D., Kóczy, L.T., Vámos, T.: Hierarchical Fuzzy Signature Structure for Complex Structured Data. In: Proceedings of ISCIII 2003 International Symposium on Computational Intelligence and Intelligent Informatics, pp. 105–109 (2003)
- [9] Ballagi, Á., Kóczy, L.T.: Fuzzy Signature-based Mobil Robot Motion Control System. In: SAMI 2008, Herlany, Slovakia (2008)
- [10] Ballagi, Á., Kóczy, L.T., Gedeon, T.D.: Fuzzy Communication in Cooperation of Mobile Robots. In: First Györ Symposium on Computational Intelligence, Györ, Hungary (2008)
- [11] Ballagi, Á., Kóczy, L.T., Gedeon, T.D.: Local Codebook Construction for Fuzzy Communication in Cooperation of Mobile Robots. *Acta Technica Jaurinensis* 1(3), 547–560 (2008)

Part III

Intelligent Control

Linear Switching Systems: Attainability and Controllability

József Bokor, Zoltán Szabó, and László Nádai

Computer and Automation Research Institute, Hungarian Academy of Sciences
Kende u. 13-17, H-1111 Budapest, Hungary
bokor@sztaki.hu, szaboz@scl.sztaki.hu, nadai@sztaki.hu

Abstract. Hybrid systems are characterized by the interaction between continuous-time dynamics (governed by differential or difference equations), and discrete dynamics and logic rules (described by temporal logic, finite state machines, etc.). Recent progress in the theory and practice of modeling and control design have caused an increasing interest in the study of hybrid systems, which is motivated not only by theoretical challenges but also by their ability to model, analyze and synthesize controllers in a large variety of application areas. This paper highlights some aspects encountered when modeling with hybrid systems through a short overview of some controllability and stabilizability results concerning linear switching systems. It was shown how classical techniques, such as geometrical control theory, Lie-algebraic techniques, convex analysis find their applicability in the study of the behavior of the hybrid systems.

1 Introduction

Motivated by the need of dealing with physical systems that exhibit a more complicated behavior than those normally described by classical continuous and discrete time domains, hybrid systems have become very popular nowadays. Hybrid models characterize systems governed by continuous differential and difference equations and discrete variables. Such systems are described by several operating regimes (modes) and the transition from one mode to another is governed by the evolution of internal or external variables or events.

Based on different characteristics of the events that determine the mode transition, it can be usually encountered two primary types of systems: *open-loop systems* (state-independent/nonautonomous), in which the events occur at fixed time and *closed-loop systems* (state-dependent/autonomous), in which the events occur when the trajectory hits a hypersurface in the extended phase space. Depending on the nature of the events there are two big classes of hybrid systems that are considered

in the control literature: *switching systems* and *impulsive systems*. In mathematical terms these systems can be described as:

$$\dot{x}(t) = f_{\sigma(t)}(x(t), u(t)), \quad (1)$$

$$y(t) = h_{\sigma(t)}(x(t), u(t)), \quad x(\tau^+) = \iota(x(\tau^-), u(\tau), \tau), \quad (2)$$

where $x \in \mathbb{R}^n$ is the state variable, $u \in \Omega \subset \mathbb{R}^m$ is the input variable and $y \in \mathbb{R}^p$ is the output variable. $\sigma: \mathbb{R}^+ \rightarrow S$ is a measurable switching function mapping the positive real line into $S = \{1, \dots, s\}$. In general the impulsive effect can be described by the relation $(\tau, x(\tau^-)) \in \mathcal{I} \times \mathcal{A}$ with \mathcal{I} a set of time instances and $\mathcal{A} \in \mathbb{R}^n$ a certain region (hypersurface) of the state space.

Switching systems are intended as the simplest class of hybrid systems. A switching system is composed of a family of different (smooth) dynamic modes such that the switching pattern gives continuous, piecewise smooth trajectories. Moreover, it is assumed that one and only one mode is active at each time instant. In a broader sense every time-varying system with measurable variations in time can be cast as a switching system, therefore it is usually assumed that the number of switching modes is finite and for practical reasons the possible switching functions (sequences) are restricted to be piecewise constant, i.e. only a finite number of transition is allowed on a finite interval. Moreover, sometimes the frequency of the transitions is also bounded – dwell time.

Impulsive control is a control paradigm based on impulsive differential equations where the system should have at least one "impulsively" changeable state variable. The boundary between impulsive plants and nonimpulsive plants is fuzzy. For example considering the variations formula, see e.g. [1], discontinuities in the dynamical equations (switching) can be equally well modeled by introducing sudden changes in the flow (impulses) and vice versa. However, if the control actions are taken in a much shorter time period comparing with the time constant, or natural period of the plant, then the possibility of modeling the system or the controller under impulsive control paradigm might arose.

In certain dynamical systems and in particular mechanical and biological systems, system state discontinuities arise naturally leading to models with multiple modes of operation involving multiple system transitions that give rise to hybrid dynamical systems. On the other hand modeling of physical systems often leads to complex nonlinear models. To get rid of the complexity of the obtained model it is often useful to apply a modeling strategy which represents the system behavior using a set of models with a simple structure, each model describing the system in a particular operating zone. Switched and impulsive systems have numerous applications in fields like mechanical systems, automotive industry, aircraft, air traffic control, network control, chaotic based secure communication, quality of service in the Internet, video coding, etc. Impulsive dynamical systems include non-smooth mechanical systems involving system collisions, shocks, and friction.

Investigations of geometrical and optimal control theory led very early to models and controllers that have discontinuous dynamics. Among the earliest investigations of dynamical systems involving continuous dynamics and discrete switchings can be traced back to relay control systems and bang-bang optimal control. Orbits, the central objects of the Nagano, Sussmann, Jurdjevic theory of attainability, are nothing else than switching sequences of vector fields, see [16, 1] while in the field of stabilizing and optimal control it turns out that even very simple systems as the Brockett's integrator:

$$\dot{x}_1(t) = u_1, \quad \dot{x}_2(t) = u_2, \quad \dot{x}_3(t) = x_2 u_1 - x_1 u_2, \quad (3)$$

cannot be stabilized by using continuous feedback control, [8].

Modern complex dynamical systems typically possess a hierarchical structure characterized by continuous-time dynamics at the lower-level units and logical decision-making units at the higher-level of hierarchy. Thus, in addition to traditional control systems, hybrid control systems involve supervising controllers which serve to coordinate the (sometimes competing) actions of the lower-level controllers. A typical range of applications that exhibit such behavior are related to the fault tolerant and reconfigurable control system paradigm.

In fuzzy control, [21], there is a more significant emphasis on the use of heuristics and there is a focus on the use of logic-based rules to represent how to control the plant rather than ordinary differential equations. This approach can offer some advantages in that the representation of knowledge in rules seems more lucid and natural for certain applications. Employing the Takagi-Sugeno fuzzy model, which utilizes local linear system description for each rule, a control methodology was developed that fully take advantage of the advances of modern control theory, [30]. A fuzzy controller, as a hybrid system, can be considered as an artificial decision maker that operates in a closed-loop system in real time.

The range of applications of hybrid and impulsive dynamical systems is not limited to controlled dynamical systems. Their usage arises in several different fields of science, including computer science, mathematical programming, and modeling and simulation. In computer science, discrete program verification and logic appears in a continuous environment giving rise to hybrid dynamical systems. In mathematical linear and nonlinear optimization with inequality constraints, changes in continuous and discrete states can be computed by a switching dynamic framework.

Hybrid dynamical systems exhibit a very rich dynamical behavior, such as Zeno solutions, noncontinuability of solutions, deadlock, etc., depending on which type of solution (e.g. Charateodory, Filippov) is considered. A Zeno solution involves a system trajectory with infinitely many resettings in finite time. Deadlock corresponds to a dynamical system state from which no continuation, continuous or discrete, is possible. These phenomena, along with the breakdown of many of the fundamental properties of classical dynamical system theory, such as continuity of solutions and continuous dependence of solutions on the system's initial conditions,

make the analysis of hybrid and impulsive dynamical systems extremely challenging.

In one paper it is impossible to catch all the different aspects of hybrid systems. In what follows a short overview will be given on theoretical issues concerning controllability and stabilizability of switching systems where the individual modes are linear time invariant systems – linear switching systems.

2 Controllability

Controllability of switching systems has been investigated mostly for the case when arbitrary switching is possible (open-loop switching) where the objective is to design a proper switching sequence to ensure controllability or stability of (usually) piecewise linear systems, see [2] [23], [35] [36], or [22] for recurrent neural networks. Usually the input set Ω is assumed to be unconstrained, i.e. $\Omega = \mathbb{R}^m$. In order to illustrate the main concepts involved in controllability problems of linear switching systems we consider here the class of bimodal systems.

Bimodal systems are special classes of switching systems, where the switch from one mode to the other one depends on the state (closed-loop switching). In the simplest case the switching condition is described by a hypersurface \mathcal{C} in the state space. To investigate controllability for this class of systems are quite difficult in general, however, for a certain class of bimodal systems controllability question can be reduced to the problem of controllability of sign constrained open-loop switching systems, i.e. the case when $\Omega = \mathbb{R}_+$, see [5].

Consider a *bimodal piecewise linear system*, i.e., a subdivision of the state space into two regions by a hyperplane \mathcal{C} . The dynamics valid within each region is

$$\dot{x}(t) = \begin{cases} A_1x(t) + B_1u(t) & \text{if } x \in \mathcal{C}_-, \\ A_2x(t) + B_2u(t) & \text{if } x \in \mathcal{C}_+, \end{cases} \quad (4)$$

where $x(t) \in \mathbb{R}^n$, $x_0 = x(t_0)$ is the state and initial state vector and $u(t) \in \mathcal{U} \subset \mathbb{R}^m$ is the input vector. \mathcal{C} denotes the hyperplane $\ker C = \{x | Cx = 0\}$ and \mathcal{C}^\pm denote the half spaces $\mathcal{C}_+ = \{x | Cx \geq 0\}$ and $\mathcal{C}_- = \{x | Cx \leq 0\}$. The state matrices are constant and of compatible dimensions and $y_s = Cx$ denotes the decision variable.

A solution (Carathéodory) of (4) on an interval I is an almost everywhere differentiable function $\varphi(t) : I \rightarrow \mathbb{R}^n$ that satisfies (4) a.e. on I . Following classical lines, (4) is said to be *completely controllable* if every point in the state space

is reachable in finite time from any other point in the state space by using bounded measurable controls.

In this paper we consider the situation when both modes have the same well defined *relative degree r*, see [14], corresponding to the output $y_s = Cx$. For sake of simplicity the results will be presented for the case when $r = 1$, i.e. the system can be transformed to the form:

$$\dot{\eta} = \begin{cases} P_1\eta + R_1y_s + Q_1u & \text{if } y_s \geq 0 \\ P_2\eta + R_2y_s + Q_2u & \text{if } y_s \leq 0 \end{cases} \quad (5)$$

$$\dot{y}_s = v. \quad (6)$$

2.1 A Separation Theorem

In order to get a deeper view on the controllability question of the bimodal system (5) it is necessary to recall some results on the unconstrained open-loop switching systems.

Consider the class of open-loop linear switched systems:

$$\dot{x}(t) = A(\sigma(t))x(t) + B(\sigma(t))u(t). \quad (7)$$

State $x \in \mathbb{R}^n$ is *controllable* at time t_0 , if there exist a time instant $t_f > t_0$, a switching function $\sigma : [t_0, t_f] \rightarrow S$, and a bounded measurable input function $u : [t_0, t_f] \rightarrow \mathbb{R}^m$ such that $x(t_f; t_0, x, u, \sigma) = 0$. The switching system (7) will be called *completely controllable* or shortly *controllable* if every state is controllable.

State $x \in \mathbb{R}^n$ is *reachable* at time t_0 , if there exist a time instant $t_f > t_0$, a switching function $\sigma : [t_0, t_f] \rightarrow S$, and a bounded measurable input function $u : [t_0, t_f] \rightarrow \mathbb{R}^m$ such that $x(t_f; t_0, 0, u, \sigma) = x$. The switching system (7) will be called *completely reachable* or shortly *reachable* if every state is reachable. We will term as reachability set the set of points reachable from the origin, and as controllability set the set of points from which the origin is reachable.

Following classical lines, (7) is said to be *globally controllable* if every point in the state space is reachable from any other point in the state space by using bounded measurable controls and a suitable switching function.

If the input set Ω is unconstrained ($\Omega = \mathbb{R}^m$) a necessary and sufficient condition for controllability can be given, see [29], [57]:

Theorem1. *System (7) is controllable if and only if*

$$\text{rank } \mathcal{R}_{\mathcal{A}, \mathcal{B}} = n, \quad (8)$$

i.e. the multivariable Kalman rank condition, holds, where the subspace $\mathcal{R}_{\mathcal{A}, \mathcal{B}}$ is defined as

$$\mathcal{R}_{\mathcal{A}, \mathcal{B}} := \text{span} \left\{ \prod_{j=1}^J A_{l_j}^{i_j} B_k \mid k = 0, \dots, s \right\} \quad (9)$$

where $J \geq 0$, $l_j \in S = \{0, \dots, s\}$, $i_j \in \{0, \dots, n-1\}$. Moreover, if one considers the finitely generated Lie-algebra $\mathcal{L}(A_0, \dots, A_s)$ which contains A_0, \dots, A_s , and a basis $\hat{A}_1, \dots, \hat{A}_K$ of this algebra, then

$$\mathcal{R}_{\mathcal{A}, \mathcal{B}} = \sum_{k=0}^s \sum_{n_1=0}^{n-1} \dots \sum_{n_K=0}^{n-1} \text{Im} (\hat{A}_1^{n_1} \dots \hat{A}_K^{n_K} B_k). \quad (10)$$

Note, that $\mathcal{R}_{\mathcal{A}, \mathcal{B}}$ is the minimal subspace invariant for all of the A_i s containing $\mathcal{B} = \sum_{i=0}^s \text{Im} B_i$.

Let us consider the open-loop switching system (5) on \mathcal{C} , formed by the modes (P_1, Q_1) and (P_2, Q_2) . Since the set $\mathcal{R}_{\mathcal{P}, \mathcal{Q}}$ contains the controllability subspaces of the individual modes, the bimodal system can be transformed, by applying a state transform and a suitable feedback, into

$$\dot{\eta}_1 = \begin{cases} P_{1,1}\eta_1 + R_{1,1}y_s + Q_1 u_1 & \text{if } y_s \geq 0 \\ P_{2,1}\eta_1 + R_{2,1}y_s + Q_2 u_2 & \text{if } y_s \leq 0 \end{cases} \quad (11)$$

$$\dot{\eta}_2 = \begin{cases} P_{1,2}\eta_2 + R_{1,2}y_s & \text{if } y_s \geq 0 \\ P_{2,2}\eta_2 + R_{2,2}y_s & \text{if } y_s \leq 0 \end{cases} \quad (12)$$

$$\dot{y}_s = v, \quad (13)$$

where, by Theorem 1, subsystem (11) is controllable on \mathcal{C} using open-loop switchings.

The bimodal system (12), (13) can be seen as a dynamic extension of

$$\dot{\eta}_2 = P_{i,2}\eta_2 + \bar{R}_{i,2}w, \quad i \in \{1, 2\}, \quad w \geq 0, \quad (14)$$

see [14]. Controllability of the dynamically extended system, provided that the original system was controllable, is by far non-trivial issue though for smooth vector fields it was proved in [22] while in the setting of bimodal systems one has the following result, [5]:

Proposition 1. *The bimodal system given by (12) and (13) is controllable if and only if the input constrained open-loop switching system (14) is controllable.*

This proposition reveals the importance of the controllability properties of the class of – possible input constrained – open-loop switching systems.

2.2 Switching Systems and Vector Fields

A control system on a smooth n -dimensional manifold M is a collection \mathcal{F} of smooth vector fields depending on independent parameters $w = [w_1, \dots, w_m] \in \Xi \subset \mathbb{R}^m$ called control inputs such that $w(t)$ belongs to a suitable class of real valued functions \mathcal{W} , called admissible controls.

A switching system can be considered as a nonlinear polysystem of the form

$$\dot{x} = f(x(t), w(t)), \quad x(0) = 0, \quad (15)$$

where in general, it is assumed that $x \in M$ and $f(\cdot, w)$, $w \in \Xi$ is an analytic (smooth) vector field on M . It is supposed that M is an n -dimensional real analytic manifold (para-compact and connected).

In our case $\Xi = S \times \Omega$ with $f_w(x) = f(x(t), w(t)) = A_i x(t) + B_i u$ where $w = (i, u)$. To system (15) can be associated in a natural way the collection of vector fields $V_f = \{f_w \mid w \in \Xi\}$, that can be used e.g. in a Lie algebraic treatment, quite suitable for unconstrained problems and small time local controllability problems.

Associated with the system (15), denote by $\mathcal{A}_{\mathcal{F}}(x, t)$ the set of all elements attainable from x at time t . For each $\mathcal{A}_{\mathcal{F}}(x) = \cup_{t \geq 0} \mathcal{A}_{\mathcal{F}}(x, t)$.

By the Filippov-Ważewski relaxation theorem the solution set of the differential inclusion defined by (7) is dense in the set of relaxed solutions, i.e., the solutions of the differential inclusion whose right hand side is the convex hull of the original set valued map, see [3], [25], [7]. This implies that the corresponding

attainable sets coincide. Hence, instead of the controllability problem defined for the original switching system (7) one can consider the controllability problem associated to the convexified differential inclusion $\dot{x} \in A_c(x)$, where

$$A_c(x) = \sum_{i=1}^s \alpha_i (A_i x + B_i u) \text{ and } \alpha_i \geq 0 \text{ and } \sum_{i=1}^s \alpha_i = 1.$$

We would like to decide (global) controllability by just examining the vector fields that define a control system without the necessity of obtaining solutions of any kind of the given system. We have already seen that it is possible to "expand" the available vector fields, e.g. by convexification, without changing the system itself, obtaining equivalent descriptions of the same system.

The following section reveals that introducing more and more redundancy in this description – by enlarging the set of vector fields that describes the system, is very useful in deciding the controllability question.

2.3 Lie Saturate

The Lie bracket of two vector fields f and g is denoted by $[f, g]$. Under the Lie bracket, and the pointwise addition, the space of all analytic vector fields on M becomes a Lie algebra; $Lie(\mathcal{F})$ denotes the subalgebra generated by \mathcal{F} . For each $q \in M$, $Lie_q(\mathcal{F})$ is a subspace of $T_q M$, the tangent space of M at q . A set of vector fields \mathcal{F} on a connected smooth manifold M is called *bracket-generating* (full-rank) if $Lie_q \mathcal{F} = T_q M$ for all $q \in M$.

Families of vector fields \mathcal{F} and \mathcal{G} are said to be (strongly) *equivalent* if $Lie(\mathcal{F}) = Lie(\mathcal{G})$ and $\overline{\mathcal{A}_{\mathcal{F}}(q, T)} = \overline{\mathcal{A}_{\mathcal{G}}(q, T)}$ for all $q \in M$ and for all $T > 0$, where the overbar denotes the closure of the sets. The Lie Saturate $LS(\mathcal{F})$ of a family of vector fields \mathcal{F} is the union of families strongly equivalent to \mathcal{F} .

In general it is difficult to construct the Lie saturate explicitly, however one can construct a completely ascending family of compatible vector fields – *Lie extension* – starting from a given set \mathcal{F} of vector fields. A vector field f is called compatible with the system \mathcal{F} if $\mathcal{A}_{\mathcal{F} \cup f}(q) \subset \overline{\mathcal{A}_{\mathcal{F}}(q)}$ for all $q \in M$. Since $LS(\mathcal{F})$ is a closed convex positive cone in $Lie(\mathcal{F})$, a possibility to obtain compatible vector fields is extension by convexification, see [16]: for $f_1, f_2 \in \mathcal{F}$ and any nonnegative functions $\alpha_1, \alpha_2 \in C^\infty(M)$ the vector fields $\alpha_1 f_1 + \alpha_2 f_2$ is compatible with \mathcal{F} . If $LS(\mathcal{F})$ contains a vector space \mathcal{V} , then $Lie(\mathcal{V}) \subset LS(\mathcal{F})$.

The importance of the Lie extension for controllability is given by the following result, [1]:

Theorem 2. *If \mathcal{F} is a bracket-generating system such that the positive convex cone generated by \mathcal{F} , i.e.,
 $\text{cone}(\mathcal{F}) = \{\sum_{i=1}^k \alpha_i f_i \mid f_i \in \mathcal{F}, \alpha_i \in C^\infty(M), \alpha_i \geq 0, k \in \mathbb{N}\}$ is symmetric, i.e.
 $\text{cone}(\mathcal{F}) = \text{cone}(-\mathcal{F})$, then \mathcal{F} is completely controllable.*

For further details on the role of the Lie saturates on controllability see also Chapter 3, Theorem 12 of [16], [1].

Remark 1. The switching system (7) can be imbedded in the class of bilinear systems with sign constrained inputs of the form: $\dot{x}(t) = \sum_{k=0}^{(m+1)s-1} \lambda_k F_k(x)$ with $\lambda_k \geq 0$ where $F_{(m+1)l} = A_{l+1}x$ and $F_{(m+1)l+j} = A_{l+1}x + e_j B_{l+1}$, with $l = 0, \dots, s-1$ and $j = 1, \dots, m$.

This embedding gives an insight in relation between the controllability of unconstrained switching systems and bang-bang type results for differential inclusions, for details see e.g. Lemma 1 and Theorem 2 of [15] and it also explains the difficulties encountered in the (weak) stabilization problem of switching systems.

In what follows, without restricting the generality, it can be assumed that the systems are single input systems.

3 Finite Number of Switchings

A *trajectory* of the switching system (7) will be defined as follows: let $x(t)$ be an absolutely continuous function. We say that $x(t)$ is a (admissible) trajectory of the system (7) on $[t_0, t_f]$ if there exists a finite subdivision $t_0 < t_1 < \dots < t_{N-1} < t_N = t_f$ of the interval $[t_0, t_f]$, such that on each subinterval (t_{k-1}, t_k) there exists an admissible function u_k such that one has $\dot{x} = A_k x + B_k u_k$.

Which function is considered as admissible, depends on the specific application. Usually it is fixed to be the set of piecewise constant functions, but could be the set of sufficiently smooth functions, too. This definition excludes problematic situations, like Zeno behavior.

Let us denote by $e^{f_w t} x_0$ the solution of the equation $\dot{\xi} = f_w(\xi)$, $\xi(0) = x_0$.

Then for a given vector field \mathcal{F} one can consider the (positive) orbits of the vector field, i.e.,

$$\Phi_{\tau, x_0}^q(\omega)(T) := e^{f_{w_q} t_q} e^{f_{w_{q-1}} t_{q-1}} \cdots e^{f_{w_2} t_2} e^{f_{w_1} t_1} x_0$$

where $\tau = (t_1, t_2, \dots, t_q)$, $t_i \geq 0$ with $T = \sum_{j=1}^q t_j$ and $\omega = (w_1, w_2, \dots, w_q) \in \Xi^q$, $f_{u_i} \in \mathcal{F}$. We will use Φ_τ^q for $\Phi_{\tau,0}^q(\omega)$ with fixed ω .

It is immediate that the trajectories of a switching systems are the (positive) orbits of the control system defined by the associated vector field. We will denote by $\Phi_{\tau,x_0}^\sigma(v)$ these orbits, where $\sigma = (s_1, s_2, \dots, s_q)$ with $s_i \in S$ and $v \in \Omega^q$.

A point $y \in M$ is called *normally reachable* from an $x \in M$ if there exist a finite sequence of vector fields $\{f_i, i = 1, \dots, q\}$ and $\bar{\tau} \in \mathbb{R}_+^q$ such that $\Phi_{\bar{\tau},x}^q = y$ and the mapping $\tau \in \mathbb{R}_+^q \rightarrow \Phi_{\tau,x}^q$, which is defined in an open neighborhood of $\bar{\tau}$, has rank $n = \dim M$ at $\bar{\tau}$.

As a consequence of the surjective mapping theorem, [4] Theorem 41.6, one has that there is a neighborhood V of y such that the points $z \in V$ are normally reachable points from x . Let us denote by $\mathcal{N}(x)$ the set of normally reachable points. It follows that if $\mathcal{N}(x)$ is not empty, then it has a nonempty interior. In the context of switching systems it means that the set of points reachable from x by using piecewise constant switchings has nonempty interior.

The (switching) system has the *normal accessibility property* if for every x the set $\mathcal{N}(x)$ is not empty. The system is *normally controllable* if y is normally reachable from x for every $x, y \in M$. In the language of the switching systems if the system is normally controllable then every two point can be joined using a finite number of switchings.

The key point here is that for a globally controllable system every point has the normal accessibility property. Actually the interior points of the reachability set are reachable by piecewise constant controls, for details see [26], [12], [58], [13].

Now we are in a position to formulate the following result:

Proposition 2. *If the switching system (7) is globally controllable than it is also globally controllable by using piecewise constant switching functions, i.e., using only a finite number of switchings.*

Moreover, there exist a bound for the necessary number of switchings, that depends only on the system matrices and Ω . There exist a universal (finite) switching sequence σ such that the time varying system $\dot{x} = A(\sigma)x + B(\sigma)u$ is globally controllable.

Remark 2. From Proposition 2 follows that there is a minimum number of switching that ensures (global) controllability. It is an open problem to give a (tight) upper bound for this number, even in the unconstrained case, see [57]. It is neither clear if this minimum can be achieved by using a single switching sequence or not.

In a general nonlinear context these questions are posed in the framework of time optimal control. The obtained results are too restrictive to be applicable for a switching system, for details see [20], [28], [31].

4 Global Controllability

Having in mind the result of the previous section we can concentrate now on the controllability problem itself. Let us apply Theorem 2 in the unconstrained situation: by constructing the Lie extension of the vector field $\mathcal{F} = \{A_i x + B_i u \mid u \geq 0\}$, one can observe that $B_i u$ is compatible with \mathcal{F} , i.e.,

$$B_i u \in LS(\mathcal{F}) \text{ Indeed, } B_i u \in \overline{co(\mathcal{F})}, \text{ since } B_i u = \lim_{\lambda \rightarrow \infty} \frac{1}{\lambda} (A_i x + \lambda B_i u).$$

If there is a vector $v \in LS(\mathcal{F})$ such that $-v \in LS(\mathcal{F})$ then $\pm A_i v \in LS(\mathcal{F})$, too, see [16].

Using these techniques in the unconstrained case it follows the assertion of Theorem 1. However, for sign constrained input one cannot find easily other compatible vector fields than B_i . Unfortunately, in general it is a hard task to prove complete controllability using Theorem 2. A result on small time controllability of the constrained switching system, that uses Lie algebraic ideas, is given [32] and [19]. These results are quite restrictive, since small time controllability requires that the convex cone generated by B_i contain a subspace, i.e.,

$$\overline{co}(\bigcup_{i=1}^s B_i) - \overline{co}(\bigcup_{i=1}^s B_i) \neq \emptyset.$$

These observations motivates the necessity to search for other methods in order to obtain a useful algorithm that might test controllability in the sign constrained case. Since $\mathcal{G} = \overline{co}\{\mathcal{F}\}$ is the Lie extension of \mathcal{F} the controllability problem for the two vector fields are equivalent.

In the more general setting of the convex processes – the set-valued analogues of linear operators – the input constrained controllability problem for LTI systems was solved in [10]. In the sequel a short overview will be given of these results followed by an extension to the input constrained controllability problem of switching systems.

4.1 Convex Processes

A convex process A from \mathbb{R}^n to itself is a set-valued map satisfying $\lambda A(x) + \mu A(y) \subset A(\lambda x + \mu y)$ for all $\lambda, \mu \geq 0$, or, equivalently, a set-valued map whose graph is a convex cone. A convex process is closed if its graph is closed and that it is strict if its domain is the whole space. With a strict

closed convex process A one can associate the Cauchy problem for the differential inclusion: $\dot{x}(t) \in A(x(t))$, $x(0) = 0$, for details see [11] and [3].

If $G \subset \mathbb{R}^n$, let us denote by G^+ its (positive) polar cone defined by

$$G^+ = \left\{ p \in \mathbb{R}^n \mid (p, x) \geq 0, \forall x \in G \right\}. \quad (16)$$

The transpose A^* of A is defined as the set-valued map defined by $p \in A^*(q) \Leftrightarrow \forall (x, y) \in \text{Graph}(A), (p, x) \leq (q, y)$. For $\lambda \in \mathbb{R}$ the eigenvectors v of A^* are the nonzero solutions of the inclusion $\lambda v \in A^*(v)$.

Motivated by the terminology used for linear systems we say that A satisfies the *rank condition* if the subspace spanned by the cone $A^k(0)$ is the whole space for some integer $k \geq 1$.

Theorem 3 ([10]). *The following conditions are equivalent:*

- a) the differential inclusion $\dot{x}(t) \in A(x(t))$, $x(0) = 0$ is controllable,
- b) the differential inclusion is controllable at some time $T > 0$,
- c) the rank condition is satisfied and A^* has no eigenvectors,
- d) for some $k \geq 1$, one has $A^k(0) = (-A)^k(0) = \mathbb{R}^n$.

Controllability of a linear control system is equivalent to the controllability of the differential inclusion defined by $\dot{x}(t) \in Ax(t) + U$, $x(0) = 0$, with $U = \overline{\text{co}}(B\Omega)$ is a closed convex cone of controls, where $\overline{\text{co}}(S)$ denotes the closure of the convex hull of the set S , see [3]. The adjoint inclusion is $-\dot{q}(t) \in A^T q(t)$, $q(t) \in U^+$, see [10]. Applying Theorem 3 one can obtain the result of Kalman, [17], for the unconstrained case and the results reported in [6] and [18] for the constrained input case.

Along these lines one can find a necessary condition for the controllability of an open-loop switching system with nonnegative control:

$$\dot{x} = A_i x + B_i u, \quad u \geq 0. \quad (17)$$

Denote by $U = \overline{\text{co}}(\cup_{i=1}^s B_i \Omega)$ and $A_c(x) = \left\{ \sum_{i=1}^s \alpha_i A_i x + U \mid \alpha_i \geq 0, \sum_{i=1}^s \alpha_i = 1 \right\}$. Then the associated differential inclusion have the same reachability set as the original switching system (17). As it was shown in the previous section, this extension is based on the geometrical framework of control theory given by the Lie theoretic approach. Even this system

does not define a convex process the result *d)* of Theorem 3 remains valid for the general case, too.

Let us consider the differential inclusion $\dot{x} \in F(x)$, $x(0) = \xi$ and the reachable set $\mathcal{R}^T(\xi) = \{x(T)\}$ where x is a solution. If F has nonempty, compact, convex values and is locally Lipschitz then $\mathcal{R}^T(\xi) = \lim_{N \rightarrow \infty} (I + \frac{T}{N}F)^N(\xi) := [\text{Exp } F](T\xi)$ for definitions and details see [33]. Extending this result, Proposition 2 of [9] shows that for a positively homogeneous inclusion, ($F(\alpha) = \alpha F(x)$, $\alpha > 0$), one has

$$[\text{Exp } F](t\xi) = \xi + \sum_{k=1}^{\infty} \frac{t^k}{k!} F^k(\xi),$$

where $F^k = F \circ F \circ \dots \circ F$. Applying this result for the differential inclusion defined by A_c the controllability condition for input constrained open-loop switching systems can be formulated as:

Proposition 3. *The following conditions are equivalent:*

- a) the switching system $\dot{x} = A_i x + B_i u$, $i \in \{1, \dots, s\}$, $u \in \Omega$ is controllable,
- b) the associated differential inclusion $\dot{x} \in A_c(x)$, $x(0) = 0$ is controllable,
- c) for some $k \geq 1$, one has $A_c^k(0) = (-A)_c^k(0) = R^n$.

Since controllability of the constrained system implies controllability of the unconstrained system, the rank condition for $A_c(x)$ can be replaced by the multivariable Kalman rank condition of Theorem 1.

The results of Proposition 3 shows that if controllability conditions are satisfied for a system defined by (A_i, B_i) then they are satisfied for a system defined by $(-A_i, -B_i)$, too. It follows that controllability of an open-loop switching system implies reachability, hence global controllability.

4.2 Examples

To illustrate the results consider the bimodal system of type (12), (13), defined by:

$$A_1 = \begin{bmatrix} 0 & 1 \\ 0 & 0 \end{bmatrix}, \quad B_1 = \begin{bmatrix} 0 \\ 1 \end{bmatrix}, \quad A_2 = \begin{bmatrix} 0 & 0 \\ 1 & 0 \end{bmatrix}, \quad B_2 = \begin{bmatrix} -1 \\ 0 \end{bmatrix}.$$

For this system the multivariable Kalman rank condition holds, but one can verify that condition c.) of Proposition 3 does not hold, i.e. the system is not controllable.

Considering the system defined by:

$$A_1 = \begin{bmatrix} 0 & 1 \\ 0 & 0 \end{bmatrix}, B_1 = \begin{bmatrix} 0 \\ 1 \end{bmatrix}, A_2 = \begin{bmatrix} 1 & 0 \\ 0 & 1 \end{bmatrix}, B_2 = \begin{bmatrix} 1 \\ -1 \end{bmatrix},$$

one can verify that condition c.) of Proposition prop:colls holds with $k = 2$, i.e. the system is controllable.

5 Stabilizability

Stability issues of switched systems, especially switched linear systems, have been of increasing interest in the recent decade, see for example [46], [44], [47], [57], [49] and these issues include several interesting phenomena, e. g., even when all the subsystems are exponentially stable, the switched systems may have divergent trajectories for certain switching signals however one may carefully switch between unstable subsystems to make the switched system exponentially stable.

The study of the switching systems is closely related to some investigations on differential inclusions. By using techniques from convex nonsmooth analysis a series of very powerful results can be deduced, for an overview of the most important ideas related to differential inclusions and stability problems related to switching systems see [54], [39], [55].

For linear time invariant (LTI) systems, $\dot{x} = Ax$, stability properties are completely determined by the matrix A . The counterpart of this fact for linear switching systems might be the strong stabilization result [51]. When there is control, i.e., $\dot{x} = Ax + Bu$, and the system is stabilizable, then the stabilization can be always done by a static state feedback $u = Kx$.

A generalization of this fact remains valid for switching systems, too, in spite of the nonlinear nature of the switching process. For the strong stability case with controls, one has that for strongly stabilizable linear controlled switching systems the feedback control always can be chosen as a "patchy", linear variable structure controller, [38]. The control is defined by a conic partition $\mathbb{R}^n = \bigcup_{k=1}^N \mathcal{C}_k$ of the state space while on each cone \mathcal{C}_k the feedback is given by $u = F_k x$.

For weak stability one has two inputs: the switching sequence and the possible control inputs of the individual subsystems. Based on the ideas of [52] it was proved that the (weak) asymptotic stabilizability of switched free linear systems by means of an event driven switching strategy can be caught in terms of a conic partition of the state space, [48], [50]. This result can be seen as a generalization of the corresponding theorem for strong stability. However, in contrast to the strong stability results, the corresponding Lyapunov function is not always convex, see [40].

In a fairly general setting a (weak) asymptotic stabilizability result of nonsmooth controlled nonlinear systems can be also given in terms of control-Lyapunov functions. By making use of the control-Lyapunov function it was possible to construct a discontinuous time-invariant feedback stabilizer that, when implemented with a

sample-and-hold strategy, guarantees semiglobal practical asymptotic stability, [43].

5.1 Strongly Stabilizable Linear Switching Systems

The zero solution of the differential inclusion $\dot{x} \in F(x)$ is called asymptotically stable (strongly stable) if for any $\varepsilon > 0$ there is a $\delta > 0$ such that for each solution the inequality $\|x(t)\| < \varepsilon$ holds for all $t \geq 0$ if $\|x(0)\| < \delta$ and if there is a $\Delta > 0$ such that for any solution with $\|x(0)\| < \Delta$ the limiting relation $\lim_{t \rightarrow \infty} x(t) = 0$ holds. The zero solution is called weakly asymptotically stable if there exists a solution for which the above conditions are fulfilled.

The necessary and sufficient conditions for asymptotic stabilizability of switched linear systems in terms of the Lyapunov functions can be summarized in the following theorem, [52], [37]:

Theorem 4. *For the asymptotic stability (weak asymptotic stability) of the zero solution of the differential inclusion $\dot{x} \in \{y = Ax \mid A \in \{A_1, \dots, A_q\}\}$ it is necessary and sufficient that there exist an $m \geq n$, a matrix $\mathcal{L} \in \mathbb{R}^{n \times m}$ with rank n and a constant $\gamma > 0$ such that the piecewise linear Lyapunov function of the polyhedral vector norm $V_{\mathcal{L}}(x) = \|\mathcal{L}x\|_{\infty}$ satisfies the inequality*

$$\sup_{y \in F(x)} D^+ V_{\mathcal{L}}(x)(x, y) \leq -\gamma V_{\mathcal{L}}(x) \quad (18)$$

(in case of weak stability

$$\inf_{y \in F(x)} D^+ V_{\mathcal{L}}(x)(x, y) \leq -\gamma V_{\mathcal{L}}(x) \quad (19)$$

respectively,) where

$$D^+ V_{\mathcal{L}}(x)(x, y) = \lim_{\varepsilon \rightarrow 0^+} \varepsilon^{-1} (V_{\mathcal{L}}(x + \varepsilon y) - V_{\mathcal{L}}(x)) \quad (20)$$

is the directional (upper right Dini) derivative of $V_{\mathcal{L}}(x)$ at x in the direction of $y \in F(x)$.

Strong stabilizability of free linear switching systems admits an algebraic characterization in terms of the system matrices, that can be viewed as the requirement imposed by the stability condition on the spectrum of an LTI operator:

Theorem 5. For the asymptotic stability of the zero solution of the differential inclusion $\dot{x} \in \{y = Ax \mid A \in \{A_1, \dots, A_q\}\}$ it is necessary and sufficient that there exist an $m \geq n$, a matrix $\mathcal{L} \in \mathbb{R}^{n \times m}$ with rank n and matrices $\Gamma_s \in \mathbb{R}^{m \times m}$ with $\gamma_{ii}^s + \sum_{j \neq i} |\gamma_{ij}^s| < 0$, $i = 1, \dots, m$; $s = 1, \dots, q$, such that $A_s \mathcal{L} = \mathcal{L} \Gamma_s$, $s = 1, \dots, q$.

For details see, e.g., [51] and the references cited therein. This condition can be seen as a generalized transformation of the system matrices A_i with a single matrix \mathcal{L} . In the special case when the Lie algebra generated by the matrices A_i is solvable, the existence of such a matrix is guaranteed with upper triangular matrices Γ_s , see [46], [44]. As an example consider the Lie algebra generated by the matrices

$$A_1 = \begin{bmatrix} -3 & 4 \\ -1 & 1 \end{bmatrix}, \quad A_2 = \begin{bmatrix} -9 & 12 \\ -4 & 5 \end{bmatrix},$$

that can be transformed to a triangular form by $T = \begin{bmatrix} 2 & 1 \\ 1 & 1 \end{bmatrix}$.

For nonautonomous linear switching systems, i.e., for differential inclusions $\dot{x} \in \{A_1 x + B_1 u, \dots, A_q x + B_q u\}$ it is not trivial, that the problem is solvable by feedback, i.e., autonomous (event driven) switching and state feedback. The key point here is that, under general conditions, asymptotic controllability implies the existence of a nonsmooth control-Lyapunov function, [56], [42], [53]. However, the explicit construction of such a control-Lyapunov function is quite difficult, in general.

Considering the difficulty of the problem in the nonlinear context, it is surprising that if the state-feedback stabilization problem can be solved by a Lyapunov function and a continuous feedback control then it can be solved by a polyhedral Lyapunov function and a linear variable structure control, see [38].

5.2 Weak Stabilization of Linear Switching Systems

Following [41] a (continuous-time) autonomous hybrid system is defined as

$$\dot{x} = f(x(t), \sigma(t)), \quad \sigma(t) = \nu(x(t), \sigma(t_-)), \quad (21)$$

where $f(\cdot, q)$, globally Lipschitz continuous, is the continuous dynamics while $\sigma(t) \in \{1, \dots, s\}$ is the finite (discrete) dynamics. The notation t_- indicates that the finite state is piecewise continuous from the right. By a controlled hybrid system we have in mind a system of the form

$$\dot{x} = f(x(t), u(t), \sigma(t)), \quad \sigma(t) = v(x(t), u(t), \sigma(t_-)). \quad (22)$$

The state evolution of a hybrid system involves two phenomena: the continuous state evolution between the switching instants and the state jumps at the switching instants. For strong stabilizability a common equilibrium is assumed to exist for all subsystems; this assumption limits the applicability of hybrid systems since a hybrid system can still be stable under appropriate switching laws even when the subsystems have different equilibria or no equilibria.

One of the main tools for analyzing stability is that of the multiple Lyapunov functions. Considering (21) let us suppose that we can find a family of Lyapunov-like functions V_i , $i \in Q = \{1, \dots, q\}$ for the vector fields f_{j_i} , i.e., a set of positive definite functions defined over a region Ω_i with negative derivatives along corresponding vector field on Ω_i . The general idea is that having $\bigcup_{i \in Q} \Omega_i = \mathbb{R}^n$ and $\sigma(t)$ defined such that $\sigma(t) = i$ if and only if $x \in \Omega_i$ (autonomous switching) and such that the sequence nonincreasing condition for a trajectory $x(t)$ holds, i.e., for consecutive switching times (t_k, t_{k+1}) one has $V_{\sigma(t_{k+1})}(x(t_{k+1})) \leq V_{\sigma(t_k)}(x(t_k))$, then the system (21) is Lyapunov stable, [41].

From the point of view of our topic it is very important that in proving stability, we can use more Lyapunov functions than constituent systems by simply introducing new discrete substates with the same continuous dynamics but different Lyapunov-like functions. This is one ingredient in the solution of the (weak) stabilizability problem of linear switched systems especially for the controlled case.

The switched linear system can be stabilized by a switching law if and only if it can be stabilized by a cone partition switching law, [50]. However, in contrast to the strong (robust) stability results, not all the weakly stabilizable switched linear systems admit a polytopic (convex) Lyapunov function, see the counterexample from [40]. This fact lefts open the question of practical construction of a conic partition that defines a switching rule that stabilizes the system.

5.3 Construction of the Stabilizing Feedback

There are essentially two approaches to design time-varying stabilizing feedbacks for general nonlinear systems. The first approach is Lie algebraic in its nature and uses open-loop control techniques of nonholonomic motion planning for

constructing time-varying feedbacks, [63]. The method is based on considering of what is known as the Lie bracket extension of the original system. Under reasonable assumptions, a stabilizing feedback control can be constructed for the extended system and the stabilizing time-invariant feedback control for the extended system is then combined with a periodic continuation of a specific solution of an open loop, finite horizon control problem. This open loop control problem is posed in terms of the logarithmic coordinates for flows and its purpose is to generate open loop controls such that the trajectories of the controlled extended system and the open loop system intersect after a finite time, independent of their common initial condition, [61]. An application of the method, based on the Wei-Norman formula, [64], was given for bilinear systems combining static feedback laws for a Lie bracket extension of the system with a solution of an open loop control problem on the associated Lie group, [59], [60].

Embedding switching systems into the class of bilinear systems is done by imposing a sign constraint on the inputs. This fact reduces the applicability of these results to stabilizing feedback construction of switching systems to the cases when the defining vector field is symmetric.

An obvious alternative is the direct Lyapunov method applied to time-variant systems, that makes use of time-variant Lyapunov functions, in general.

There are several constructive propositions in the literature how to stabilize classes of linear switched system without input signals, see for instance [45]. These methods are restricted to switched closed-loop linear systems consisting of (possibly unstable) linear vector fields for which there exists a stable convex combination of the corresponding matrices, [67]. These methods guarantee stability by using a common quadratic Lyapunov function and often they can be cast in terms of linear matrix inequalities (LMI), [68].

Stabilization of linear switching systems that have control inputs is solved essentially for the same class of systems, i.e. for systems where after applying linear static feedbacks the obtained set of autonomous systems fit in the given category, [66], [57].

There has not been found yet a method to solve the feedback stabilization problem for general linear switching systems. The fact that switching systems are related to bilinear systems having signed constrained control inputs and that there are stabilizable linear switching systems that do not possess a convex Lyapunov function indicate the sources of the difficulties of this challenging problem.

Conclusions

Hybrid systems are characterized by the interaction between continuous-time dynamics (governed by differential or difference equations), and discrete dynamics and logic rules (described by temporal logic, finite state machines, if-then-else conditions, discrete events, etc.). Recent progress in the theory and practice of modeling and control design have caused an increasing interest in the study of

hybrid systems, which is motivated not only by theoretical challenges but also by their ability to model, analyze and synthesize controllers in a large variety of application areas.

This paper highlights some aspects encountered when modeling with hybrid systems through a short overview of some controllability and stabilizability results concerning linear switching systems. It was shown how classical techniques, such as geometrical control theory, Lie-algebraic techniques, convex analysis find their applicability in the study of the behavior of the hybrid systems.

The problems are often quite difficult, that is illustrated by the fact that hybrid dynamics are often so complex, even considering only linear vector fields, that a satisfactory feedback controller cannot be synthesized by using analytical tools similar to those that pertain to linear systems or to certain classes of nonlinear smooth systems. The encountered difficulties induce an intensive research work where the new methods and new results will have a great impact on our knowledge on control design for nonlinear systems, in general.

Acknowledgments. The effort was sponsored by the Hungarian National Science Foundation (OTKA) under the grant CNK78168 and by the Air Force Office of Scientific Research, Air Force Material Command, USAF, under the grant number FA8655-08-1-3016. The U.S Government is authorized to reproduce and distribute reprints for Governmental purpose notwithstanding any copyright notation thereon. The support of the Control Engineering Research Group of H.A.S. at Budapest University of Technology and Economics is also gratefully acknowledged.

References

- [1] Agrachev, A.A., Sachkov, Y.L.: *Control Theory from the Geometric Viewpoint*. Encyclopaedia of Mathematical Sciences, vol. 87. Springer, Heidelberg (2004)
- [2] Altafini, C.: The Reachable Set of a Linear Endogenous Switching System. *Systems and Control Letters* 47(4), 343–353 (2002)
- [3] Aubin, J.P., Cellina, A.: *Differential Inclusions*. Springer, Berlin (1984)
- [4] Bartle, R.: *The Elements of Real Analysis*, 2nd edn. Wiley, New York (1976)
- [5] Bokor, J., Szabó, Z., Balas, G.: Controllability of Bimodal LTI Systems. In: Proceedings of Joint CCA, ISIC and CACSD, Munich, Germany (2006)
- [6] Brammer, R.F.: Controllability in Linear Autonomous Systems with Positive Controllers. *SIAM Journal on Control* 10(2), 329–353 (1972)
- [7] Bressan, A., Piccoli, B.: A Baire Category Approach to the Bang-Bang Property. *J. Differential Equations* 116, 318–337 (1995)
- [8] Brockett, R.W.: Asymptotic Stability and Feedback Stabilization, Differential Geometric Control Theory. *Birkhäuser* (1983)
- [9] Cabot, A., Seeger, A.: Multivalued Exponentiation Analysis. Part I: Maclaurin Exponentials. *Set-Valued Analysis* 14(4), 347–379 (2006)
- [10] Frankowska, H., Olech, C., Aubin, J.P.: Controllability of Convex Processes. *SIAM Journal on Control* 24(6), 1192–1211 (1986)
- [11] Filippov, A.F.: Differential Equations with Discontinuous Right Hand Sides. *Translations of the American Mathematical Society* 62 (1960)
- [12] Grasse, K.A.: Structure of the Boundary of the Attainable Set in Certain Nonlinear Systems. *Mathematical Systems Theory* 18(1), 57–77 (1985)

- [13] Grasse, K.A., Sussmann, H.J.: Global Controllability by Nice Controls. In: Nonlinear Controllability and Optimal Control, pp. 33–79. Dekker, New York (1990)
- [14] Isidori, A.: Nonlinear Control Systems. Springer, Heidelberg (1989)
- [15] Jurdjevic, V., Sallet, G.: Controllability Properties of Affine Systems. SIAM Journal on Control and Optimization 22(3), 501–508 (1984)
- [16] Jurdjevic, V.: Geometric Control Theory. Cambridge University Press, Cambridge (1997)
- [17] Kalman, R.E.: Contributions to the Theory of Optimal Control. Boletin de la Sociedad Matematica Mexicana 5, 102–119 (1960)
- [18] Korobov, V.I.: A Geometric Criterion of Local Controllability of Dynamical Systems in the Presence of Constraints on the Control. Differential Equations 15, 1136–1142 (1980)
- [19] Krastanov, M., Veliov, V.: On the Controllability of Switching Linear Systems. Automatica 41(4), 663–668 (2005)
- [20] Krener, A.J.: Generalization of Chow’s Theorem and the Bang-Band Theorem to Nonlinear Control Problems. SIAM Journal on Control 12(1), 43–52 (1974)
- [21] Passino, K.M., Yurkovich, S.: Fuzzy Control. Addison Wesley Longman, Menlo Park (1998)
- [22] Sontag, E., Qiao, Y.: Further Results on Controllability of Recurrent Neural Networks. Systems and Control Letters 36, 121–129 (1999)
- [23] Sun, Z., Ge, S.S., Lee, T.H.: Controllability and Reachability Criteria for Switched Linear Systems. Automatica 38(5), 775–786 (2003)
- [24] Sun, Z., Ge, S.S.: Switched Linear Systems. Control and Design. Springer, Heidelberg (2005)
- [25] Suslov, S.I.: Nonlinear Bang-Bang Principle. Mathematical Notes 49(5), 518–523 (1991)
- [26] Sussmann, H.: Some Properties of Vector Field Systems that are not Altered by Small Perturbations. Journal of Differential Equations 20, 292–315 (1976)
- [27] Sussmann, H.J.: Reachability by Means of Nice Controls. In: Proceedings of 26th IEEE CDC, Los Angeles, pp. 1368–1373 (1987)
- [28] Sussmann, H.J.: A Bang-Bang Theorem with Bound on the Number of Switchings. SIAM Journal on Control 17(5), 629–651 (1979)
- [29] Stikkel, G., Bokor, J., Szabó, Z.: Necessary and Sufficient Condition for the Controllability of Switching Linear Hybrid Systems. Automatica 40(6), 1093–1098 (2004)
- [30] Tanaka, K., Wang, H.O.: Fuzzy Control Systems Design and Analysis: A Linear Matrix Inequality Approach. John Wiley & Sons, Inc., New York (2001)
- [31] Vakhrameev, S.: A Bang-Bang Theorem with a Finite Number of Switchings for Nonlinear Smooth Control Systems. Journal of Mathematical Science 85(3), 2002–2016 (1997)
- [32] Veliov, V., Krastanov, M.: Controllability of Piecewise Linear Systems. Systems and Control Letters 7, 335–341 (1986)
- [33] Wolenski, P.R.: The Exponential Formula for the Reachable Set of a Lipschitz Differential Inclusion. SIAM Journal on Control and Optimisation 28(5), 1148–1161 (1990)
- [34] Wonham, W.M.: Linear Multivariable Control - A Geometric Approach, 3rd edn. Springer, New York (1985)
- [35] Xie, G., Wang, L.: Necessary and Sufficient Conditions for Controllability of Switched Linear Systems. In: American Control Conference, 2002. Proceedings of the 2002, vol. 3, pp. 1897–1902 (2002)

- [36] Yang, Z.: An Algebraic Approach towards the Controllability of Controlled Switching Linear Hybrid Systems. *Automatica* 38, 1221–1228 (2002)
- [37] Azhmyakov, V.: Stability of Differential Inclusions: a Computational Approach. *Math. Probl. Eng.* Art. ID 17837 (2006)
- [38] Blanchini, F.: Nonquadratic Lyapunov Functions for Robust Control. *Automatica* 31(3), 451–461 (1995)
- [39] Blanchini, F.: Set Invariance in Control. *Automatica* 35, 1747–1767 (1999)
- [40] Blanchini, F., Savorgnan, C.: Stabilizability of Switched Linear Systems does not Imply the Existence of Convex Lyapunov Functions. In: Proc. of the 45th IEEE Conference on Decision and Control, San Diego, pp. 119–124 (2006)
- [41] Branicky, M.S.: Multiple Lyapunov Functions and Other Analysis Tools for Switched and Hybrid Systems. *IEEE Transactions on Automatic Control* 43(4), 475–482 (1998)
- [42] Clarke, F.H., Ledyaev, Y.S., Sontag, E.D., Subbotin, A.I.: Asymptotic Controllability Implies Feedback Stabilization. *IEEE Transactions on Automatic Control* 42(10), 1394–1407 (1997)
- [43] Kellett, C.M., Teel, A.R.: Weak Converse Lyapunov Theorems and Control-Lyapunov Functions. *SIAM Journal on Control and Optimisation* 42(6), 1934–1959 (2004)
- [44] Liberzon, D., Agrachev, A.: Lie-Algebraic Stability Criteria for Switched Systems. *SIAM Journal on Control and Optimisation* 40(1), 253–269 (2001)
- [45] Liberzon, D., Morse, A.S.: Basic Problems in Stability and Design of Switched Systems. *IEEE Control System Magazine* 19(5), 59–70 (1999)
- [46] Liberzon, D., Hespanha, J.P., Morse, A.S.: Stability of Switched Systems: a Lie-Algebraic Condition. *Systems and Control Letters* 37(3), 117–122 (1999)
- [47] Liberzon, D.: *Switching in Systems and Control. Systems and Control: Foundations and Applications*. Birkhauser, Boston (2003)
- [48] Lin, H., Antsaklis, P.J.: A Necessary and Sufficient Condition for Robust Asymptotic Stabilizability of Continuous-Time Uncertain Switched Linear Systems. In: Proc. of the 43rd IEEE Conference on Decision and Control, Bahamas, vol. 4, pp. 3690–3695 (2004)
- [49] Lin, H., Antsaklis, P.J.: Stability and Stabilizability of Switched Linear Systems: A Short Survey of Recent Results. In: Proc. of the 13th IEEE Mediterranean Conference on Control and Automation, Limassol, pp. 24–29 (2005a)
- [50] Lin, H., Antsaklis, P.J.: A Converse Lyapunov Theorem for Uncertain Switched Linear Systems. In: Proc. of the European Control Conference. CDC-ECC 2005, Sevilla, pp. 3291–3296 (2005b)
- [51] Liu, D., Molchanov, A.: Criteria for Robust Absolute Stability of Time-Varying Nonlinear Continuous-Time Systems. *Automatica* 38(4), 627–637 (2002)
- [52] Molchanov, A.P., Pyatnitskiy, Y.S.: Criteria of Asymptotic Stability of Differential and Difference Inclusions Encountered in Control Theory. *Systems and Control Letters* 13(1), 59–64 (1989)
- [53] Rifford, L.: Semiconcave Control-Lyapunov Functions and Stabilizing Feedbacks. *SIAM Journal on Control and Optimisation* 41(3), 659–681 (2002)
- [54] Smirnov, G.V.: Weak Asymptotic Stability of Differential Inclusions. II. *Avtomat. i Telemekh.* 8, 56–63 (1990)
- [55] Smirnov, G.V.: *Introduction to the Theory of Differential Inclusions*. Graduate Studies in Mathematics, vol. 41. American Mathematical Society, Providence, RI (2002)
- [56] Sontag, E.D., Sussmann, H.J.: “Nonsmooth Control-Lyapunov Functions”. In: Proc. of the IEEE Conf. Decision and Control, New Orleans, pp. 2799–2805 (1995)
- [57] Sun, Z., Ge, S.S.: *Switched Linear Systems. Control and Design*. Springer, Heidelberg (2005)

- [58] Sussmann, H.J.: Reachability by Means of Nice Controls. In: Proceedings of 26th IEEE CDC, Los Angeles, CA, pp. 1368–1373 (1987)
- [59] Michalska, H., Torres-Torriti, M.: Time-Varying Stabilizing Feedback Design for Bilinear Systems. In: Proceedings of 19th IASTED International Conference: Modelling, Identification and Control - MIC 2000, Innsbruck, Austria, pp. 93–99 (2000)
- [60] Torres-Torriti, M., Michalska, H.: Stabilization of Bilinear Systems with Unstable Drift. In: Proceedings of American Control Conference, Anchorage, Alaska, USA, pp. 3490–3491 (2002)
- [61] Liu, W.: An Approximation Algorithm for Nonholonomic Systems. SIAM Journal on Control and Optimisation 35, 1328–1365 (1997)
- [62] Sarychev, A.V.: Lie- and Chronologico-Algebraic Tools for Studying Stability of Time-Varying Systems. Systems and Control Letters 43(1), 59–76 (2001)
- [63] Lafferriere, G., Sussmann, H.J.: A Differential Geometric Approach to Motion Planning. In: Li, Z., Canny, J.F. (eds.) Nonholonomic Motion Planning, pp. 235–270. Kluwer Academic Publishers, Dordrecht (1993)
- [64] Wei, J., Norman, E.: On Global Representations of the Solutions of Linear Differential Equations as Products of Exponentials. Proceedings of the American Mathematical Society, 327–334 (1964)
- [65] Johannson, M., Ranzer, A.: Computation of Piecewise Quadratic Lyapunov Functions. IEEE Transactions on Automatic Control 43(1), 555–559 (1998)
- [66] Pettersson, S.: Controller Design of Switched Linear Systems. In: Proceedings of American Control Conference, Boston, Massachusetts, USA (2004)
- [67] Peleties, P., DeCarlo, R.: Asymptotic Stability of m-Switched Systems Using Lyapunov-like Functions. In: Proceedings of American Control Conference, Boston, Massachusetts, USA, pp. 1679–1684 (1991)
- [68] Pettersson, S., Lennartson, E.: Hybrid System Stability and Robustness Verification Using Linear Matrix Inequalities. International Journal on Control 75(16), 1335–1355 (2002)

Indirect Adaptive Control Using Hopfield-Based Dynamic Neural Network for SISO Nonlinear Systems

Ping-Cheng Chen¹, Chi-Hsu Wang², and Tsu-Tian Lee¹

¹ Department of Electrical Engineering, National Taipei University of Technology, Taiwan
pcchen@ntut.edu.tw; ttlee@ntut.edu.tw

² Department of Electrical and Control Engineering, National Chiao Tung University

Abstract. In this paper we propose an indirect adaptive control scheme using Hopfield-based dynamic neural network for SISO nonlinear systems with external disturbances. Hopfield-based dynamic neural networks are used to obtain uncertain function estimations in an indirect adaptive controller, and a compensation controller is used to suppress the effect of approximation error and disturbance. The weights of Hopfield-based dynamic neural network are on-line tuned by the adaptive laws derived in the sense of Lyapunov, so that the stability of the closed-loop system can be guaranteed. In addition, the tracking error can be attenuated to a desired level by selecting some parameters adequately. Simulation results illustrate the applicability of the proposed control scheme. The designed parsimonious structure of the Hopfield-based dynamic neural network makes the practical implementation of the work in this paper much easier.

Keywords: Hopfield-based dynamic neural network, dynamic neural network, Lyapunov stability theory, indirect adaptive control.

1 Introduction

Recently, static neural networks (SNNs) and dynamic neural networks (DNNs) are wildly applied to solve the control problems of nonlinear systems. Some static neural networks, such as feedforward fuzzy neural network (FNN) or feedforward radius basis function network (RBFN), are frequently used as a powerful tool for modeling the ideal control input or nonlinear functions of systems [1]-[2]. However, the complex structures of FNNs and RBFNs make the practical implementation of the control schemes infeasible, and the numbers of the hidden neurons in the NNs' hidden layers (in general more than the dimension of the controlled system) are hard to be determined. Another well-known disadvantage is that SNNs

are quite sensitive to the major change which has never been learned in the training phase. On the other hand, DNNs have an advantage that a smaller DNN is possible to provide the functionality of a much larger SNN [3]. In addition, SNNs are unable to represent dynamic system mapping without the aid of tapped delay, which results in long computation time, high sensitivity to external noise, and a large number of neurons when high dimensional systems are considered [4]. This drawback severely affects the applicability of SNNs to system identification, which is the central part in some control techniques for nonlinear systems. On the other hand, owing to their dynamic memory, DNNs have good performance on identification, state estimation, trajectory tracking, etc., even with the unmodeled dynamics. In [5]-[7], researchers first identify the nonlinear system according to the measured input and output, and then calculate the control law based on the NN model. The output of the nonlinear system is forced by the control law to track either a given trajectory or the output of a reference model. However, there are still some drawbacks. In [5], although both identification and tracking errors are bounded, the control performance shown in the simulations is not satisfactory. In [6], two DNNs are utilized in the iterative learning control system to approximate the nonlinear system and mimic the desired system output and thus increase the complexity of the control scheme and computation loading. The work in [7] requires a prior knowledge of the strong relative degree of the controlled nonlinear system. Besides, an additional filter is needed to obtain higher derivatives of the system output. These drawbacks restrict the applicability of the above works to practical implementation.

Hence, we try to fix the above drawbacks by an indirect adaptive control scheme using Hopfield-based DNNs. Hopfield model was first proposed by Hopfield J. J. in 1982 and 1984 [8]-[9]. Because a Hopfield circuit is quite easy to be realized and has the property of decreasing in energy by finite number of node-updating steps, it has many applications in different fields. In this paper, a so-called indirect adaptive control scheme using Hopfield-based dynamic neural network (IACHDNN) for SISO nonlinear systems is proposed. The Hopfield-based DNN can be viewed as a special kind of DNNs. The control object is to force the system output to track a given reference signal. The uncertain parameters of the controlled plant are approximated by the internal states of Hopfield-based DNNs, and a compensation controller is used to dispel the effect of the approximation error and bounded external disturbance. The synaptic weights of the Hopfield-based DNNs are on-line tuned by adaptive laws derived in the Lyapunov sense. The control law and adaptive laws provide stability for the closed-loop system with external disturbance. Furthermore, the tracking error can be attenuated to a desired level provided that the parameters of the control law are chosen adequately. The main contributions of this paper are summarized as follows. 1) The structure of the used Hopfield-based DNN contains only one neuron, which is much less than the number of neurons in SNNs or other DNNs for nonlinear system control. 2) The simple Hopfield circuit greatly improves the applicability of the control scheme to practical implements. 3) No strong assumptions or prior knowledge of the controlled plant are needed in the development of IACHDNN.

2 Hopfield-Based Dynamic Neural Model

2.1 Descriptions of the DNN Model

Consider a DNN described by the following nonlinear differential equation [5]

$$\dot{\chi} = \mathbf{A}\chi + \mathbf{BW}\sigma(\mathbf{V}_1\chi) + \mathbf{B\Psi}\varphi(\mathbf{V}_2\chi)\gamma(\bar{\mathbf{u}}) \quad (1)$$

where $\chi = [\chi_1 \ \chi_2 \ \cdots \ \chi_n]^T \in R^n$ is the state vector, $\bar{\mathbf{u}} = [\bar{u}_1 \ \bar{u}_2 \ \cdots \ \bar{u}_m]^T \in R^m$ is the input vector, $\sigma : R^r \rightarrow R^k$, $\mathbf{A} \in R^{n \times n}$ is Hurwitz matrix, $\mathbf{B} = \text{diag}\{b_1, b_2, \dots, b_n\} \in R^{n \times n}$, $\mathbf{W} \in R^{n \times k}$, $\mathbf{V}_1 \in R^{r \times n}$, $\mathbf{V}_2 \in R^{s \times n}$, $\varphi : R^s \rightarrow R^{l \times n}$, and $\gamma : R^m \rightarrow R^n$. In (1), χ is the state of the DNN, \mathbf{W} and $\mathbf{\Psi}$ are the weight matrices describing output layer connections, \mathbf{V}_1 and \mathbf{V}_2 are the weight matrices describing the hidden layer connections, $\sigma(\cdot)$ is a sigmoid vector function responsible for nonlinear state feedbacks, and $\gamma(\cdot)$ is a differentiable input function. A DNN in (1) satisfying

$$r = s = l = n, \quad \mathbf{V}_1 = \mathbf{V}_2 = I_{n \times n}, \quad \varphi(\cdot) = I_{n \times n} \quad (2)$$

is the simplest DNN without any hidden layers and can be expressed as

$$\dot{\chi} = \mathbf{A}\chi + \mathbf{BW}\sigma(\chi) + \mathbf{B\Psi}\gamma(\bar{\mathbf{u}}) \quad (3)$$

To simplify our further analysis, we follow the literatures [5] to choose $k = n$, $\mathbf{A} = \text{diag}\{-a_1 - a_2 \ \cdots - a_n\}$ with $a_i > 0$, $i=1, 2, \dots, n$, and $\gamma(\bar{\mathbf{u}}) = [\bar{\mathbf{u}} \ \mathbf{0}]^T \in R^n$ with $n \geq m$ and $\mathbf{0} \in R^{n-m}$ being a zero vector. Let $\mathbf{\Psi} = [\Theta \ \Theta_r]^T$, where $\Theta \in R^{n \times m}$ and $\Theta_r \in R^{n \times (n-m)}$. Then, the expression in (3) can be modified as

$$\dot{\chi} = \mathbf{A}\chi + \mathbf{BW}\sigma(\chi) + \mathbf{B}\Theta\bar{\mathbf{u}} \quad (4)$$

From (4), we have

$$\dot{\chi}_i = -a_i\chi_i + b_i W_i^T \sigma(\chi) + b_i \Theta_i^T \bar{\mathbf{u}}, \quad i = 1, 2, \dots, n \quad (5)$$

where $W_i^T = [w_{i1} \ w_{i2} \ \cdots \ w_{im}]$ and $\Theta_i^T = [\theta_{i1} \ \theta_{i2} \ \cdots \ \theta_{im}]$ are the i^{th} rows of \mathbf{W} and Θ , respectively. Solving the differential equation (5), we obtain

$$\begin{aligned} \chi_i &= b_i \left(W_i^T \xi_{W,i} + \Theta_i^T \xi_{\Theta,i} \right) + e^{-a_i t} \chi_i(0) - e^{-a_i t} b_i \left[W_i^T \xi_{W,i}(0) + \Theta_i^T \xi_{\Theta,i}(0) \right], \\ i &= 1, 2, \dots, n. \end{aligned} \quad (6)$$

where $\chi_i(0)$ is the initial state of χ_i ; $\xi_{W,i} \in R^n$ and $\xi_{\Theta,i} \in R^m$ are the solutions of

$$\dot{\xi}_{W,i} = -a_i \xi_{W,i} + \sigma(\chi) \quad (7)$$

and

$$\dot{\xi}_{\Theta,i} = -a_i \xi_{\Theta,i} + \bar{\mathbf{u}} \quad (8)$$

respectively; $\xi_{W,i}(0)$ and $\xi_{\Theta,i}(0)$ are initial states of $\xi_{W,i}$ and $\xi_{\Theta,i}$, respectively. Note that the terms $e^{-a_i t} \chi_i(0)$ and $e^{-a_i t} b_i \left[W_i^T \xi_{W,i}(0) + \Theta_i^T \xi_{\Theta,i}(0) \right]$ in (6) will exponentially decay with time owing to $a_i > 0$.

2.2 Hopfield-Based DNN Approximator

A DNN approximator for continuous functions can be defined as

$$\chi_i = b_i \left(\hat{W}_i^T \xi_{W,i} + \hat{\Theta}_i^T \xi_{\Theta,i} \right) + e^{-a_i t} \chi_i(0) - e^{-a_i t} b_i \left[\hat{W}_i^T \xi_{W,i}(0) + \hat{\Theta}_i^T \xi_{\Theta,i}(0) \right], \quad i = 1, 2, \dots, n \quad (9)$$

where \hat{W}_i and $\hat{\Theta}_i$ are the estimations of W_i and Θ_i , respectively. For a continuous vector function $\Phi = [\Phi_1 \Phi_2 \dots \Phi_n]^T \in R^n$, we first define optimal vectors W_i^* and Θ_i^* as

$$(W_i^*, \Theta_i^*) = \arg \min_{\hat{W}_i \in \Omega_{W_i}, \hat{\Theta}_i \in \Omega_{\Theta_i}} \left\{ \sup_{x \in D_x, u \in D_U} \left| \Phi_i - \left\{ b_i \left(\hat{W}_i^T \xi_{W,i} + \hat{\Theta}_i^T \xi_{\Theta,i} \right) + e^{-a_i t} \chi_i(0) - e^{-a_i t} b_i \left[\hat{W}_i^T \xi_{W,i}(0) + \hat{\Theta}_i^T \xi_{\Theta,i}(0) \right] \right\} \right| \right\} \quad (10)$$

where $D_x \subset R^N$ and $D_U \subset R^m$ are compact sets; $\Omega_{W_i} = \left\{ \hat{W}_i : \|\hat{W}_i\| \leq M_{W_i} \right\}$ and $\Omega_{\Theta_i} = \left\{ \hat{\Theta}_i : \|\hat{\Theta}_i\| \leq M_{\Theta_i} \right\}$ are constraint sets for \hat{W}_i and $\hat{\Theta}_i$. Then, Φ can be expressed as

$$\Phi_i = b_i \left(W_i^{*T} \xi_{W,i} + \Theta_i^{*T} \xi_{\Theta,i} \right) + e^{-a_i t} \chi_i(0) - e^{-a_i t} b_i \left[W_i^{*T} \xi_{W,i}(0) + \Theta_i^{*T} \xi_{\Theta,i}(0) \right] + \Delta_i \quad i = 1, 2, \dots, n \quad (11)$$

where Δ_i is the approximation error. Note that the optimal vectors W_i^* and Θ_i^* are difficult to be determined and might not be unique. The modeling error vector $\tilde{\chi} = [\tilde{\chi}_1 \ \tilde{\chi}_2 \cdots \tilde{\chi}_n]^T$ can be defined from (9) and (11) as

$$\tilde{\chi}_i = \Phi_i - \chi_i$$

$$= b_i \left(\tilde{W}_i^T \xi_{W,i} + \tilde{\Theta}_i^T \xi_{\Theta,i} \right) - e^{-a_i t} b_i \left[\tilde{W}_i^T \xi_{W,i}(0) + \tilde{\Theta}_i^T \xi_{\Theta,i}(0) \right] + \Delta_i, \quad i = 1, 2, \dots, n \quad (12)$$

where $\tilde{W}_i = W_i^* - \hat{W}_i$, and $\tilde{\Theta}_i = \Theta_i^* - \hat{\Theta}_i$.

In this paper, a Hopfield-based dynamic neural network is adopted as the approximator. It is known as a special case of DNN with $a_i = 1/(R_i C_i)$ and $b_i = 1/C_i$, where $R_i > 0$ and $C_i > 0$ representing the resistance and capacitance at the i^{th} neuron, respectively [7]. The sigmoid function vector $\sigma(\chi) = [\sigma_1(\chi_1) \ \sigma_2(\chi_2) \cdots \sigma_n(\chi_n)]^T$ is defined by a hyperbolic tangent function as

$$\sigma(\chi_i) = \tanh(\kappa_i \chi_i), \quad i = 1, 2, \dots, n \quad (13)$$

where κ_i is the slope of $\tanh(\cdot)$ at the origin. It is known that tangent function is bounded by $-1 < \tanh(\cdot) < 1$.

3 Problem Formulation

Let $S \subset R^n$ and $Q \subset R^n$ be an open sets, $D_s \subset S$ and $D_q \subset Q$ be and compact sets. Consider the n^{th} -order nonlinear dynamic system of the form

$$x^{(n)} = f(\mathbf{x}) + g(\mathbf{x})u + d$$

$$y = x \quad (14)$$

where $\mathbf{x} = [x_1 \ x_2 \ \cdots \ x_n]^T = [x \ \dot{x} \ \cdots \ x^{(n-1)}]^T$ is the state vector; $f : D_s \rightarrow R$ and $g : D_q \rightarrow R$ are uncertain continuous functions; $u \in R$ and $y \in R$ are the continuous control input and output of the system, respectively; $d \in R$ is a bounded external disturbance. We consider only the nonlinear systems which can be represented as (14). It is required that $g \neq 0$ so that (14) is controllable. Without losing generality, we assume that $0 < g < \infty$. The control objective is to force the system output y to follow a given bounded reference signal $y_r \in C^h$, $h \geq n$. The error vector e is defined as

$$\mathbf{e} = [e, \dot{e}, \dots, e^{(n-1)}]^T \in R^n \quad (15)$$

with $e = y_r - x = y_r - y$.

If $f(\mathbf{x})$ and g are known and the system is free of external disturbance, the ideal controller can be designed as

$$u_{ideal} = \frac{1}{g(\mathbf{x})} [-f(\mathbf{x}) + y_r^{(n)} + \mathbf{k}_c^T \mathbf{e}] \quad (16)$$

where $\mathbf{k}_c = [k_n \ k_{n-1} \ \dots \ k_1]^T$. Applying (16) to (14), we have the following error dynamics

$$e^{(n)} + k_1 e^{(n-1)} + \dots + k_n e = 0. \quad (17)$$

If $k_i, i=1, 2, \dots, n$ are chosen so that all roots of the polynomial $H(s) \triangleq s^n + k_1 s^{n-1} + \dots + k_n$ lie strictly in the open left half of the complex plane, then we have $\lim_{t \rightarrow \infty} e(t) = 0$ for any initial conditions. However, since the system dynamics may be unknown or perturbed, the ideal feedback controller u_{ideal} in (16) cannot be implemented.

4 Design of IACHDNN

To solve this problem, a new indirect adaptive control scheme using Hopfield-based dynamic neural network (IACHDNN) for SISO nonlinear systems is proposed. Two Hopfield-based DNNs are used to estimate the uncertain continuous functions f and g , respectively. The indirect adaptive controller u_{id} takes the following form

$$u_{id} = \frac{1}{\hat{g}} \left[-\hat{f} + y_r^{(n)} + \mathbf{k}_c^T \mathbf{e} - u_c \right] \quad (18)$$

where \hat{f} and \hat{g} are the estimations of f and g , respectively; u_c is the compensation controller employed to compensate the effects of external disturbance and the approximation error introduced by the Hopfield-based DNN approximations (described later). Substituting (18) into (14) and using (16) yield

$$\begin{aligned} \dot{\mathbf{e}} &= \mathbf{A}_c \mathbf{e} - \mathbf{B}_c \left[(f - \hat{f}) + (g - \hat{g}) u_{id} \right] + \mathbf{B}_c u_c - \mathbf{B}_c d \\ &= \mathbf{A}_c \mathbf{e} - \mathbf{B}_c (\tilde{f} + \tilde{g} u_{id}) + \mathbf{B}_c u_c - \mathbf{B}_c d \end{aligned} \quad (19)$$

$$\text{where } \mathbf{A}_c = \begin{bmatrix} 0 & 1 & 0 & \cdots & 0 \\ \vdots & \ddots & \ddots & \ddots & 0 \\ 0 & \cdots & \cdots & 0 & 1 \\ -k_n & -k_{n-1} & \cdots & \cdots & -k_1 \end{bmatrix} \in R^{n \times n}; \quad \mathbf{B}_c = [0 \ 0 \ 0 \ 1]^T \in R^n;$$

$\tilde{f} = f - \hat{f}$; $\tilde{g} = g - \hat{g}$. According to the discussion in Sec. 2.2, the Hopfield-based DNNs used to approximate f and g containing only a single neuron and can be expressed as

$$\hat{f} = \frac{1}{C_f} \left(\hat{W}_f \xi_{w_f} + \hat{\Theta}_f^T \xi_{\Theta_f} \right) + e^{-\frac{1}{R_f C_f} t} \hat{f}(0) - \frac{1}{C_f} e^{-\frac{1}{R_f C_f} t} \left[\hat{W}_f \xi_{w_f}(0) + \hat{\Theta}_f^T \xi_{\Theta_f}(0) \right] \quad (20)$$

and

$$\hat{g} = \frac{1}{C_g} \left(\hat{W}_g \xi_{w_g} + \hat{\Theta}_g^T \xi_{\Theta_g} \right) + e^{-\frac{1}{R_g C_g} t} \hat{g}(0) - \frac{1}{C_g} e^{-\frac{1}{R_g C_g} t} \left[\hat{W}_g \xi_{w_g}(0) + \hat{\Theta}_g^T \xi_{\Theta_g}(0) \right] \quad (21)$$

where $\hat{f}(0)$ and $\hat{g}(0)$ are the initial value of \hat{f} and \hat{g} ; the subscripts (and the secondary subscripts) f and g indicate that the variables correspond to the estimations \hat{f} and \hat{g} in this paper. Note that \hat{W}_f , \hat{W}_g , ξ_{w_f} , and ξ_{w_g} are scalars, and the input signals of the Hopfield-based DNNs are $\bar{u} = [x \dot{x} \cdots x^{(n-1)}]^T$. Fig. 1 shows the electric circuit of the Hopfield-based DNN containing only a single neuron. Substituting (20) and (21) into (19) yields

$$\dot{\mathbf{e}} = \mathbf{A}_c \mathbf{e} - \mathbf{B}_c (\bar{f} + \bar{g} u_{id}) + \mathbf{B}_c u_c - \mathbf{B}_c \varepsilon \quad (22)$$

where

$$\begin{aligned} \bar{f} &= \frac{1}{C_f} \tilde{W}_f \left[\xi_{w_f} - e^{-\frac{1}{R_f C_f} t} \xi_{w_f}(0) \right] + \frac{1}{C_f} \tilde{\Theta}_f^T \left[\xi_{\Theta_f} - e^{-\frac{1}{R_f C_f} t} \xi_{\Theta_f}(0) \right], \\ \bar{g} &= \frac{1}{C_g} \tilde{W}_g \left[\xi_{w_g} - e^{-\frac{1}{R_g C_g} t} \xi_{w_g}(0) \right] + \frac{1}{C_g} \tilde{\Theta}_g^T \left[\xi_{\Theta_g} - e^{-\frac{1}{R_g C_g} t} \xi_{\Theta_g}(0) \right], \end{aligned}$$

and

$\varepsilon = \Delta_f + \Delta_g u_{id} + d$, where Δ_f and Δ_g are the approximation errors defined in the same way as that in (11). In order to derive the main theorem in this paper, the following assumption and lemma is required.

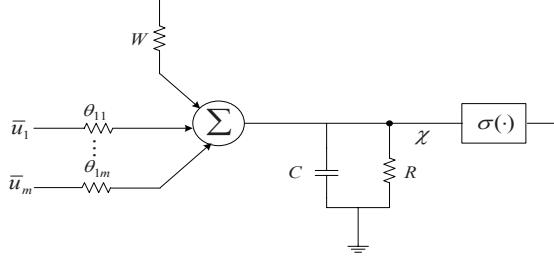


Fig. 1. Electric circuit of the Hopfield-based DNN containing only a single neuron

Assumption: Assume that there exists a finite constant μ so that

$$\int \varepsilon^2 d\tau \leq \mu, \quad 0 \leq t < \infty. \quad (23)$$

Lemma: Suppose $\mathbf{P} = \mathbf{P}^T > 0$ satisfies

$$\mathbf{A}_c^T \mathbf{P} + \mathbf{P} \mathbf{A}_c + \mathbf{Q} + \mathbf{P} \mathbf{B}_c \left(\frac{1}{\rho^2} - \frac{1}{\delta} \right) \mathbf{B}_c^T \mathbf{P} = 0 \quad (24)$$

where $\mathbf{Q} = \mathbf{Q}^T > 0$; $\rho > 0$ and $\delta > 0$ satisfies $\frac{1}{\rho^2} - \frac{1}{\delta} \leq 0$. Let $\hat{W}_f(0) \in \Omega_{w_f}$, $\hat{W}_g(0) \in \Omega_{w_g}$, $\hat{\Theta}_f(0) \in \Omega_{\Theta_f}$, and $\hat{\Theta}_g(0) \in \Omega_{\Theta_g}$, where $\hat{W}_f(0)$, $\hat{W}_g(0)$, $\hat{\Theta}_f(0)$ and $\hat{\Theta}_g(0)$ are the initial values of \hat{W}_f , \hat{W}_g , $\hat{\Theta}_f$, and $\hat{\Theta}_g$, respectively. If the adaptive laws are designed as

$$\dot{\hat{W}}_f = -\hat{W}_f = \begin{cases} -\frac{\beta_{w_f}}{C_f} \mathbf{e}^T \mathbf{P} \mathbf{B}_c \left[\xi_{w_f} - e^{-\frac{1}{R_f C_f} t} \xi_{w_f}(0) \right] \\ \text{if } |\hat{W}_f| < M_{w_f} \text{ or } \left(|\hat{W}_f| = M_{w_f} \text{ and } \mathbf{e}^T \mathbf{P} \mathbf{B}_c \hat{W}_f \left[\xi_{w_f} - e^{-\frac{1}{R_f C_f} t} \xi_{w_f}(0) \right] \geq 0 \right), \\ \Pr \left\{ \frac{\beta_{w_f}}{C_f} \mathbf{e}^T \mathbf{P} \mathbf{B}_c \left[\xi_{w_f} - e^{-\frac{1}{R_f C_f} t} \xi_{w_f}(0) \right] \right\} \\ \text{if } |\hat{W}_f| = M_{w_f} \text{ and } \mathbf{e}^T \mathbf{P} \mathbf{B}_c \hat{W}_f \left[\xi_{w_f} - e^{-\frac{1}{R_f C_f} t} \xi_{w_f}(0) \right] < 0 \end{cases} \quad (25)$$

$$\dot{\hat{W}}_g = -\dot{\tilde{W}}_g = \begin{cases} -\frac{\beta_{w_g}}{C_g} \mathbf{e}^T \mathbf{P} \mathbf{B}_c \left[\xi_{w_g} - e^{-\frac{1}{R_g C_g} t} \xi_{w_g}(0) \right] \\ \text{if } |\hat{W}_g| < M_{w_g} \text{ or } \left(|\hat{W}_g| = M_{w_g} \text{ and } \mathbf{e}^T \mathbf{P} \mathbf{B}_c \hat{W}_g \left[\xi_{w_g} - e^{-\frac{1}{R_g C_g} t} \xi_{w_g}(0) \right] \geq 0 \right), \quad (26) \\ \Pr \left\{ \frac{\beta_{w_f}}{C_g} \mathbf{e}^T \mathbf{P} \mathbf{B}_c \left[\xi_{w_g} - e^{-\frac{1}{R_g C_g} t} \xi_{w_g}(0) \right] \right\} \\ \text{if } |\hat{W}_g| = M_{w_g} \text{ and } \mathbf{e}^T \mathbf{P} \mathbf{B}_c \hat{W}_g \left[\xi_{w_g} - e^{-\frac{1}{R_g C_g} t} \xi_{w_g}(0) \right] < 0 \end{cases}$$

$$\dot{\hat{\Theta}}_f = -\dot{\tilde{\Theta}}_f = \begin{cases} -\frac{\beta_{\Theta_f}}{C_f} \mathbf{e}^T \mathbf{P} \mathbf{B}_c \left[\xi_{\Theta_f} - e^{-\frac{1}{R_f C_f} t} \xi_{\Theta_f}(0) \right] u_{id} \\ \text{if } \|\hat{\Theta}_f\| < M_{\Theta_f} \text{ or } \left(\|\hat{\Theta}_f\| = M_{\Theta_f} \text{ and } \mathbf{e}^T \mathbf{P} \mathbf{B}_c \hat{\Theta}_f \left[\xi_{\Theta_f} - e^{-\frac{1}{R_f C_f} t} \xi_{\Theta_f}(0) \right] u_{id} \geq 0 \right), \quad (27) \\ \Pr \left\{ \frac{\beta_{\Theta_f}}{C_f} \mathbf{e}^T \mathbf{P} \mathbf{B}_c \left[\xi_{\Theta_f} - e^{-\frac{1}{R_f C_f} t} \xi_{\Theta_f}(0) \right] u_{id} \right\} \\ \text{if } \|\hat{\Theta}_f\| = M_{\Theta_f} \text{ and } \mathbf{e}^T \mathbf{P} \mathbf{B}_c \hat{\Theta}_f \left[\xi_{\Theta_f} - e^{-\frac{1}{R_f C_f} t} \xi_{\Theta_f}(0) \right] u_{id} < 0 \end{cases}$$

$$\dot{\hat{\Theta}}_g = -\dot{\tilde{\Theta}}_g = \begin{cases} -\frac{\beta_{\Theta_g}}{C_g} \mathbf{e}^T \mathbf{P} \mathbf{B}_c \left[\xi_{\Theta_g} - e^{-\frac{1}{R_g C_g} t} \xi_{\Theta_g}(0) \right] u_{id} \\ \text{if } \|\hat{\Theta}_g\| < M_{\Theta_g} \text{ or } \left(\|\hat{\Theta}_g\| = M_{\Theta_g} \text{ and } \mathbf{e}^T \mathbf{P} \mathbf{B}_c \hat{\Theta}_g \left[\xi_{\Theta_g} - e^{-\frac{1}{R_g C_g} t} \xi_{\Theta_g}(0) \right] u_{id} \geq 0 \right), \quad (28) \\ \Pr \left\{ \frac{\beta_{\Theta_g}}{C_g} \mathbf{e}^T \mathbf{P} \mathbf{B}_c \left[\xi_{\Theta_g} - e^{-\frac{1}{R_g C_g} t} \xi_{\Theta_g}(0) \right] u_{id} \right\} \\ \text{if } \|\hat{\Theta}_g\| = M_{\Theta_g} \text{ and } \mathbf{e}^T \mathbf{P} \mathbf{B}_c \hat{\Theta}_g \left[\xi_{\Theta_g} - e^{-\frac{1}{R_g C_g} t} \xi_{\Theta_g}(0) \right] u_{id} < 0 \end{cases}$$

where β_{w_f} , β_{w_g} , β_{Θ_f} , and β_{Θ_g} are positive learning rates; the projection operators $\Pr\{\cdot\}$ are defined as

$$\Pr \left\{ \frac{\beta_{w_f}}{C_f} \mathbf{e}^T \mathbf{P} \mathbf{B}_c \left[\xi_{w_f} - e^{-\frac{1}{R_f C_f} t} \xi_{w_f}(0) \right] \right\} = \frac{\beta_{w_f}}{C_f} \mathbf{e}^T \mathbf{P} \mathbf{B}_c \left\{ - \left[\xi_{w_f} - e^{-\frac{1}{R_f C_f} t} \xi_{w_f}(0) \right] + \frac{\hat{W}_f \left[\xi_{w_f} - e^{-\frac{1}{R_f C_f} t} \xi_{w_f}(0) \right]}{|\hat{W}_f|^2} \hat{W}_f \right\},$$

$$\Pr\left\{\frac{\beta_{w_g}}{C_g} \mathbf{e}^T \mathbf{PB}_c \left[\xi_{w_g} - e^{-\frac{1}{R_g C_g} t} \xi_{w_g}(0) \right]\right\} = \frac{\beta_{w_g}}{C_g} \mathbf{e}^T \mathbf{PB}_c \left\{ - \left[\xi_{w_g} - e^{-\frac{1}{R_g C_g} t} \xi_{w_g}(0) \right] + \frac{\hat{W}_g \left[\xi_{w_g} - e^{-\frac{1}{R_g C_g} t} \xi_{w_g}(0) \right]}{\|\hat{W}_g\|^2} \hat{W}_g \right\},$$

$$\Pr\left\{\frac{\beta_{\Theta_f}}{C_f} \mathbf{PB}_c \left[\xi_{\Theta_f} - e^{-\frac{1}{R_f C_f} t} \xi_{\Theta_f}(0) \right] u_{id}\right\} = \frac{\beta_{\Theta_f}}{C_f} \mathbf{e}^T \mathbf{PB}_c \left\{ - \left[\xi_{\Theta_f} - e^{-\frac{1}{R_f C_f} t} \xi_{\Theta_f}(0) \right] u_{id} + \frac{\hat{\Theta}_f^T \left[\xi_{\Theta_f} - e^{-\frac{1}{R_f C_f} t} \xi_{\Theta_f}(0) \right] u_{id}}{\|\hat{\Theta}_f\|^2} \hat{\Theta}_f \right\},$$

$$\Pr\left\{\frac{\beta_{\Theta_g}}{C_g} \mathbf{PB}_c \left[\xi_{\Theta_g} - e^{-\frac{1}{R_g C_g} t} \xi_{\Theta_g}(0) \right] u_{id}\right\} = \frac{\beta_{\Theta_g}}{C_g} \mathbf{e}^T \mathbf{PB}_c \left\{ - \left[\xi_{\Theta_g} - e^{-\frac{1}{R_g C_g} t} \xi_{\Theta_g}(0) \right] u_{id} + \frac{\hat{\Theta}_g^T \left[\xi_{\Theta_g} - e^{-\frac{1}{R_g C_g} t} \xi_{\Theta_g}(0) \right] u_{id}}{\|\hat{\Theta}_g\|^2} \hat{\Theta}_g \right\},$$

then \hat{W}_f , \hat{W}_g , $\hat{\Theta}_f$ and $\hat{\Theta}_g$ are bounded by $|\hat{W}_f| \leq M_{w_f}$, $|\hat{W}_g| \leq M_{w_g}$, $\|\hat{\Theta}_f\| \leq M_{\Theta_f}$, and $\|\hat{\Theta}_g\| \leq M_{\Theta_g}$ for all $t \geq 0$ [10]. Now we are prepared to state the main theorem of this paper.

Theorem: Suppose the **Assumption** (23) holds. Consider the plant (14) with the control law (18). The function estimations \hat{f} and \hat{g} are given by (25) and (21) with the adaptive laws (25)-(28). The compensation controller u_s is given as

$$u_c = -\frac{1}{2\delta} \mathbf{B}_c^T \mathbf{P} \mathbf{e} \quad (29)$$

Then, the overall control scheme guarantees the following properties:

$$\begin{aligned} i) \quad & \frac{1}{2} \int_0^t \mathbf{e}^T \mathbf{Q} \mathbf{e} d\tau \leq \frac{1}{2} \mathbf{e}(0)^T \mathbf{P} \mathbf{e}(0) + \frac{\tilde{W}_f(0) \dot{\tilde{W}}_f(0)}{2\beta_{w_f}} + \frac{\tilde{W}_g(0) \dot{\tilde{W}}_g(0)}{2\beta_{w_g}} + \frac{\tilde{\Theta}_f^T(0) \dot{\tilde{\Theta}}_f(0)}{2\beta_{\Theta_f}} \\ & + \frac{\tilde{\Theta}_g^T(0) \dot{\tilde{\Theta}}_g(0)}{2\beta_{\Theta_g}} + \frac{\rho^2}{2} \int_0^t \varepsilon^2 d\tau \end{aligned} \quad (30)$$

for $0 \leq t < \infty$, where $\mathbf{e}(0)$, $\tilde{W}_f(0)$, $\tilde{W}_g(0)$ and $\tilde{\Theta}_f(0)$, $\tilde{\Theta}_g(0)$ are the initial values of \mathbf{e} , \tilde{W}_f , \tilde{W}_g , $\tilde{\Theta}_f$, and $\tilde{\Theta}_g$, respectively.

ii) The tracking error $\|\mathbf{e}\|$ can be expressed in terms of the lumped uncertainty as

$$\|\mathbf{e}\| \leq \sqrt{\frac{2V(0) + \rho^2 \mu}{\lambda_{\min}(\mathbf{P})}} \quad (31)$$

where $V(0)$ is the initial value of a Lyapunov function candidate defined later and $\lambda_{\min}(\mathbf{P})$ is the minimum eigenvalue of \mathbf{P} .

Proof:

i) Define a Lyapunov function candidate as

$$V = \frac{1}{2} \mathbf{e}^T \mathbf{P} \mathbf{e} + \frac{1}{2\beta_{W_f}} \tilde{W}_f^2 + \frac{1}{2\beta_{W_g}} \tilde{W}_g^2 + \frac{1}{2\beta_{\Theta_f}} \tilde{\Theta}_f^T \dot{\tilde{\Theta}}_f + \frac{1}{2\beta_{\Theta_g}} \tilde{\Theta}_g^T \dot{\tilde{\Theta}}_g \quad (32)$$

Differentiating (32) with respect to time and using (22) yield

$$\begin{aligned} \dot{V} &= \frac{1}{2} \mathbf{e}^T \mathbf{P} \dot{\mathbf{e}} + \frac{1}{2} \dot{\mathbf{e}}^T \mathbf{P} \mathbf{e} + \frac{1}{\beta_{W_f}} \tilde{W}_f \dot{\tilde{W}}_f + \frac{1}{\beta_{W_g}} \tilde{W}_g \dot{\tilde{W}}_g + \frac{1}{\beta_{\Theta_f}} \tilde{\Theta}_f^T \dot{\tilde{\Theta}}_f + \frac{1}{\beta_{\Theta_g}} \tilde{\Theta}_g^T \dot{\tilde{\Theta}}_g \\ &= \frac{1}{2} \mathbf{e}^T (\mathbf{A}_{c_c}^T \mathbf{P} + \mathbf{P} \mathbf{A}_c) \mathbf{e} - \mathbf{e}^T \mathbf{P} \mathbf{B}_c (\bar{f} + \bar{g} u_{id}) + \mathbf{e}^T \mathbf{P} \mathbf{B}_c u_c - \mathbf{e}^T \mathbf{P} \mathbf{B}_c \mathcal{E} + \frac{1}{\beta_{W_f}} \tilde{W}_f \dot{\tilde{W}}_f + \frac{1}{\beta_{W_g}} \tilde{W}_g \dot{\tilde{W}}_g \\ &\quad + \frac{1}{\beta_{\Theta_f}} \tilde{\Theta}_f^T \dot{\tilde{\Theta}}_f + \frac{1}{\beta_{\Theta_g}} \tilde{\Theta}_g^T \dot{\tilde{\Theta}}_g \\ &= \frac{1}{2} \mathbf{e}^T (\mathbf{A}_{c_c}^T \mathbf{P} + \mathbf{P} \mathbf{A}_c) \mathbf{e} + \mathbf{e}^T \mathbf{P} \mathbf{B}_c u_c - \mathbf{e}^T \mathbf{P} \mathbf{B}_c \mathcal{E} + V_{W_f} + V_{W_g} + V_{\Theta_f} + V_{\Theta_g} \end{aligned} \quad (33)$$

where

$$\begin{aligned} V_{W_f} &= \tilde{W}_f \left\{ -\frac{1}{C_f} \mathbf{e}^T \mathbf{P} \mathbf{B}_c \left[\xi_{W_f} - e^{-\frac{1}{R_f C_f} t} \xi_{W_f}(0) \right] + \frac{1}{\beta_{W_f}} \dot{\tilde{W}}_f \right\}, \\ V_{W_g} &= \tilde{W}_g \left\{ -\frac{1}{C_g} \mathbf{e}^T \mathbf{P} \mathbf{B}_c \left[\xi_{W_g} - e^{-\frac{1}{R_g C_g} t} \xi_{W_g}(0) \right] + \frac{1}{\beta_{W_g}} \dot{\tilde{W}}_g \right\}, \\ V_{\Theta_f} &= \tilde{\Theta}_f^T \left\{ -\frac{1}{C_f} \mathbf{e}^T \mathbf{P} \mathbf{B}_c \left[\xi_{\Theta_f} - e^{-\frac{1}{R_f C_f} t} \xi_{\Theta_f}(0) \right] u_{id} + \frac{1}{\beta_{\Theta_f}} \dot{\tilde{\Theta}}_f \right\}, \\ V_{\Theta_g} &= \tilde{\Theta}_g^T \left\{ -\frac{1}{C_g} \mathbf{e}^T \mathbf{P} \mathbf{B}_c \left[\xi_{\Theta_g} - e^{-\frac{1}{R_g C_g} t} \xi_{\Theta_g}(0) \right] u_{id} + \frac{1}{\beta_{\Theta_g}} \dot{\tilde{\Theta}}_g \right\}. \end{aligned}$$

Substituting (29) into (33) and using (24), we have

$$\begin{aligned} \dot{V} &= \frac{1}{2} \mathbf{e}^T (\mathbf{A}_{c_c}^T \mathbf{P} + \mathbf{P} \mathbf{A}_c) \mathbf{e} - \frac{1}{2\delta} (\mathbf{e}^T \mathbf{P} \mathbf{B}_c)(\mathbf{B}_c \mathbf{P} \mathbf{e}) + \mathbf{e}^T \mathbf{P} \mathbf{B}_c \mathcal{E} + V_{W_f} + V_{W_g} + V_{\Theta_f} + V_{\Theta_g} \\ &= \frac{1}{2} \mathbf{e}^T (\mathbf{A}_{c_c}^T \mathbf{P} + \mathbf{P} \mathbf{A}_c - \frac{1}{\delta} \mathbf{P} \mathbf{B}_c \mathbf{B}_c^T \mathbf{P}) \mathbf{e} + \mathbf{e}^T \mathbf{P} \mathbf{B}_c \mathcal{E} + V_{W_f} + V_{W_g} + V_{\Theta_f} + V_{\Theta_g} \\ &= \frac{1}{2} \mathbf{e}^T (-\mathbf{Q} - \frac{1}{\rho^2} \mathbf{P} \mathbf{B}_c \mathbf{B}_c^T \mathbf{P}) \mathbf{e} + \mathbf{e}^T \mathbf{P} \mathbf{B}_c \mathcal{E} + V_{W_f} + V_{W_g} + V_{\Theta_f} + V_{\Theta_g} \end{aligned}$$

$$= -\frac{1}{2} \mathbf{e}^T \mathbf{Q} \mathbf{e} - \frac{1}{2} \left[\frac{1}{\rho} \mathbf{B}_c^T \mathbf{P} \mathbf{B}_c - \rho \varepsilon \right]^2 + \frac{1}{2} \rho^2 \varepsilon^2 + V_{w_f} + V_{w_g} + V_{\Theta_f} + V_{\Theta_g} \quad (34)$$

Using (25), we have

$$V_w = \begin{cases} 0 & \text{if } \left| \hat{W}_f \right| < M_{w_f} \text{ or } \left(\left| \hat{W}_f \right| = M_{w_f} \text{ and } \mathbf{e}^T \mathbf{P} \mathbf{B}_c \hat{W}_f \left[\xi_{w_f} - e^{-\frac{1}{R_f C_f} t} \xi_{w_f}(0) \right] \geq 0 \right) \\ -\frac{1}{C_f} \mathbf{e}^T \mathbf{P} \mathbf{B}_c \frac{\hat{W}_f \left[\xi_{w_f} - e^{-\frac{1}{R_f C_f} t} \xi_{w_f}(0) \right]}{\left| \hat{W}_f \right|^2} \tilde{W}_f \hat{W}_f & \text{if } \left| \hat{W}_f \right| = M_{w_f} \text{ and } \mathbf{e}^T \mathbf{P} \mathbf{B}_c \hat{W}_f \left[\xi_{w_f} - e^{-\frac{1}{R_f C_f} t} \xi_{w_f}(0) \right] < 0 \end{cases} \quad (35)$$

For the condition $\left(\left| \hat{W}_f \right| = M_{w_f} \text{ and } \mathbf{e}^T \mathbf{P} \mathbf{B}_c \hat{W}_f \left[\xi_{w_f} - e^{-\frac{1}{R_f C_f} t} \xi_{w_f}(0) \right] < 0 \right)$, we have $\left| \hat{W}_f \right| = M_{w_f} \geq \left| W_f^* \right|$ because W_f^* belongs to the constraint set Ω_{w_f} . Using this fact, we obtain $\tilde{W}_f \hat{W}_f = \frac{1}{2} (W_f^{*2} - \hat{W}_f^2 - \tilde{W}_f^2) \leq 0$. Thus, the second line of (35) can be rewritten as

$$V_w = -\frac{1}{2C_f} \mathbf{e}^T \mathbf{P} \mathbf{B}_c \frac{\hat{W}_f^T \left[\xi_{w_f} - e^{-\frac{1}{R_f C_f} t} \xi_{w_f}(0) \right]}{\left| \hat{W}_f \right|^2} (\left| W_f^* \right|^2 - \left| \hat{W}_f \right|^2 - \left| \tilde{W}_f \right|^2) \leq 0. \quad (36)$$

Thus, in (35), we obtain $V_{w_f} \leq 0$. Similarly, we can also obtain that $V_{w_g} \leq 0$, $V_{\Theta_f} \leq 0$, and $V_{\Theta_g} \leq 0$. Using this knowledge, we can further rewrite (34) as

$$\dot{V} \leq -\frac{1}{2} \mathbf{e}^T \mathbf{Q} \mathbf{e} + \frac{1}{2} \rho^2 \varepsilon^2 \quad (37)$$

Integrating both sides of the inequality (37) yields

$$V(t) - V(0) \leq -\frac{1}{2} \int_0^t \mathbf{e}^T \mathbf{Q} \mathbf{e} d\tau + \frac{\rho^2}{2} \int_0^t \varepsilon^2 dt \quad (38)$$

for $0 \leq t < \infty$. Since $V(t) \geq 0$, we obtain

$$\frac{1}{2} \int_0^t \mathbf{e}^T \mathbf{Q} \mathbf{e} d\tau \leq V_0 + \frac{\rho^2}{2} \int_0^t \varepsilon^2 dt. \quad (39)$$

Substituting (32) into (39), we obtain (30).

ii) From (37) and since $\int_0^t \mathbf{e}^T \mathbf{Q} \mathbf{e} dt \geq 0$, we have

$$2V(t) \leq 2V(0) + \rho^2 \mu, \quad 0 \leq t < \infty \quad (40)$$

From (32), it is obvious that $\mathbf{e}^T \mathbf{P} \mathbf{e} \leq 2V$, for $t \geq 0$. Because $\mathbf{P} = \mathbf{P}^T \geq 0$, we have

$$\lambda_{\min}(\mathbf{P}) \|\mathbf{e}\|^2 = \lambda_{\min}(\mathbf{P}) \mathbf{e}^T \mathbf{e} \leq \mathbf{e}^T \mathbf{P} \mathbf{e} \quad (41)$$

Thus, we obtain

$$\lambda_{\min}(\mathbf{P}) \|\mathbf{e}\|^2 \leq \mathbf{e}^T \mathbf{P} \mathbf{e} \leq 2V(t) \leq 2V(0) + \rho^2 \mu \quad (42)$$

from (39)-(40). Therefore, from (42), we can easily obtain (31), which explicitly describe the bound of tracking error $\|\mathbf{e}\|$. If initial state $V(0) = 0$, tracking error $\|\mathbf{e}\|$ can be made arbitrarily small by choosing adequate ρ . Equation (31) is very crucial to show that the proposed IACHDNN will provide the closed-loop stability rigorously in the Lyapunov sense under the **Assumption** (23). **Q. E. D.**

The block diagram of IACHDNN is shown in Fig. 2.

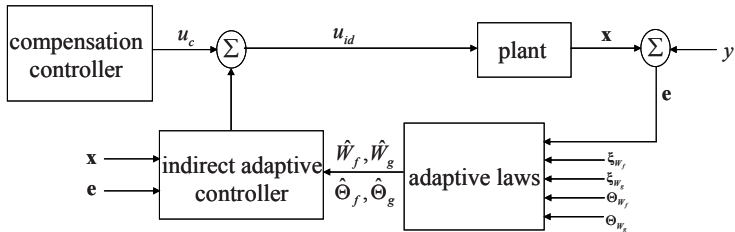


Fig. 2. The Block diagram of IACHDNN

Remark: Equation (31) describes the relations among $\|\mathbf{e}\|$, ρ , and $\lambda_{\min}(\mathbf{P})$. To get more insight of (31), we first choose $\rho^2 = \delta$ in (24) to simplify the analysis. Thus, from (24), we can see that $\lambda_{\min}(\mathbf{P})$ is fully affected by the choice of $\lambda_{\min}(\mathbf{Q})$ in the way that a larger $\lambda_{\min}(\mathbf{Q})$ leads to a larger $\lambda_{\min}(\mathbf{P})$, and vice

versa. Now, one can easily observe from (31) that the norm of tracking error can be attenuated to any desired small level by choosing ρ and $\lambda_{\min}(\mathbf{Q})$ as small as possible. However, this may lead to a large control signal which is usually undesirable in practical systems.

5 Simulation Results

In this section, simulation results are presented to illustrate the effectiveness of the proposed control scheme. It should be emphasized that the development of the IACHDNN does not need to know the exact dynamics of the controlled system.

Example: Consider an inverted pendulum system. Let x_1 (rad) be the angle of the pendulum with respect to the vertical line. The dynamic equations of the inverted pendulum are [10]

$$\dot{x}_1 = x_2$$

$$\dot{x}_2 = \frac{g_v \sin x_1 - \frac{mlx_2^2 \cos x_1 \sin x_1}{m_c + m}}{l\left(\frac{4}{3} - \frac{m \cos^2 x_1}{m_c + m}\right)} + \frac{\frac{\cos x_1}{m_c + m}}{l\left(\frac{4}{3} - \frac{m \cos^2 x_1}{m_c + m}\right)} u + d \quad (43)$$

where $g_v = 9.8 \text{ m/s}^2$ is the acceleration due to gravity; m_c is the mass of the cart; m is the mass of the pole; l is the half-length of the pole; u is the applied force (control) and d is the external disturbance. The reference signal here is $y_r = (\pi/30)\sin t$, and d is a square wave with the amplitude ± 0.05 and period 2π . Also we choose $m_c = 1$, $m = 0.5$, and $l = 0.5$. The initial states are $[x_1(0) \ x_2(0)]^T = [0.2 \ 0.2]^T$. The learning rates of weights adaption are selected as $\beta_{w_f} = \beta_{\Theta_f} = 0.2$ and $\beta_{w_g} = \beta_{\Theta_g} = 0.005$; the slope of $\tanh(\cdot)$ at the origin are selected as $\kappa_f = k_g = 1$ and $\delta = 0.1$ for the compensation controller. The resistance and capacitance are chosen as $R_f = R_g = 10 \Omega$ and $C_f = C_g = 0.001 F$. For a choice of $\mathbf{Q} = 15\mathbf{I}$, $\mathbf{k}_c = [2 \ 1]^T$, we solve the Riccati-like equation (24) and obtain $\mathbf{P} = \begin{bmatrix} 22.5 & 7.5 \\ 7.5 & 7.5 \end{bmatrix}$. The simulation results for are shown in Fig. 3, where the tracking responses of state x_1 and x_2 are shown in Figs. 3(a) and 3(b), respectively, the associated control inputs are shown Fig. 3(c). From the simulation results, we can see that the proposed IACHDNN can achieve favorable tracking performances with external disturbance. This fact shows the strong disturbance-tolerance ability of the proposed system.

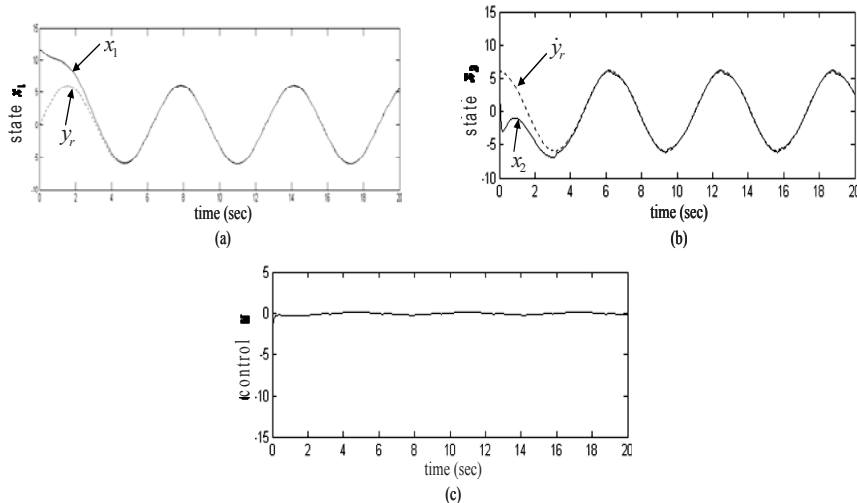


Fig. 3. Simulation results

Conclusions

An indirect adaptive control scheme using Hopfield-based dynamic neural networks for SISO nonlinear systems is proposed in this paper. The simple Hopfield-based DNNs are used to approximate the uncertain parameters of the controlled plant and the synaptic weights Hopfield-based DNNs are tuned on-line by the adaptive laws. A compensation controller is merged into control law to compensate the effect of modeling error and external disturbance. By the Lyapunov stability analysis, we prove that the closed-loop system is stable, and the tracking error can be attenuated to a desired level. Note that no strong assumptions and prior knowledge of the controlled plant are needed in the development of IACHDNN. Simulation results demonstrate the effectiveness and robustness of the proposed IACHDNN in the presence of external disturbance. The parsimonious structure of the Hopfield-based DNN (only one neuron is contained) and the simple Hopfield circuit make the IACHDNN much easier to implement and more reliable in practical purposes.

References

- [1] Chen, B.S., Lee, C.H., Chang, Y.C.: H^∞ Tracking Design of Uncertain Nonlinear SISO Systems: Adaptive Fuzzy Approach. *IEEE Trans. Fuzzy Syst.* 4, 32–43 (1996)
- [2] Li, Y., Qiang, S., Zhang, X., Kaynak, O.: Robust and Adaptive Backstepping Control for Nonlinear Systems Using RBF Neural Networks. *IEEE Trans. Neural Networks* 15, 693–701 (2004)

- [3] Lin, C.T., George Lee, C.S.: Neural Fuzzy Systems: a Neuro-Fuzzy Synergism to Intelligent Systems. Prentice-Hall, Englewood Cliffs (1996)
- [4] Pham, D.T., Liu, X.: Dynamic System Identification Using Partially Recurrent Neural Networks. *J. Syst. Eng.* 2, 90–97 (1992)
- [5] Poznyak, A.S., Yu, W., Sanchez, D.N., Perez, J.P.: Nonlinear Adaptive Trajectory Tracking Using Dynamic Neural Networks. *IEEE Trans. Neural Networks* 10, 1402–1411 (1999)
- [6] Chow, T.W.S., Li, X.D., Fang, Y.: A Real-Time Learning Control Approach for Nonlinear Continuous-Time System Using Recurrent Neural Networks. *IEEE Trans. Ind. Electronics*. 47, 478–486 (2000)
- [7] Ren, X.M., Rad, A.B., Chan, P.T., Lo, W.L.: Identification and Control of Continuous-time Nonlinear Systems via Dynamic Neural Networks. *IEEE Trans. Ind. Electronics* 50, 478–486 (2003)
- [8] Hopfield, J.J.: Neural Networks and Physical Systems with Emergent Collective Computational Abilities. *Proceedings of National Academy of sciences, USA* 79, 2554–2558 (1982)
- [9] Hopfield, J.J.: Neurons with Graded Response Have Collective Computational Properties Like Those of Two-State Neurons. *Proceedings of National Academy of sciences, USA* 81, 3088–3092 (1984)
- [10] Wang, L.X.: Adaptive Fuzzy Systems and Control - Design and Stability Analysis. Prentice-Hall, Englewood Cliffs (1994)

Fuzzy Immune Controller Synthesis for ABR Traffic Control in High-Speed Networks

Georgi M. Dimirovski¹, Yuanwei Jing², and Tao Ren²

¹Dogus University, Computer Engineering Dept., Acibadem, Istanbul 34722, R. Turkey, and SS Cyril & Methodius University, FEIT, ASE, Karpos 2 BB, 1000 Skopje, R. Macedonia
gdimirovski@dogus.edu.tr

²Northeastern University, College of Information Science & Engineering, Shenyang, Liaoning, 110004, P.R. China
ywjjing@mail.neu.edu.cn; chinarentao@163.com

Abstract. An end-to-end congestion control design synthesis algorithm for the available-bit-rate traffic in high speed asynchronous-transfer-mode networks is studied via applying the synergy of fuzzy-based intelligence and immune control laws. A fuzzy immune controller is designed to overcome the adverse effects in the network caused by unavoidable uncertainties such as number of users, available bit-rate bandwidth, and propagated transmission delays. Also an algorithm is proposed that can guarantee the minimum cell rate in order to ensure the fair and full utilization of the bandwidth. Simulation investigation has been carried out and the results show the proposed control synthesis is robust and the system performs effectively in adaptive mode. Hence the network's quality-of-service is guaranteed too.

1 Introduction

In order to place this study into prospect a few facts about high-speed network technologies are recalled first [1], [2], [3]. The Asynchronous Transfer Mode (ATM) technology has been defined as the transport technology to be used in Broadband Integrated Service Digital Networks (B-ISDN) communication services. In due time ATM Forum has defined five service classes to support multi-media traffic; these are: the constant bit-rate (CBR) class, the real-time and non-real-time variable bit-rate (VBR) class, the unspecified bit-rate (UBR) class, and the available bit-rate (ABR) class, which is a best effort class. Furthermore, in ATM network the priority of ABR is lower than those of VBR or CBR hence ABR gets the leftover capacity after VBR or CBR communication services have been transmitted. In turn, the bandwidth of ABR may be changing frequently. The ABR is known to be the only class that responds to network congestion by means

of an in-built feedback control mechanism in order to improve network utilization by minimizing data loss and retransmissions [4], [5], [6]. It is therefore more suitable for solving the congestion induced problems in the network itself [7], [8]. The aim of controlling the ABR source rates is to avoid overflow of the buffer caused by the varying bandwidth and to utilize the bandwidth to the full [4], [5], [6]. Ultimately, the goal is to ensure the network operates as high quality-of-service (QoS) network system [9].

The rate-based feedback control strategy has been adopted as the standard method by the ATM Forum [1]. This control scheme makes use of resource management (RM) cells to convey the feedback control information and implement the controlling action. In fact, there are two different schemes for the rate-based feedback control method: (a) binary feedback (BFB) scheme; and (b) explicit rate (ER) scheme. Moreover, the earlier research endeavors have yielded schemes based on more traditional control-theoretic views [10]-[18] whereas fairly recently composite methods combining computational intelligence techniques with control-theoretic views have emerged [19]-[26].

Further presentation of is organized as follows. Section 2 is devoted to provide a brief overview on the most relevant previous works. In Section 3, there is given a representation model for the ATM high-speed networks. Thereafter in Section 4 there is presented the proposed fuzzy-immune controller design. In Section 5, there are presented the obtained simulation results and discussed the feasible operating performance of high-speed networks. The concluding section and references follow thereafter.

2 An Overview of Some Previous Studies

In the sequel a brief overview to some relevant previous works in the literature is presented, albeit it is far from exhaustive. The interested reader should consult the references in those that are overviewed in here for a more comprehensive awareness about the subject topics as well as better understanding of the issues involved.

The delicate problem of ABR control in ATM networks and its essential issues has been well elaborated in [8] along with certain possible advanced solutions and associated difficulties in practical implementation. In contrast, work [9] is focused on a rather practical approach for achieving QoS provisions in the Internet. An thorough analysis of congestion control mechanisms versus the best effort service model has been carried out in [10]. Works [11] and [12] have studied the application of BFB based method due to its simplicity and tried to achieve the outmost performance. However, in both these synthesis designs the proposed controls still exhibit oscillatory dynamics and require large buffer storage in order to avoid packet losses. Besides, there is no guarantee against instability troubles.

The ER based scheme and associated algorithms have been investigated too. The study [13], for instance, developed an analytic method for the design of closed-loop congestion controllers along with tackling the important issues of both

fairness and stability. The authors proposed a PD control design based on a robust adaptive design philosophy. Yet, given the fact that a number of parameters need to be updated frequently this control design could be costly to implement since it has to include provision for frequent parameter adaptation, which would inevitably invoke higher-order dynamical version. The authors of work [14], on the other hand, proposed a dual PD controller design in which the control parameters can be determined so as to ensure the loop stability in a control-theoretic sense over a wide range of traffic patterns and propagation delays in the network. This method has been shown to exhibit good performance and it possesses a solid theoretical foundation. Nonetheless it does require a complicated procedure to obtain the proper controller parameters hence its practical usage is hard to implement. The authors of paper [15] have provided a control-theoretic investigation and novel solution on ABR explicit rate algorithm for ATM Switches. In [16], [17] and [18] there has been proposed a control scheme employing a Smith predictor along with a proportional controller. This design synthesis has been shown can not only lower the average queue level but also to improve disturbance rejection. However, the scheme requires knowledge of the round-trip delays between the source and the switches along the connection path. Moreover, if the propagation delays change the system may become unstable while the occurrence of these changes seems rather vaguely uncertain. Thus the issue on how to design an efficient, and yet implementable, congestion controller that can cope with poorly understood ABR and VBR traffic models, large propagation delay, and a variety of uncertainties existing in ATM network traffic remained open up to nowadays.

Since, one hand, most of the traditional control theories are analytically mathematical and model-based, and the process to be controlled involves not only nonlinearity but also uncertainties and vagueness in their occurrence, normally, the applications of one or another category of computational intelligence was appealing. Not surprisingly, a tendency towards exploiting fuzzy-logic and neural networks emerged soon. For it is believed they may prove as viable techniques for dealing with complicated uncertain features and varying environment in ATM high-speed networks, which cannot be captured by an exact mathematical modeling analysis.

One group of research works [19]-[22] within this tendency seems to be inspired by achieving learning capacity in addition to adaptation in congestion control. In work [19] such a neural-network based solution was proposed for congestion control in ATM multiplexers. Their design synthesis employed learning approximation and generalization potential of neural networks. Authors of [20] have developed an adaptive congestion control protocol with learning capability for wider usage in high-speed networks. Work [21] also contributed a congestion control for high-speed networks but the solution is based on cooperative multi-agent technology. Yet another kind of contribution based on simulated-annealing Q-learning algorithms has been developed in paper [22].

Another group of research works within this tendency [23]-[26] has been focused on exploiting results of fuzzy reasoning-based computational intelligence in synergy with control-theoretic approach to congestion control problem in

high-speed networks. The authors of [23] proposed to design a predictive self-tuning fuzzy- logic control technique. They have shown their control design is efficient and stable as well as it outperforms other proposed ABR rate controllers in a variety of network environments. A nonlinear PID controller employing fuzzy-tuned immune feedback law has been proposed in [24]. Subsequently, this idea inspired the authors of [25] to develop a novel simple yet efficient fuzzy immune PID controller for ABR traffic control over ATM networks. Finally, in work [26] another variant of fuzzy immune flow control synthesis for ATM networks has been proposed.

Our research followed this streamline within the context of employing fuzzy sets and fuzzy reasoning [27], [28], [29] for deriving fuzzy control applications [30], [31], [32].

Present study, which is a completion of our paper [25], is a further exploration of the explicit rate scheme based on a fuzzy immune controller endowed with a certain machine intelligence capability for adjusting ABR source rate in due time and with an algorithm that guarantees minimum cell rate (MCR). This design synthesis aims to exploit the synergy of some fuzzy-computing intelligence within the category of immune control laws. Thus it represents a kind of hybrid fuzzy and analytical control synthesis for ABR traffic control. It should be noted further, our fuzzy-immune control synthesis achieves capacity to tune the parameters on-line and ensure the QoS traffic in ATM high-speed networks, which is not the case in other proposed designs. In addition, the saturation feature of output queue length, the course sending rate, and variation of the propagation delay are also accounted for. It has been tested by extensive simulation experiments the results of which demonstrated the proposed design synthesis possesses properties of adaptation and robustness in varying network traffic environment while retaining its effectiveness as well as implementation simplicity.

3 Representation Model of the ATM Network Transmission

A single bottleneck link of ATM switching network visually can be described as depicted in Figure 1. Such a network can be considered as a graph structure consisting of source (S) and a destination (D) as well as a switch node (SN). The network traffic is contributed by source/destination pairs (S, D), i.e. the connected links in the network's graph. Each (S, D) connection is associated with a virtual circuit (VC) that being is set up before starting the actual communication transmission. Each switch node has a processing capacity of $c_{pr} = 1/\tau_{pr}$ (cells/s), where τ_{pr} is the time between the moment a cell is received by the switch node and the moment it is placed in the queue of its outgoing link. Each link is characterized by the transmission capacity $c_s = 1/\tau_s$ (cells/s), where τ_s is the transmission

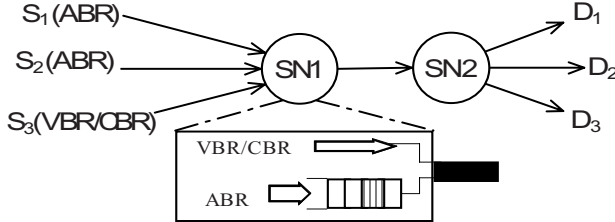


Fig. 1. A schematic presentation of a typical single bottleneck ATM network with three traffics competing for the available resource

time of a cell. Generally speaking, $c_{pr} > c_s$, so congestion is caused by transmission capacity not by processor of the switch node.

In [6], [7], [11], and [12], the respective authors implemented Per-VC FIFO queuing for the switch by which the congestion control algorithms can be effectively and easily run at the source and assure the fairness of bandwidth sharing (at a short time scale). However, this kind of switch is not scalable and may costly to be implemented. Therefore, we implement a commonly used FIFO queue switch whose buffer is shared by all VC's. Associated with each buffer is an ER computation engine that determines the rate for each ABR VC switched through this buffer. The source generates resource management (RM) cells, at a rate proportional to its current data cell rate. The destination terminal will turn around and route the RM cells back to the source. The RM cells contain some special fields including explicit rate (ER) field. ER denotes the rate the switch can support. Each node encountered by the RM cell along the VC path, stamps the computed value for the input rate on the RM cell only if this value results to be less than the rate already stored. The node that has the smallest ER value is called bottleneck node. Moreover we assume that there is only one bottleneck node for each VC. The RM cells will return source from bottleneck node after a delay T_b , where T_b denotes the forward propagation delay. On receiving the RM cell, the source sets the input rate to this value, which is bounded by minimum cell rate (MCR) and peak cell rate (PCR). The effect of the new rate becomes apparent at the switch under consideration after another delay T_f , where T_f denotes the backward propagation delay. The sum of propagation delay in the forward and the backward path represents the round-trip propagation delay, denoted by $T_{rtt} = T_b + T_f$. In this study it is assumed that the propagation delay is dominant in comparison to other delays (processing, queuing, etc.) that occur and persist.

Let $x_j(t)$ be the queue level associated with the j^{th} link of the bottleneck switch node. Upon adoption at $t = 0$ of the initial conditions $x(0) = 0$, the flow conservation equations may be written down as

$$x_j(t) = \text{Sat}_{x_c} \left\{ \int_0^t \sum_{i=0}^N u_{ij}(\tau - T_{rtti}) d\tau - \int_0^t d_j(\tau) d\tau \right\} \quad (1)$$

where

$$\text{Sat}_{x_c}(z) = \begin{cases} 0 & \text{if } z < 0 \\ x_c & \text{if } z > x_c \\ z & \text{otherwise} \end{cases} \quad (1-a)$$

Other quantities represent: N denotes the number of VC's sharing the j^{th} link of the switch node under consideration; $u_{ij}(t)$ denotes the input rate of the i^{th} VC; T_{rtti} denotes the round-trip propagation delay of the i^{th} VC; $d_j(\tau)$ denotes the bandwidth of j^{th} link.

4 Fuzzy Immune Control Law

Let T_{\max} represent the maximum round-trip propagation delay among all the VC's, because the round-trip propagation delay is the main factor affecting the performance of network, we design the controller under the worst environment where $T_{rtti} = T_{\max}$ ($i = 1, 2, \dots, N$). Then (1) can be rewritten as:

$$x_j(t) = \text{Sat}_{x_c} \left\{ \int_0^t \sum_{i=0}^N u_{ij}(\tau - T_{\max}) d\tau - \int_0^t d_j(\tau) d\tau \right\} \quad (2)$$

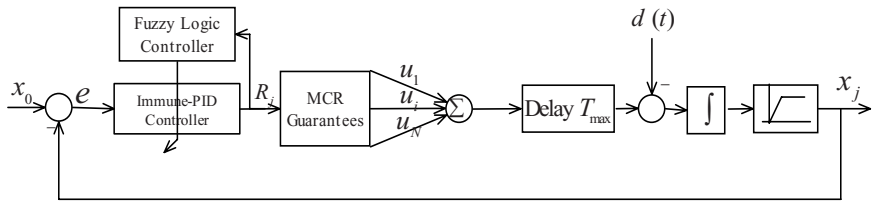


Fig. 2. A Block diagram representation of the ABR flow control system

Figure 2 depicts a block-diagram representation of the control system architecture of the ABR flow control. Since it can be difficult to measure the available ABR bandwidth, $d_j(t)$ is here modeled as a disturbance. In the sequel, the design

of immune PID controller and the fuzzy law as well as the algorithm of guaranteeing minimum cell rate (MCR), respectively, we will be discussed in more detail. It should be noted, the here proposed intelligent controller comprises three co-operating algorithms: immune PID control law; fuzzy-logic self-tuning emulator; and minimum MCR provider.

4.1 Immune PID Controller Design

It is well known by and large the implemented industrial controllers are of the linear three-term category, namely the one based on proportional-plus-integral-derivative control law that emulates reasonably well a highly skilled human operator [31], [32]. For classical linear PID controllers have the advantage of a simple and well understood algorithm that is easy to implement in both analogue and digital version, and also easily maintained and retuned. However, on the other hand, its parameters can be tuned only if an accurate model of the process-to-be-controlled is available; besides it is hard to ensure the robustness and the effectiveness when process model is rather uncertain as is the case of ABR flow control. Still, it appeared to be a rather good point of departure towards the fuzzy-computing base intelligent controller proposed in here.

The equation of the discrete-time version of the PID control laws is well-known and given as follows:

$$R(k) = k_p e(k) + k_i \sum_{j=0}^k e(j) + k_d \left[\frac{e(k) - e(k-1)}{T} \right] \quad (3)$$

Should this control algorithm be endowed by immunity ability, then its performance would be far beyond the standard one.

On the other hand, the natural immune system in living organisms, whose function is to identify and to eliminate foreign material, is capable of teaming, memorizing, and recognizing patterns [13]. It should be noted, the immune system has many remarkable abilities such as adapting, evolving, learning, self-organizing, etc. There exist various cells that are involved in the biological immune system. The most important cells of the immune system are lymphocytes.

There are mainly two classes of lymphocytes, namely T cells and B cells. Antibody (Ab) molecules are synthesized and secreted by B cells, and this particular process is regulated by T cells. The T cells can either help or suppress B cells' response to a stimulus. The principle cells that are involved in the interaction are antibody (Ab), antigen (Ag), B cells (B), help T cells (T_H) and suppressor T cells (T_S). The Ag is taken in by B cells and appears on the surface of B cells. It exhibits the antigen presentation. The antigen presentation is

recognized by the T_H and secretes the interleukin (IL^+) that activates the immune response. Thus the IL^+ becomes a second signal of B cells. The B cells divide into plasma cells, then synthesize Ab , and finally secrete Ab . If the Ag is excluded by the Ab , then immune response is finished. This is to say, if Ab is increased, then the T_S are stimulated to secrete interleukin (IL^-) that suppress the immune response. If the generation of Ab stops, the immune response is ended up [13].

In this feedback regulating mechanism of T cells the background concept adopted is the following simple immune feedback control law. The amount of antigens at the k^{th} generation is defined as $\varepsilon(k)$. In turn, the output from the T_H stimulated by the antigens is defined as $T_H(k)$ and the effect of the T_S on B cells as $T_S(k)$. Thus the total stimulation received by the B cells is given as follows:

$$S(k) = T_H(k) - T_S(k) \quad (4)$$

Notice that in here $T_H(k) = k_1 \varepsilon(k)$ and $T_S(k) = k_2 f[\Delta S(k)] \varepsilon(k)$ where k_1 represents the stimulation factor whereas k_2 represents a suppression factor. Function $f(\cdot)$ is a nonlinear function that accounts for the effect of the reaction of B cells and the antigens. Now, let observe the amount of the antigens $\varepsilon(k)$ observed as the control error between a given set point and the output of the feedback system mechanism, and the total stimulation $S(k)$ received by B cells as a controlling input. Then the immune feedback control law in discrete time

$$R(k) = K[1 - \eta f(R(k), \Delta R(k))]e(k) \quad (5)$$

follows at once. In here, gain parameter $K = k_1$ is employed to control the response speed, and parameter $\eta = k_2/k_1$ is employed to control the stabilization effect. It should be noted, controller (5) based on the immune feedback mechanism is a nonlinear proportional (P) controller in which $f(\cdot)$ models the reaction effect of B cells and the antigens hence plays a crucial role.

The above analysis discussion justifies put forward the equation output of an immune PID controller as follow:

$$R(k) = K[1 - \eta f(R(k), \Delta R(k))]e(k) + k_i \sum_{j=0}^k e(j) + k_d \left[\frac{e(k) - e(k-1)}{T} \right] \quad (6)$$

In order to avoid complicated computations and save the memorizing of the switches, instead we propose the PID equation below

$$R(k) = R(k-1) + k_p' [(e(k) - e(k-1))] + k_i e(k) + k_d \left[\frac{e(k) - 2e(k-1) + e(k-2)}{T} \right] \quad (7)$$

where

$$k_p' = K[1 - \eta f(R(k), \Delta R(k))] \quad (7-a)$$

is the time varying gain of the integral control mode, which is to be computed on line.

4.2 Design of Fuzzy Self-tuning Emulator

In order to develop an intelligent yet feasible immune PID control synthesis, we propose to employ a fuzzy-logic control synthesis to emulate the analytically unknown nonlinear function $f(\cdot)$. Furthermore, this fuzzy emulator should be constructed so as to capture the reaction effect of B cells and the antigens; hence it should be conceived as a semantic driven one on the grounds of the available qualitative knowledge on the biological background.

Remark 1: The alternative effective method to construct a nonlinear functional approximator by applying an artificial neural network would not allow for using to the full the available biological qualitative knowledge.

Since the design of fuzzy controllers imply applications of fuzzy sets and fuzzy inference in control theory, in our study the design procedure is organized in the three typical stages.

(1) *Fuzzification.* The procedure to define appropriate membership functions hence fuzzy sets for $R(k)$, $\Delta R(k)$, and $f(\cdot)$ following the biological analysis above outlined in the previous section. For $R(k)$ and $\Delta R(k)$, respectively, the fuzzy sets “positive” (P) and “negative” (N) have been adopted. And for $f(\cdot)$ the three fuzzy sets “positive” (P), “zero” (Z), and “negative” (N) have been adopted. The defining membership functions are considered over $(-\infty, +\infty)$ due to not precisely known quantitative information. The Z model, the S model, and the Triple model functions are chosen to describe the fuzzy sets of input and output variables.

(2) *Inference.* On the grounds of the above qualitative analysis, the following four fuzzy rules have been developed:

- a. If R is P and ΔR is P then $f(R, \Delta R)$ is N
- b. If R is P and ΔR is N then $f(R, \Delta R)$ is Z
- c. If R is N and ΔR is P then $f(R, \Delta R)$ is Z
- d. If R is N and ΔR is N then $f(R, \Delta R)$ is P

Moreover, in these rules Zadeh's AND fuzzy-logic operator has been employed.

(3) *Defuzzification*. The center of gravity method has been chosen to calculate the output of fuzzy controller.

It should be noted, control law (7) can ensure the negative feedback control operation provided $f(R, \Delta R) \leq 1$. Moreover, if happens $\eta = 0$ or $f(R, \Delta R) = 0$, then fuzzy immune PID controller will operate temporarily as the standard linear PID controller. The above proposed synthesis of fuzzy immune PID control can equally distribute the bandwidth to each ABR user who has the rate R_j .

4.3 Algorithm Design for MCR Guarantee and Fairness

The basic definition of service fairness in ATM networks stets that no set of ABR connections should be arbitrarily discriminated against and that no set of connections should be arbitrarily favored. In fact, in the previous sections was assumed that all the active ABR connections have zero MCR so that the same feedback rate is sent to all active VC's. However, ABR connections may happen to have different nonzero MCR requirements. Thus other fairness criteria ought to be considered and ATM networks there have been defined a few of them. One of those is called "MCR plus equal share" and defined for VC_i as follows:

$$ER_{ij}(k) = MCR_i + R_j(k) \quad (8)$$

When it happens $MCR_i = 0$ ($i = 1, 2, \dots, N$), then $ER_{ij}(k) = R_j(k)$. On the other hand, when $MCR_i > 0$, then (8) should and can guarantee all MCR minimum. Thus the common rate in steady state will have to converge to:

$$R_s = \frac{C^{\text{abr}} - \sum_i^N MCR_i}{N} \quad (9)$$

where C^{abr} is the ABR bandwidth of the considered link established. Furthermore, after meeting the requirements of the VC's with $\text{MCR} > 0$ the remaining ABR capacity is readily shared equally among all the VBR users.

5 Investigation of Performance via Simulation Experiments

In this section, we present the investigation of the transient performance of ATM network with the proposed fuzzy-immune controller under a variety of networking conditions and loads. For this purpose, we have chosen the operating scenarios simulation experiments as those proposed by Kolarov and Ramamurthy in their study [14].

The network system is assumed to have two switches with 1680 cell buffers each and two groups of ABR sources, with each group consisting of five persistent sources and one group of VBR source consisting of four VBR sources (see Fig. 3). The sampling interval is chosen as $T = 1\text{ms}$, and this is a reasonable compromise between the computational cost and consequent impact on performance. The buffer set point $x_0 = 50\text{cells}$. All links have been assumed to possess capacity of 365 cells/ms (155 Mb/s). Obviously the link between the two switch setups is the trouble causing bottleneck link.

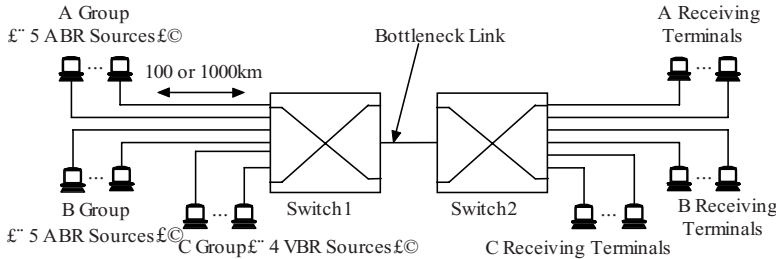


Fig. 3. The model of single bottleneck link on which the simulation experiments have been carried out

In the sequel, solely a sample set of typical simulation results is being presented and discussed.

5.1 Simulation in LAN Network

The distance from the sources A and B to the switch1 is 100 km and the round-trip propagation is 1 ms, while the distance from the receiving terminals to the switch1 is 1 km (neglected in here). The source parameters are chosen as follows:

$\text{PCR}=365\text{cells/ms}$, $\text{ICR}=\text{MCR}=4\text{cells/ms}$. Sources in group A start transmission at time $t = 1\text{ms}$, while Sources in group B start at time $t = 300\text{ms}$.

Figure 4 shows the rate for each source. When the sources in group A start transmission, the rates converge to stable value 73 cells/ms ($365/5$). When group B sources start transmission, all source rates stabilize around a new equilibrium of 36.5 cells/ms ($365/10$).

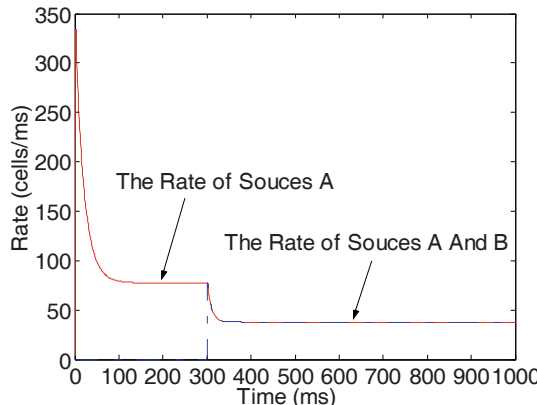


Fig. 4. Responses for the ABR source rates in LAN network exhibiting $T_{rtt} = 1\text{ms}$

In Figure 5 there are depicted the queue lengths. As seen in Fig. 5, the queue length converges to 50 cells, which is the buffer set point, after 105 ms and there no overshoot occurs. When group B sources start at time $t = 300\text{ms}$, the queue level attains its stable value after 70 ms with very small overshoot (1.4 cells) indeed.

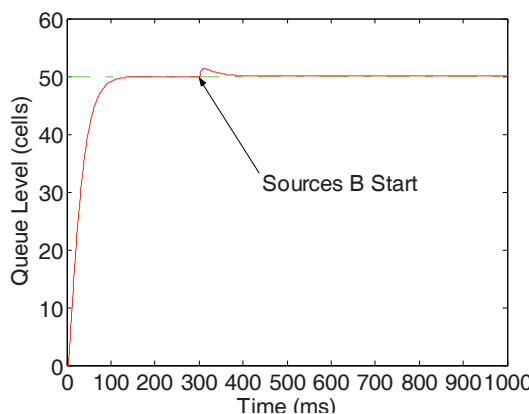


Fig. 5. Responses for the buffer queue levels in LAN network exhibiting $T_{rtt} = 1\text{ms}$

These results are rather encouraging and suggest the affirmative conclusion about the achieved controlled performance. Thus it may readily be concluded that the proposed fuzzy immune controller timely responds to the changes in network load and makes the rate of sources and queue stabilize rapidly. Thus the prospect of practical implementation in LAN networks is promising.

5.2 Simulation in WAN Network

In this case study, the distance from the sources A and B to the switch1 is set to be 1000 km, and the round-trip propagation time is set to be 10 ms. The other conditions remained the same as the LAN simulation experiment. The corresponding results are depicted in Figures 6 and 7, respectively.

As it is seen from Fig. 6, the settling time for the source-rate transient response shows only a slight degradation with respect to that performance in a LAN environment. In precise terms, it appears to last only 50 ms longer.

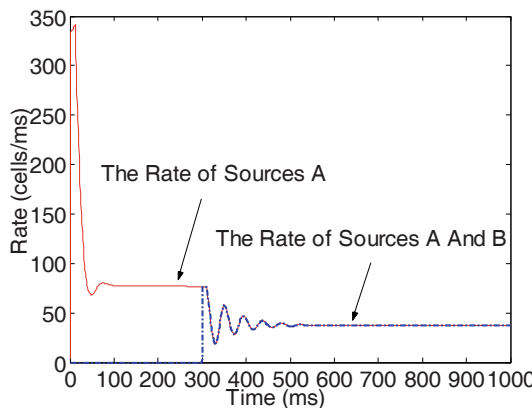


Fig. 6. Responses for the ABR source rates in WAN network exhibiting $T_{rt} = 10\text{ms}$.

It is apparent from Fig. 7 that there are no cell losses during the transient periods. The queue length settles around the buffer set point (50 cells) specified.

Notice that, although the time delay is ten times longer, not only the rates of all ABR sources but also the queue length converge quickly to stable values. Again it is clearly demonstrated that the fuzzy immune controller can better overcome the adverse effect caused on controlled variables by the considerably long time delays.

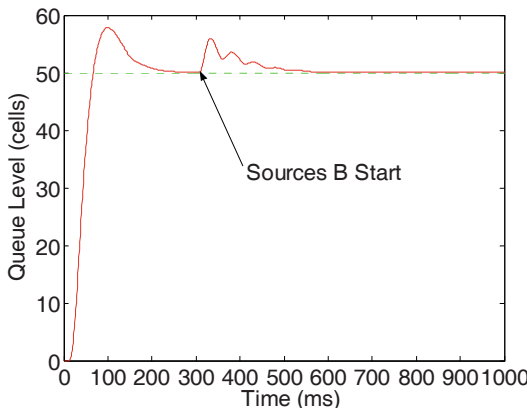


Fig. 7. Responses for the buffer queue levels in LAN network exhibiting $T_{rtt} = 10\text{ms}$

5.3 Simulation with VBR Existing in WAN

Next, the performance of fuzzy immune controller in a WAN environment when the available rate for ABR service continuously changes with time is explored. For this purpose, four video MPEG sources at switch1 with a peak rate of 35 cells/ms and an average rate of 21 cells/ms have been added. The MPEG sources have service priority over ABR sources and start the respective transmission at time $t = 1\text{ms}$. The ABR sources (with infinite backlog) are persistent nonetheless.

Next Figure 8 depicts the transient response under the aggregated rate of the four MPG at about 73 Mb/s. As seen from Fig. 8, After $t = 1\text{ms}$ and $t = 300\text{ms}$, the rate of ABR sources stabilize around 58 cells/ms and 29 cells/ms, respectively, with little transient oscillations. Importantly, no cell loss occurred. This simulation investigation indicated that the proposed fuzzy immune controller can reduce the sensitivity to varying ABR bandwidth. Thus it may well be inferred it does possess a certain good range of robustness.

The insofar discussed three simulation experiments have been carried out with the same MCR values of all the ABR sources.

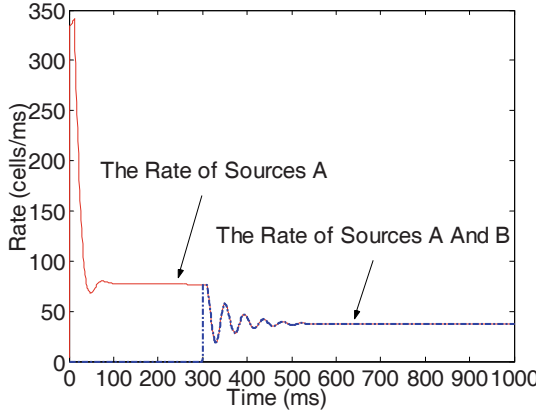


Fig. 8. Response of ABR source rate with $T_{rtt} = 10\text{ms}$ when priority VBR flows exist

5.4 Simulation with Different MCR in WAN

It is shown in this subsection that the control scheme with the proposed design synthesis of the fuzzy immune controller algorithm can achieve fairness and does support minimum rate guarantee ($\text{MCR} > 0$). Recall that the ER is being computed by using (8).

The following MCR values have been assigned to the ten ABR sources:

- (1) Sources A(1), A(2), and A(3) (group S1) have $\text{MCR} = 49 \text{ cells/ms}$;
- (2) Sources A(4), A(5), and B(1) (group S2) have $\text{MCR} = 38 \text{ cells/ms}$;
- (3) Sources B(2), B(3), B(4), and B(5) (group S3) have $\text{MCR} = 26 \text{ cells/ms}$.

Sources in group A start transmission at time $t = 1\text{ms}$. The obtained simulation responses are depicted in Figure 9.

The following observation analysis of Fig. 9 readily yields the following facts:

The remaining bandwidth after the MCR guarantees are satisfied, namely $365 - 105 - 48 = 212 \text{ cells/ms}$, is equally shared among the five sources of the group A. In other words, sources in group S1 get $35 + 212/10 = 56 \text{ cells/ms}$ each, whereas sources in group S2 [A(4) and A(5)] get $24 + 212/10 = 45 \text{ cells/ms}$.

When sources from group B become active at time $t = 300\text{ms}$, the sum of all the MCR values becomes 225 cells/ms and the remaining bandwidth $365 - 225 = 140 \text{ cells/ms}$ is equally shared among the ten sources.

It appears, each source gets an additional bandwidth of 14 cells/ms on the top of its own MCR guarantee.

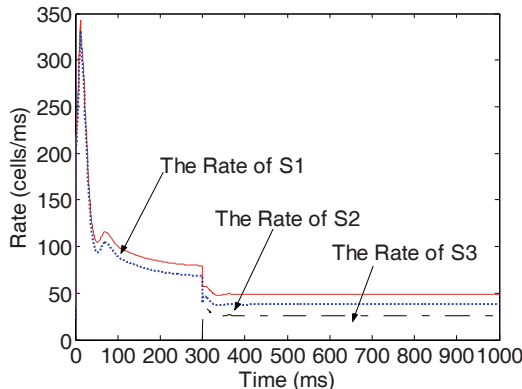


Fig. 9. Response of the ABR source rates with $T_{rt} = 10\text{ms}$ and different MCR guarantees

Indeed, Figure 9 clearly shows that after the transients settle down the bandwidth states become:

- 1/. Sources in group S1 get 49 cells/ms each;
- 2/. Sources in group S2 get 38 cells/ms each;
- 3/. Sources in group S3 get 26 cells/ms each.

These figures confirm that the proposed fuzzy immune control synthesis, regardless its simplicity, also ensures the fairness transmission service of ATM networks.

Conclusion

In the article two contributions we have been given: firstly, a control-theoretic approach to the design a closed-loop rate-based flow controller in high-speed networks has been elaborated; and secondly, the compatible usage of fuzzy computing emulator and immune version of the analytical PID control law. In turn, a fuzzy immune design synthesis for control of rate-based flows in ATM networks has been achieved which possess asymptotic stability and practical robustness. Furthermore, the proposed fuzzy immune controller can be fairly easy implemented in practice. Despite its simplicity and primitive fuzzy computing intelligence, the propose control synthesis copes rather well with the adverse effects caused by time delays and uncertainties of the network.

Thus the source rates respond timely and rapidly to the changes in the network traffic hence the congestion avoidance is effectively enabled. Furthermore, the proposed synthesis also guarantees the MCR fairness values and leads to no cell loss and full link utilization. Results from simulation experiments have been gathered

for LAN and WAN environments, and WAN in composite VBR existing operation. All these have demonstrated the synthesized scheme possesses both effective adaptability and good robustness, which are important in a variety of operating applications in high-speed networks.

Acknowledgments. Professors Georgi M. Dimirovski and Yuan-Wei Jing acknowledge with gratitude their home universities, SS Cyril & Methodius of Skopje and Northeastern of Shenyang, and the respective Ministries of Education & Science of R. Macedonia and P.R. China for supporting in part their decade long academic co-operation. Tao Rent expresses his acknowledgement to the authorities for Education & Science of P.R. of China the received support under NSF Grant 60274009 and Doctoral Program of Higher Education Grant 20020145007 as well as under the funding scheme for Key Laboratory of Process Industry Automation. Lastly but not least, Georgi M. Dimirovski would also like to acknowledge the authorities of Dogus University in Istanbul, Turkey, for the travel funding provided insofar.

References

- [1] ATM Technical Committee: Traffic Management Specification, Version 4.1, af-tm-0121.000. ATM Forum, 43–55 (March 1999)
- [2] Stallings, W.: High-Speed Networks: TCP/IP and ATM Design Principles. Prentice-Hall, Upper Saddle River (1998)
- [3] Bertsekas, D., Galager, R.: Data Networks, 2nd edn. Prentice Hall, Englewood Cliffs (1992)
- [4] Jacobson, V.: Congestion Avoidance and Control. Computer Communications Review 18, 316–329 (1988)
- [5] Jain, R.: Congestion Control and Traffic Management in ATM Networks: Recent Advance and A Survey. Computer Networks & ISDN Systems 28(13), 1723–1738 (1991)
- [6] Ait-Hellal, O., Altman, E., Basar, T.: Rate-based Flow Control with Bandwidth Information. European Trans. on Telecommunications 8, 55–65 (1997)
- [7] Imer, O.C., Basar, T.: Control of Congestion in High-Speed Networks. European J. Control, Special Issue 7, 132–144 (2001)
- [8] Imer, O.C., Compans, S., Basar, T.R.: Srikant: ABR Congestion Control in ATM IEEE Control Systems Magazine 21, 38–56 (2001)
- [9] Xiao, X., Telkamp, T., Fineberg, V., Chen, C., Ni, L.M.: A Practical Approach for Providing QoS in the Internet Backbone. IEEE Communications Magazine 40, 56–62 (2002)
- [10] Gervos, P., Crowcroft, J., Kirsten, P.S., Bhati, S.: Congestion Control Mechanisms and the Best effort Service Model. IEEE Network 15, 16–26 (2001)
- [11] Ramakrishnan, K., Jain, R.: A Binary Feedback Scheme for Congestion Avoidance in Computer Networks with A Connectionless Network Layer. ACM Trans. on Computer Systems 8, 158–181 (1990)
- [12] Bonomi, F., Mitra, D., Seery, J.B.: Adaptive Algorithms for Feedback-Based Flow Control in High-Speed, Wide-Area ATM Networks. IEEE J. on Selected Areas in Communications 13, 1267–1283 (1995)
- [13] Benmohamed, L., Meerkov, S.M.: Feedback Control of Congestion in Packet Switching Networks: The Case of A Single Congested Node. IEEE/ACM Trans. on Networking 1, 693–707 (1993)
- [14] Kolarov, A., Ramamurthy, G.: A Control-Theoretic Approach to the Design of An Explicit Rate Controller for ABR Service. IEEE/ACM Trans. on Networking 7, 741–753 (1999)

- [15] Benmohamed, L., Wang, Y.T.: A Control-Theoretic ABR Explicit Rate Algorithm for ATM Switches with Per-VC Queuing. In: Proceedings of the 1998 IEEE INFOCOM, San Diego, CA, vol. 1, pp. 183–191 (1998)
- [16] Mascolo, S., Cavendish, D., Gerla, M.: ATM Rate Based Congestion Control Using A Smith Predictor: An EPRCA Implementation. In: Proceedings of the 1996 IEEE INFOCOM, San Francisco, CA, pp. 569–576. The IEEE, Piscataway (1996)
- [17] Mascolo, S.: Smith's Principle for Congestion Control in High Speed ATM Networks. In: Proceedings of the 36th IEEE Conference on Decision and Control, San Diego, CA, pp. 4595–4600. The IEEE, Piscataway (1997)
- [18] Mascolo, S.: Congestion Control in High-Speed Communication Networks Using the Smith Principle. *Automatica* 35, 1921–1935 (1999)
- [19] Habib, I., Tarraf, A., Saadawi, T.: A Neural Network Controller for Congestion Control in ATM Multiplexers. *Computer Networks & ISDN Systems* 29, 325–334 (1997)
- [20] Lestas, M., Pitsilides, A., Ioannu, P., Hadjipollas, G.: Adaptive Congestion Protocol: A Congestion Control Protocol with Learning Capability. *Computer Networks: Intl. J. of Computer & Telecommunications Networking* 51, 3773–3798 (2007)
- [21] Kwang, K.S., Tan, S.W., Hsiao, M.C., Wu, C.S.: Cooperative Multiagent Congestion Control for High-speed Networks. *IEEE Trans. on Systems, Man & Cybernetics, Part B: Cybernetics* 35, 255–268 (2005)
- [22] Li, X., Zhou, Y.C., Dimirovski, G.M., Jing, Y.W.: Simulated Annealing Q-learning Algoritam for ABR Traffic Control of ATM Networks. In: Proceedings of the 27th American Control Conference, Seaatle, WA, pp. 4462–4467. The AACC and IEEE, Piscataway (2008)
- [23] Hu, R.Q., Petr, D.W.: A Predictive Self-Tuning Fuzzy-Logic Feedback Rate Controller. *IEEE/ACM Trans. on Networking* 8, 697–709 (2000)
- [24] Ding, Y.S.: A Nonlinear PID Controller Based on Fuzzy-Tuned Immune Feedback Law. In: Proceedings of the 3rd World Congress on Intelligent Control and Automation, Beijing, P.R. China, pp. 1576–1580 (2000)
- [25] Ren, T., Dimirovski, G.M., Jing, Y.W.: ABR Traffic Control over ATM Networks Using Fuzzy Immune PID Controller. In: Proceedings of the 25th American Control Conference, Minneapolis, MN, pp. 4876–4881 (2006)
- [26] Ren, T., Gao, Z., Kong, W., Jing, Y., Yang, M., Dimirovski, G.M.: Performance and Robustness Analysis of a Fuzzy Immune Flow Controller in ATM Networks with Time-varying Multiple Time-delays. *J. Control Theory & Applications* 6, 253–258 (2008)
- [27] Klir, G.J., Yuan, B.: *Fuzzy Sets and Fuzzy Logic: Theory and Applications*. Prentice-Hall, Upper Saddle River (1995)
- [28] Ross, T.J.: *Fuzzy Logic with Engineering Applications*, 2nd edn. John Wiley & Sons, Chichester (2005)
- [29] Siler, W., Buckley, J.J.: *Fuzzy Expert Systems and Fuzzy Reasoning*. John Wiley & Sons Inc., Hoboken (2005)
- [30] Berenji, H.R.: Fuzzy Logic Controllers. In: Yager, R.R., Zadeh, L.A. (eds.) *An Introduction to Fuzzy Logic Applications in Intelligent Systems*, pp. 69–76. Kluwer Academic, Boston (1993)
- [31] Palm, R., Driankov, D., Hellendoorn, H.: *Model Based Fuzzy Control*. Springer, Heidelberg (1997)
- [32] Yen, J., Langari, R.: *Fuzzy Logic: Intelligence, Control, and Information*. Prentice Hall, Upper Saddle River (1999)

Takagi-Sugeno Type Fuzzy Automaton Model

Janos L. Grantner and George A. Fodor

Western Michigan University, Kalamazoo, MI, USA

janos.grantner@wmich.edu

ABB AB, SE-72159 Västerås, Sweden

george.a.fodor@se.abb.com

Abstract. Tracking the status of an event-driven, large control system is a difficult problem. Those systems often encounter unexpected events in an uncertain environment. Using a fuzzy automaton offers an effective approximation method to model continuous and discrete signals in a single theoretical framework. A Max-Min automaton can successfully model a cluster of relevant states when a decision is to be made on the next state of a goal path at the supervisory level. However, to provide analytical proof for stability and other key properties of a fuzzy controller a Takagi-Sugeno (TS) model is preferred. In this paper a TS-type fuzzy automaton is proposed.

Keywords: fuzzy logic, fuzzy automata, Takagi-Sugeno fuzzy model.

1 Introduction

Among the problems that characterize industrial process control innovation, and which are not domain-related, some of the difficult ones are as follows: (a) how can new knowledge be introduced into a system, (b) how can the system activate stored domain knowledge in an autonomous way, (c) how can the knowledge be validated (or otherwise detected as inappropriate) and (d) how can the system recover if the new, activated knowledge (or the currently active knowledge) is not suitable to handle the situation at hand.

The use of agent technology can help to answer question (a). According to its general definition an agent is an architecture-neutral, mobile software entity that can act on behalf of a human and have decision making capabilities similar to a human [4]. The theory of software dynamical architectures describes the dynamics of the environment in which agents can act. The software architecture, using an architecture broker, mediates the information flow among agents in order to achieve overall population-level goals, and also makes various resources (computational power, sensors, and actuators) available to the agent.

The activation of the appropriate knowledge is accomplished via identification operations performed by agents that are capable of finding the right model among a set of available models. Thus the answer to problem (b) is defined as the appropriate interaction among the software architecture mechanisms and the agents. Agents with model-based target seeking algorithms utilizing fuzzy logic that interact in a distributed large system are strong candidates to replace traditional communications channels among units of a distributed system at a higher system level. Thus agents both require more advanced architectures and also the revision of the architecture. Fuzzy automata can implement new knowledge by means of the states of the goal path of an event-driven, sequential control algorithm while providing an effective approximation method to model continuous and discrete signals in a single theoretical framework.

With respect to problem (c): knowledge validation is achieved by quantifying the degree of deviation from the nominal operating conditions due to unexpected events caused by either abrupt, or gradual changes in the system, or in the environment of the system.

With respect to problem (d): there is a need for computationally inexpensive fault detection and identification (FDI) algorithms, and automated recovery from faults. One aspect of FDI and automated recovery from faults is the evaluation of the state transitions between states of a large, complex system. It can be accomplished by focusing only on clusters of relevant states along the goal path to find a suitable next state. A reconfigurable virtual Max-Min fuzzy automaton (also referred to as the Hybrid Fuzzy-Boolean Finite State Machine, HFB-FSM) can be used to model those clusters of states. The other aspect of recovery is devising actuator values in the chosen new state that facilitate the recovery while keeping the system stable. A TS-type fuzzy automaton is proposed to achieve this goal as well.

The rest of the paper is organized as follows: in Section 2 the key properties of the HFB-FSM model are summarized. In Section 3 the definition of the proposed TS-type fuzzy automaton model (TSTFA) that has been developed from the HFB-FSM is given. In Section 4 the concept of the virtual TSTFA automaton is described. In Section 5 a simulation example is discussed. Conclusions are given in Section 6.

2 Extended HFB-FSM Model

The model of the Hybrid Fuzzy-Boolean Finite State machine was presented in [1]. It was extended in [2] to address the modeling requirements of a complex hybrid system at a higher, more flexible level. The notion of this fuzzy automaton is based upon the premises as follows: the fuzzy automaton can stay in some crisp states simultaneously, to a certain degree in each. Those degrees are defined by a state membership function. For each fuzzy state there is just one dominant (crisp) state, though, for which the state membership is a 1 (full membership). Each dominant state is associated with a linguistic model for inference. For each fuzzy

state a composite linguistic model is devised using the composition of the linguistic models of those contributing crisp states that has a greater than 0 state membership degree in that fuzzy state.

The transitions between fuzzy states are based upon the transitions defined between their dominant crisp states. There is an underlying Boolean finite state machine to implement the fuzzy automaton. The states of this Boolean automaton are the dominant crisp states of the fuzzy automaton.

The fuzzy inputs (and even fuzzy outputs, as an option) are mapped to sets of two-valued logic variables using the B algorithm [1]. The analog inputs with threshold also yield two-valued logic variables. In addition, the automaton may have two-valued inputs as well. All of these Boolean variables are used to devise the next states of the two-valued state variables of the underlying Boolean automaton. Two-valued outputs are devised using possibly all types of inputs and the current dominant state. Fuzzy outputs are obtained through the compositional rule of inference. Defuzzified outputs are calculated by using a suitable defuzzification algorithm.

Formally, a HFB-FSM automaton with p states is defined by the set of equations below:

$$S_{Fk} : S_k, g_{Sk} \quad (1)$$

$$R^* = f(G, R_S) \quad (2)$$

$$G = \begin{bmatrix} \beta_1^1 \dots \beta_p^1 \\ \dots \\ \beta_1^k \dots \beta_p^k \\ \dots \\ \beta_1^p \dots \beta_p^p \end{bmatrix} \quad (3)$$

$$Z_F = X_F \circ R^* \quad (4)$$

$$Z_C = DF(Z_F) \quad (5)$$

$$X_T \text{ is TRUE if } X_A \geq X_{AT} \quad (6)$$

$$X_B = B(X_F) \quad (7)$$

$$Z_B = B(Z_F) \quad (8)$$

$$Y_B = f_y(X_B, W_B, X_T, Z_B, y_B) \quad (9)$$

$$U_B = f_u(X_B, W_B, X_T, y_B) \quad (10)$$

In Equation (1) a fuzzy state is defined by a dominant crisp (Boolean) state along with a state membership function: S_{Fk} stands for fuzzy state k, S_k represents crisp state k, and g_{Sk} is the state membership function associated with S_k ($k=1,\dots,p$). G stands for the matrix of state membership functions. X_F , W_B , and X_A stand for fuzzy, two-valued (Boolean) and analog inputs with associated X_{AT} threshold values, respectively. A threshold comparator module compares the value of each analog signal with its associated threshold value to set the corresponding X_T signal as true, or false. Z_F , Z_C , and U_B stand for fuzzy, crisp (defuzzified), and two-valued (Boolean) outputs, respectively. In Equation (2) R^* is the composite linguistic model, and \circ is the operator of composition in Equation (4). Each crisp state of the HFB-FSM is characterized by an aggregated, overall linguistic model, R_S or by a set of linguistic sub-models in the case of multiple-input-single-output (MISO), and multiple-input-multiple-output (MIMO) systems. For each fuzzy state of the HFB-FSM model, a R^* composite linguistic model is created from the finite set of R_{Si} overall linguistic models ($i=1,\dots,p$). Let the HFB-FSM be in fuzzy state S_{Fk} , then

$$R_k^* = \max[\min(\beta_1^k, R_{S1}), \dots, \min(\beta_p^k, R_{Sp})] \quad (11)$$

where $\beta_1^k, \dots, \beta_p^k$ stand for the degrees of state membership function g_{Sk} and R_{S1}, \dots, R_{Sp} are the aggregated linguistic models [1] in crisp states S_1, \dots, S_p , respectively. In fact, Equation (11) is the computational algorithm for Equation (2). By modifying the β degrees of the state membership functions on-line, new R^* composite linguistic models can be created under real-time conditions.

The R^* composite linguistic model is one of the key concepts in defining the HFB-FSM automaton. It determines how fuzzy outputs are inferred from the knowledge base in different fuzzy states. In other words, it reflects the fact of a fuzzy state transition by inferring different fuzzy outputs even for identical fuzzy inputs in two different states.

X_B , Z_B , Y_B , and y_B stand for two-valued Boolean inputs, Boolean outputs (both devised from input and output fuzzy sets using the B algorithm) and next states

and present states of the state variables, respectively. The Z_C crisp values of the fuzzy outputs are obtained by evaluating a defuzzification strategy, DF.

The transitions between active composite linguistic models are determined by the state transitions of the HFB-FSM. The state transitions of the HFB-FSM are specified by means of a sequence of changes in the states of the fuzzy inputs (optionally, fuzzy outputs, too), of the analog inputs with threshold, as well as of the two-valued inputs. The changes in the states of the fuzzy inputs are mapped into a corresponding sequence of changes of Boolean input variable sets using the B algorithm. In this two-valued domain, those changes are joined by the state changes of the two-valued inputs and the true/false logic values of the analog inputs with threshold. This combined Boolean input sequence specification is used to synthesize the crisp finite state machine section of the HFB-FSM. Hence, the HFB-FSM model allows the integration of fuzzy, analog and two-valued logic specifications to describe a system's dynamic behavior. The integrated treatment of fuzzy, analog with threshold, and two-valued signals is of great importance for designing complex hybrid systems.

3 TS-Type Fuzzy Automaton Model (TSTFA)

The TSTFA model has been developed from the HFB-FSM one such that the computational algorithm for the linguistic model of Equation (2) and the inference algorithm of Equation (4) are replaced by new equations to comply with the Takagi-Sugeno (TS) model of fuzzy systems [3]. Equation (5) is dropped because there is no need for it in a TS system. Equation (8) is also dropped because no fuzzy output is inferred from the linguistic model anymore. Equations (1), (3) and (6)-(10) remain in effect, however, Equation (9) is slightly revised due to the drop of Z_B .

In the TS model [3] the format of implications is proposed as follows:

$R : If \ x_1 \ is \ A_1, \dots, x_k \ is \ A_k \ then \ y = g(x_1, \dots, x_k)$ and g is a linear function such that

$$g = p_0 + p_1 x_1 + \dots + p_k x_k \quad (12)$$

where A_1, \dots, A_k are fuzzy sets, x_1, \dots, x_k are fuzzy inputs and output y is obtained as a crisp value. Suppose there are n implications R^i ($i=1, \dots, n$) of the above format. When the fuzzy inputs are given as singletons

$$x_1 = x_1^0, \dots, x_k = x_k^0$$

then the final output y is inferred in the following steps.

1) For each implication R^i ($i = 1, \dots, n$) y^i is calculated by the function g^i in the consequence

$$y^i = p_0^i + p_1^i x_1^0, \dots, + p_k^i x_k^0. \quad (13)$$

2) The truth value of the proposition $y=y^i$ is calculated by the equation

$$|y=y^i| = (A_1^i(x_1^0) \wedge \dots \wedge A_k^i(x_k^0)) \wedge |R^i| \quad (14)$$

where $|*|$ means the truth value of proposition $*$, \wedge stands for min operation and $A(x^0)$ stands for the grade of membership of x^0 in fuzzy set A . For simplicity, $|R^i|=1$ is assumed.

3) The final output y inferred from n implications is given as the average of all y^i with the weights $|y=y^i|$:

$$y = \frac{\sum |y=y^i| \times y^i}{\sum |y=y^i|} \quad (15)$$

In the TSTFA model the Takagi-Sugeno version of the IF THEN rules is adopted as it is given in Equation (12). The only change in the notation is that Z is used for output rather than y .

$R : \text{If } x_1 \text{ is } A_1, \dots, x_k \text{ is } A_k \text{ then } Z = g(x_1, \dots, x_k)$ and g is a linear function such that

$$Z = p_0 + p_1 x_1 + \dots + p_k x_k \quad (16)$$

In each crisp state S_k the final output Z_{Sk} is calculated according to Equations (14) and (15) above:

$$|Z_{Sk} = Z_{Sk}^i| = (A_1^i(x_1^0) \wedge \dots \wedge A_k^i(x_k^0)) \wedge |R^i| \quad (17)$$

$$Z_{Sk} = \frac{\sum |Z_{Sk} = Z_{Sk}^i| \times Z_{Sk}^i}{\sum |Z_{Sk} = Z_{Sk}^i|} \quad (18)$$

The notion of composite output Z^* is introduced to reflect the contribution of the output values devised from the TS linguistic models that are attached to crisp states to the final output in a fuzzy state. Let the TSTFA be in fuzzy state S_{Fk} , then

$$Z_k^* = \frac{\beta_1^k Z_{S1} + \dots + \beta_p^k Z_{Sp}}{\sum_i \beta_i^k} \quad (i=1, \dots, p) \quad (19)$$

It is clear from Equation (19) that only those crisp states that have greater than 0 degree of state membership in fuzzy state S_{Fk} contribute to the final output.

Formally, a TSTFA automaton with p states is defined by the following set of equations:

$$S_{Fk} : S_k, g_{Sk} \quad (20)$$

$$R_S = TS(X_F, Z_S) \quad (21)$$

$$G = \begin{bmatrix} \beta_1^1 \dots \beta_p^1 \\ \dots \\ \beta_1^k \dots \beta_p^k \\ \dots \\ \beta_1^p \dots \beta_p^p \end{bmatrix} \quad (22)$$

$$Z^* = TS(X_F^0, R_S, G) \quad (23) \quad X_T \text{ is TRUE if } X_A \geq X_{AT} \quad (24)$$

$$X_B = B(X_F^0) \quad (25)$$

$$Y_B = f_y(X_B, W_B, X_T, y_B) \quad (26)$$

$$U_B = f_u(X_B, W_B, X_T, y_B) \quad (27)$$

TS stands for a reference to the Takagi-Sugeno model. The detailed representation of Equation (21) is given by Equation (16). The computational algorithm for Equation (23) is given by Equations (17)–(19). X_F^0 stands for singleton fuzzy inputs. The block diagram of the TSTFA automaton is shown in Fig. 1.

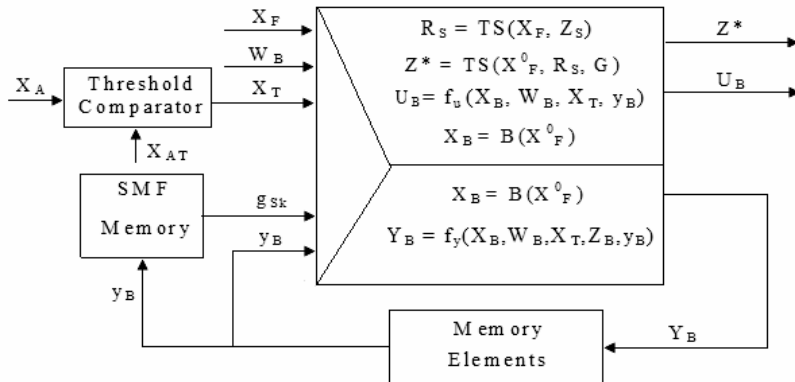


Fig. 1. TSTFA Automaton Block Diagram

One can notice that the B algorithm that maps changes in a fuzzy input to changes of the states of a set of Boolean input variables will be executed much faster for the TSTFA than for the HFB-FSM. It is due to the fact that there is no need to run a defuzzification step if the fuzzy inputs are singletons.

4 Virtual TSTFA Automata

The concept of the virtual fuzzy automaton was introduced in [2]. Hardware accelerator for reconfigurable fuzzy automata was proposed in [5]. Since the state set of a complex system may consist of tens of thousands of states, it would be impractical to design a fuzzy automaton of that size. However, as it is shown in [6], when the current goal state can be computed and all possible disturbances are known, only a small partition of the total state space is relevant to make a decision on the next state along a goal path. A supervisory algorithm monitoring the flow of states first determines a segment of the transition graph (a cluster of relevant states) prior to the decision on the next state transition. Then it creates an instance of the virtual TSTFA to implement it. In other words, it defines a TSTFA model of the relevant cluster of states of the goal path.

The following information will be downloaded to the reconfigurable TSTFA: the active sets of fuzzy, analog with threshold, and Boolean inputs and fuzzy and two-valued outputs, respectively, state membership function degrees, the actual mapping scheme between fuzzy and Boolean subintervals of the B algorithm, threshold values, the initial state, the state transition graph along with the conditions, the mapping function for two-valued outputs, the Takagi-Sugeno linguistic models and then the current status of all active input signals of any kind.

The TSTFA will then make a decision on the transition to the next state, infer outputs (if needed), and pass all these information back to the supervisory algorithm. The configuration process will repeat each time when a new instance of the TSTFA should be created to track the current segment of the state graph.

5 Simulation Example

A control application of the TSTFA model for cold-rolling mills is in the works. A simulator using Matlab for the TSTFA model has been developed to help this research. What follows is a brief summary of some of the current results.

In cold-rolling mills, a metal strip that is subject to different degrees of reduction across its width will be elongated in varying length over different sections of the strip. The reduction is carried out in the rolling gap. A number of actuators can slightly modify the gap such that the stress profile can be controlled such that some predefined target flatness will be achieved. The difference between the measured strip flatness and the target flatness curve is the flatness error. The flatness error can be gauged by sensors, which provide the input signal to a multiple-input-multiple-output (MIMO) control system. The output signals of the MIMO controller are sent to different actuators that are to modify the rolling gap. This control loop has a simple linear mathematical model. In Fig. 2 a cold-rolling mill control configuration is depicted. More details on the control system can be found in [7].

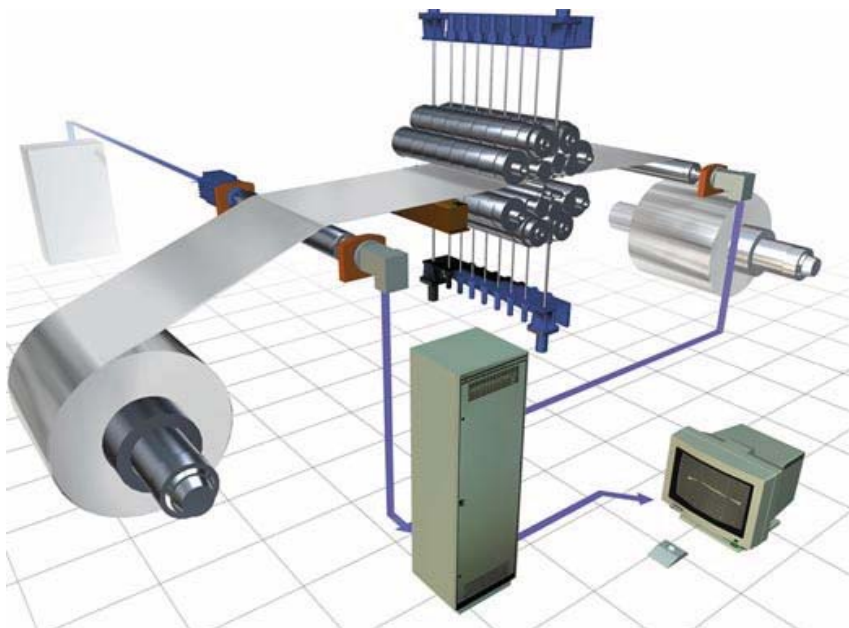


Fig. 2. Cold-rolling mill control system

The flatness sensors are placed on a deflecting roll with measuring zones across the width of the strip. In our example there are 32 measuring zones. We consider a typical actuator set that has three mechanical actuators. These actuators have different capabilities to correct flatness errors. The control strategy may assign weights for the degree by which an actuator performs relative to others. For three

actuators, a control algorithm will operate with four states as follows: states S1, S2 and S3 in which actuators 1, 2, and 3, respectively, act stronger than the other two actuators and state S4 in which the control error is small and all three actuators act with the same weight. The technologically feasible state transitions for the MIMO controller are shown in Fig. 3.

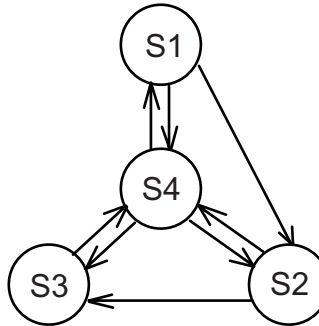


Fig. 3. States of the MIMO controller

As an illustration, the Takagi-Sugeno fuzzy model of the control system in a particular state is given by the rules as follows:

RULE (1):

IF X5 is low and X6 is low and X7 is low THEN
 $Z1=(1/3)*(x5+x6+x7)$ and $Z2=(1/3)*(x5+x6+x7)$ and $Z3=(1/3)*(x5+x6+x7)$ and
 $Z4=1-0.66*(x5+x6+x7)$ and $Z5=1-0.66*(x5+x6+x7)$ and
 $Z6=1-0.66*(x5+x6+x7)$

RULE (2):

IF X5 is medium and X6 is low and X7 is low THEN
 $Z1=x5$ and $Z2=(1/2)*(x6+x7)$ and $Z3=(1/2)*(x6+x7)$
and $Z4=x5$ and $Z5 =1-(1/2)*(x6+x7)$ and $Z6=1-(1/2)*(x6+x7)$

RULE (3):

IF X5 is low and X6 is medium and X7 is low THEN
 $Z1=x6$ and $Z2=x6$ and $Z3=(1/2)*(x5+x7)$ and
 $Z4 =1-(1/2)*(x5+x7)$ and $Z5=x6$ and $Z6=1-(1/2)*(x5+x7)$

The TS model employs linear functions with a support point being the strength that could take care of the flatness error if an actuator acted alone. The TS inference of Eq. (18) creates a combination of actuator functions with good control properties. The plot of the resulting control residual $r=e-Ax$ is given in Fig. 4 and the flatness profile in Fig. 5, respectively. The simulated state transitions are depicted in Fig. 6. Fig. 6 illustrates that the TSTFA-based control system stays in those states in which one actuator having more weight (i.e., S1, S2 and S3) for a shorter period of time. It stays in state S4 in which all actuators act together on a small error for a longer time period.

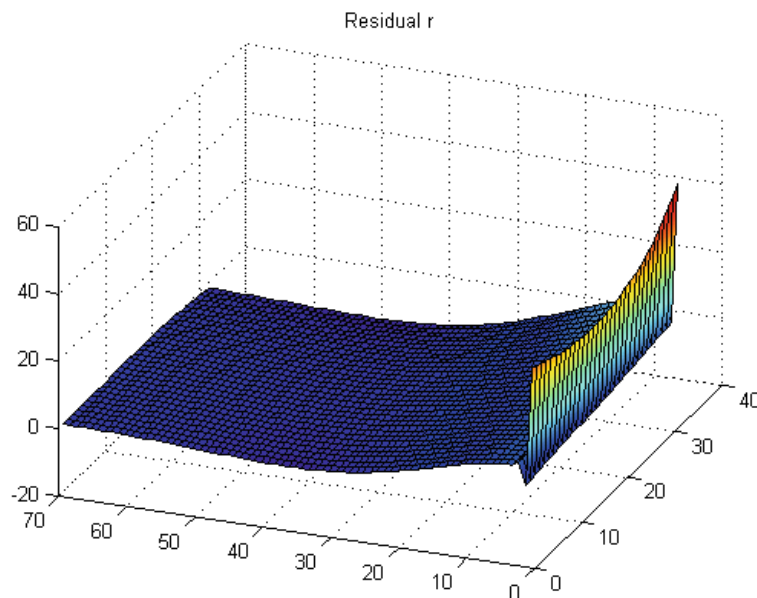


Fig. 4. Flatness residual

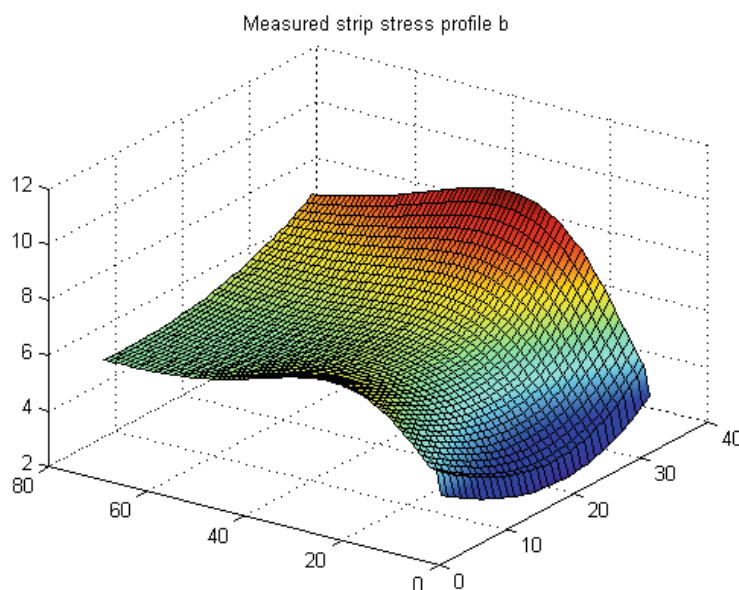


Fig. 5. Flatness profile

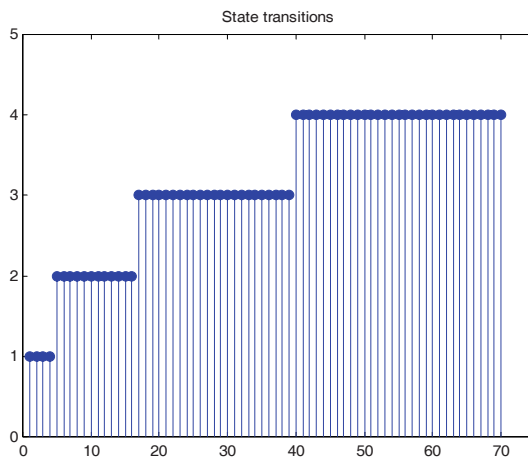


Fig. 6. TSTFA state transitions

Conclusions

Software agents, when enhanced with fuzzy automata, can perform a learned, model-based reconfiguration that optimizes what type of system behavior has priority in the current situation. A Takagi-Sugeno type fuzzy automaton model is introduced that can support decision making with respect to automatic recovery from faults. In addition to assisting in the selection of a suitable state for recovery the TSTFA automaton can also be used to calculate actuator signal values through TS inference.

References

- [1] Grantner, J.L., Fodor, G., Driankov, D.: Hybrid Fuzzy-Boolean Automata for Ontological Controllers. In: Proceedings of the 1998 IEEE World Congress on Computational Intelligence, FUZZ-IEEE 1998, Anchorage, Alaska, May 4-9, 1998, vol. I, pp. 400–404 (1998)
- [2] Grantner, J.L., Fodor, G.A., Driankov, D.: The Virtual Fuzzy State Machine Approach - A Domain-Independent Fault Detection and Recovery Method for Object-based Control Systems. In: Proceedings of 18th International Conference of the North American Fuzzy Information Processing Society - NAFIPS 1999, New York, NY, June 10-12, 1999, pp. 158–162 (1999)
- [3] Takagi, T., Sugeno, M.: Fuzzy Identification of Systems and Its Application in Modeling and Control. *IEEE Trans. System, Man and Cybernetics* 15, 116–132 (1985)
- [4] Knapik, M., Johnson, J.: Developing Intelligent Agents for Distributed Systems, Exploring Architecture, Technologies and Applications. McGraw-Hill, New York (1998)
- [5] Grantner, J.L., Tamayo, P.A., Gottipati, R., Fodor, G.A.: Reconfigurable Fuzzy Automaton for Software Agents. In: Proceedings of the BISCSE 2005 Conference, University of California, Berkeley, CA, on CD, November 2-5 (2005)
- [6] Fodor, G.A.: Ontologically Controlled Autonomous Systems: Principles, Operations and Architecture. Kluwer Academic Publishers, Boston (1998)
- [7] <http://www.abb.com/pressductor>

Control and Dynamics of Fractional Order Systems

J.A. Tenreiro Machado, Isabel S. Jesus, Ramiro S. Barbosa, and Manuel F. Silva

Institute of Engineering of Porto, Porto, Portugal
`{jtm, isj, rsb, mss}@isep.ipp.pt`

Abstract. Fractional Calculus (FC) goes back to the beginning of the theory of differential calculus. Nevertheless, the application of FC just emerged in the last two decades due to the progress in the area of nonlinear dynamics. This article discusses several applications of fractional calculus in science and engineering, namely: the control of heat systems, the tuning of PID controllers based on fractional calculus concepts and the dynamics in hexapod locomotion.

1 Introduction

The generalization of the concept of derivative D^α [$f(x)$] to non-integer values of α goes back to the beginning of the theory of differential calculus [1, 2].

The FC deals with derivatives and integrals to an arbitrary order (real or, even, complex order). The mathematical definition of a derivative/integral of fractional order has been the subject of several different approaches [1, 2]. One commonly used definition is given by the Riemann-Liouville expression ($\alpha > 0$):

$$_a D_t^\alpha x(t) = \frac{1}{\Gamma(n-\alpha)} \frac{d^n}{dt^n} \int_a^t \frac{x(\tau)}{(t-\tau)^{\alpha-n+1}} d\tau, \quad n-1 < \alpha < n \quad (1)$$

where $x(t)$ is the applied function and $\Gamma(x)$ is the Gamma function of x . Another widely used definition is given by the Grünwald-Letnikov approach ($\alpha \in \Re$):

$$_a D_t^\alpha f(t) = \lim_{h \rightarrow 0} \frac{1}{h^\alpha} \sum_{k=0}^{[\frac{t-a}{h}]} (-1)^k \binom{\alpha}{k} f(t-kh) \quad (2)$$

where h is the time increment and $[x]$ means the integer part of x .

The 'memory' effect of these operators is demonstrated by (1) and (2), where the convolution integral in (1) and the infinite series in (2), reveal the unlimited memory of these operators, ideal for modelling hereditary and memory properties in physical systems and materials.

An alternative approach to (1) and (2), is given by the Laplace definition:

$$D^\alpha x(t) = L^{-1} \left\{ s^\alpha X(s) - \sum_{k=0}^{n-1} s^k D^{\alpha-k-1} x(t) \Big|_{t=0} \right\} \quad (3)$$

where $X(s) = L \{ x(t) \}$, $n-1 < \alpha \leq n$, $\alpha > 0$.

Based on the proposed definitions it is possible to calculate the fractional-order integrals/derivatives of several functions (Table 1).

Table 1. Fractional-Order Integrals of Several Functions

$\varphi(x)$, $x \in \Re$	$(I_+^\alpha \varphi)(x)$, $x \in \Re$, $\alpha \in C$
$(x-a)^{\beta-1}$	$\frac{\Gamma(\beta)}{\Gamma(\alpha+\beta)}(x-a)^{\alpha+\beta-1}$, $\text{Re}(\beta) > 0$
$e^{\lambda x}$	$\lambda^{-\alpha} e^{\lambda x}$, $\text{Re}(\lambda) > 0$
$\begin{cases} \sin(\lambda x) \\ \cos(\lambda x) \end{cases}$	$\lambda^{-\alpha} \begin{cases} \sin(\lambda x - \alpha \pi/2) \\ \cos(\lambda x - \alpha \pi/2) \end{cases}$, $\lambda > 0$, $\text{Re}(\alpha) > 1$
$e^{\lambda x} \begin{cases} \sin(\gamma x) \\ \cos(\gamma x) \end{cases}$	$\frac{e^{\lambda x}}{(\lambda^2 + \gamma^2)^{\alpha/2}} \begin{cases} \sin(\gamma x - \alpha \phi) \\ \cos(\gamma x - \alpha \phi) \end{cases}$, $\phi = \arctan(\gamma/\lambda)$, $\gamma > 0$, $\text{Re}(\lambda) > 1$

In recent years fractional calculus (FC) has been a fruitful field of research in science and engineering [1, 2]. In fact, many scientific areas are currently paying attention to the FC concepts and we can refer its adoption in viscoelasticity and damping, diffusion and wave propagation, electromagnetism, chaos and fractals, heat transfer, biology, electronics, signal processing, robotics, system identification, traffic systems, genetic algorithms, percolation, modelling and identification, telecommunications, chemistry, irreversibility, physics, control systems, economy and finance.

Having these ideas in mind, this article is organized as follows. Section 2 introduces the fundamental aspects of fractional order control. Section 3 applies a fractional PID controller to a heat diffusion system, while section 4 proposes a methodology for tuning PID controllers based on fractional order concepts. Section 5 investigates the dynamics in hexapod locomotion. Finally, section 6 draws the main conclusions.

2 Fractional-Order Control

In this section, we present a brief review of the basic concepts of fractional-order control systems.

2.1 Basic Concepts

An important aspect of fractional-order algorithms can be illustrated through the elemental control system of Fig. 1, with open-loop transfer function:

$$L(s) = \left(\frac{\omega_c}{s} \right)^\gamma, \quad 1 < \gamma < 2 \quad (4)$$

where ω_c is the gain crossover frequency, that is $|L(j\omega_c)| = 1$. The parameter γ is the slope at the gain crossover frequency and may assume integer as well noninteger values.

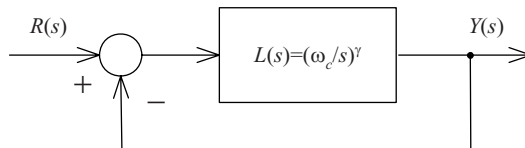


Fig. 1. Elemental fractional-order control system

The Bode diagrams of amplitude and phase of $L(s)$ are illustrated in Fig. 2. The amplitude curve is a straight line of constant slope -20γ dB/dec, and the phase curve is a horizontal line at $-\gamma\pi/2$ rad. This choice of $L(s)$ gives a closed-loop system with the desirable property of being insensitive to gain changes. If the gain changes the crossover frequency ω_c will change but the phase margin of the system remains $PM = \pi(1 - \gamma/2)$ rad, independently of the value of the gain [3].

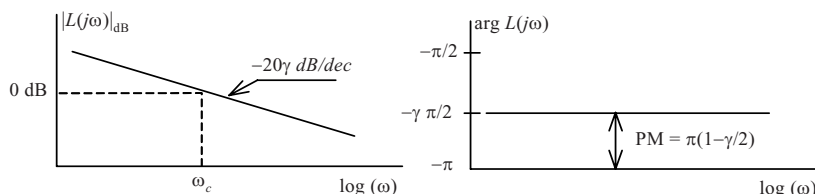


Fig. 2. Bode diagrams of amplitude and phase of $L(jw)$ for $1 < \gamma < 2$

The closed-loop transfer function, $T(s) = Y(s)/R(s)$, is given by:

$$T(s) = \frac{L(s)}{1 + L(s)} = \frac{1}{(0.7ex0.7ex)^{\gamma} + 1}, \quad \gamma \in \Re^+ \quad (5)$$

The unit step response of $T(s)$ is:

$$y(t) = L^{-1} \left\{ \frac{\omega_c^{\gamma}}{s(s^{\gamma} + \omega_c^{\gamma})} \right\} = 1 - \sum_{n=0}^{\infty} \frac{[-(\omega_c t)^{\gamma}]^n}{\Gamma(1+\gamma n)} = 1 - E_{\gamma} [-(\omega_c t)^{\gamma}] \quad (6)$$

where $E_{\gamma}(x)$ is the one-parameter Mittag-Leffler function [2]. This function is a generalization of the common exponential function since for $\gamma = 1$ we have $E_1(x) = e^x$.

2.2 Controller Implementation

The generalized PID controller $G_c(s)$ has a transfer function of the form:

$$G_c(s) = \frac{M(s)}{E(s)} = K_p \left[1 + \frac{1}{T_i s^{\alpha}} + T_d s^{\beta} \right] \quad (7)$$

where α and β are the orders of the fractional integrator and differentiator, respectively. The constants K_p , T_i and T_d are correspondingly the proportional gain, the integral time constant and the derivative time constant.

Clearly, taking $(\alpha, \beta) = \{(1, 1), (1, 0), (0, 1), (0, 0)\}$ we get the classical {PID, PI, PD, P} controllers, respectively. The $PI^{\alpha}D^{\beta}$ controller is more flexible and gives the possibility of adjusting more carefully the closed-loop system characteristics.

As can be seen in expression (7), fractional controllers are defined by irrational continuous transfer functions, in the Laplace domain, or infinite dimensional discrete transfer functions, in the Z domain. Therefore, when analyzing fractional systems, we usually adopt continuous or discrete integer-order approximations of fractional-order operators [4, 5].

The usual approach for obtaining discrete equivalents of continuous operators of type s^{α} adopts the Euler, Tustin and Al-Aloui generating functions. It is well known that rational-type approximations frequently converge faster than polynomial-type approximations and have a wider domain of convergence in the complex

domain. Thus, by using the Euler operator $w(z^{-1}) = (1 - z^{-1})/T$, and performing a power series expansion of $[w(z^{-1})]^\alpha = [(1 - z^{-1})/T]^\alpha$ gives the discretization formula corresponding to the Grünwald-Letnikov definition (2):

$$D^\alpha (z^{-1}) = \left(\frac{1 - z^{-1}}{T} \right)^\alpha = \sum_{k=0}^{\infty} h^\alpha(k) z^{-k} = \sum_{k=0}^{\infty} \left(\frac{1}{T} \right)^\alpha \binom{k - \alpha - 1}{k} z^{-k} \quad (8)$$

A rational-type approximation can be obtained by applying the Padé approximation method to the impulse response sequence $h^\alpha(k)$, yielding the discrete transfer function:

$$H(z^{-1}) = \frac{b_0 + b_1 z^{-1} + \dots + b_m z^{-m}}{1 + a_1 z^{-1} + \dots + a_n z^{-n}} = \sum_{k=0}^{\infty} h(k) z^{-k} \quad (9)$$

where $m \leq n$ and the coefficients a_k and b_k are determined by fitting the first $m+n+1$ values of $h^\alpha(k)$ into the impulse response $h(k)$ of the desired approximation $H(z^{-1})$. Thus, we obtain an approximation that has a perfect match to the desired impulse response $h^\alpha(k)$ for the first $m+n+1$ values of k . Note that the above Padé approximation is obtained by considering the Euler operator but the determination process will be exactly the same for other types of discretization schemes.

3 Fractional Order Control of a Heat Diffusion System

In this section, we apply the FC concepts to the control of a heat diffusion system.

3.1 Heat Diffusion

The heat diffusion is governed by a linear unidimensional partial differential equation (PDE) of the form:

$$\frac{\partial u}{\partial t} = k \frac{\partial^2 u}{\partial x^2} \quad (10)$$

where k is the diffusivity, t is the time, u is the temperature and x is the space coordinate. The system (10) involves the solution of a PDE of parabolic type for which the standard theory guarantees the existence of a unique solution [6, 7, 8].

For the case of a planar perfectly isolated surface we usually apply a constant temperature U_0 at $x = 0$ and analyzes the heat diffusion along the horizontal coordinate x . Under these conditions, the heat diffusion phenomenon is described by a non-integer order model:

$$U(x, s) = \frac{U_0}{s} G(s), \quad G(s) = e^{-x\sqrt{\frac{s}{k}}} \quad (11)$$

where x is the space coordinate, U_0 is the boundary condition and $G(s)$ is the system transfer function.

In our study, the simulation of the heat diffusion is performed by adopting the Crank-Nicholson implicit numerical integration method [6, 7, 8, 9].

3.2 $PI^\alpha D^\beta$ Tuning Using Optimization Indices

In a previous work was demonstrated that the PID^β controller applied to an heat system reveals better results than the classical PID controller tuned through the Ziegler-Nichols open loop (ZNOL) heuristic [3, 8]. In fact, the ZNOL does not produce satisfactory results giving a significant overshoot, a large settling time and a time delay. The fractional dynamics of the system points out other strategies, namely the adoption of fractional control algorithms.

In this sub-section we analyze the closed-loop system of Fig. 3 under the action of the fractional $PI^\alpha D^\beta$ controller given by the transfer function (7) with $0 \leq \alpha \leq 1$ and $0 \leq \beta \leq 1$. The fractional integral ($1/T_i s^\alpha$) and derivative ($T_d s^\beta$) terms in expression (7) are implemented through a 4th order Padé discrete rational transfer function of type (9) and it is used a sampling period of $T = 0.1$ s.

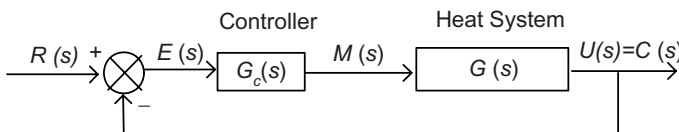


Fig. 3. Closed-loop system with PID controller $G_c(s)$

The $PI^\alpha D^\beta$ controller is tuned by minimizing the integral square error (ISE) performance index, defined as [8, 9]:

$$\text{ISE} = \int_0^{\infty} [r(t) - c(t)]^2 dt \quad (12)$$

Another important performance index consists in the energy E_m at the $\text{PI}^\alpha \text{D}^\beta$ controller output $m(t)$ given by the expression:

$$E_m = \int_0^{T_e} m^2(t) dt \quad (13)$$

where T_e is the time window needed to stabilize the systems output $c(t)$.

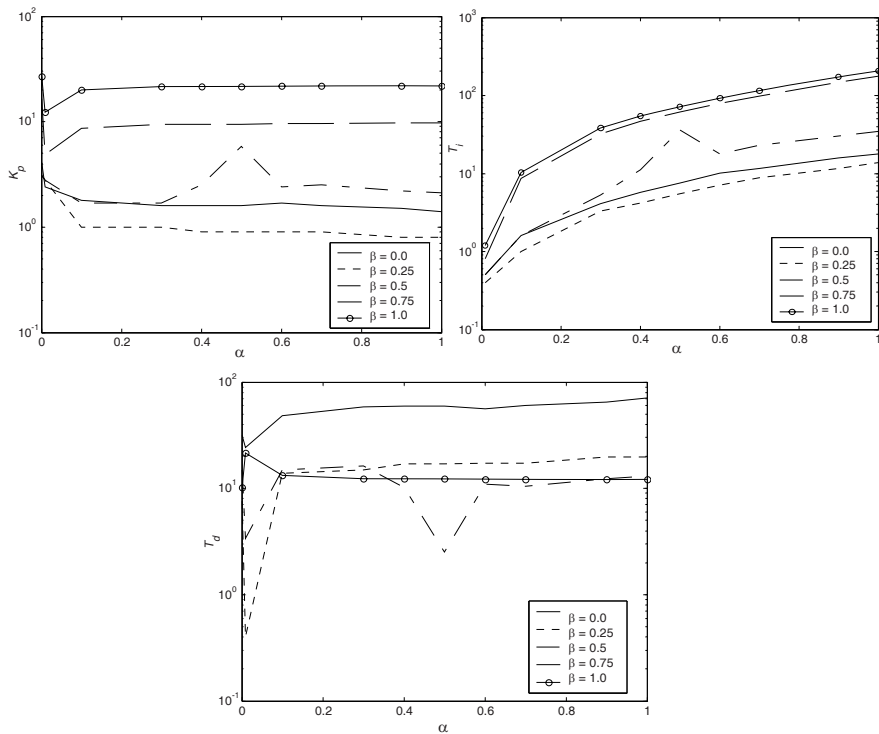


Fig. 4. The $\text{PI}^\alpha \text{D}^\beta$ (K_p , T_i , T_d) versus $\{\alpha, \beta\} = \{0.0, 0.25, 0.50, 0.75, 1.0\}$, when optimizing the ISE criteria, $x=3.0$ m, $k=0.042 \text{ m}^2 \text{s}^{-1}$

A step reference input $R(s) = 1/s$ is applied at $x = 0.0$ m and the output $u(t) = c(t)$ is analyzed for $x = 3.0$ m. The heat system is simulated for a period of

3000 seconds. Figure 4 illustrates the variation of the controller parameters (K_p , T_i , T_d) as function of the integrative order's α for $\beta = \{0.0, 0.25, 0.50, 0.75, 1.0\}$ when optimizing the tuning in the perspective of the ISE criteria.

The curves reveal that for integer order $\beta = \{0.0, 1.0\}$ the parameters (K_p , T_i , T_d) are larger than the fractional ones.

Figure 5 depicts the variation of the transient response parameters, namely the settling time t_s , the rise time t_r , the peak time t_p and the percent overshoot $ov(\%)$, for the closed-loop response with the $PI^\alpha D^\beta$ tuned thought the minimization of the ISE index.

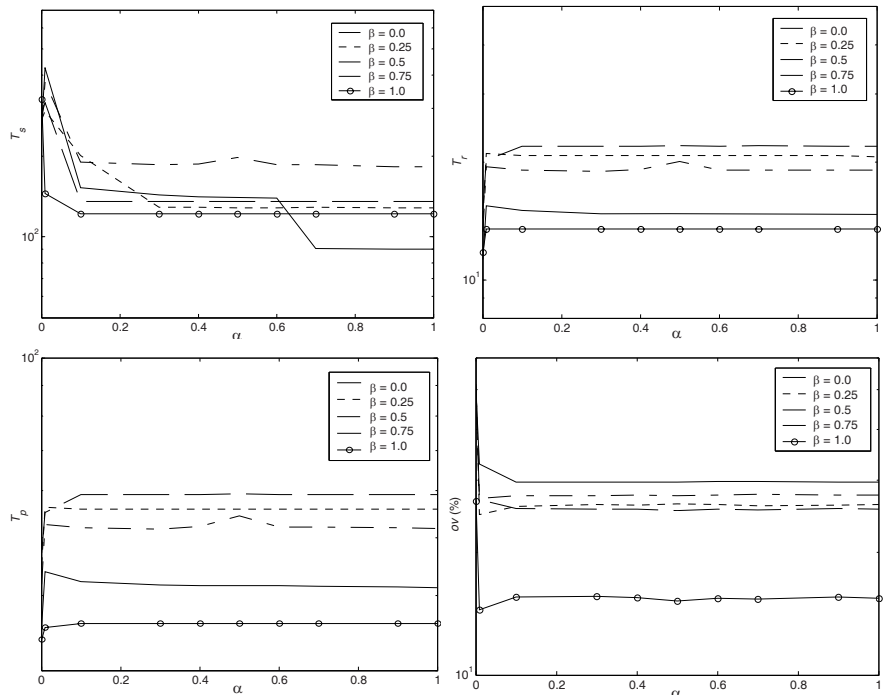


Fig. 5. Parameters t_s , t_r , t_p , $ov(\%)$ for the step responses of the closed-loop system with a $PI^\alpha D^\beta$, when optimizing the ISE, $x=3.0$ m, $k=0.042$ m s^{-1}

Figure 6 depicts the energy E_m of the control action *versus* the index ISE. For a given pair of values of the orders (α, β) this locus gives the best controller tuning in the perspective of the index ISE. It was found numerically that the curve follows approximately the logistic model $E_m = a / (1 + be^{-cISE})$, $a = 4552.37$,

$b = 378.44$, $c = 0.32$. The 'best' solution is the one that leads to the smallest values of ISE and E_m . However, as often occurs when considering several optimization objectives, when one index decreases the other increases, and vice-versa. Therefore, the locus makes possible not only to get the best ISE between all tested pairs, but also, as a secondary goal, to get a good valued for the energy index. The smallest ISE value occurs for $(\alpha, \beta) = (1.0, 1.0)$ which is 72.75% of the worst value found at $(\alpha, \beta) = (1.0, 0.0)$. On the other hand, the smallest value of the control action energy E_m is found for $(\alpha, \beta) = (1.0, 0.0)$ which corresponds to 0.68% of the highest value that occurs at $(\alpha, \beta) = (1.0, 1.0)$. In this line of thought, the locus makes possible to establish a compromise between both indices. For example, for $(\alpha, \beta) = (0.3, 0.5)$ we can have a reduction of the ISE to 88.83%, which is near the optimum, while the energy E_m has a dramatic reduction to 0.95%.

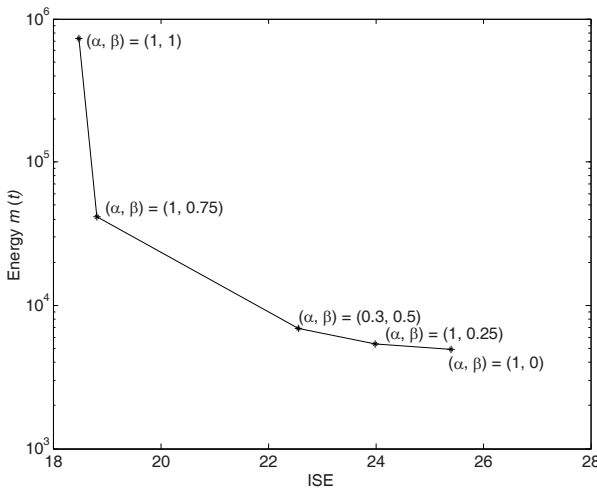


Fig. 6. ISE index versus the control action energy E_m for the best β

4 PID Tuning Based on Fractional Concepts

In this section we address the closed-loop system with the fractional-order integrator $L(s) = (\omega_c/s)^\gamma$ in the forward path (Fig. 1) as the reference system for PID tuning [3]. With the order γ and the gain crossover frequency ω_c we can establish the overshoot and the speed of the output response, respectively.

The design of the PID controller will consist on the determination of the optimum PID set gains (K , T_i , T_d) that minimizes the integral of the square error (ISE), which is defined as:

$$J(K, T_i, T_d) = \int_0^{\infty} [y(t) - y_r(t)]^2 dt \quad (14)$$

where $y(t)$ is the step response of the closed-loop system with the PID controller and $y_r(t)$ is the desired step response of the fractional-order transfer function given by expression (5). For the case under study, the order γ may assume real noninteger values such that $1 < \gamma < 2$.

To illustrate the effectiveness of the proposed methodology we tune the PID controller for different specifications of (γ, ω_c) . We plot the curves for gain variations around the nominal gain ($K_p = 1$) corresponding to $K_p = \{0.6, 0.8, 1.0, 1.2, 1.4\}$, that is, for a variation up to $\pm 40\%$ of its nominal value. In Fig. 7 it is shown the step responses and the Bode diagrams of phase of the plant transfer function $G_p(s) = 1/(s+1)^4$, for $\gamma = 4/3$ ($PM = 60^\circ$), $\omega_c = 0.5$ rad/s. We observe that the step responses have an almost constant overshoot independently of the variation of the plant gain around the gain crossover frequency ω_c . Therefore, with the proposed algorithm we are capable of producing closed-loop systems robust to gain variations and step responses exhibiting an iso-damping property.

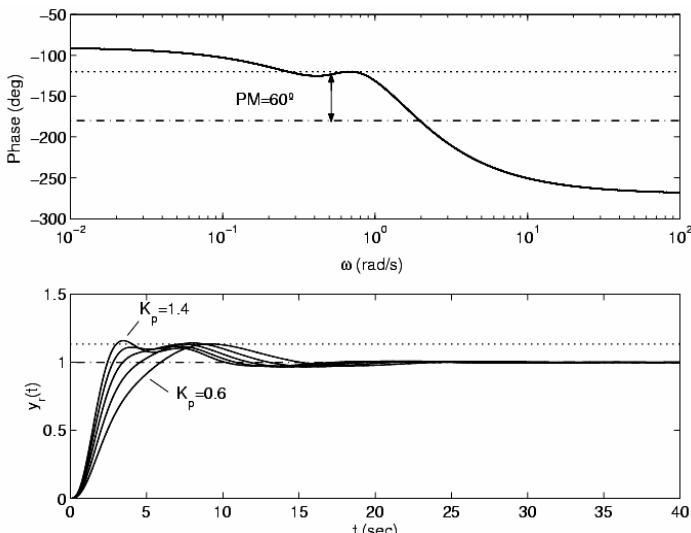


Fig. 7. Bode phase diagram and step responses for the closed-loop system with a PID controller (tuned by the proposed methodology) for $G_p(s)=1/(s+1)^4$

5 Complex-Order Dynamics in Hexapod Locomotion

The present section evaluates foot-ground interaction during legged robot locomotion, for several walking conditions, and analyzes its dynamics in the viewpoint of fractional calculus.

The main interest of this study stems from previous works showing that fractional dynamics arise in systems with 'mixed' characteristics, such as the cases of a liquid interaction with a porous wall [10], in biological systems where there is the growth of tumors in healthy tissues [11] and in backlash systems with continuous-discrete interactions [12].

The system under analysis [13] reveals a behavior of this kind, namely with multiple periodic collisions among the robot feet and the ground.

5.1 Hexapod Robot Model and Control Architecture

Figure 8 presents the kinematic and dynamic model for the hexapod body and foot-ground interaction. We consider a hexapod walking system with $n = 6$ legs, equally distributed along both sides of the robot body, having each one two rotational joints (*i.e.*, $j = \{1, 2\} \equiv \{\text{hip, knee}\}$) [13].

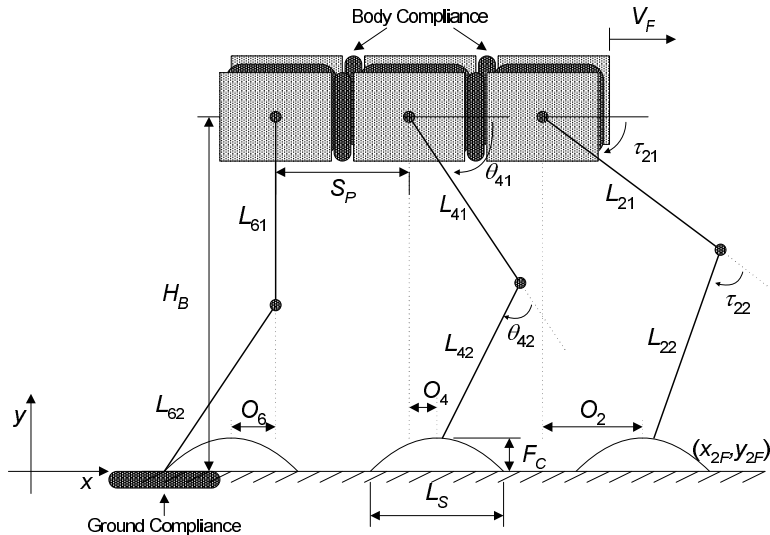


Fig. 8. Kinematic and dynamic quadruped robot model

It is considered the existence of robot body compliance because walking animals have a spine that allows supporting the locomotion with improved stability. The robot body is divided in n identical segments (each with mass $M_b n^{-1}$) and a

linear spring-damper system (with parameters defined so that the body behaviour is similar to the one expected to occur on an animal) is adopted to implement the intra-body compliance [13]. The contact of the i^{th} robot feet with the ground is modelled through a non-linear system [13], being the values for the parameters based on the studies of soil mechanics [13].

The general control architecture of the multi-legged locomotion system is presented in Fig. 9 [14]. We adopt the $G_{c1}(s)$ parameters that establish a compromise in what concerns the simultaneous minimization of E_{av} and ε_{xyH} [14], and a proportional controller G_{c2} with gain $Kp_j = 0.9$ ($j = 1, 2$).

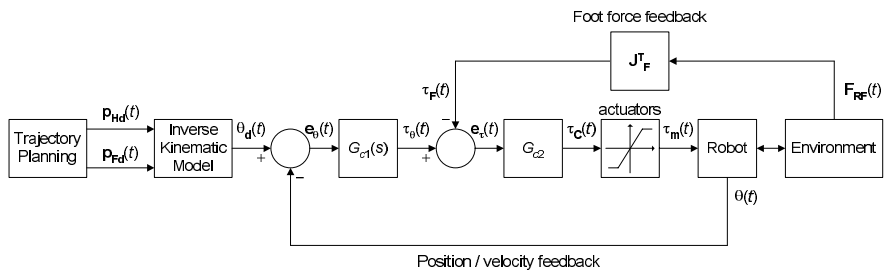


Fig. 9. Quadruped robot control architecture

5.2 Locomotion System Transfer Function

In order to obtain the transfer functions (TF) of the system (robot and environment), the frequency response of the locomotion system is computed numerically. For that purpose, small amplitude sinusoidal exciting signals $\delta \mathbf{p}_d(t)$ are superimposed, separately, on the frequency range under analysis, over the x and y feet desired Cartesian trajectories, according to the block diagram presented in Fig. 10. The resulting feet reference trajectories are given by:

$$\mathbf{p}_d(t) + \delta \mathbf{p}_d(t) = \begin{bmatrix} x_{id}(t) + \delta x_{id}(t) \\ y_{id}(t) + \delta y_{id}(t) \end{bmatrix} \quad (15)$$

$$\mathbf{p}_d(t) + \delta \mathbf{p}_d(t) = \Psi [\Theta_d(t) + \delta \Theta_d(t)] \Rightarrow \Theta_d(t) + \delta \Theta_d(t) = \Psi^{-1} [\mathbf{p}_d(t) + \delta \mathbf{p}_d(t)] \quad (16)$$

where $\mathbf{p}_d(t) + \delta \mathbf{p}_d(t)$ are the i^{th} feet desired Cartesian trajectories (relatively to their hip) perturbed with a sinusoidal signal of small amplitude and $\Theta_d(t) + \delta\Theta_d(t)$, are the corresponding perturbed joint trajectories. During the robot locomotion simulation, the perturbations propagate to the torques demanded to the robot leg joint actuators by the controller (resulting $\Gamma_c(t) + \delta\Gamma_c(t)$) and to the robot real feet trajectories (that become $\mathbf{p}_F(t) + \delta\mathbf{p}(t)$).

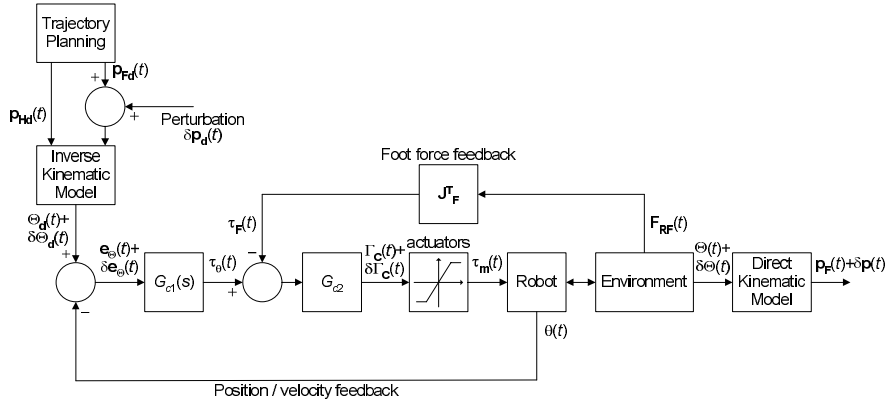


Fig. 10. Block diagram adopted for the calculation of the TF $G_{xj}(s)$ and $G_{yj}(s)$, $j=1,2$

The system TFs are given by ($j = 1, 2$):

$$G_{xj}(j\omega) = \frac{F\{\delta x_{1F}(t)\}}{F\{\delta\tau_{1jC}(t)\}}, \quad G_{yj}(j\omega) = \frac{F\{\delta y_{1F}(t)\}}{F\{\delta\tau_{1jC}(t)\}} \quad (17)$$

where $\delta x_{1F}(t)$ and $\delta y_{1F}(t)$ are the resulting leg 1 foot trajectory perturbations, $\delta\tau_{11C}(t)$ and $\delta\tau_{12C}(t)$ are the corresponding joint demanded torques perturbations and $F\{\cdot\}$ represents the Fourier transform operator.

5.3 Transfer Function Computation

In order to determine G_{xj} and G_{yj} ($j = 1, 2$), the TFs of the robot-environment, the locomotion is simulated while the robot is moving on a perfectly flat surface without obstacles in its path. For this purpose, sinusoidal perturbations, with maximum amplitudes of $\delta x_{id}(t) = 10^{-4}$ m and $\delta y_{id}(t) = 10^{-4}$ m in the x

and y directions, respectively, are superimposed, separately, over the planned robot feet Cartesian trajectories, in the range of frequencies $0.001 \text{ rads}^{-1} \leq \omega \leq 100.0 \text{ rads}^{-1}$ during $T_{\text{sim}} \approx 40000$ steps. Figure 11 presents charts of the sinusoidal perturbation $\delta x_{id}(t)$, for $\omega = 100.0 \text{ rads}^{-1}$, and the corresponding feet trajectory perturbations $\delta x_{1F}(t)$ and joint torque perturbations $\delta \tau_{11C}(t)$ and $\delta \tau_{12C}(t)$.

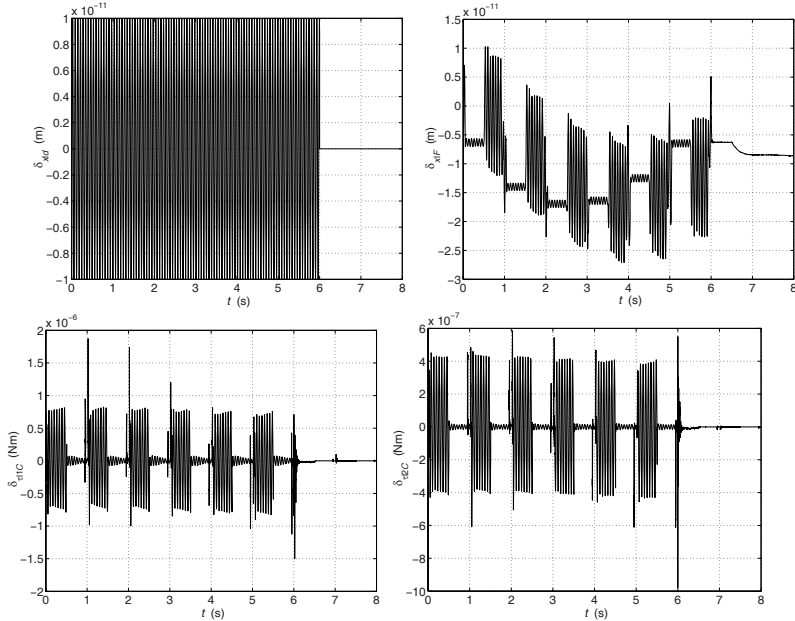


Fig. 11. Sinusoidal perturbation $\delta x_{id}(t)$, for $\omega = 100.0 \text{ rads}^{-1}$ (top, left), and the corresponding feet trajectory perturbations $\delta x_{1F}(t)$ (top, right) and joint torque perturbations $\delta \tau_{11C}(t)$ (lower, left) and $\delta \tau_{12C}(t)$, for $V_F = 1.0 \text{ ms}^{-1}$

We start with G_{xj} for a robot forward locomotion speed of $V_F = 1.0 \text{ ms}^{-1}$. As can be observed from the Nichols chart presented in Fig. 12, G_{x1} presents different asymptotes for different frequency ranges. At low frequencies ($A \equiv [0.001; 0.05] \text{ rads}^{-1}$) the asymptote can be approximated by the expression:

$$G_{xj}(s) \approx \frac{k_{xj}}{\iota(s^{\alpha_{xj} + i\beta_{xj}})}, \quad \iota = \sqrt{-1}, \quad \alpha_{xj}, \beta_{xj} \in \Re, \quad j = 1, 2 \quad (18)$$

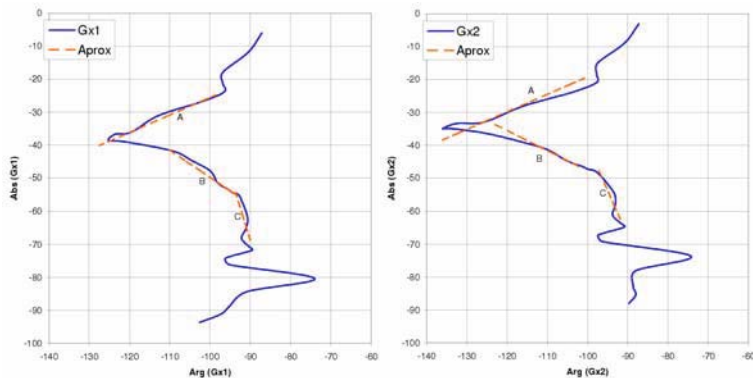


Fig. 12. Nichols charts of $G_{x1}(j\omega)$ and $G_{x2}(j\omega)$, and their approximations at low (A), medium (B) and high frequencies (C), for $V_F = 1.0 \text{ ms}^{-1}$

The values of the parameters α_{xj} and β_{xj} for the low frequency asymptotic approximation of G_{x1} are presented in Table 2.

Table 2. Parameters values for the asymptotic approximations of the Nichols charts of G_{x1} and G_{x2} , with $V_F = 1.0 \text{ ms}^{-1}$

$V_F = 1.0 \text{ ms}^{-1}$	G_{x1}			G_{x2}		
Frequency Range	k_{x1}	α_{x1}	β_{x1}	k_{x2}	α_{x2}	β_{x2}
Low (A)	0.001	0.72	0.18	0.001	0.77	0.22
Medium (B)	0.0014	0.84	-0.20	0.0022	1.03	-0.19
High (C)	0.00068	1.02	-0.01	0.002	1.04	-0.04

At medium and at high frequencies (regions B $\equiv [0.05; 0.5] \text{ rads}^{-1}$ and C $\equiv [0.5; 5.0] \text{ rads}^{-1}$), the resulting TFs can be approximated by an expression of the type:

$$G_{xj}(s) \approx \frac{k_{xj}}{s^{\alpha_{xj} + i\beta_{xj}}}, \quad \alpha_{xj}, \beta_{xj} \in \Re, \quad j = 1, 2 \quad (19)$$

The values of the parameters α_{xj} and β_{xj} for the asymptotic approximations in these frequency ranges are also presented in Table 2.

These results reveal a complex order dynamics that is a consequence of the foot-ground interaction, with several free-impact-contact-impact-free dynamical states. Complex order dynamics have already been addressed in modelling and control [15, 16, 17, 18].

We verify that the Nichols chart of G_{x2} has similar features to those of G_{x1} , as can be observed in Fig. 12. The asymptotic approximations at low, medium and high frequencies, can be described by identical expressions and occur in the same frequency ranges as for the case of G_{x1} . The same can be concluded by comparing the values of the parameters α_{xj} and β_{xj} , for the asymptotic approximations of G_{x2} and G_{x1} (Table 2).

In a second phase, the study is repeated for a robot velocity of $V_F = 2.0 \text{ ms}^{-1}$ and the conclusions are identical. The asymptotic approximations at low, medium and high frequencies, obey to the same expressions as in the case for $V_F = 1.0 \text{ ms}^{-1}$ ((18) and (19), for low and medium and high frequencies, respectively).

The meaning of the imaginary factor i in the denominator of expression (18) is not yet clear. However, the authors believe on the existence of an expression unifying the asymptotic behavior of the TF both at low and medium frequencies, which is currently under investigation.

Conclusions

We have presented several applications of the FC concepts. It was demonstrated the advantages of using the FC theory in different areas of science and engineering. In fact, this paper studied a variety of different dynamic systems, namely:

- Tuning of PID controllers using fractional calculus concepts
- $\text{PI}^\alpha \text{D}^\beta$ controller of a heat diffusion systems
- Complex-order dynamics in hexapod locomotion

The results demonstrate the importance of FC in the modelling and control of many systems and motivate for the development of new applications.

References

- [1] Oldham, K.B., Spanier, J.: *The Fractional Calculus: Theory and Application of Differentiation and Integration to Arbitrary Order*. University of Michigan Press, New York (1974)
- [2] Podlubny, I.: *Fractional Differential Equations*. University of Michigan Press, San Diego (1999)
- [3] Barbosa, R.S., Machado, J.A.T., Ferreira, I.M.: *Nonlinear Dynamics* 38(1/4), 305 (2004)
- [4] Vinagre, B.M., Chen, Y., Petráš, I.: *Franklin Institute* 340(5), 349 (2003)
- [5] Barbosa, R.S., Machado, J.A.T., Silva, M.F.: *Signal Processing* 86(10), 2567 (2006)
- [6] Gerald, C.F., Wheatley, P.O.: *Applied Numerical Analysis*. Addison-Wesley, USA (1999)

- [7] Farlow, S.J.: *Partial Differential Equations for Scientists and Engineers*. Wiley, Chichester (1993)
- [8] Jesus, I.S., Machado, J.A.T.: *Journal of Advanced Computational Intelligence and Intelligent Informatics* 11(9), 1086 (2007)
- [9] Jesus, I.S., Machado, J.A.T.: *Nonlinear Dynamics* 54(3), 263 (2008)
- [10] Oustaloup, A.: *La Commande CRONE: Commande Robuste d'Ordre Non Entier* Éditions Hermès (1991)
- [11] Chen, W., Holm, S.: *Proceedings of the Sixth International Conference on Theoretical and Computational Acoustics* (2003)
- [12] Barbosa, R.S., Machado, J.A.T.: *Nonlinear Dynamics* 29(1-4), 235 (2002)
- [13] Silva, M.F., Machado, J.A.T., Lopes, A.M.: *Robotica* 23(5), 595 (2005)
- [14] Silva, M.F., Machado, J.A.T., Lopes, A.M.: *Machine Intelligence and Robotic Control*, pp. 33–44 (2003)
- [15] Sabatier, J., Poullain, S., Latteux, P., Thomas, J.L., Oustaloup, A.: *Nonlinear Dynamics* 38(1-4), 383 (2004)
- [16] Hartley, T.T., Lorenzo, C.F., Adams, J.L.: *Proceedings of the VIB, – ASME International 20th Biennial Conference on Mechanical Vibration and Noise*, ASME, Long Beach, California, USA (2005) DECT2005-84951
- [17] Nigmatullin, R.R., Trujillo, J.J.: *Proceedings Fifth EUROMECH Nonlinear Dynamics Conference*, Eindhoven, The Netherlands, pp. 1402–1408 (2005)
- [18] Hartley, T.T., Adams, J.L., Lorenzo, C.F.: *Proceedings of the VIB, – ASME International 20th Biennial Conference on Mechanical Vibration and Noise*, ASME, Long Beach, California, USA (2005) DECT2005-84952

Adaptive Control Using Fixed Point Transformations for Nonlinear Integer and Fractional Order Dynamic Systems

József K. Tar and János F. Bitó

Institute of Intelligent Engineering Systems, John von Neumann Faculty of Informatics,
Budapest Tech, Bécsi út 96/B, H-1034 Budapest, Hungary
tar.jozsef@nik.bmf.hu, bito@bmf.hu

Abstract. In this paper an automatic learning based adaptive approach elaborated for the control of nonlinear dynamic systems is analyzed from various points of view concerning the imprecision and incompleteness of the available system model used by the controller. The proposed approach is compared to the most elaborated classical techniques using Lyapunov functions and dynamic models that are exact in their mathematical form but imprecise in their parameters, yield globally and asymptotically stable solutions but do not allow the presence of permanent external perturbations. It is shown that the novel control allows both numerical imprecision and enduring external disturbances unknown by the controller, but generally cannot guarantee global stability. It is also shown that its simple structure makes it a prospective candidate for the control of fractional order dynamic phenomena in which the conventional techniques based on the application of integer order time-derivatives of quadratic Lyapunov functions have great difficulties. The possible implementation of the proposed method is mathematically tackled and expounded from various backgrounds as the application of Cauchy Sequences in complete, linear, normed metric (Banach) spaces, and the use of coupled differential equations that may also be obtained from simple quadratic Lyapunov functions the decreasing nature of which generally can be guaranteed only within bounded regions. The operation of the proposed method is illustrated by simulation examples made for integer and fractional order dynamical systems as examples.

1 Introduction

In the present paper the problem of controlling integer and fractional order are briefly overviewed separately due to the different nature of the mathematical difficulties/possibilities characteristic to these fields.

1.1 The Adaptive Control of Integer Order Systems

In the wide set of control approaches applicable to integer order systems two typical limit cases can be identified. The so-called “Model Based Approaches” assume the availability of precise and complete system model on the basis of which the required controller can be designed in advance. Such controllers need only some simple error-feedback to operate properly and often are referred to as “Model Predictive Controllers (MPC)” (e.g. [1]). MPCs normally are combined with the formal mathematical framework of “Optimal Control” as e.g. the so called “Receding Horizon Control” either in the control of mechanical systems [2] or e.g. chemical processes [3]. The fact that in many cases the linear approximation of the nonlinear model is satisfactory in the vicinity of certain typical trajectory, and by choosing appropriately simple cost functions and constraints linear matrix equalities or inequalities can be obtained for the solution of which software packages are commercially available made this approach actual in our days, too [4].

The other extreme approach corresponds to the case in which no any analytical model is available for the controlled system. For such problems references to Soft Computing based modeling approaches (e.g. [5]), “Model Free Controllers” (e.g. [6]), and “Grey System Models” (e.g. [7, 8]) can be found in the current literature. These approaches try to fit more or less uniform schemes to the controlled system that is observed during the control process. The Soft Computing based applications try to develop complete, everlasting, and precise models formulated in a non-analytical way relying on Kolmogorov’s Approximation Theorem [9], and have significant limits in the case of complex, multiple dimensional systems [10]. The Grey Systems make do with simple structures needing continuous maintenance.

In the great variety of practical cases a formally exact analytical model of the system to be controlled is available. For instance, the closed analytical dynamic model of robots normally takes the form as follows:

$$\mathbf{H}(\mathbf{q})\ddot{\mathbf{q}} + \mathbf{C}(\mathbf{q}, \dot{\mathbf{q}})\dot{\mathbf{q}} + \mathbf{g}(\mathbf{q}) = \mathbf{Q} \quad (1)$$

in which $\mathbf{q} \in \mathbb{R}^n$ denotes the physical state of the system, \mathbf{Q} describes the generalized forces to be exerted by the controller through the drives of the robot, \mathbf{H} denotes the symmetric, positive definite inertia matrix, the array \mathbf{g} describes the gravitational terms, and the \mathbf{C} and \mathbf{H} matrices are deduced from the Lagrangian of the whole robot, consequently they are not independent of each other. It can be shown that due to this interdependence it holds that

$$\left(\frac{1}{2} \dot{\mathbf{H}} - \mathbf{C} \right)^T = - \left(\frac{1}{2} \dot{\mathbf{H}} - \mathbf{C} \right), \quad (2)$$

i.e. this matrix is skew-symmetric [11]. If the kinematical structure of the robot is precisely known, that is a common situation, the expressions in (1) and (2) are

constructed of precisely known functions of the state variable and its time-derivatives and, and \mathbf{Q} only linearly depends on the imprecisely known dynamic parameters so that the coefficients of this linear dependence depend on \mathbf{q} and its time-derivatives. Though in different depths of details, both the “Adaptive Inverse Dynamics Control” and the “Slotine-Li Adaptive Control” utilize the available formal information for developing appropriate parameter tuning rules due to which the control that initially starts its operation by the use of approximate dynamic parameters eventually can exactly learn them. Since this latter method is the more sophisticated one not requiring the inverse of roughly estimated matrices its behavior was analyzed in details in [12] regarding its robustness against unknown external perturbations. For making comparisons with the here proposed approach it is worth analyzing this approach to the tune of a few sentences.

The main deficiency of this method that it assumes that the generalized forces are exactly known and they are equal with effects of the system’s drives commanded by the controller. This assumption excludes the successful compensation of lasting and unknown external perturbations because generally they need not be restricted to a form that can originate from the variation of the parameters in the left hand side of (1). The exerted forces are calculated as

$$\mathbf{Q} = \hat{\mathbf{H}}(\mathbf{q})\dot{\mathbf{v}} + \hat{\mathbf{C}}\mathbf{v} + \hat{\mathbf{g}} - \mathbf{K}_D[\dot{\mathbf{e}} + \Lambda\mathbf{e}] \equiv \mathbf{Y}(\mathbf{q}, \dot{\mathbf{q}}, \mathbf{v}, \dot{\mathbf{v}})\hat{\mathbf{p}} - \mathbf{K}_D[\dot{\mathbf{e}} + \Lambda\mathbf{e}] \quad (3)$$

in which \mathbf{K}_D and Λ are symmetric positive definite matrices, the quantities denoted by the caret symbol denote the actual approximate model values (\mathbf{p} means the parameter vector and \mathbf{Y} the exactly known matrix of the coefficients in the dynamic model), and $\mathbf{e} := \mathbf{q} - \mathbf{q}^N$ denotes the error of tracking the nominal trajectory. The parameter tuning rule, i.e. the time-derivative of the actual estimation of the constant \mathbf{p} vector, $\dot{\hat{\mathbf{p}}}$, is obtained by guaranteeing non positive time-derivative of the Lyapunov function U ($dU/dt \leq 0$), for which the information conveyed by (2) is necessary:

$$U := \frac{1}{2}\mathbf{S}^T \mathbf{H} \mathbf{S} + \frac{1}{2}\tilde{\mathbf{p}}^T \mathbf{G} \tilde{\mathbf{p}}, \quad \mathbf{S} := \dot{\mathbf{e}} + \Lambda\mathbf{e}, \quad \tilde{\mathbf{p}} := \hat{\mathbf{p}} - \mathbf{p}, \quad \dot{\hat{\mathbf{p}}} = -\mathbf{G}^{-1} \mathbf{Y}^T \mathbf{S} \quad (4)$$

where \mathbf{G} is a positive definite matrix influencing the speed of learning. Its worth noting that the Lyapunov function itself is unknown by the controller (it is constructed from the elements of the unknown exact model and the parameter estimation errors), only its existence and appropriate properties have to be guaranteed. [The tuning rule in (4) evidently does not utilize unknown information.]

The great advantage of Lyapunov’s stability theory developed in the 19th Century [13] when people generally were in lack of useful computing power consisted in the fact that it could guarantee certain properties of the motion without knowing other details of the solution. Essentially the same philosophy can be applied when using Lyapunov functions in control technology, therefore Lyapunov’s method

obtained fundamental significance in linear and nonlinear control, and his work was issued a long time after his death, too [14]. However, it can be noted that from practical point of view the application of Lyapunov function cannot be done without extensive simulation investigations since the details of the nonlinear transients generated also may have practical significance. To obtain information on them the only possible way is the application of numerical simulations in general. Therefore from this point of view the Lyapunov function based methods are not really far better than the simple local approach proposed in this paper, for which the simulations are needed because it cannot guarantee global convergence.

Furthermore, in the generalization of the Lyapunov-function based methods difficulties arise in the case of non-integer order systems that can be characterized with response functions that are not integer order derivatives of their state variables. As it will be shown in the sequel, while the integer order derivatives of a quadratic Lyapunov function behave conveniently by yielding integer order derivatives of the state variables, the non-integer order derivatives do not have this useful and nice property.

1.2 *The Adaptive Control of Fractional Order Systems*

Though the formal mathematical idea of introducing non-integer order derivatives can be traced from the 17th Century in a letter by L'Hospital in which he asked Leibniz what would be the meaning of $D^n y$ if $n = 1=2$ in 1695 [15], it was better outlined only in the 19th Century [16-18]. Due to the lack of clear physical interpretation their first applications in Physics appeared only later, in the 20th Century, in connection with visco-elastic phenomena [19, 20]. The topic later obtained quite general attention [21-23], and also found new applications in material science [24], analysis of earthquake signals [25], control of robots [26], and in the description of diffusion [27], etc. The concept of fractional derivatives has many different definitions, e.g. by Riemann-Liouville, Caputo, Grünwald-Letnikov, Hadamard, Marchaud, Riesz, etc. In this paper, for its lucidity and simplicity, we use the discrete time resolution approximation of the form introduced by Caputo as follows:

$${}_a^C u_t^{n-1+\beta}(t) \equiv u^{(n-1+\beta)}(t) := \int_a^t \frac{u^{(n)}(\tau)(t-\tau)^{-\beta}}{\Gamma(1-\beta)} d\tau \quad (5)$$

in which $(n-1+\beta)$ denotes the order of differentiation, n is positive integer constant, $0 < \beta < 1$, a is some initial instant, and Γ denotes the gamma function. For physical applications (5) can be restricted to limited length of memory as $a=t-L$ where L denotes the limited memory-length of the system. This definition has the interesting property that if $u^{(n)}=const.$ then $u^{(n-1+\beta)}=const.$, too, since by substitution in the integral $\xi := t-\tau$, $d\xi = -d\tau$, it is obtained that

$$u^{(n-1+\beta,L)}(t) := -u^{(n)} \int_0^t \frac{\xi^{-\beta}}{\Gamma(1-\beta)} d\xi = \frac{-u^{(n)}[0^{1-\beta} - L^{1-\beta}]}{\Gamma(1-\beta)(1-\beta)}. \quad (6)$$

The expression in (6) immediately suggests the following approximation for non constant classical $(n-1+\beta)$ derivative: let us divide the $[t-L,t]$ interval into small sub-intervals as $[t-T\delta t, t-(T-1)\delta t]$, $[t-(T-1)\delta t, t-(T-2)\delta t]$, $[t-(T-2)\delta t, t-(T-3)\delta t]$, ..., $[t-\delta t, t]$ ($L=T\delta t$), and let us suppose that $u(n) \equiv \text{const.}$ within these small intervals:

$$\begin{aligned} u^{(n-1+\beta,T,\delta t)}(t) &:= \sum_{s=0}^T \frac{\delta t^{1-\beta} u^{(n)}(t-s\delta t) [(s+1)^{1-\beta} - s^{1-\beta}]}{\Gamma(2-\beta)} = \\ &= \sum_{s=0}^T G_s u^{(n)}(t-s\delta t), \quad G_s := \frac{\delta t^{1-\beta} [(s+1)^{1-\beta} - s^{1-\beta}]}{\Gamma(2-\beta)}. \end{aligned} \quad (7)$$

By the use of matrix technique in [28] it was shown that according to the approximation defined in (7) the solution of the differential equation $u^{(1+\beta)} = -ku$ ($0 < \beta \leq 1$) corresponds to damped oscillations approaching to $u(t) \equiv 0$ as $t \rightarrow \infty$ the details of which are determined by the “preceding history of the system”, i.e. by the value of the integer order $u^{(n)}$ in the grid-points of the $[-T, 0]$ interval if the solution of this equation is investigated in the $[0, \infty]$ interval.

On the above basis a non-integer order dynamic system can be defined by a state propagation equation as follows:

$$x^{(1+\beta)}(t) = f(x(t), \dot{x}(t), Q). \quad (8)$$

where x denotes the physical state, Q stands in the position/role of the actual physical agent by setting of which the instantaneous value of the state propagation, that is $x^{(1+\beta)}(t)$ can be influenced. The inherent internal memory of the fractional order systems in this approach manifests in the actual value of $x^{(1+\beta)}(t)$ that contains the linear combination of the past values of $x^{(2)}$ that cannot be manipulated in the present time due to causality. (A simple example of a similar case is the control of the position of the last pearl of a truncated necklace when we have direct access to the instantaneous acceleration of the first pearl only: the effects of this action reach the last pearl only through a chain of local interactions between the neighboring pearls, so such systems have inherent internal memory, too.) Therefore, if for the trajectory tracking error e a simple relaxation of P-type can be achieved as $e^{(1+\beta)} = -Pe$ the tracking error asymptotically will converge to zero. In the next section it will be shown that such a convergence can be achieved by the same manner for integer and fractional (real) β , too.

2 The Proposed Adaptive Approach

Many control tasks can be formulated by using the concepts of the "excitation" \mathbf{Q} of the controlled system to which it is expected to respond by some prescribed or "desired response" \mathbf{r}^d . The appropriate excitation can be computed by the use of some incomplete and imprecise dynamic model $\mathbf{Q} = \phi(\mathbf{r}^d)$. Due to the modeling errors the actual response determined by the system's exact dynamics, Ψ , results in a realized response \mathbf{r}^r that differs from the desired one: $\mathbf{r}^r = \psi(\phi(\mathbf{r}^d)) = \mathbf{f}(\mathbf{r}^d)$. It is worth noting that these functions may contain various hidden parameters that partly correspond to the dynamic model of the system, and partly pertain to unknown external dynamic forces acting on it. Normally the controller can manipulate or "deform" the input value from \mathbf{r}^d so that $\mathbf{r}^d = \mathbf{f}(\mathbf{r}_*^d)$ i.e. so that the realized response obtained for the deformed input just equals with the desired response. In this manner it is satisfactory to determine \mathbf{r}^d on purely kinematical basis to achieve asymptotically zero error trajectory tracking. For finding the appropriate deformation for Single Input-Single Output (SISO) systems an iterative learning process was proposed that was obtained from a nonlinear deformation of the response function as follows: $r(t_{n+1}) = G(r(t_n); r^d(t_{n+1}))$ in which

$$\begin{aligned} G(r; r^d) &= (r + K)[1 + B \tanh(A[f(r) - r^d])] - K \\ G(r_*; r^d) &= r_*, \quad G(-K; r^d) = -K \\ G' &= (r + K) \frac{ABf'(r)}{\cosh^2(A[f(r) - r^d])} + \\ &\quad [1 + B \tanh(A[f(r) - r^d])] \\ G'(r_*; r^d) &= (r_* + K)ABf'(r_*) + 1 \end{aligned} \quad . \quad (9)$$

The solution of the equation $f(r_*) = r^d$ evidently is a fixed point of function G for fixed r^d . For achieving convergent sequences in the vicinity of r_* the *contractivity* of G is required in a local region around r_* . If $|G'(r; r^d)| \leq K < 1$, then evidently $|G(b; r^d) - G(a; r^d)| = \left| \int_a^b G'(\tau; r^d) d\tau \right| \leq \int_a^b |G'(\tau; r^d)| d\tau \leq K|b - a|$, therefore the proposed sequence will be self-convergent and must converge to one of the fixed points of G : if $r_n \rightarrow u$ then

$$\begin{aligned} |G(u) - u| &= |G(u) - r_n + r_n - u| \leq \\ &\leq |G(u) - r_n| + |r_n - u| \leq \\ &\leq |G(u) - G(r_{n-1})| + |r_n - u| \leq \\ &\leq K|u - r_{n-1}| + |r_n - u| \rightarrow 0 \text{ as } r_n \rightarrow u \end{aligned} \quad . \quad (10)$$

For guaranteeing such a convergence the derivatives of G have to be considered around r_* in (9). With an affine approximation of $f(r)$ in the vicinity of r_* it evidently can be shown that the transformation defined in (9) has a proper and a false fixed point, but by properly manipulating the A , B and K control parameters the good fixed point can be located within the basin of attraction of r_* , and the requirement of $|G'(r_*; r^d)| < 1$ can be guaranteed, too.

If r^d is not fixed but varies slowly in time, but the internal dynamics of the iteration is fast enough this approach can be used tracking time-varying trajectories to which time-varying response pertains. If the time-difference between the steps of the iteration Δt is small the operation can be approximated by a differential equation as follows:

$$\begin{aligned} \dot{r}(t_{n+1}) &\approx \frac{r(t_{n+1}) - r(t_n)}{\Delta t} = \frac{G(r(t_n); r^d(t_{n+1})) - G(r(t_n); r^d(t_n))}{\Delta t} \approx \\ &\approx \frac{\partial G}{\partial r} \frac{r(t_n) - r(t_{n-1})}{\Delta t} + \frac{\partial G}{\partial r^d} \frac{r^d(t_{n+1}) - r^d(t_n)}{\Delta t} \approx \\ &\approx \frac{\partial G}{\partial r} \dot{r}(t_n) + \frac{\partial G}{\partial r^d} \dot{r}^d(t_{n+1}) \end{aligned} \quad . \quad (11)$$

For small Δt this roughly corresponds to

$$\begin{aligned} \frac{d}{dt} \dot{r}(t_{n+1}) &\approx \frac{\dot{r}(t_{n+1}) - \dot{r}(t_n)}{\Delta t} \approx \frac{\partial G}{\partial r} \frac{r(t_n) - r(t_{n-1})}{\Delta t} + \frac{\partial G}{\partial r^d} \frac{r^d(t_{n+1}) - r^d(t_n)}{\Delta t} \approx \\ &\approx \frac{\frac{\partial G}{\partial r} - 1}{\Delta t} \dot{r}(t_n) + \frac{\frac{\partial G}{\partial r^d}}{\Delta t} \dot{r}^d(t_{n+1}) \end{aligned} \quad . \quad (12)$$

For constant or slowly varying r^d desired response (12) corresponds to exponentially damped $\dot{r}(t) \rightarrow 0$ solution: the smaller the cycle time Δt is the faster convergence is achieved. The limit $\dot{r}(t) = 0$ corresponds to constant r , i.e. to constant sequence $r(t_{n+1}) = r(t_n)$ that is a fixed point of function G has been achieved. Further possibility for making the idea more familiar to the everyday engineering practice is considering a scalar Lyapunov function and its time-derivative as

$$V := \frac{1}{2} \dot{r}^2 \geq 0, \quad \dot{r} = 0 \Leftrightarrow V = 0, \quad \dot{V} = \dot{r} \ddot{r} = \dot{r} \frac{\frac{\partial G}{\partial r} - 1}{\Delta t} \dot{r}. \quad (13)$$

Evidently, $\dot{V} < 0$ can be achieved as well as the situation that from $\dot{V} = 0$ it follows that $\dot{r} = 0$. That corresponds to the conventional application of the Lyapunov function technique. In our case the decrease of V can be guaranteed only in a local basin of attraction. In the sequel examples will be shown for the

application of this simple idea. It is worth noting that by the use of the norm for $x \in \mathbb{R}^n$ quantities as $\|x\| := \sum_{s=1}^n |x_s|$ the above considerations can be generalized for Multiple Input Multiple Output (MIMO) systems of type $\mathbb{R}^n \rightarrow \mathbb{R}^n$, too.

3 Application Examples via Simulation

For obtaining numerical results the INRIA's SCILAB-SCICOS software packages were used. SCILAB (Scientific Laboratory) is a software package freely available for download at the Internet. Its main advantage is that it offers a very practical open computing environment mainly for scientific applications that made it a popular tool for a wide circle of users [29]. One of its services, the SCICOS (Scilab Connected Object Simulator) provides its users with a graphical interface by the use of which its professional ODE (Ordinary Differential Equations) Solver can conveniently and lucidly utilized. This solver can automatically and adaptively select between various numerical integration methods depending on the stiffness of the problem to be solved. In this tool the objects can be represented by the combination of ready-made (they can be copied from the standard palettes) and user-defined function blocks created according to C, FORTRAN or SCILAB syntaxes, and can graphically be interconnected instead of using more abstract function calls. To ease the simulation of dynamic systems the time as variable is distinguished and dealt with in special manner, and the SCICOS library offers various event generators, clocks, shift registers, etc., that is tools the operation of which is physically related to the elapsed time. In the sequel various examples will be considered as paradigms.

3.1 Adaptive Control of the 2D Generalization of the Φ -type Van der Pol Oscillator

The equation of motion of the “original” single variable Van der Pol oscillator was formulated in 1927 to model the behavior of an electrical circuit containing a triode valve [30]. The generalization of this system for 2D yields the following equations of motion:

$$\begin{aligned} m\ddot{x}_1 - \mu(1-x_1^2-x_2^2)\dot{x}_1 + \omega_0^2 x_1 + \alpha x_1^3 + \lambda x_1^5 &= Q_1 \\ m\ddot{x}_2 - \mu(1-x_1^2-x_2^2)\dot{x}_2 + \omega_0^2 x_2 + \alpha x_2^3 + \lambda x_2^5 &= Q_2 \end{aligned} \quad (14)$$

in which (in our case) the exact model values were as follows: $m=1 \text{ kg}\times\text{m}$, $\mu=0.4 \text{ N}\times\text{s}$, $\omega_0=0.46 \text{ N}^{1/2}$, $\alpha=1 \text{ N}$, and $\lambda=0.1 \text{ N}$. x_1 and x_2 are non-dimensional coordinates, and Q_1 and Q_2 are the manipulating agents in N. The appropriate imprecise

model values were $\hat{m} = 0.7 \text{ kg}\times\text{m}$, $\hat{\mu} = 0.38 \text{ N}\times\text{s}$, $\hat{\omega}_0 = 0.43 \text{ N}^{1/2}$, $\hat{\alpha} = 0 \text{ N}$, and $\hat{\lambda} = 0 \text{ N}$. The kinematical trajectory tracking control was of a PD-type with pre-scribed tracking error relaxation $\ddot{e} = -Pe - D\dot{e}$ with $P = \Lambda^2$, $D = 2\Lambda$, $\Lambda = 12 \text{ 1/s}$.

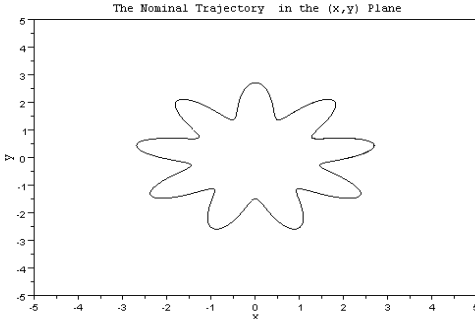


Fig. 1. The nominal trajectory in the (x,y) plane

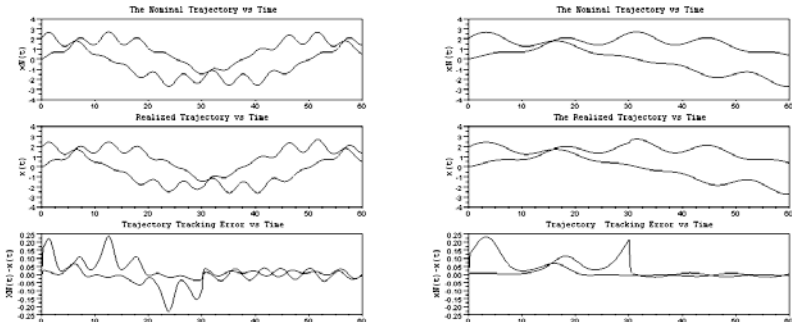


Fig. 2. Trajectory tracking for relatively fast (LHS) and slow (RHS) motion

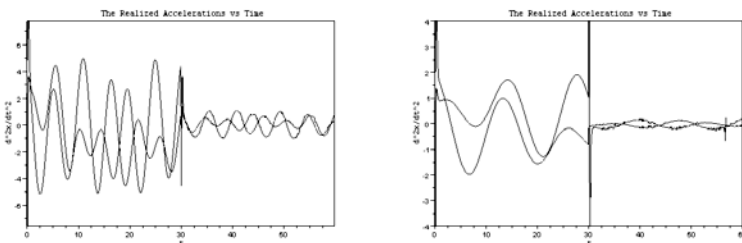


Fig. 3. Setting the acceleration of the coordinates for relatively fast (LHS) and slow (RHS) motion

The nominal trajectory to be traced in the (x,y) plane is given in Fig. 1. The nominal and realized trajectories and the tracking error versus time for relatively fast and slow motion are given in Fig. 2. The adaptive loop was computed with the causal time-shift $t_{n+1}-t_n=0.01 \text{ s}$, and it was switched on in the 30th second of the

simulation. It can well be seen that turning on adaptivity considerably improves the precision of trajectory tracking, especially for the slower motion. It can be pointed out that the improvement in trajectory tracking originates from properly setting the acceleration of the coordinates [Fig. 3].

The next paradigm considered serves as a counterpart of the strictly model-based approach in (4) without using any Lyapunov function. In contrast to the more traditional approaches it is not sensitive to unknown external perturbations.

3.2 The Adaptive Control of a 2D System under Unknown External Disturbances

The system to be controlled is a wheel that can be translated along the vertical axis (generalized coordinate q_1) and also be rotated around it (generalized coordinate q_2). One point of the wheel is connected to a string attracting it into the direction of a point of Cartesian coordinates $[X, Y, Z]$. The equation of motion is as follows:

$$\begin{bmatrix} M & 0 \\ 0 & \Theta \end{bmatrix} \begin{bmatrix} \ddot{q}_1 \\ \ddot{q}_2 \end{bmatrix} + \begin{bmatrix} -Mg - k(q_1 - Z) \\ -k(R \sin q_2 - Y)R \cos q_2 + k(R \cos q_2 - X)R \sin q_2 \end{bmatrix} = \begin{bmatrix} Q_1 \\ Q_2 \end{bmatrix} \quad (15)$$

The exact model parameters are $M=20$ kg, $\Theta=35$ kg×m², $k=3.1$ N/m, $g=9.81$ m/s², $X=3.9$ m, $Y=2.1$ m, $Z=0.53$ m, $R=0.89$ m. The imprecise model values are $\hat{M}=25$ kg, $\hat{\Theta}=40$ kg×m², $\hat{k}=3$ N/m, $\hat{g}=10$ m/s², $\hat{X}=3.5$ m, $\hat{Y}=2.5$ m, $\hat{Z}=0.5$ m, $\hat{R}=0.8$ m. The controller applied is a common Variable Structure / Sliding Mode one prescribing the error metrics S that is only a part in a more sophisticated control in (4) as follows: $\dot{S}_i = -K \tanh(S_i/w)$ with $w=0.1$, $K=100$, and $\Lambda=30$. In the non-adaptive controller this strategy is only approximated on the basis of the imprecise model. The adaptive loop is used for realizing this strategy more precisely.

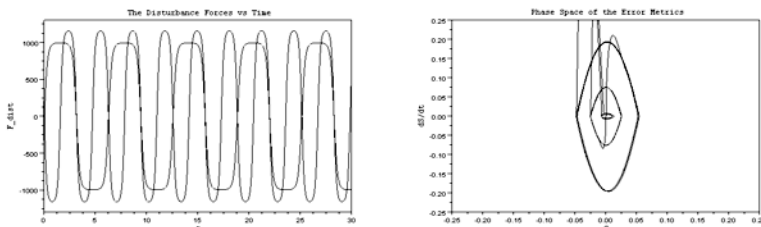


Fig. 4. The disturbance forces (LHS) and the phase space of the error metrics (RHS)

In Fig. 4 the external disturbance forces and the phase space of the error metrics are described. The wider phase trajectories pertain to the non-adaptive stage, the narrower ones belong to the adaptive one. The trajectory tracking is described in Fig. 5.

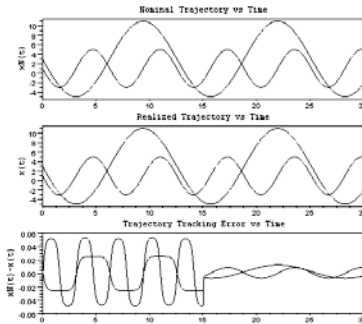


Fig. 5. Trajectory tracking of the VS/SM controller without adaptive loop (till 30 s), and with adaptivity (after the 30th s)

Figure 5 well reveals the efficient compensation of the external disturbances of the adaptive control: before switching on adaptivity the tracking error is in close correlation with the external forces that reveals that the main source of errors were the external influences; after switching on the adaptive loop the errors correlate with the trajectories to be tracked since these characteristics are physically related to the model imprecision. In the next section the control of fractional order systems are considered.

3.3 The Adaptive Control of Fractional Order Systems

The conventional approach in adaptive control normally starts with the construction of some Lyapunov function that is quadratic function of the tracking and estimation errors like the Slotine-Li controller with its Lyapunov function defined in (4). According to the rules of integer order derivation the product of two functions separately contains the original functions and their derivatives in the given instant as $(uv)'(\tau) = u'(\tau)v(\tau) + u(\tau)v'(\tau)$. In the case of the various definitions for the fractional order derivatives these multiplied expressions must be inserted into an integration therefore the value of the fractional order derivative in a given time-instant cannot be constructed from the instantaneous values of the original functions and their derivatives. For instance, in the definition suggested by Caputo in (5) these products have to be integrated. As a consequence the traditional technique that can derive the instantaneous values of the integer order derivatives from the derivative of the Lyapunov function fails in the realm of the fractional order systems. Similar problems arise when attempts are made for generalizing the extremum principles

of Classical Physics for fractional order systems. In [31] a modified Hamilton Principle was derived by introducing two types of canonical transformations, and the Hamilton-Jacobi equations using generalized mechanics with fractional and higher-order derivatives were obtained. Normally both left- and right-sided Riemann-Liouville fractional derivatives appear in the equations obtained from the variational principle [32], [33]. The here proposed method does not cope with any difficulty if the system dynamics described by (8) is substituted into the role of the “system response”. If the approximation (7) is used in the possession of the integer order derivatives in the grid defining the “preceding history” and the actual value of $x^{(1+\beta)}$ the appropriate instantaneous 2nd order can be obtained from the fractional order one and common integration can applied in the simulations for which the SCILAB/SCICOS packages provide excellent ready-made blocks. In the present section the adaptive control of a (8)-type system, the fractional order generalization of the one dimensional Van der Pol oscillator is considered that obeys the state propagation equation as follows:

$$mx^{(1+\beta)} - \mu(1-x^2)\dot{x} + \omega_0^2 x + \alpha x^3 + \lambda x^5 = Q \quad (16)$$

is considered with the following parameter settings: $m=1$, $\mu=0.4$, $\omega_0=0.46$, $\alpha=1$, and $\lambda=0.1$, x is a non-dimensional coordinate, and Q is the manipulating agent. (Since we consider this hypothetical system from purely mathematical point of view we omit the dimensions of the appropriate terms that depend on the order of derivation in general.) The appropriate imprecise model values were $\hat{m}=0.5$, $\hat{\mu}=0.3$, $\hat{\omega}_0=0.4$, $\hat{\alpha}=0.8$, and $\hat{\lambda}=0.05$. In the proportional control $P=36$ (its dimension is intentionally omitted), $\delta t=0.01$ s discrete time-resolution in the approximation of the Caputo derivatives and 10 step memory length were applied.

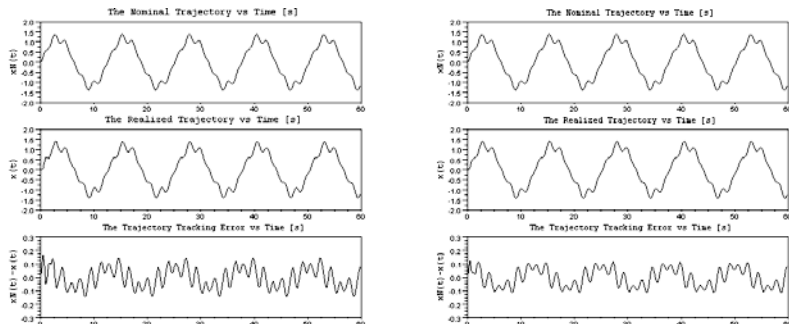


Fig. 6. Trajectory tracking of the non-adaptive (LHS) and the adaptive (RHS) control in the case of the fractional order (1.75) Van der Pol oscillator

As it can be seen if Fig. 6 the improvement in the tracking accuracy is not very significant that can physically be understood if we take into account that in the “response” of the fractional order system in (8) the instantaneous integer order derivative is “mixed” with the combination of its past values that (due to the principle

of causality) cannot be manipulated in the given instant: these excited “degrees of freedom” live their own life without further active control possibility like in the case of the control of the sequentially connected pearls by directly manipulating the acceleration of the first one. For instance, in the case of linear spring connections between three pearls the 3rd one’s 6th time-derivative can be instantaneously be manipulated by the force action on the 1st pearl. The relaxation of the effects of the appropriate initial conditions means the “internal memory” of such systems. Similar phenomenon takes place whenever a vehicle like a lorry pulling a connected cart turns up: in a given stage the initial conditions determine what happens and the driver cannot exert appropriate instantaneous action to evade the accident. However, according to Fig. 7 the improvement in the fractional order response caused by adaptivity is quite significant, therefore as much as such systems can be controlled this approach can control them. The control parameters of the fixed point transformation were as follows: $A=1/(4\times 2000)$, $B=4$, $K=-4000$.

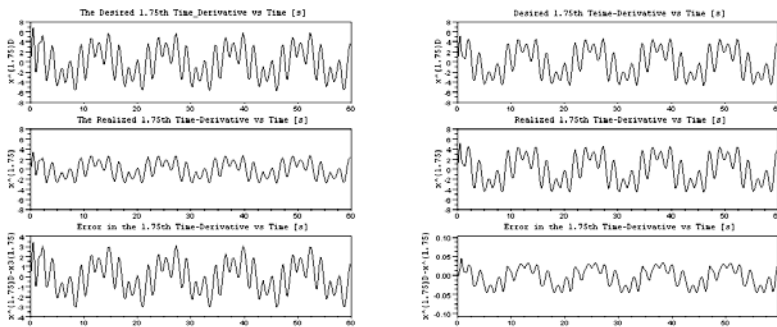


Fig. 7. The fractional order derivatives (1.75) in the case of the non-adaptive (LHS) and adaptive (RHS) control of the generalized Van der Pol oscillator

Conclusions

In this paper the application and possible implementation and operation of a novel, fixed point transformations based adaptive controller was demonstrated via simulation using the professional ODE solver package of the SCILAB/SCICOS pack. It was found that the proposed method is far simpler than the conventional approaches based on the use of some Lyapunov functions. The method was applied for integer and fractional order nonlinear dynamic systems. The special finite element approach proposed was constructed of “standard” counters, event clocks, shift registers, integer order integrators and derivators, and simple function blocks of the use of if / then rules, multiplications and divisions, additions and subtractions, and the \tanh nonlinear function. On this basis it can be expected that such controllers can be realized by the combination of commercially available components. Regarding our future researches it seems to be expedient to study the

applicability of this method for the adaptive control of other causal systems with memory in when the “memory property” is not necessarily related to integer or fractional order derivatives.

Acknowledgments. The authors gratefully acknowledge the support by the Hungarian National Research Fund (OTKA) within the project No. K063405. This research was also supported by the National Office for Research and Technology (NKTH) in Hungary using the resources of the Research and Technology Innovation Fund within the project No. RET-10/2006.

References

1. Mosca, E., Zhang, J.: Stable Design of Predictive Control. *Automatica* 28, 1229–1233 (1992)
2. Varga, A., Lantos, B.: Predictive Control of Powered Lower Limb Prosthetic. In: Proceedings of International Conference of Climbing and Walking Robots, CLAWAR, Brussels, Belgium, pp. 204–214 (2006)
3. Moldoványi, N.: Model Predictive Control of Crystallisers, PhD Dissertation, Department of Process Engineering, University of Pannonia, Veszprém, Hungary (2008)
4. Varga, A., Lantos, B.: Eigenvalue Properties of Discrete Time Linear Receding Horizon Control Systems. In: Proceedings of IEEE International Conference on Mechatronics, Budapest, Hungary, pp. 531–536 (2006)
5. Yu, X., Kacprzyk, J. (eds.): Applied Decision Support with Soft Computing. Studies in Fuzziness and Soft Computing, vol. 124. Springer, Heidelberg (2003)
6. Han, Z.-G.: The Application of Model Free Controller. *Control Engineering of China* 9(4), 22–25 (2002) (in Chinese)
7. Lin, Y., Liu, S.: A Historical Introduction to Grey Systems Theory. In: Proc. of the IEEE International Conference on Systems, Man and Cybernetics, The Netherlands, vol. 1, pp. 2403–2408 (2004)
8. Deng, J.L.: Introduction to Grey System Theory. *The Journal of Grey System* 1, 1–24 (1989)
9. Kolmogorov, A.N.: On the Representation of Continuous Functions of Many Variables by Superpositions of Continuous Functions of One Variable and Addition. *Doklady Akademii Nauk USSR* 114, 953–956 (1957) (In Russian)
10. Tikk, D., Kóczy, L.T., Gedeon, T.D.: A Survey on the Universal Approximation and its Limits in Soft Computing Techniques," Research Working Paper RWP-IT-01-2001, School of Information Technology, Murdoch University, Perth, W.A, p. 20 (2001)
11. Slotine, J.-J.E., Li, W.: Applied Nonlinear Control. Prentice Hall, International, Inc., Englewood Cliffs (1991)
12. Tar, J.K., Rudas, I.J., Gy, H., Bitó, J. F., Tenreiro Machado, J.A.: On the Robustness of the Slotine-Li and the FPT/SVD-based Adaptive Controllers. *WSEAS Transactions on Systems and Control* 9(3), 686–700 (2008)
13. Lyapunov, A.M. (1892) A General Task about the Stability of Motion (in Russian), PhD Thesis (1892)
14. Lyapunov, A.M.: Stability of Motion. Academic Press, New-York (1966)
15. Tenreiro Machado, J.A.: Fractional Calculus and Dynamical Systems. Invited plenary lecture at the IEEE International Conference on Computational Cybernetics (ICCC 2006), Tallinn, Estonia, August 20-22 (2006)

16. Lacroix, S.: *Traité du calcul différentiel et du calcul intégral*, Courcier, Paris, France (1819)
17. Liouville, J.: Mémoire sur le calcul des différentielles à indices quelconques. *J. Ecole Polytechn* 13, 71–162 (1832)
18. Grünwald, A.K.: Über 'begrenzte' Derivationen und deren Anwendung. *Zeitschrift für angewandte Mathematik und Physik* 12, 41–48 (1867)
19. Gemant, A.: Method of Analyzing Experimental Results Obtained from Elasto Viscous Bodies. *Physics* 7, 311–317 (1936)
20. Gemant, A.: On Fractional Differentials. *The Philosophical Magazine* 25, 540–549 (1938)
21. Oldham, K.B., Spanier, J.: *The Fractional Calculus: Theory and Application of Differentiation and Integration to Arbitrary Order*. Academic Press, London (1974)
22. Miller, K.S., Ross, B.: *An Introduction to the Fractional Calculus and Fractional Differential Equations*. John Wiley and Sons, Chichester (1993)
23. Podlubny, I.: *Fractional Differential Equations*. Academic Press, San Diego (1999)
24. Torvik, P.J., Bagley, R.L.: On the Appearance of the Fractional Derivative in the Behaviour of Real Materials. *ASME Journal of Applied Mechanics* 51, 294–298 (1984)
25. Koh, C.G., Kelly, J.M.: Application of Fractional Derivatives to Seismic Analysis of Base-isolated Models. *Earthquake Engineering and Structural Dynamics* 19, 229–241 (1990)
26. Machado, J.A., Azenha, A.: Fractional-Order Hybrid Control of Robot Manipulators. In: Proc. of the IEEE International Conference on Systems, Man and Cybernetics, pp. 788–793 (1998)
27. Agrawal, O.P.: Solution for a Fractional Diffusion-wave Equation in a Bounded Domain. *Nonlinear Dynamics* 29, 145–155 (2002)
28. Tar, J.K., Rudas, I.J., Bitó, J.F., Tenreiro Machado, J.A., Kozłowski, K.: Adaptive Controller for Systems of Fractional Dynamics Based on Robust Fixed Point Transformations. In: Proc. of the 7th International Symposium on Applied Machine Intelligence and Informatics (SAMI 2009), Herlany, Slovakia, pp. 117–123 (2009)
29. Campbell, S.L., Chancelier, J.P., Nikoukhah, R.: *Modeling and Simulation in Scilab/Scicos*. Springer, Heidelberg (2006)
30. Van der Pol, B.: *Philos. Mag.* 7(3), 65 (1927)
31. Riewe, F.: Mechanics with Fractional Derivatives. *Phys. Rev., E* 55, 3581–3592 (1997)
32. Klimek, M.: Lagrangian Fractional Mechanics a Noncommutative Approach. *Czechoslovak Journal of Physics* 55(11) (November 2005)
33. Baleanu, D., Avkar, T.: Lagrangians with Linear Velocities within Riemann-Liouville Fractional Derivatives. *Il Nuovo Cimento B* 119(1), 73–79 (2004)

Author Index

- Aoyama, Tadayoshi 101
Ballagi, Áron 147
Barbosa, Ramiro S. 235
Bejczy, Antal K. 123
Bitó, János F. 253
Bokor, József 167
Borovac, Branislav 79
Chen, Ping-Cheng 189
Dimirovski, Georgi M. 205
Dong, Fangyan 129
Fodor, George A. 223
Fodor, János 25
Fukuda, Kazuya 129
Fukuda, Toshio 101
Gedeon, Tamás D. 147
Grantner, Janos L. 223
Hasegawa, Yasuhisa 101
Hirota, Kaoru 129
Jesus, Isabel S. 235
Jing, Yuanwei 205
Kóczy, László T. 147
Kojima, Shigetaka 101
Le, Phuc Quang 129
Lee, Tsu-Tian 189
Matsuura, Yui 129
Nádai, László 167
Oikawa, Hitoho 129
Pap, Endre 3
Ren, Tao 205
Sekiyama, Kosuke 101
Silva, Manuel F. 235
Szabó, Zoltán 167
Takagi, Hideyuki 65
Tar, József K. 253
Tenreiro Machado, J.A. 235
Vu, Hai An 129
Vukobratović, Miomir 79
Wang, Chi-Hsu 189
Wilamowski, Bogdan M. 51
Yamazaki, Yoichi 129